ENHANCED OIL RECOVERY IN HIGH SALINITY HIGH TEMPERATURE RESERVOIR BY CHEMICAL FLOODING

A Dissertation

by

MOHAMMED ABDULLAH BATAWEEL

Submitted to the Office of Graduate Studies of
Texas A&M University
in partial fulfillment of the requirements for the degree of

DOCTOR OF PHILOSOPHY

December 2011

Major Subject: Petroleum Engineering

ENHANCED OIL RECOVERY IN HIGH SALINITY HIGH TEMPERATURE RESERVOIR BY CHEMICAL FLOODING

A Dissertation

by

MOHAMMED ABDULLAH BATAWEEL

Submitted to the Office of Graduate Studies of
Texas A&M University
in partial fulfillment of the requirements for the degree of

DOCTOR OF PHILOSOPHY

Approved by:

Chair of Committee,	Hisham A Nasr-El-Din
Committee Members,	David Schechter
	Gioia Falcone
	Mahmoud El-Halwagi
Head of Department,	Stephen A. Holditch

December 2011

Major Subject: Petroleum Engineering

ABSTRACT

Enhanced Oil Recovery in High Salinity High Temperature Reservoir by Chemical Flooding. (December 2011)
Mohammed Abdullah. Bataweel, B.S., King Fahad University of Petroleum and Minerals;
M.S., Herriot-Watt University
Chair of Advisory Committee: Dr. Hisham A. Nasr-El-Din

Studying chemical enhanced oil recovery (EOR) in a high-temperature/high-salinity (HT/HS) reservoir will help expand the application of chemical EOR to more challenging environments. Until recently, chemical EOR was not recommended at reservoirs that contain high concentrations of divalent cations without the need to recondition the reservoir by flooding it with less saline/ less hardness brines. This strategy was found ineffective in preparing the reservoir for chemical flooding. Surfactants used for chemical flooding operating in high temperatures tend to precipitate when exposed to high concentrations of divalent cations and will partition to the oil phase at high salinities. In this study amphoteric surfactant was used to replace the traditionally used anionic surfactants. Amphoteric surfactants show higher multivalent cations tolerance with better thermal stability. A modified amphoteric surfactant with lower adsorption properties was evaluated for oil recovery. Organic alkali was used to eliminate the water softening process when preparing the chemical solution and reduce potential scale problems caused by precipitation due to incompatibility between chemical slug containing alkali and formation brine.

Using organic alkali helped in minimizing softening required when preparing an alkali-surfactant-polymer (ASP) solution using seawater. Solution prepared with organic alkali showed the least injectivity decline when compared to traditional alkalis (NaOH and Na_2CO_3) and sodium metaborate. Adding organic alkali helped further reduce IFT values when added to surfactant solution.

Amphoteric surfactant was found to produce low IFT values at low concentrations and can operate at high salinity / high hardness conditions. When mixed with polymer it improved the viscosity of the surfactant-polymer (SP) solution when prepared in high salinity mixing water (6% NaCl). When prepared in seawater and tested in reservoir temperature (95^{o}C) no reduction in viscosity was found. Unlike the anionic surfactant that causes reduction in viscosity of the SP solution at reservoir temperature. This will not require increasing the polymer concentration in the chemical slug. Unlike the case when anionic surfactant was used and more polymer need to be added to compensate the reduction in viscosity.

Berea sandstone cores show lower recovery compared to dolomite cores. It was also found that Berea cores were more sensitive to polymer concentration and type and injectivity decline can be a serious issue during chemical and polymer injection. Dolomite did not show injectivity decline during chemical and polymer flooding and was not sensitive to the polymer concentration when a polymer with low molecular weight was used.

CT scan was employed to study the displacement of oil during ASP, SP, polymer and surfactant flooding. The formation and propagation oil bank was observed during these core flood experiments. ASP and SP flooding showed the highest recovery, and formation and propagation of oil bank was clearer in these experiments compared to surfactant flooding. It was found that in Berea sandstone with a permeability range of 50 to 80 md that the recovery and fluid flow was through some dominating and some smaller channels. This explained the deviation from piston-like displacement, where a sharp change in saturation in part of the flood related to the dominated channels and tapered front with late arrival when oil is recovered from the smaller channels. It was concluded that the recovery in the case of sandstone was dominated by the fluid flow and chemical propagation in the porous media not by the effectiveness of the chemical slug to lower the IFT between the displacing fluid and oil.

DEDICATION

This dissertation is dedicated

To my mother, for her effort to make me who I am;
To my father, who would be proud of my accomplishment in his grave;
To my beloved wife, who offered me an unconditional love and support during our journey;
To my children, Nawaar, Abdullah, and Omar, the source of joy and hope in my life;
To all my brothers and sister, thank you for believing in me and wishing to celebrate more of your great accomplishments.

ACKNOWLEDGMENTS

All praises and thanks to Almighty Allah most Gracious, most Merciful, for his help and blessing for making this accomplishment possible. May his peace and blessing be upon all his messengers, prophets and all humankind alive and dead, Amen.

I would like to express my sincere thanks to my supervising professor, Dr. Hisham A. Nasr-El-Din. I am grateful for his assistance and guidance throughout my studies and research. Also, I am heartily thankful for his encouragement, supervision and support from the preliminary to the concluding level which enabled me to develop an understanding of this subject. Working with him was a fruitful experience and I thank him for being a mentor during this journey. I wish to extend my appreciation to Dr. Goia Falcone, Dr. Schechter, and Dr. El-Halwagi for devoting their invaluable time to review my research work and evaluate its results. Their comments during the course of my studies are highly appreciated.

I would like to thank the graduate and undergraduate students who assisted me in my research. Special thanks go to Yadhalli Shivaprasad, Prakash Ilando, Ashish Reddy, and Ryan L. Strubeck for help conducting different lab experiments that made completing this work possible. Thanks to the Dr. Nasr-El-Din group for making my study and research exciting and enjoyable.

Thanks also go to my friends, colleagues, and the faculty and staff for making my time at Texas A&M University a great experience. Special thanks goes to John Maldonado, facilities and safety coordinator, for his help and support during building of the labs and maintaining experimental setups.

Many thanks to Saudi ARAMCO for providing a scholarship during my Ph.D. studies at Texas A&M University. Special thanks goes to EXPEC ARC and OSD management for believing in me and selecting me to join this program. Thanks go to Aramco Service Company for their support during my arrival and stay.

I would like to thank the technical staff at Oil Chem. Technology for their help in providing chemicals and technical support of this project. Also, I would like to thank Stepan, Sasol and SNF for providing chemical samples and technical data.

Thanks go also to Professor George Hirasaki and Dr. Yu Bian at Rice University for spending time to help me evaluate evaporative light scattering detector (ELSD) technology in their lab and for sharing with us some useful data and information.

I wish to express my love and gratitude to my beloved family (my parents Abdullah and Thuria Bataweel; my wife, my kids, my brothers and sisters) for their understanding, believing in me, and the endless love they have shown throughout the duration of my study.

NOMENCLATURE

a	Acceleration associated with the body force, almost always gravity
A^-	Water soluble anionic surfactant can be produced from oleic-phase acid (HAo)
AMPS	2-acrylamido-2methyl propane sulfonate and acrylamide
CMC	Critical micelle concentration
D	Average pore diameter; microns
E_A	Aerial displacement efficiency, fraction
E_I	Vertical displacement efficiency, fraction
E_V	Volumetric displacement efficiency, fraction
HAo	Oleic-phase acid
HAw	Aqueous phase acid
HEC	Hydroxyethylcellulose
HLB	Hydrophilic-lipophilic balance
HPAM	Hydrolyzed polyacrylamides
IFT	Interfacial tension
k	Flow consistency index
K_i	Effective permeability
k_{ro}	Relative permeabilities to oil
k_{rw}	Relative permeabilities to water
L	Characteristic length scale', e.g. radius of a drop or the radius of a capillary tube
M	Mobility control is discussed in terms if mobility ratio
n	Power low index
N_b	Bond numbers a dimensionless number expressing the ratio of gravitational to capillary forces

N_c	Capillary number
P_c	Capillary pressure
PEO	Polyethylene oxide
r	Radius of the oil droplet or capillary
S_{oi}	Initial oil saturation
S_{orc}	Residual oil saturation after chemical flooding
S_{orw}	Residual oil saturation after water flooding
$\Delta\rho$	Density difference between aqueous solution and the crude oil
ϕ	Porosity, fraction
φ	Contact angle
μ	Steady shear viscosity
μ_{app}	Apparent viscosity of the injected fluid
μ_o	Oil viscosity
μ_0	Shear viscosity for the lower Newtonian region
μ_w	Water viscosity
μ_∞	Shear viscosity for the upper Newtonian region
ν	Darcy velocity, m/s
ω	Rotational speed
τ	Time constant (inverse of the critical shear rate where lower Newtonian region ends and shear thinning region starts)
σ_{ow}	Interfacial tension between water and oil
σ_{os}	Interfacial tension between oil and solid
σ_{ws}	Interfacial tension between water and oil
λi	Fluid mobility is the ratio between effective permeability and it's viscosity
ρ	Density, or the density difference between fluids

γ	Shear rate

TABLE OF CONTENTS

CHAPTER Page

CHAPTER Page

CHAPTER Page

CHAPTER Page

LIST OF FIGURES

Page

Page

Page

Page

Page

Page

Page

Page

Page

LIST OF TABLES

Page

CHAPTER I
INTRODUCTION

Oil Recovery

Oil recovery processes are classified in to: Primary, secondary and tertiary or enhanced oil recovery EOR processes (Green and Willhite 98). In primary recovery driving mechanisms depend on the natural energy present in the reservoir. This natural energy is used to displace the oil to producing wells. The source for the natural drive are solution gas, gas cap, water drive, fluid and rock expansion, gravity drive or combination of two or more of the driving mechanism.

In secondary recovery water and gas are injected to increase the natural energy of the reservoir by either displacing hydrocarbon to producers or by pressure maintenance by voidage replacement of the produced oil. This can be done by either injection to gas cap in case of gas injection for pressure maintenance or to the oil-column wells for immiscible displacement. The most used secondary recovery is water flooding due to its availability and efficiency when compared to gas injection.

Tertiary recovery or EOR is result of injection gas, chemical, hot water or steam to recovery oil that was not extracted during the previous recovery processes. The injected fluids during EOR operation interacts with reservoir rock and oil to create favorable conditions for oil recovery. These interactions can result in lowering interfacial tension (IFT), oil swelling, reduction of oil viscosity, wettability alteration, mobility modification, or favorable phase behavior.

This dissertation follows the style of *SPE Journal*.

Enhanced Oil Recovery EOR Processes

Enhanced Oil Recovery, or "EOR," is the use of any process or technology that enhances the displacement of oil from the reservoir, other than primary recovery methods. For effective recovery by any EOR method an efficient displacement need to be accomplished. Displacement efficiency is given by Eq.1:

$$E = E_D x E_V \quad \text{.....(1)}$$

where E is displacement efficiency (frac), E_D is microscopic displacement efficiency (frac), and E_V is macroscopic (volumetric sweep) displacement efficiency (frac).

Microscopic displacement is related to mobilization of oil from the porous media on pore scale level. E_D measures the effectiveness of displacing fluid to mobilize oil contacted by injected fluid and lower residual oil saturation.

Macroscopic displacement E_V measures the effectiveness in displacing fluid to sweep the oil toward the production wells. The volumetric sweep efficiency is the product of areal and vertical sweep efficiencies (**Fig. 1)** and given by Eq.2:

$$E_V = E_A x E_I \quad \text{.....(2)}$$

where E_A is areal displacement efficiency (frac), and EI is vertical displacement efficiency (frac).

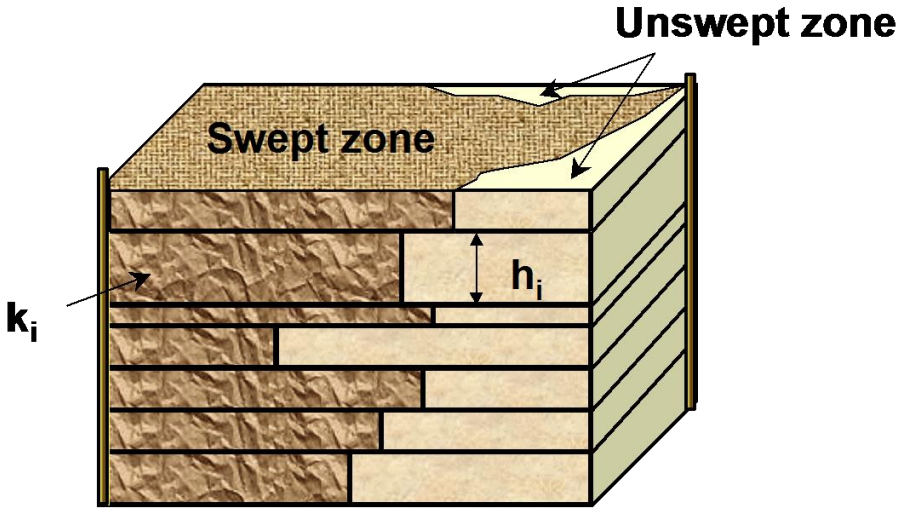

Fig. 1—Areal and vertical sweep of reservoir section.

Microscopic Displacement in Porous Media

In immiscible displacement process, such as water flooding, part of the crude oil is trapped as isolated drops (**Fig. 2**), stringers, or pendular rings, depending on wettability (Green and Willhite, 1998). When this condition is reached relative permeability to oil will reduce to zero and displacing phase flows around to trapped oil and losses its displacing effectiveness (Green and Willhite, 1998). The oil doses not move in the flowing stream because of capillary forces prevent oil deformation and passage through constrictions in the pore passages.

Factors that affect the microscopic displacement are (Shah and Schechter, 1977):

1. Geometry of the pore structure.
2. Fluid-fluid interaction, such as interfacial tension, density difference, bulk viscosity ratio, and phase behavior.
3. Fluid-rock interaction, such as wettability, ion exchange, and adsorption.
4. Applied pressure gradient and gravity.

The capillary and viscous forces govern the phase trapping that affect the microscopic displacement efficiency (Green and Willhite 1998). The ability to alter these forces can help improving the microscopic and macroscopic displacement efficiency. In the following sections the description of these forces, how they operate and methods to alter them will be discussed. This discussion will be essential to understand how different recovery mechanisms work and how they can be used in enhanced oil recovery (EOR).

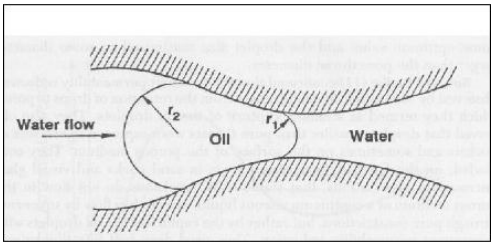

Fig. 2—Blocking mechanism for a trapped oil droplet in porous media (from McAuliffe, 1973a).

Capillary forces

a. Interfacial tension (IFT)

When two immiscible fluids exist in the porous media interfacial tension occurs. Interfacial tension results from the attractive van der Waals forces between molecules of the same fluid (cohesion) which will be equal for the molecules in the bulk of the fluid. However, at the interface between two different fluids the equilibrium forces are disturbed by unequal forces between dissimilar fluids. This imbalance pulls the molecules at the interface toward the interior of the fluid, resulting in surface area to minimize (Schramm, 2000, Green and Willhite 1998, Liu 2007, Zhang 2005). **Fig.3** shows the interaction between molecules that cause the IFT phenomena.

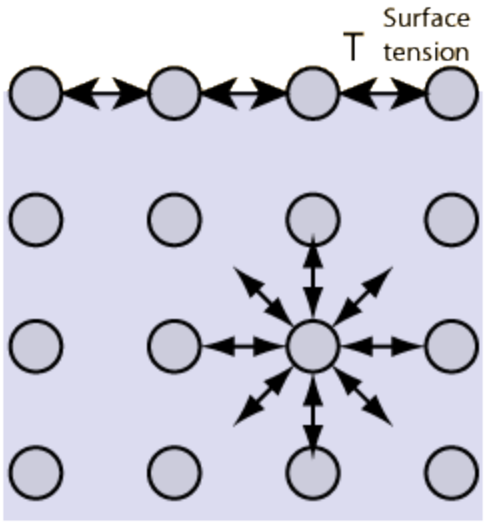

Fig. 3—Interaction between water molecule in bulk and surface of the water droplet that cause surface tension.

b. Wettability (Abdullah et al. 2007)

Wettability is the tendency of one fluid to spread on or adhere to a solid surface in the presence of a second fluid (Green and Willhite 1998, Standnes, 2001, Anderson, 1986). The wettability in porous media effects the distribution of fluids in the media, fluid saturation and relative permeability (Anderson, 1986). Thus practical implications of reservoir wettability will influence productivity and oil recovery, during primary, secondary and tertiary processes. The wettability effect on the distribution of fluids in the reservoir has two folds: microscopically and macroscopically. Microscopically or pore-level view, fluid in the wetting phase covers the walls of the pores and non-wetting phase remains the center of the pore. Secondly, wetting phase will occupy the small pores whereas non-wetting will cover large pores (Abdullah et al. 2007; Anderson. 1986 & 1987). **Fig.4** shows the distribution of fluids in pore scale for three wettability cases: water-wet, mixed-wet, and oil-wet.

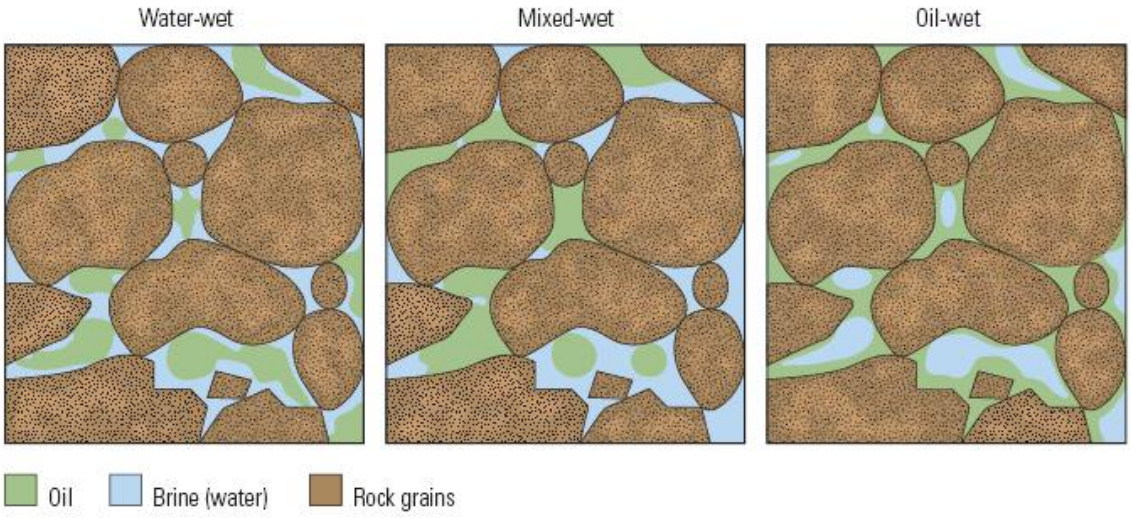

Fig. 4—Oil and water distribution inside the porous media for water-wet, mixed-wet, and oil-wet (from Abdullah et al. 2007).

On the other hand, wettability macroscopically or in reservoir-level affects the capillary pressure in the reservoir which will have an influence on the transition zone from high oil saturation in the top to high water saturation in the bottom. In water-wet reservoir, transition zone is long and the change in saturation from high oil saturation to high water saturation is long and capillary pressure is positive. On the other hand, oil-wet reservoir has a short transition zone with negative capillary pressure (Abdullah et al., 2007).

When two immiscible liquids (brine and oil) are in contact with a solid surface, interfacial tension deforms the liquids and generates what is known contact angle (θ). The balance between different interfacial tension forces causes the characteristic contact angle for the oil-water-solid system as can be seen in **Fig. 5**. The force balance at the line of interaction of oil-water-solid system yields Young's equation (Standnes, 2001; Young, 1805):

$$\sigma_{os} = \sigma_{ws} + \sigma_{ow} .\cos\theta \quad \text{.....(3)}$$

where σ_{os} is oil-solid IFT (N/m), σ_{ws} is water-solid IFT (N/m), σ_{ow} is oil-water IFT, (N/m), and θ is Contact angle, (degree).

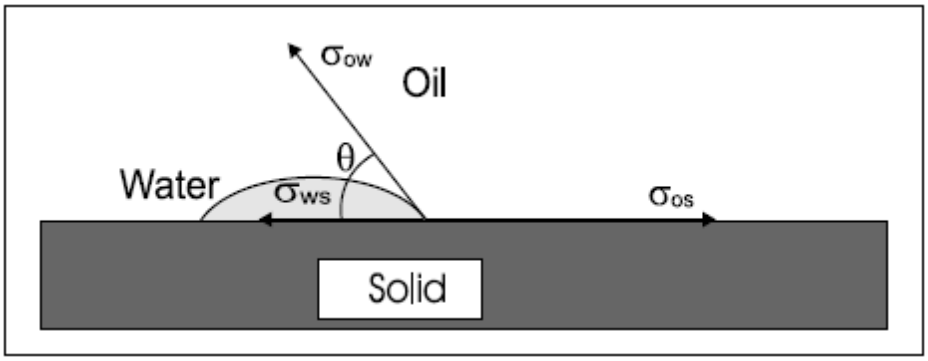

Fig. 5—Force balance at the oil-water-solid contact line defining the contact angle ϕ (from Standnes 2001).

Contact angle gives an indication of wettability state of solid surface. A solid surface can be water-wet, oil-wet, intermediate wet or mixed wet. **Fig.6** shows three wettability state and its relation with contact angle:

a. Water –wet when contact angle < 90^o.
b. Oil-wet at contact angle > 90^o.
c. Neutral-wet around 90^o.

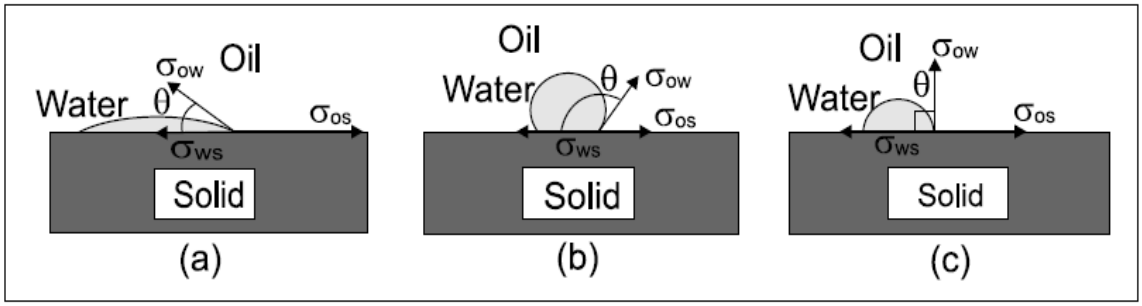

Fig. 6—Three surfaces with different wettability. (a) Water-wet ($\theta < 90^o$), (b) Oil-wet ($\theta > 90^o$), and (c) Neutral-wet ($\theta = 90^o$).

The wettability type is a function of rock and oil composition, and saturation history (Green and Willhite 1998). Intermediate wettability occurs when both fluids oil and water tend to wet equally or with one phase is slightly more wetting than the other. Mixed wettability results from the variation of chemical composition of the rock surfaces (Green and Willhite 1998). The type of rock wettability of the rock will have a great impact on the recovery resulted from chemical flooding when wettability alteration is the main recovery mechanism.

c. Capillary pressure

The existence of two fluids in capillary tube or in pore in reservoir rock results in pressure difference across the interface. This pressure is called capillary pressure and is very important in forming the saturation distribution in the transition zone between the free water level and the oil saturated zone. Capillary pressure can be calculated using the following equation:

$$\boldsymbol{P_c = \frac{2\sigma_{ow} COS\theta}{r}} \quad \text{..... (4)}$$

where P_c: is capillary pressure (psi), and r is capillary radius (cm). As can be seen from the above equation the capillary pressure is a function of oil-water IFT, wettability presented by θ, and pore throat and pore body radius. Capillary pressure can be positive in water-wet system and negative in oil-wet rocks.

d. Viscous forces

Viscous forces in the porous media are reflected in the pressure drop created by the fluid flow in the media. Darcy's law is an expression of this force. Viscous forces in porous media are dominated by the flow velocity and fluid viscosity.

e. Gravitational forces

Due to the multi-phase flow in hydrocarbon reservoir the difference in density of the fluids gravitational forces will play an important role in fluid segregation and fluid flow in the porous media. Gravitational forces will be pronounced when viscous and capillary forces are negligible or the difference in fluids density is large.

Flow Regime Characterization

Multi-phase flow in porous media is affected by capillary, viscous, and gravitational force and the interplay between them (Green and Willhite 1998). The flow regime caused by the interaction between these forces is represented by capillary and bond number.

- Capillary Number

  Capillary number is a dimensionless number expressing the ratio of viscous to capillary forces

$$\boldsymbol{N_c = \frac{v\mu}{\sigma \cos \emptyset}} \quad \text{.....(5)}$$

where N_c: is capillary number (dimensionless), ν is interstitial velocity, and μ viscosity of displacing fluid (cp).

- Bond Number

  Bond number notated N_b, is a dimensionless number expressing the ratio of gravitational to capillary forces:

$$\boldsymbol{N_b = \frac{\rho a L^2}{\sigma}} \quad \text{.....(6)}$$

where ρ is the density, or the density difference between fluids, *a* the acceleration associated with the body force, almost always gravity, *L* the

'characteristic length scale', e.g. radius of a drop or the radius of a capillary tube, and σ is the surface tension of the interface.

EOR Methods

Taber et al. (1997) prepared a table of more than 20 EOR methods that were evaluated in laboratories and field tests. These methods can be group in three main methods: gas, improve water flooding (chemical) and thermal methods. These EOR methods will be discussed in the following paragraphs.

However, with much of the easy-to-produce oil already recovered from U.S. oil fields, producers have attempted several tertiary, or enhanced oil recovery (EOR), techniques that offer prospects for ultimately producing 30 to 60 percent, or more, of the reservoir's original oil in place. Three major categories of EOR have been found to be commercially successful to varying degrees:

- Thermal recovery, which involves the introduction of heat such as the injection of steam to lower the viscosity, or thin, the heavy viscous oil, and improve its ability to flow through the reservoir. Thermal techniques account for over 50 percent of U.S. EOR production, primarily in California.
- Gas injection, which uses gases such as natural gas, nitrogen, or carbon dioxide that expand in a reservoir to push additional oil to a production wellbore, or other gases that dissolve in the oil to lower its viscosity and improves its flow rate. Gas injection accounts for nearly 50 percent of EOR production in the United States.
- Chemical injection, which can involve the use of long-chained molecules called polymers to increase the effectiveness of water floods, or the use of detergent-like surfactants to help lower the surface tension that often prevents oil droplets from moving through a reservoir. Chemical techniques account for less than one percent of U.S. EOR production.

Each of these techniques has been hampered by its relatively high cost and, in some cases, by the unpredictability of its effectiveness. (Department of energy)

Gas methods

Gas injection is one of the oldest EOR methods in petroleum industry. An extensive experimental work in the area helped develop a reasonable understanding of the method. Oil production from CO_2 injection continued to increase USA in spite of fluctuation in oil price during the years. Most of the produced oil from EOR methods is by gas injection (Liu 2007). Gases used for gas injection are nitrogen, flue gas, hydrocarbon and CO2.

Gas injection to the reservoir can enhance recovery either by using miscible and immiscible processes. In low pressure immiscible process will dominate, however, miscible displacement dominates in high pressures. Other than pressure, oil composition affects the mode of displacement to be miscible or immiscible (Taber 1997, Green and Willhite 1998). Miscible displacement can be classified as first-contact miscible (FCM) or multiple-contact miscible (MCM) (Green and Willhite 1998).

Recovery mechanisms related to immiscible processes are oil swilling, viscosity reduction, interfacial tension reduction near to the miscible region, blow-down or solution gas recovery and enhance gravity drainage in dipping reservoirs (Mangalsingh 1996; Taber 1997b). This mostly happen during nitrogen, flue gas or CO2 injection before reaching the miscibility pressure.

On the other hand, recovery related to miscible flooding, which is achieved by displacing the oil with injected fluid that is miscible with the oil by forming a single phase when mixed at all proportions with oil (Green and Willhite 1998). The two miscible displacement classes that were mentioned earlier are first-contact miscibility (FCM) and multiple-contact miscibility (MCM). In FCM process, the injected fluids are directly miscible with oil at reservoir pressure and temperature. A small slug of liquefied petroleum gas (LPG) will be injected to displace the oil. This will be followed with a larger volume of less expensive (i.e. dry gas) for displacement.

In case of MCM, the injected fluid is not miscible at first contact with oil. In this process modification of injected fluids and oil in the reservoir is achieved by multiple contacts between the different fluids in the reservoir and mass transfer of some components between the fluids. Under proper pressure, temperature and modified composition miscibility between displacing fluid and oil is generated in-situ. The MCM processes are classified as vaporizing-gas (lean gas) displacement, condensing and condensing/vaporizing-gas (enriched-gas) displacements, and CO2 displacements.

In the vaporizing-gas process, lean gases, which contain methane and low-molecular weight hydrocarbons, is injected to the reservoir. The composition of the injected fluid will change (enriched) due to vaporization of the intermediate components from the oil caused by the multiple contacts between the injected gas and the reservoir oil. The modified injected fluid will become miscible with the oil in some point in the reservoir and miscible displacement will start from that point on.

In the condensing-gas (enriched-gas) process, the injected fluid contains larger amounts of intermediate-molecular-weight

Gas methods, particularly carbon dioxide (CO_2), recover the oil mainly by injecting gas into the reservoir. Gas methods sometimes are called solvent methods or miscible process. Currently, gas methods account for most EOR production and are very successful especially for the reservoirs with low permeability, high pressure and lighter oil (Lake, 1989; Green and Willhite 1998). However, gas methods are unattractive if the reservoir has low pressure or if it is difficult to find gas supply. (Liu 2007)

Thermal methods (Green and Willhite 1998, Taber et al. 1997, Doghaish 2009)

Three main processes are used:

1. Steam-Drive

Stream-drive or steam-flooding process involves injection of steam into injection wells to displace viscous crude oil toward producing wells. As steam losses energy when it is following in the reservoir hot water condensation will occur. This process consists of hot water flooding in the region where condensation occurred and followed by the steam

injection. **Fig. 7** depicts steam flooding process and formation of four different regions by this type of thermal recovery:

1) water and oil at reservoir temperature toward the production well

2) followed by oil bank,

3) condensed hot water

4) injected steam close to the injection well.

The main recovery mechanisms are viscosity reduction of crude oil, oil swilling, steam stripping and steam-vapor drive (Green and Willhite 1998, Taber et al. 1997 part-2).

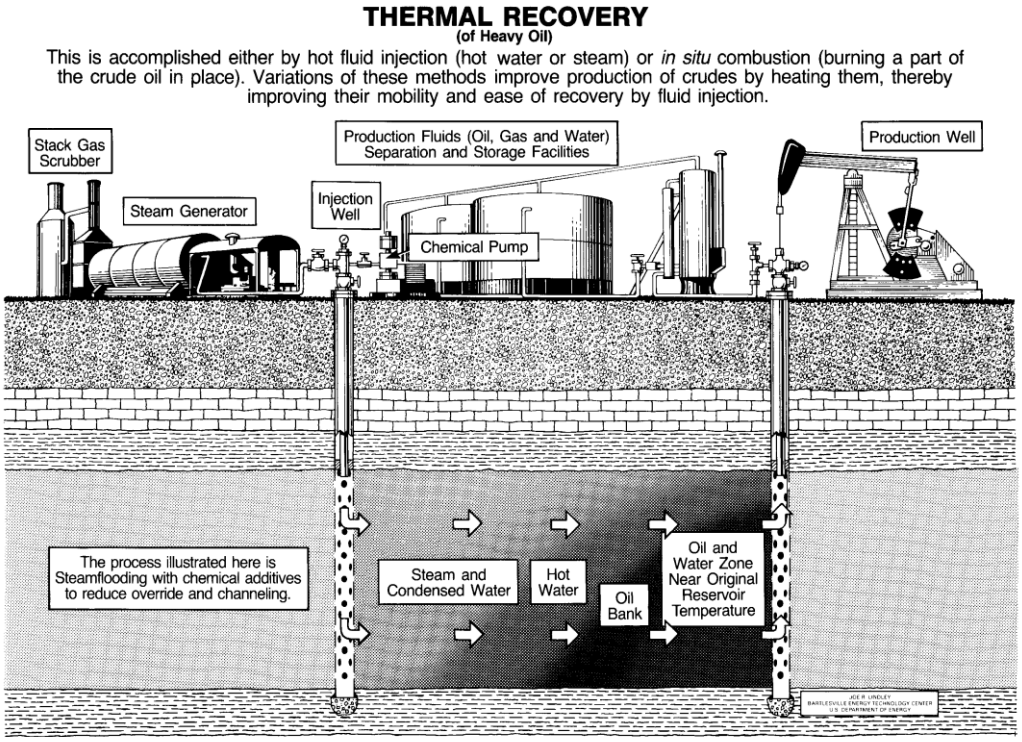

Fig. 7—Steam flooding process (Adapted from Green and Willhite, 1998; courtesy of DOE).

2. In-situ Combustion

In-situ combustion or fire flooding involves generation of thermal energy in the reservoir by combustion. This is initiated by electrical heater, gas burner or spontaneous ignition.

Spontaneous ignition occurs if the reservoir temperature is high (above 131 °F) or if there is sufficient heat released by the oxidation of the oil and it usually takes few days for the spontaneous ignition to start (Doghaish, 2008). To sustain this operation air should be continuously injected. Two techniques are used for the fire-front to propagate in the reservoir: forward combustion where reservoir is ignited in the injection well and air is injected to advance the front away from injection well toward the production well. The second technique is the reverse combustion where the reservoir is ignited in the production well and air injection is initiated in adjacent wells. Recovery mechanisms by the in-situ combustion:

1. Lowering oil viscosity from heating
2. Vaporization of fluids
3. Thermal cracking
4. Pressure supplied by the injected air

3. Cyclic Steam Stimulation

Also called the huff and puff method, which is a single well process where steam is injected to the reservoir and then shut down for sufficient time, usually for week or two, to allow the steam to heat the area around the well. After that the well is open for production until production is diminished then the operation is repeated. **Fig. 8** illustrates the cyclic steam stimulation process. Recovery Mechanisms by cyclic steam stimulation:

1. viscosity reduction
2. Steam flushing
3. oil swilling
4. steam stripping

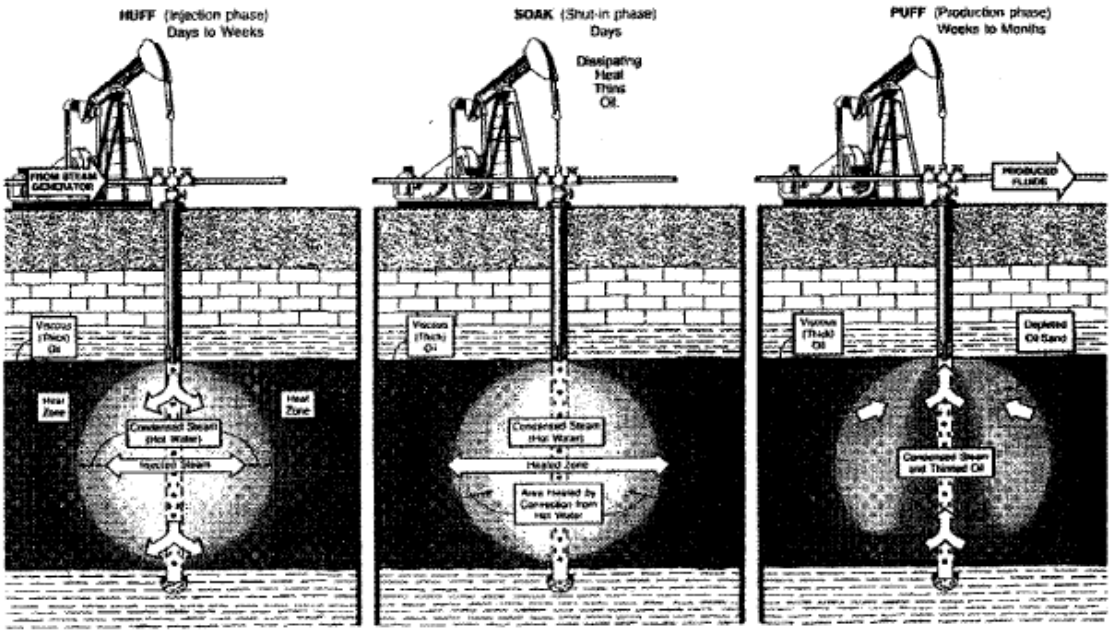

Fig. 8—Cyclic Steam Stimulation (Adapted from Green and Willhite 1998; courtesy of DOE).

Chemical methods

Chemical processes involve injection of specific solutions that effectively displace oil because of their phase-behavior properties, which results in low IFT values between the displacing and displaced fluids (Green and Willhite 1998). When solution in the main chemical slug get in contact with residual oil drops, they will deform under pressure gradient due to low IFT values and are displaced through the pore throats. The coalescence of the oil drops results in oil bank formation and propagation a head of the displacing fluid (Green and Willhite 1998). Chemical EOR is used to achieve one or more of the following microscopic displacement mechanisms: interfacial tension (IFT) reduction, wettability alteration, and mobility control (Zhang. 2005; Green and Willhite. 1998; Taber et al. 1997).

The capillary number discussed earlier is related to residual oil saturation through the desaturation curve (**Fig.9**). A critical capillary number should be reached before oil recovery started and break in desaturation curve is noticed. The critical capillary number

and shape of the desaturation curve is a function of following rock properties (Schramm 2000, page 206):

- aspect ratios, ratio of body to pore throat diameter.
- Pore size distribution.
- Wettability.

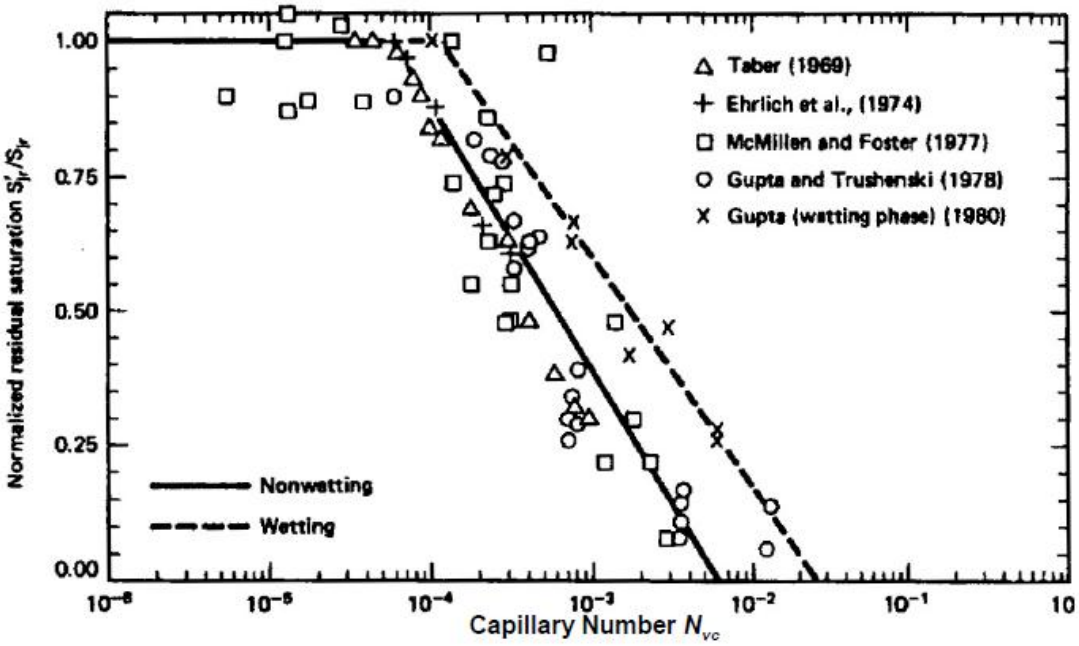

Fig. 9—Capillary desaturation curves for sandstone cores (Delshad 1986; Lake 1989).

Chemicals Used in EOR

Chemicals used in chemical EOR application will be discussed in the following sections.

Alkali

Alkalis are water-soluble substances that release hydroxide ions (OH^-) when dissolve in water. Alkalis can be categorized by being inorganic or organic or can be divided to strong or weak. Alkalis are used in chemical flooding to accomplish the following:

interact with carboxylic acid in the crude to generate in-situ surfactant, wettability alteration and reduce surfactant losses.

Role of Alkali in Chemical Flooding

In-situ Generation of Petroleum Soap

One of the recovery mechanisms by alkali flooding is the in-situ generation of the surface-active soap. Most crude oil contains carboxylic acids as part of its constituents. The variation of the amount of this acid in crude oil results in different acid numbers for different cruds. Different crude oils with different acid numbers will cause a wide variety in behavior upon contact with alkali during alkaline or ASP flooding. Acid in crude oil have low solubility in aqueous phase at neutral pH so it will not be extracted during water flooding. deZabala et al. (1982) suggested a chemical model for the alkali-oil saponification. **Fig. 10** demonstrates the chemical model by deZabala. At high pH flooding the acidic components in the oil will react with alkali solution and will generate water soluble anion salt. In their model, they represented the mixture of active acid species with a single component HA.

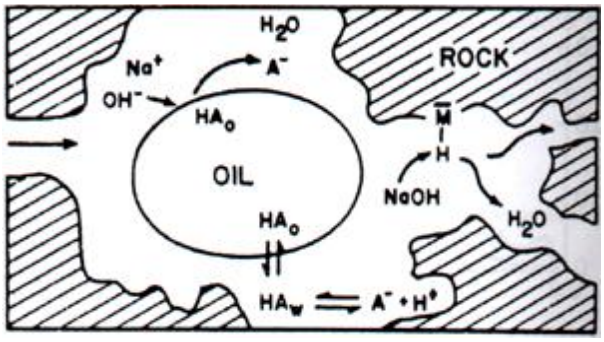

Fig. 10—Chemical model for reaction between oil and alkali solution in recovery process. (deZabala et al. 1982).

This acid in the oil will have some aqueous solubility and will distribute itself between the oleic and aqueous phases represented by Eq.7:

$$HAo \leftrightarrow HAw \quad \text{.....(7)}$$

where HAo is the oleic-phase acid, HAw is the aqueous phase acid. Water soluble anionic surfactant (A^-) can be produced from oleic-phase acid (HAo) by the following hydrolysis and extraction equation:

$$HAo + NaOH \leftrightarrow NaA + H_2O \quad \text{.....(8)}$$

Or can be produced from the aqueous-phase acid (HAw) by aqueous hydrolysis:

$$HAw \leftrightarrow H^+ + A^- \quad \text{.....(9)}$$

The existence of alkali in the aqueous phase will lead to the reduction of the H+ and will result in forward dissociation of HAw. The generated A^- ion will adsorb at oil-water interfaces and lower the interfacial tension.

Reduce Surfactant Loss

One of the important roles of alkali is the reduction of the surfactant adsorption to the formation minerals (Hirasaki. 2008). Several factors affect the surfactant adsorption including temperature, pH, salinity, type of surfactant and type of minerals found in the rock (Wesson and Harwell. 2000). The main reason for surfactant adsorption is the electrostatic interaction between charged minerals on the rock and the charged head-group in the surfactant (Wesson and Harwell. 2000, Hirasaki. 2008, Zhang and Somasundaran. 2006, Liu. 2007, Nelson et al. 1984). To minimize surfactant adsorption to the rock repulsion forces between the surfactant and rock should be maintained or generated. Since most surfactants used for chemical flooding are anionic, then creating a negative potential between brine and rock will help creating a repulsive forces that can result in reduction in surfactant adsorption. For this reason alkalis are added to the chemical slug to increase the pH and generate a negatively charged environment to reduce surfactant consumption. Hirasaki and Zhang (2003) and Zhang (2005) found a

positive zeta potential of the surface of calcite with 0.02 M NaCl for pH 6-8. They found a negative Zeta potential for calcite at lower pH values down to pH of 7 when 0.1 N $Na_2CO_3/NaHCO_3$ brine was used. This is because the potential determining ions for calcite are Ca^{2+} and CO^{2-}. The access amount of CO^{2-} anions make the surface negatively charged (Hirasaki and Zhang. 2003, Liu. 2007). Al-Hashim et al. (1996) evaluated the effect of adding 1 % of $NaHCO_3$:Na_2CO_3 with ratio of 1:1, to surfactant adsorption on limestone and found a reduction of more than 85% at low surfactant concentrations. Changing the pH of the of the fluid will cause the iso-electric point of the limestone to be exceeded and the surface will be negatively charged causing an electrostatic repulsion between the charged anionic surfactant and the rock which will reduce adsorption (Berger and Lee. 2006).

Wettability Alteration

When two interfaces such as solid-water and water-oil approaches each other surface forces between them will either keep these surfaces apart or will draw them closer to each other (Abdullah et al. 2007). The opposite charges between the two surfaces result in electrostatic attraction between the interfaces and collapse the brine film. This will bring the oil in direct contact with the reservoir rock (Hirasaki and Zhang. 2003). The surface force components between two interfaces are electrostatic, van der Waals, and structural or salvation interactions (Hirasaki. 1991, Abdullah et al. 2007). The electrostatic force depends on brine pH and salinity, crude oil composition, and reservoir mineral (Hirasaki 1991).

Hirasaki and Zhang (2003) determined the zeta potential for crude oil-brine interface and of the calcite-brine interface. They found that the zeta potential of the oil-brine interface for the system they tested is negative for pH greater than 3 and that the calcite is negative down to pH 7 when the brine is 0.1 N $Na_2CO_3/NaHCO_3$ plus HCl to adjust the pH. The excess of the carbonate anions (which is a potential determining ion for calcite surface) in the above system makes the surface negatively charged. Since both the oil-brine interface and calcite-brine interface are negative there will be electrical

repulsion between the two surfaces that will tend to stabilize brine film between the two surfaces and alter wettability to water-wet.

Nasr-el-din et al. (1992) observed wettability reversal for Berea disaggregated particles from water-wet to oil-wet when sodium carbonate concentration was increased above 1 wt% in ASP formulation used in their study. They found that increasing alkali concentration caused the synthetic surfactant partitioned into the oil phase and the other portion adsorbed onto the surface of particles, which causes the wettability reversal.

Surfactants

The word surfactant originated from the surface active agent (Broze 1999). Surfactant is the substance that adsorb onto the surfaces or interfaces of the system and altering the degree of surface or interfacial free energies of those surfaces or interfaces (Rosen 2004). The surfactant molecules form oriented monolayers at the interface and show surface activity (i.e., lowering the interfacial tension between the two phases) (Schramm 2000). The interface is the boundary between any two immiscible phases; the term surface donates an interface where one phase is a gas (Rosen 2004). Definition of interfacial free energy is the minimum amount of work required to create unit area of the interface to expand it by unit area (Rosen 2004). The ability of surfactants to adsorb to the different interfaces is due to the structure of the surfactant molecule, which contain a hydrophilic head group and hydrophobic (lipophilic) tail (Schramm 2000; Green and Willhite 1998). **Fig.11** shows a Schematic representation of a surfactant molecule. The head group can be polar or ionic and interact strongly with the aqueous environment and solvated via dipole-dipole or ion-dipole interactions (Schramm 2000; Broze 1999). The nature of the head group of the surfactant molecule is used to classify main groups of surfactants to anionic, cationic, amphoteric and nonionic (Schramm 2000; Broze 1999). The hydrophobic or tail section of the surfactant molecule is mostly composed of hydrocarbon chain which can be linear or branched (Broze 1999). In some specialized surfactant, the tail can be non-hydrocarbon chain such as a polydimethylsiloxane or a perfluorocarbon (Broze 1999). The amphiphilic nature (polar and non-polar group in

same molecule) of surfactants gives the raise to its special properties (Goddard and Ananthapadmanabhan 1993). In aqueous solutions the surfactants have the tendency to minimize the contact of their hydrophobic groups with water by either adsorbing at the interfaces or association in the solutions.

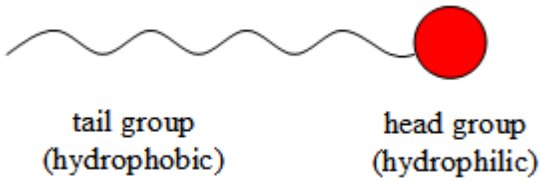

Fig. 11—Schematic of general surfactant molecule.

Surfactant Types

Anionic

Anionic surfactants are the oldest and the most common type of surfactants. They are produced economically with large volumes (Broze 1999). In aqueous solution the surfactant molecule ionize and head group will carry a negative charge (Broze 1999; Green and Willhite 1998). Anionic surfactant can be divided to the following: carboxylate, sulfate, sulfonate, and phosphate (Broze, 1999). They are the sodium salts of alkylbenzene sulfonates, alkyl xylene sulfonates, alkyl toluene sulfonates, alkoxylated alkylphenol sulfonates, alkoxylated alkylphenol sulfonates, alkoxylated linear or branched alcohol sulfates, alkoxylated linear or branched alcohol sulfonates, alkyl diphenylether sulfonates, sulfonated alpha-olefins, and alkoxylated mono and di phosphate esters.

Cationic

A surfactant molecule that can dissociate to yield a surfactant ion whose polar group is positively charged (Broze, 1999). When compared to other type of surfactants cationic

surfactants have more tendencies to change the surface properties of solids. For this reason they are used to alter solids wettability (Broze 1999). Examples for cationic surfactant are the following:

Nonionic

A surfactant molecule whose polar group is not electrically charged. Example include alkoxylated alkylphenols, alkoxylated linear or branched alcohols, and alkyl polyglucosides.

Amphoteric

A surfactant molecule for which the ionic character of the polar group depends on the solution pH. Where it will be positively charged at low pH and neutral at intermediate pH. Examples of some amphoteric surfactant include betaines, sulfobetaines, amidopropyl betaines, and amine. Application of amphoteric surfactant in chemical EOR will be discussed in coming section.

Micelle formation and aggregation

At very low surfactant concentrations, the dissolved surfactant molecules are dispersed as monomers. When surfactant quantity increased to a critical concentration called the critical micelle concentration (CMC) the molecules starts to aggregate and forms micelles. In these micelles, the hydrophobic tails associate in the interior of the aggregate leaving the hydrophilic parts facing the aqueous medium (Schramm 2000), Green and Willhite 1998). These micelles consist of 50 or more surfactant molecules in each aggregate. The assembly of surfactant molecules to form micelle with increasing concentration of surfactant is shown in **Fig.12**. The formation of micelles is a result of the alkyl chain tendency to avoid the energetically unfavorable contact with an aqueous phase and the need of the polar parts to stay in contact with water (Schramm 2000). Increase in the surfactant concentration above the CMC will result in increase in micelle concentration with little change in monomer concentration. Many of the surfactant

solution will have a change in its properties with increasing surfactant concentration until CMC is reached, where no change in these properties will occur beyond this point. Interfacial tension is one of these properties that show this change. At low concentrations (below CMC) increasing the surfactant concentration decreases the surface and interfacial tension of the solution. When CMC is reached increasing the surfactant concentration will not change the surface or interfacial values any more. **Fig.13** shows the change in surface tension as function of surfactant concentration until CMC is reached where no further change was seen even with increasing the surfactant concentration.

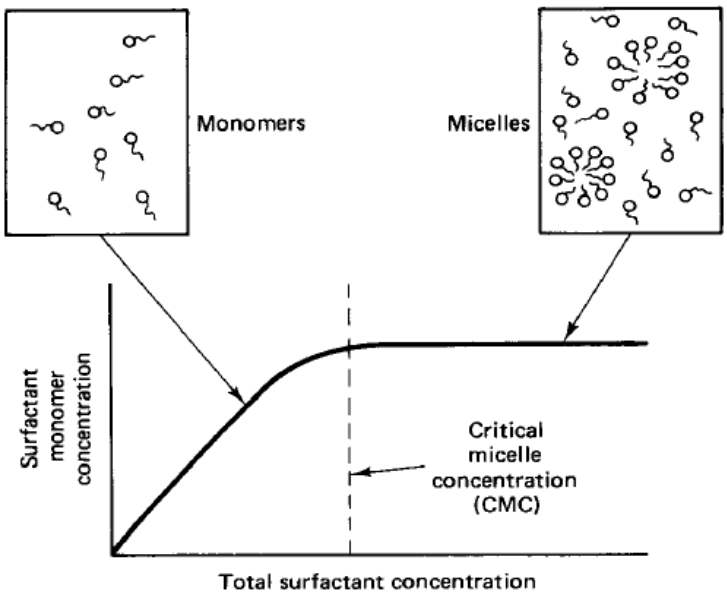

Fig. 12—Schematic definition of critical micelle concentration, CMC (Lake 1989).

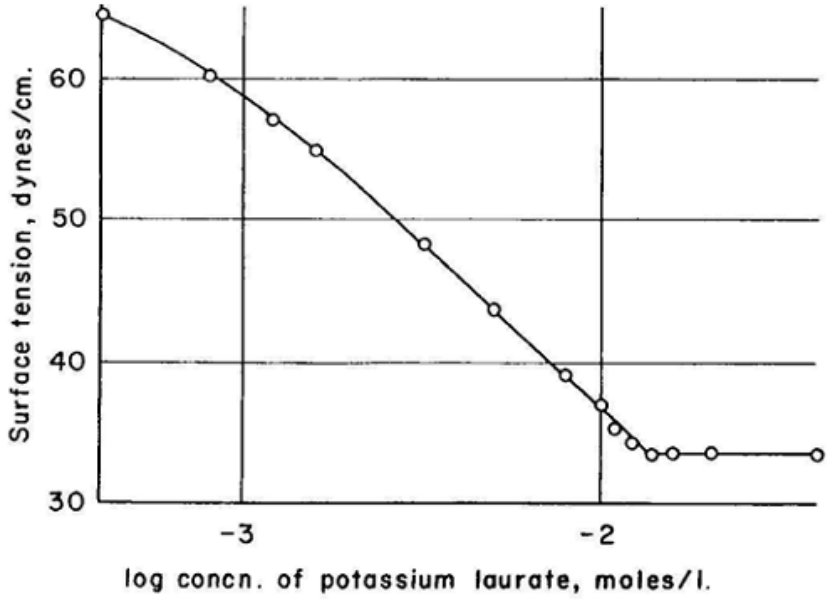

Fig. 13—Interfacial tension as a function of surfactant concentration (Miller and Neogi 1985).

Phase behavior of microemulsion

Phase behavior of the microemulsion is a technique used to screen different formulations at different parameters. One of the most used scans in the designing chemical solution is the salinity scan. Where chemical formulation, oil-water ratio, pressure and temperature are kept constant and salinity in the aqueous solution is changed on each scan. **Fig.14** is an example of a phase behavior experiment with as salinity scan to find the optimum salinity that can be used for given conditions. As can be seen in the figure, at low and high salinities two phases are formed, in the intermediate salinities a three phases area formed with middle phase size changing from one salinity to the second. The salinity with maximum middle phase is called optimum salinity, with over optimum at high salinity and under optimum at low salinity. Microemulsions are divided to three classes: lower-phase microemulsion, upper-phase microemulsion and middle phase microemulsion. Other way to categorize microemulsion is to use the Winsor-type system

(Winsor 1954). Winsor Type I microemulsion consist of oil-swollen micelles in a water continuum (equivalent to lower-phase microemulsion), Winsor Type II consist of water-swollen reverse micelles in oil phase (upper-phase). Type III microemulsion consist of numerous swollen micelle that touch each other, in which water parts are forming a continuous phase and oil part forming continuous phase forming a bicontinuous structure (Salager et al. 2005). **Fig.15** shows different type of microemulsion types with oil-swollen and water-swollen micelles. When bicontinuous microemulsion is formed it enhances the ability of the solution to solubilize both water and oil. During these studies the target is to have the highest solubilization value for the formulation design.

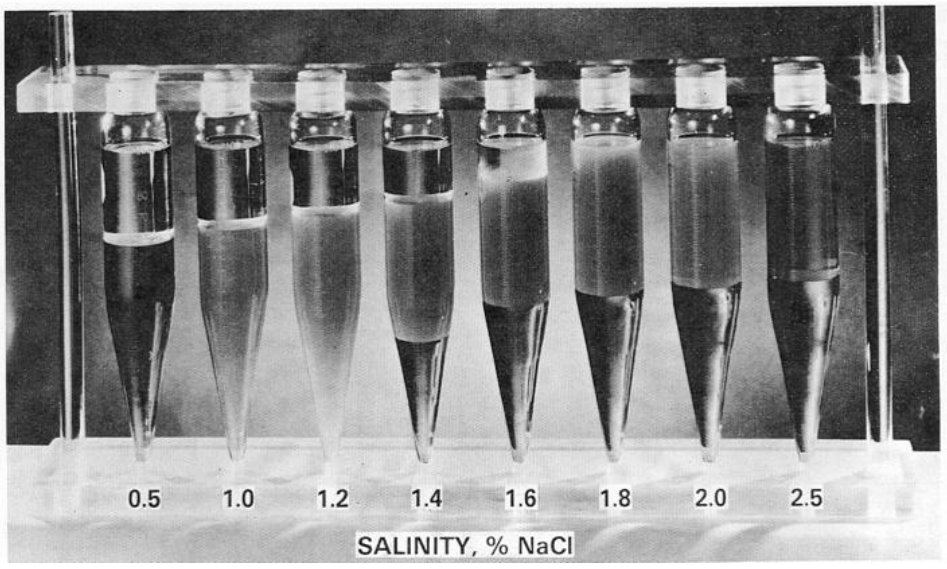

Fig. 14—Effect of salinity on microemulsion phase behavior (Reed and Healy 1977).

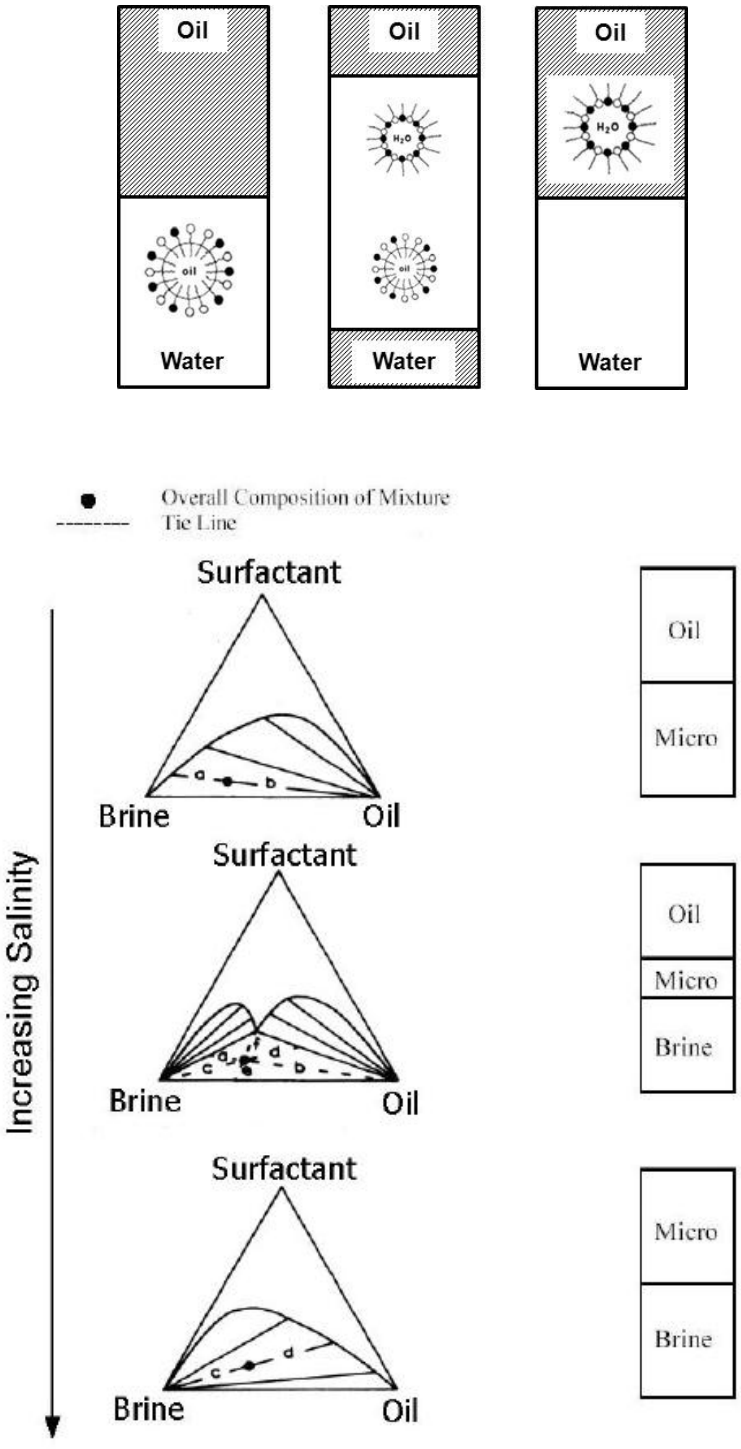

Fig. 15—Types of microemulsion with oil-swollen and water-swollen micelles and its representation in ternary diagram.

Fig.16 shows the change in solubilization factor as function of salinity. To apply the findings of salinity screening in the field this will require in many cases injecting a preflush to create a similar salinity gradient. Then the main chemical slug will be prepared and injected in salinity close to the optimum salinity to have the highest solubility by the microemulsion phase. More discussion about implementation of these strategies in the field is given in coming section.

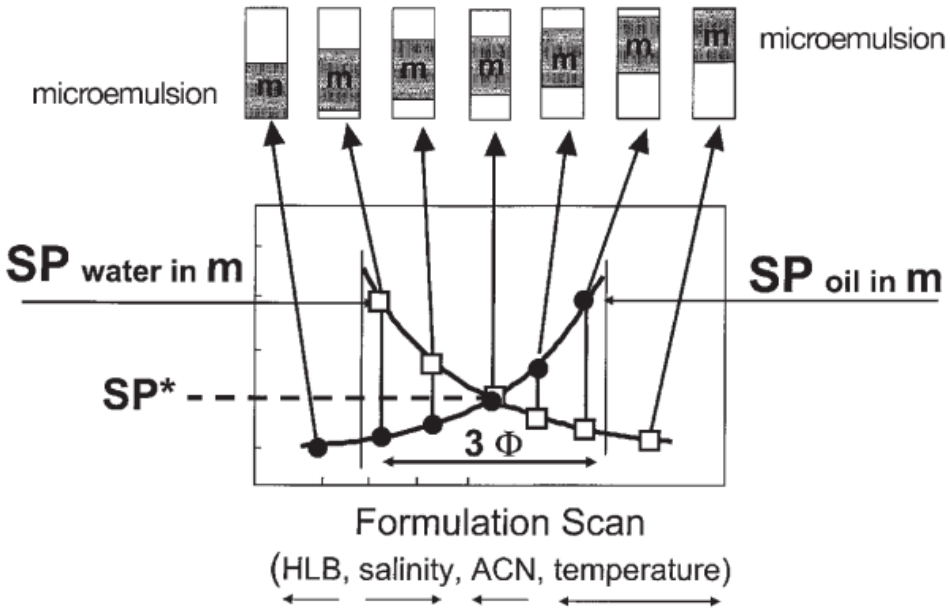

Fig. 16—Solubilization variation along a formulation scan expressed as solubilization parameters, SP (Salager et al. 2005).

Formulation Concepts and Requirements for Surfactant Slug

For successful displacement of trapped oil by chemical flooding, chemical slug should achieve the following (Hirasaki et al. 2008; Levitt et al. 2009; Flaaten et al. 2010):

1. Ultra-low IFT and maintain the ultra-low IFT during the displacement process.
2. Mobility control for microscopic and macroscopic displacement.

3. Compatibility with mixing and formation brine to prevent surfactant precipitation or separation in presence of high divalent ions.
4. Low surfactant adsorption at the reservoir rock.
5. Compatibility between surfactant and polymer to minimize separation.

To design chemical slug for challenging reservoir requirements researchers used several chemical components to overcome these challenges. Following are the different chemical components for the main stage in the chemical flood:

Chemical Composition of Traditional Chemical Slug

Co-solvent can be used to enhance the properties and to help solubilize the other ingredients in the composition. Co-solvents include, but are not limited to, low molecular weight alcohols, glycols, and ethers such as iso-propanol, iso-butanol, hexanol, 2-ethylhexanol, ethylene glycol monobutyl ether, ethylene glycol, propylene glycol, diethylene glycol. The co-solvents are generally used in concentrations from about 0% to 20% by weight of the total injection fluid.

Polymer

Several polymers were considered for polymer flooding. These polymers include biopolymers such as Xanthan gum and synthetic polymers such as hydrolyzed polyacrylamide (HPAM), polyacrylamide, polyacrylic acid, copolymers of polyacrylamide (PAM) and acrylamido methyl propane sulfonate (AMPS) and copolymers of acrylamide and acrylic acid. Polyethylene oxide (PEO) and hydroxyethylcellulose (HEC) are other examples (Magbagbeola, 2008). Polymers commonly used in chemical flooding; are the biopolymers, HPAM, and copolymer (Schramm, 2000, page212, Nasr-el-din, 1991). Two good biopolymer candidates are xanthan and scleroglucan. Xanthan is negatively charged double helix when mixed in saline brine, whereas, scleroglucan is uncharged triple helix in solution. Polymers forming helix hides there hydrophobic sections in the interior of the helix which minimize the formation of surfactant-polymer complex when prepared together. Both

polymers shows high tolerance to salinity and hardness, and can be prepared in seawater (Schramm, 2000).

HPAM is water-soluble polyelectrolyte with negative charges along the polyacrylamide chain (Lee, 2009, Nasr-el-din, 1991). When polymers hydrolyze in water, polyacrylamide chain is stretched due to the electrostatic repulsion between the negative charges in the carboxylate groups on the chain (Nasr-el-din, 1991). Viscosity enhancement will occur because of the chain extension and physical entanglement of the solvated chains (Khan and et al. 2009). HPAM are the mostly used polymer in chemical flooding and has better resistance to biodegradation when compared to biopolymers (Magbagbeola, 2008).

Copolymer is a polymer derived from two (or more) monomeric species, as opposed to a homopolymer where only one monomer is used. AMPS is copolymers composed of acrylamide and sodium 2-acrylamide-2-methylpropane sulfonate are designed to tolerate temperature and seawater (Schramm 2000).

Surfactant -polymer interaction

The interactions between surfactant molecules and synthetic polymers in aqueous solutions affects the rheological properties of solutions, adsorption characteristics at solid-liquid interfaces, stability of colloidal dispersions, the solubilization capacities in water for sparingly soluble molecules, and liquid-liquid interfacial tensions (Nagarajan 2001). When polymer and surfactant mutually exist in a solution one or more of the following forms can be found (Nagarajan 2001):

1. Single dispersed polymer molecules.
2. Single dispersed surfactant molecules.
3. Intermolecular complexes between polymer and surfactant molecules.
4. Surfactant aggregates.

Studying interaction between polymer and surfactants involve three branches (**Table 1**):

Table 1— Polymer surfactant interaction studies

Study	Analytical Technique	Notes
morphology of polymer-surfactant complexes in solution	nuclear magnetic resonance (NMR), neutron scattering and fluorescence spectroscopy	elucidate the structure of polymer-surfactant complexes and to estimate the size of the polymer-bound micelles
quantitative measurement of the amount of surfactant associating with the polymer molecules	dialysis, surface tension, viscosity , electrical conductivity, dye solubilization, specific ion activity	some surfactants do not associate at all with polymers while others do so significantly. Also, the solution properties exhibit critical behavior at one or two surfactant concentrations in some systems but not in others
phase behavior of polymer-surfactant solutions with or without the presence of additional components like electrolytes and oil		

Structure of polymer-surfactant complexes depend on molecular structure of the polymer and surfactant, and on the nature of the interaction forces between the solvent, the surfactant and the polymer (Nagarajan 2001). The first form is when there is no interaction between polymer and surfactant due to both the polymer and the surfactant carry the same type of ionic charges or polymer is relatively rigid and for steric reasons does not interact with ionic or nonionic surfactants. Other reason can be that both the polymer and the surfactant are uncharged and no obvious attractive interactions promoting association between them. **Fig. 17** shows the polymer molecule implying no polymer-surfactant interaction. This is due to similar charge on polymer and surfactant.

Fig. 17—Polymer molecule implying no surfactant-polymer interaction.

Fig. 18 illustrates a system where the polymer and the surfactant carry opposite electrical charges. The association is caused by electrostatic attractions that create a complex with reduced charge and hence, reduced hydrophilicity. This can lead to the precipitation of these complexes from solution.

Fig. 18—Association due to electrostatic attractions between oppositely charged surfactant and polymer molecules.

Fig. 19 shows that polymer and surfactant have opposite charges. Surfactant molecule can cause interamolecular bridging by binding to multiple sites on the same molecule. Surfactant also can bind to more than one polymer molecule and have inter-molecular bridging between several molecules.

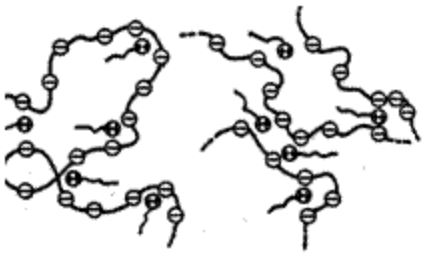

Fig. 19—Surfactant molecules causing intermolecular bridging by binding to multiple sites in the same polymer molecule or binding to more than one molecule.

Fig. 20 depicts the interaction between surfactant and copolymer. Random or multi-block copolymer molecules or blocks will segregate because dissimilar segments of varying polarity. Polymer segregation can take different forms, like formation of polymeric micelles. Surfactant molecules locate themselves at the interface between segregated regions.

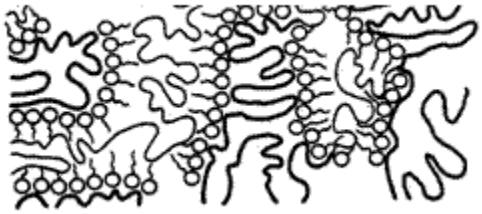

Fig. 20—Interaction between surfactant and copolymer.

Fig. 21 shows the interaction of surfactant with hydrophobically modified polymer. At low surfactant concentration individual surfactant molecules associate with one or more of the hydrophobic modifiers on a single polymer molecule or multiple polymer molecules. No conformational changes on the polymer caused by this type of interaction.

Fig. 21—Interaction of surfactant with hydrophobically modified polymer.

At higher surfactant concentration cluster of surfactant molecules associate with multiple hydrophobic modifiers in single polymer molecule. This interaction causes significant change polymer conformation as seen in **Fig. 22.**

Fig. 22—Interaction between high surfactant concentrations with multiple hydrophobic modifiers in single polymer molecule.

Fig. 23 depicts the interaction between hydrophobically modified polymers with larger surfactant concentrations, surfactant aggregates associate with multiple hydrophobic modifiers on single polymer molecule.

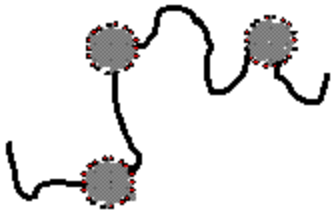

Fig. 23—Interaction between micelles and hydrophobically modified polymer.

When surfactant concentration is above the critical micelle concentration (CMC) and micelles are formed, polymer molecule penetrates and wraps around the polar head group region of the micelle (**Fig.24**). In this form of complex, a single polymer molecule can associate with one or more surfactant micelles. Such structure describes the interaction between nonionic or ionic polymer associated with surfactant micelles or oppositely charged micelles.

Fig. 24—Interaction between micelles and polymer molecules.

Surfactant-polymer Flooding

Two different strategies are followed when using surfactant to formulate a chemical solution for EOR application. First one uses high concentrations of surfactant in the chemical slug with different components including co-surfactant, co-solvent (alcohol), polymer and salt. Salt are used to create proper salinity gradient for the solution to reach to a favorable phase behavior condition, this is to achieve optimum solubilization values.

The low molecular weight alcohol is needed to design a gel-free formulation and to improve polymer-surfactant solution compatibility (Schramm 2000; Austad 1994). In this approach (called micellar-surfactant flooding) the flood is designed to form a thermodynamically stable microemulsion phase between the oil and displacing fluid (water). The development of microemulsion phase requires optimum condition, where equal solubilization of oil and ware into the middle phase. To achieve this optimum condition proper salinity should be maintained ahead, within, and behind the main chemical slug. Negative salinity gradient should be imposed by preconditioning the reservoir. The negative salinity gradient is established by pre-flushing the reservoir with monovalent cation to remove divalent cations and have better control on the salinity. The salinity gradient is designed to have high salinity (over optimum) ahead of the slug, optimum salinity in the slug and lower salinity (under optimum) behind the main slug. As explained in previous section the optimum salinity for the oil-aqueous-chemical solution is identified using salinity screening test. The phase behavior achieved is a function of the chemical composition, salinity, hardness, temperature and oil. Any change in one of these parameters can cause shift in the phase behavior of the system. This shift can cause the system to be in an over optimum mode and cause surfactant losses due to phase trapping in the oil. Three phase fluid flow regime resulted from this flooding type: aqueous, microemulsion, and oil. From reservoir engineering point of view it is very difficult to handle flow of three liquid phases in porous medium. Controlling reservoir conditions to guaranty optimum parameter for effective solubilization is extremely challenging task especially in field scale operation.

When using micellar-polymer flooding several challenges results in problems during injection

Preflushes to remove excessive salinity and divalent cations have been ineffective on the field scale application (Murtada and Marx 1982; Hamaker and Franzier 1978). Researchers are working on improving the chemical EOR technology by (Schramm 2000):

- Simplifying the flooding process.

- Improving the efficiency of the surfactants.
- Developing new chemicals.
- Reducing the cost and operation.

Use of amphoteric surfactants in chemical EOR

Stournas (1984) prepared several amphoteric surfactants and conducted an experimental work to evaluate their solubility characteristics at high salinity and high hardness brines. He also, studied the interfacial properties of these surfactants at low concentrations ranging from 0.005 to 1 % prepared in high salinity brines and find that IFT can reach to ultra-low values of 10^{-3} and 10^{-4} mN/m. He examined the chemical and thermal stability of the surfactant at high salinity brine of 20% (with relative cation concentration of at molar ration of: Na^{+} :Ca^{2+} : Mg^{2+} = 10 : 2 :1) and under temperature of 103^{o}c for one month and did not find any change in surfactant concentration or IFT values. Recovery experiments were conducted using sand pack columns of diameter and length of 1.5 cm and 1 m, respectively. The crushed sandstone (4-325 mesh) gives porosity of 35% and brine permeability of 3 darcies. Oil recovery values of 30 to 40% of residual oil were found using amphoteric surfactants.

Kalpakci and Chan (1985) proposed the use of 0.001 to 5 wt.% of amphoteric surfactant with polymer with high injection volume (more than 0.5 PV) to recover residual oil after water flooding. They propose to use amphoteric surfactant with polymer prepared in seawater. In their study the conducted core flood experiment using Berea sandstone cores and found that their proposed method recovered 18.9%.

Wang et al. (2008) synthesized a series of amphoteric surfactants by adjusting the hydrophobic group. These surfactants were evaluated for their IFT and found to reach ultra-low values of 10^{-3} to 10^{-4} mN/m at concentration ranges of 10 to 3,000 ppm (wt). When tested in high salinity brine (153,000 ppm) and hardness of 1,500 ppm the surfactant solution maintained ultra-low IFT values with Daqing field crude. They evaluate the oil recovery by conducting core flooding experiment using SP flood with amphoteric surfactant and found that it can achieve higher recovery efficiency than ASP

using anionic surfactant. The recovery values of 70% OOIP or higher on SP flood was used with lower surfactant concentrations when compared to surfactant used ASP. They suggest that using this type of surfactant can improve the economics of chemical flooding since low concentration of surfactant is needed. They conducted a micro-visual oil displacement test and found that this type can change the wettability and increase the recovery value.

Berger and Berger (2009) found that the degree of unsaturation and the distribution of carbon chain length in the lipophilic base are of extreme importance to lower IFT for wide range of oil and brines. They claim that relatively small pore volume slug of mixture of amphoteric surfactants is required to effectively recover oil. They design the amphoteric surfactant to have low IFT values over a wide range of surfactant concentrations, compare to others that show low IFT values in limited surfactant concentrations.

Wang et al. (2010) put forward conditions for surfactants to attain ultra-low IFT at low concentrations. They suggested that using these conditions will help in development in surfactants that fit oil and brine requirement for the reservoir. The conditions are as follows: 1) the attraction between hydrophobic bases, hydrophilic bases, crude oil molecules and water molecules must be equal, which will cause the surfactant molecules to mobilize at the oil-water interface. 2) the effective area occupied by the hydrophobic base and the hydrophilic base at the oil-water interface should be about equal. This will guarantee the surfactant will form a tight film and no other molecules will be at the interface to increase the IFT. The authors' claim that satisfying these two conditions; surfactant solutions do not require salt, alkali, co-surfactant, and co-surfactant to attain ultra-low IFT values. Taking in mined the two conditions discussed above the authors designed six types of surfactants and evaluated them and found that they achieve the low IFT values required. In their work they evaluated the performance of these surfactants with three different crudes at temperatures of 45, 80 and 98^{o}C, and brines with salinities up to 229,000 ppm, and divalent ions 21,000 ppm . These surfactants were able to attain

IFT values less than $9X10^{-3}$ mN/m. Regarding recovery experiments they found values similar to their finding in 2008 study (Wang et al. 2008).

Objectives

The objectives of this work are:

- Evaluate new type of amphoteric surfactant for chemical flooding in sandstone and carbonate reservoirs.
- Study the effect of surfactant type, pore volume injected, type and concentration of polymer on the recovery enhancement in Berea sandstone and dolomite cores.
- Assess core injectivity decline caused by conventional and new alkalis injected in high salinity/high hardness formation brines.
- Evaluate core injectivity decline caused by polymer and surfactant retention using sandstone and carbonate cores.
- Use CT scan to characterize fluid flow inside the core during chemical flooding.

CHAPTER II
ALKALI IN CHEMICAL EOR*

Summary

Using inorganic alkali in alkaline/surfactant/polymer (ASP) flooding resulted in scale precipitation when multivalent cations exist in mixing and formation brine in some extended field studies. This issue can be critical in the un-swept zones, which are the major target for EOR process, where formation brines can have high concentrations of Ca^{2+} and Mg^{2+}. Any precipitation can result in plugging the pores in the target zone and result in loss of injectivity.

Several alkalis were evaluated to assess their potential to form scale in high salinity formation brines and seawater as mixing brine at high temperature applications. Four alkalis are evaluated; three inorganic NaOH, Na_2CO_3, sodium metaborate and one organic alkali.

Eliminating the need to soften the mixing brine will result in expanding the ASP application to more challenging applications and will reduce the softening cost for the mixing water. Preventing precipitation of scale when chemical slug enters the unswept zones will result in improving the efficiency of the ASP flood, reduces chemical consumption and prevent scale precipitation that can cause formation damage and operational problems in the producers.

*Reprinted with permission from "Minimizing Scale Precipitation in Carbonate Cores Caused by Alkalis in ASP Flooding in High Salinity/High Temperature Applications" by Bataweel, M.A., and Nasr-El-Din, H.A.2011, Paper SPE 141451 presented at International Symposium on Oilfield Chemistry.

Introduction

The scaling problem caused by ASP injection in the Daqing pilot site was discussed by Wang et al. (2004). In the pilot test production wells in Daqing, scale was found in the wellbores and pumps, which resulted in a shutdown period of 114 days to replace and check the affected pumps, after that frequent pump malfunctions occurred from scale accumulations. Serious scale problems were found on the ground collecting and gathering system such as ground pipe walls, oil transferring stations, multipurpose stations, oil/water separating system, produced water disposal system, valves, pump heads and flow-meters. The authors studied the scaling mechanism and found that the injection of high-pH fluid will interact with formation brine and cause HCO_3^- to produce CO_3^{2-}. This will precipitate carbonate and hydroxide (Wang et al. 2004).

Strong alkalis have high reactivity with different reservoir rock minerals and hard ions in the formation and injected brines. Some researchers suggested using different alkalis to overcome these complications. Recently, two alkalis were suggested, sodium metaborate and organic alkali (Flateen et al. 2008, Berger and Lee. 2006). Flateen et al. (2008) proposed sodium metaborate as a weaker alkali to avoid problems caused by strong alkalis in the ASP floods. The sodium metaborate showed a promising results and more tolerance to hard ions. Berger and Lee (2006) suggested using organic alkalis to replace inorganic alkalis in ASP process. They found that organic alkali can be mixed with similar chemicals used to formulate ASP with more tolerance for high-salinity and high-divalent cations concentrations. In our work we will investigate using these alkalis to reduce the negative impacts caused by interactions by strong alkalis.

Berger and Lee (2006) compared an organic alkali with an inorganic alkali, sodium carbonate, and studied their effect on scale precipitation, pH, IFT, adsorption of on calcite and the viscosity of the ASP slug. They found that the organic alkali showed better tolerance to brines that have high TDS and hard ions and no precipitation was found when using organic alkali. No reduction in pH values was noticed when organic alkali was used compare to reduction in pH values when Na_2CO_3 was used with unsoftened brine. No noticeable difference in the IFT values using organic alkali with

unsoftened brine compare to Na_2CO_3 prepared in softened brine. When comparing the effect of the two alkalis on ASP slug viscosity using softened water and formation brine; reduction in viscosity from 14.6 to 13.8 cP when organic alkali was used, compared to reduction from 9.3 to 2.7 cP with Na_2CO_3 were mixed with softened or unsoftened brine, respectively. A summary of their experimental results of their work is given in **Table 2**. Detailed discussion of role of alkalis in chemical EOR can be found in Chapter I.

Table 2— Effect of brine on chemical slug properties.*

Alkali	**Organic Alkali**		**Na_2CO_3**	
Brine	**Softened**	**Un-softened**	**Softened**	**Un-softened**
pH	10.6	10.7	12.3	11.6
IFT,	-	0.005	0.006	-
Viscosity, cP	14.6	13.8	9.3	2.7

*Berger & Lee (2006)

Alkalis tested

Total of four alkalis were used in this paper; sodium hydroxide, sodium carbonate, sodium metaborate, and organic alkali. Two of the mostly used alkalis in enhanced oil recovery are sodium hydroxide and sodium carbonate. Green and Willhite (1998) give the dissociation equation of NaOH and Na_2CO_3 in aqueous phase. Dissociation of strong alkali in water (NaOH)

$$NaOH \rightarrow Na^+ + OH^- \text{……..……..(10)}$$

Dissociation of sodium carbonate (Na_2CO_3) in water is given by the following reaction:

$$Na_2CO_3 \rightarrow 2Na^+ + CO_3^{2+} \text{……...…(11)}$$

This is followed by the hydrolysis reaction:

$$CO_3^{2-} + H_2O \leftrightarrow HCO^- + OH^- \quad \text{.....(12)}$$

Sodium Metaborate has been introduced recently as an alternative of conventional alkalis (Flaaten et al. 2008-a, Flaaten et al. 2008-b, Zhang et al. 2008, Hirasaki 2008). Sodium Metaborate sequester divalent ions Ca^{2+} and Mg^{2+} by complex formation, and can tolerate precipitation for divalent ions up to 6,000 ppm (Flaaten et al. 2008-a, Flaaten et al. 2008-b, Zhang et al. 2008). Multivalent ions such as Ca^{2+} and Mg^{2+} could be complexed with borate ions, monovalent electrolytes, and divalent ions sequestrate to increase their effective solubility in an aqueous phase. Flaaten et al. (2008) and Zhang et al. (2008) observed that the borate ions at first form an amorphous precipitate with calcium and magnesium that dissolves as the divalent ion concentration increases. Like all other alkali metal borates, monomeric borate ion ($B(OH)^{4-}$) is strongly hydrolyzed to form polymeric borate ions when its concentration and solution pH change (Flaaten et al. 2008-a, Flaaten et al. 2008-b, Zhang et al. 2008).

Using conventional inorganic alkalis can cause some operational problems when using it for ASP process. Mixing water for the chemical slug should be softened to prevent the precipitation of hard ions when get in contact with alkalis like sodium hydroxide and sodium carbonate. Strong inorganic alkalis caused corrosion and scale problems during ASP flooding at Daqing. Inorganic alkalis will affect the polymer performance and more polymer concentration is required to achieve the desired viscosity.

An alternative organic alkali was suggested to overcome the mentioned problems and provide the positive effects of including the alkali in the ASP process. This organic alkali is non-toxic, biodegradable and can be used for environmentally sensitive areas. The organic alkali in this study is derived from sodium salts of polyaspartic acid (Berger and Lee. 2006, Berger and Lee. 2008). **Fig. 25** shows the structure of the sodium salt of polyaspartic acid. The chelating and solid dispersion properties of this alkali allow it to be used in water containing divalent ions like; Ca^{2+}, Mg^{2+}, Fe^{2+}, Sr^{2+} and Ba^{2+} (Berger and Lee. 2008). Less than 1:1 molar-to-molar ratio of the polyaspartic salt to the divalent

cations is required to provide chelation and solid dispersing properties needed (Berger and Lee. 2008).

In this study we will compare the two of the most used alkalis in EOR application (sodium hydroxide and sodium carbonate) and two of the newly proposed: sodium metaborate and organic alkali.

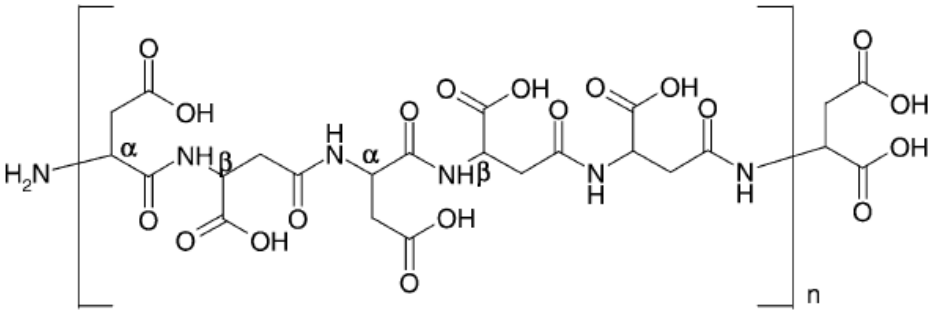

Fig. 25—Organic alkali (polyaspartic acid) structure (Berger and Lee 2008).

Experimental Studies

Materials

Several alkalis were used to study their interaction with brines containing hard water for ASP slug preparation. The water used in all experiment was obtained from a water system with resistivity greater than 18 MΩ.cm at 25^{o}C. Sodium chloride, calcium chloride, magnesium chloride, sodium bicarbonate, sodium carbonate and sodium sulfate used to prepare different brine were an analytical grade. Alkalis used in this study are sodium hydroxide, sodium carbonate, sodium metaborate and Organic alkali. Core samples used in this study were carbonate.

Fluid compatibility in brines containing divalent cations

Compatibility experiments were conducted to evaluate the fluid-fluid interaction between injection water used to prepare chemical slugs and the water in the formation. In this study the seawater was used for secondary recovery and interaction between

seawater and different alkalis were evaluated. The second scenario evaluated in this paper is the interaction between alkalis and formation brine in upswept zones or areas of the field subjected to re-injection of produced formation brine. The interaction with two formation water was evaluated in this study. Seawater and formation brine samples were prepared and alkalis were added at different weight percentages. The samples were mixed in glass tubes and was heated to 90^{o}C and kept for 5 days. Samples were checked twice a day for any leak of evaporation. The compatibility test was visual and presence of any solid like material was en evidence of incompatibility. At end of experiment samples were removed and were photographed.

Coreflood studies

A coreflood apparatus was designed and built to simulate fluid flow in porous media in the reservoir. The schematic diagram of the coreflood apparatus is shown in **Fig. 26**. Positive displacement pump was used to deliver fluids at constant flow rates at variable speeds up to 200 cm^3/min and pressure up to 2,000 psi. Accumulators with floating pistons rated up to 3,000 psi. and 300^{o}F were used to store fluids. The coreholder can accommodate a core plug with diameter of 1.5 inches and length up to 6 inches. Pressure transducers were used to measure the pressure drop across the core. Back pressure regulator was used to control the flowing pressure downstream of the core. A second back pressure regulator was used control the confining pressure on the core plug. A convection oven was used to heat up the core holder and was controlled using temperature controller and thermocouples. Data acquisition system was used to collect data from the pressure transducer. Fraction collector was connected to the outlet to collect effluent from the core during the flooding experiment.

Dry core samples were weighed then were vacuum saturated with brine. Saturation brine and alkali solution was filled in two separate transfer vessels with floating pistons. The saturated core samples were flooded with several pore volumes with the same brine to make sure it is saturated. Saturated samples were weighed again and difference in weight was used to calculate the core pore volume. After that samples were stored in

brine until the time of the experiment. Core sample was loaded to the core-holder and put inside oven. The confining pressure was applied using hand pump and pore pressure was increased in the core by injecting the brine from inlet and outlet side of the core. The confining pressure and pore pressure were 1,000 and 500 psi, respectively. After that the brine was injected to the core at a constant low flow rate of 0.5 cm^3/min at room temperature. Pressure drop across the core sample was recorded when pressure stabilize to calculate initial permeability. After that the temperature in the oven was set to 90^oC and was left the heat-up minimum for 2 hours while continuing fluid injection this is done to expedite the heating process. The pressure drop at the core was measured at the high temperature. After that 2 pore volume of alkali solution was injected into the core at the same rate. The effluent from the sample was collected in test tubes every 5 cm^3 for further analysis.

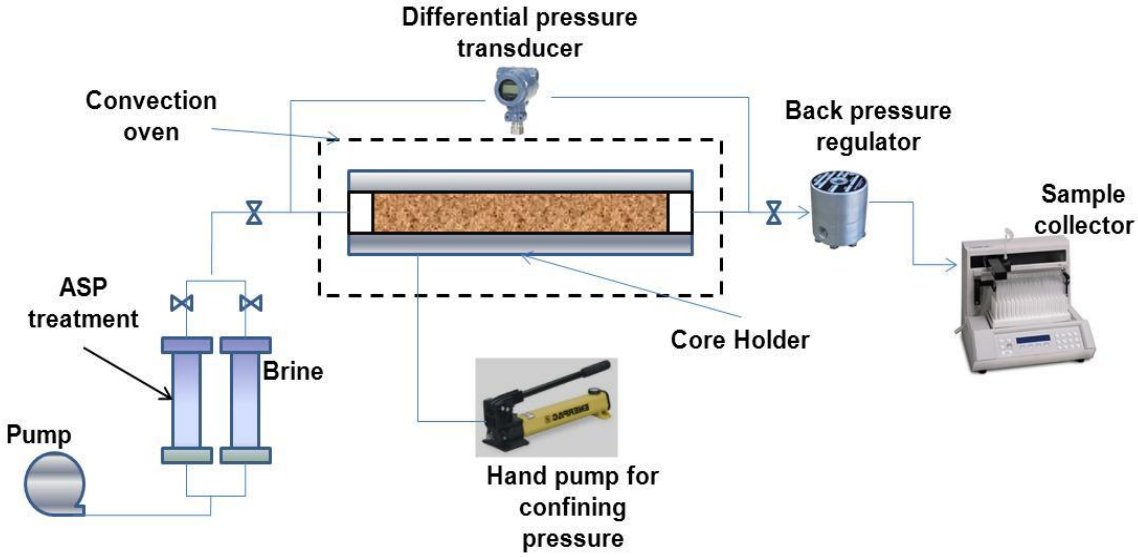

Fig. 26—Schematic for core flood set-up.

Core flood experiments were conducted to study reduction in permeability resulted from alkali precipitation and interaction between alkali and rock. Core-flood samples

used in this study were carbonate. Two flooding scenarios were investigated in these experiments. The first series of experiments were to study alkali interaction with reservoir pre-flushed with seawater during secondary recovery. Core samples in this case were saturated with seawater and then flooded with chemical slug. The slug containing alkali was prepared in soften seawater if alkali shows precipitation in compatibility test, otherwise, it was prepared in seawater. Four alkalis used in these experiments were sodium carbonate, sodium hydroxide, sodium metaborate and organic alkali.

Second series of experiments were designed to simulate the injection of chemical slug in zone pre-flushed with produced water (formation brine) or upswept zones during secondary recovery. Chemical slug will mix with formation brine and can cause precipitation of divalent ion in pores and result in plugging the formation. This is very important in carbonate reservoir with high calcium and magnesium ions in the brine. In this work calcium and magnesium levels in the formation brine are around 30,000 and 4,000 mg/L, respectively.

Result and Discussion

Compatibility studies

The objective of this study is to evaluate the ability of different alkaline solutions to tolerate divalent ions in mixing and formation brines. The first series of tests were done to evaluate using seawater as mixing water for the chemical slug. The chemical composition of seawater is given in **Table 3**.

Table 3— Formation brine used compatibility test.

	Concentration, mg/L	
Ions	**High Salinity Formation Brine**	**Seawater**
Na^{+}	51,187	16,877
Ca^{2+}	29,760	664
Mg^{2+}	4,264	2,279
Ba^{2+}	10	0
Sr^{2+}	1,035	0
HCO_3^{-}	351	193
Cl^{-}	143,285	31,107
SO_4^{2-}	108	3,560
CO_3^{-}	0	0
TDS	230,000	54,680

Three concentrations of each alkali were prepared in seawater (0.1 , 0.5 and 1.0 wt%) and heated to 90^{o}C for 5 days. The samples were shaken twice a day during the period of the experiment. As can be seen in **Fig. 27**, all inorganic alkalis showed precipitation when mixed with seawater, except the organic alkali. Organic alkali was compatible with seawater in all three concentrations. During visual inspection of the sample it was noticed that the precipitates from sodium metaborate are more flocculent when compared to sodium hydroxide and sodium carbonate.

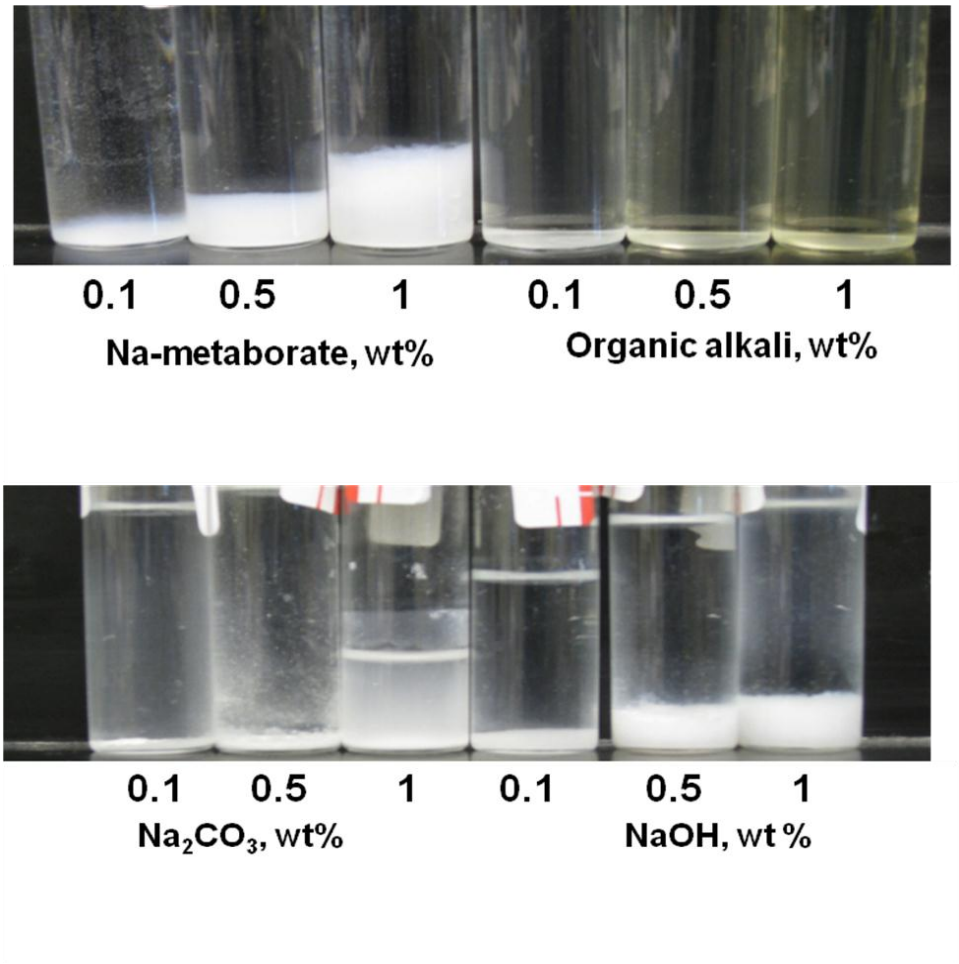

Fig. 27—Precipitation of alkalis in seawater.

Fig. 28 shows the pH values for alkalis at soften seawater at different concentrations (0.1, 0.5, and 1.0 wt%). When prepared in seawater there was a noticeable decrease in the pH values of NaOH and Na_2CO_3 compared to less reduction in pH for sodium metaborate and organic alkali (**Fig. 29**). The decrease in pH can be explained by the precipitation of hard ions (Ca^{2+} and Mg^{2+}). The same experiment was repeated using high salinity formation brine (**Table 3**) for Na_2CO_3, sodium metaborate and organic alkali. This brine has high concentration of Ca^{2+} more than 13,000 mg/L.

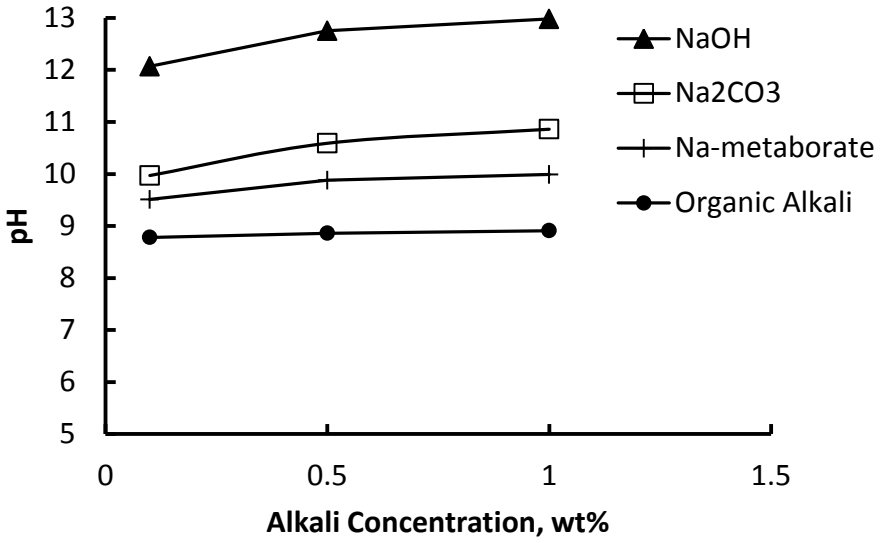

Fig. 28—pH values of alkalis mixed in softened seawater.

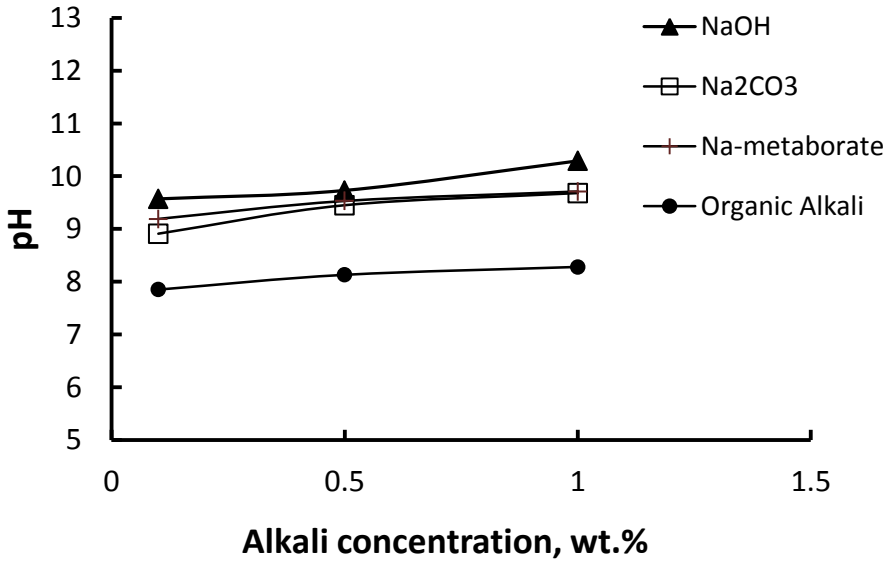

Fig. 29—Reduction in pH values when mixing alkalis in un-softened seawater. pH of seawater is 7.71.

Fig. 30 shows the pH values of the brine without alkali and with alkalis. A reduction in pH values even below the formation brine was noticed when sodium carbonate was added. This can be explained be excessive precipitation and loss of alkalinity. When sodium metaborate and organic alkali were added and increase in pH values was noticed with much improvement in values shown given by the sodium metaborate.

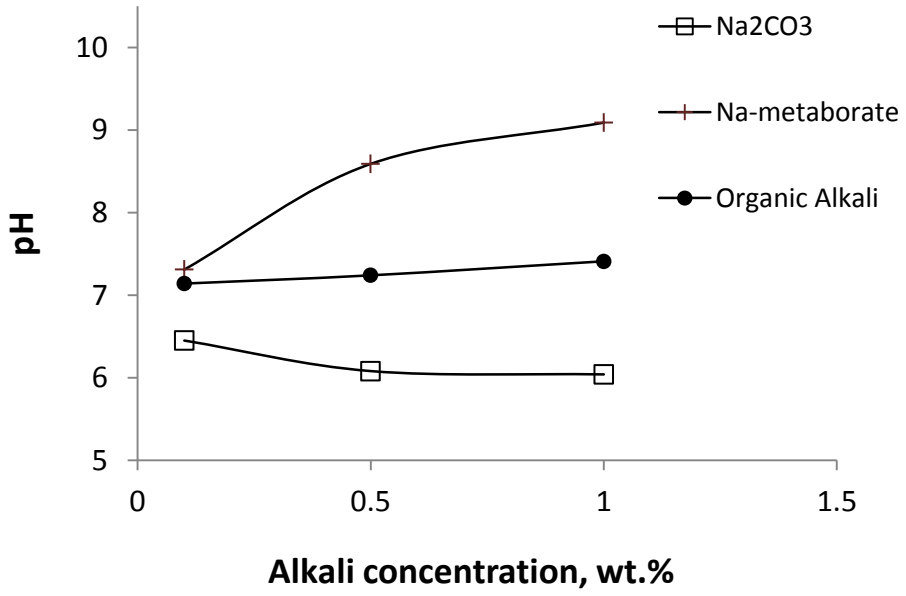

Fig. 30—Alkali in low salinity formation brine. pH of formation brine is 6.52.

Core flooding studies

Total of seven core flood experiments were conducted to study the impact of interaction between alkali solution and saturation brine in the core samples. **Table 4** gives the basic information of core samples used in this study. These experiments were conducted to study two flooding scenarios.

Table 4— Core sample data used to study the impact of interaction between alkali solution and saturation brine in core sample.

Sample #	Length, cm	Diameter, cm	Pore volume, cm^3	Porosity, %	Permeability, md	Notes	Brine
1	9.69	3.73	32.77	30.88	101	Organic Alkali	Seawater
2	10.07	3.73	32.68	29.64	141	Na-metaborate	
3	10.31	3.73	35.94	31.83	150	Na_2CO_3	
5	9.77	3.75	32.57	30.25	130	NaOH	
4-d	11.43	3.81	22.97	17.62	143	Na_2CO_3	High salinity formation brine
5-d	12.66	3.81	24.95	17.28	102	Organic Alkali	
6-d	13.02	3.81	25.35	17.08	54	Na-metaborate	

Case-1 Cores Preflushed with Seawater

Four core flood experiments were conducted in this series to evaluate the interaction of seawater with alkali solutions. The samples were saturated with seawater and, alkali solution was injected to the core. In the first experiment sodium hydroxide was used and effluent was collected from the sample. The sodium hydroxide was prepared in softened seawater since precipitation was noticed when mixed with seawater during the compatibility experiments. After injecting sodium hydroxide and aging it for 8 hours; permeability of the core was measured again and 21.3 % reduction was noticed. Both sodium carbonate and sodium metaborate were prepared in soften seawater and showed no reduction in permeability after been injected to core samples. The organic alkali was prepared in seawater without softening since no precipitation was noticed during the compatibility study. Also, no reduction in permeability was noticed. **Fig. 31** shows core permeability before and after alkali injection. Injection of sodium hydroxide caused reduction in core permeability. When comparing the permeability result between sodium hydroxide and sodium carbonate our finding is in agreement with Cheng (1986) where sodium hydroxide is more damaging. Although both sodium hydroxide and sodium carbonate showed precipitation during the compatibility test, however sodium carbonate did not show damage. This can be explained in three ways: first solubility of magnesium

hydroxide is less than calcium hydroxide and more magnesium ions exist in seawater this increase the possibility of more precipitation when hydroxide mix with seawater. Secondly, the sodium carbonate will precipitate calcium carbonate from seawater but less quantities of calcium exist in seawater and the effect is further reduced by dilution of the calcium ions when softened seawater was injected. Third, morphology and nature of the precipitated salts caused by hydroxide and carbonate are different. In case of hydroxide the precipitates are hydrated, flocculent and damaging compared to granular less damaging carbonate precipitate (Cheng, 1986).

Fig. 32 shows initial and final permeabilites for cores injected with sodium metaborate and organic alkali with no reduction in permeability. To best to our knowledge this is the first time these two alkalis are tested for permeability damage experiments. The current findings are encouraging for using ASP with seawater. When organic alkali was injected effluent were collected to examine if any precipitation was noticed.

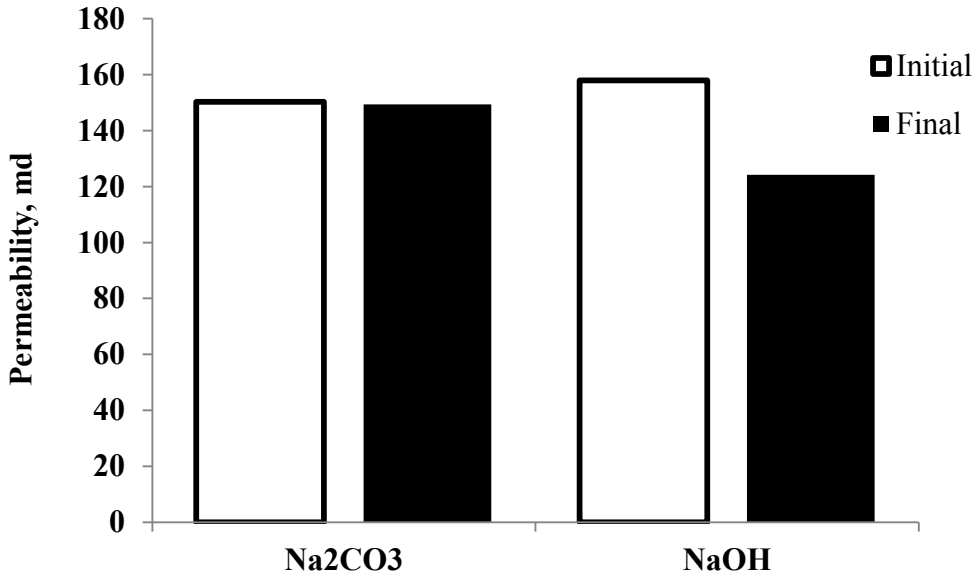

Fig. 31—Reduction in permeability caused by sodium carbonate and sodium hydroxide injection in seawater.

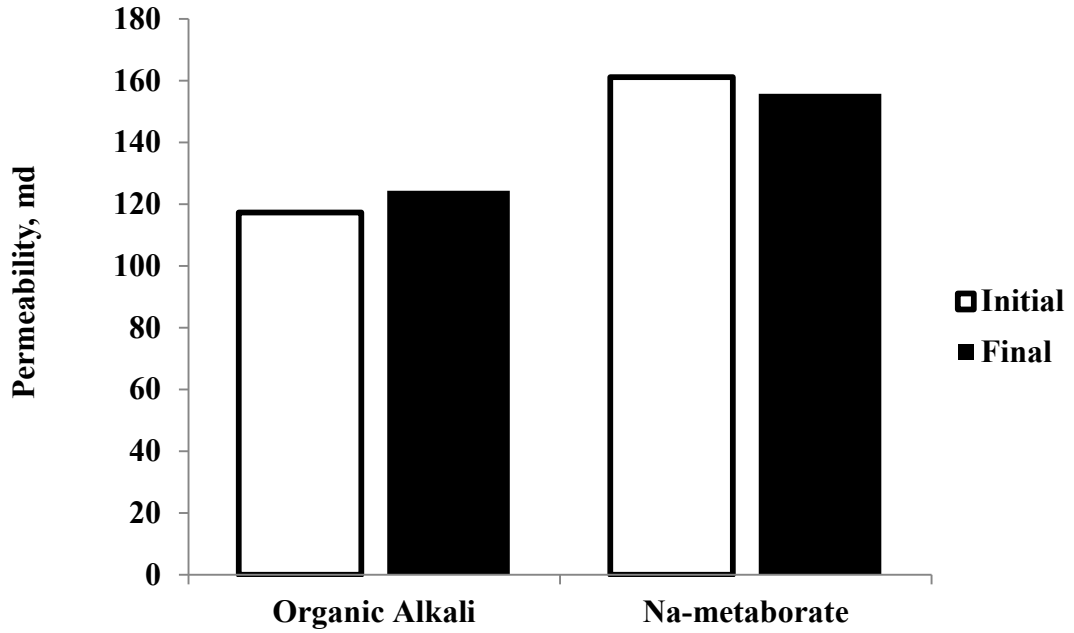

Fig. 32—Reduction in permeability caused by organic alkali and sodium metaborate injection in seawater.

Fig 33 shows the magnesium and calcium concentration profile during the core flood experiment with organic alkali and as can be seen no change in hard ion concentration, which is an indication of no precipitation.

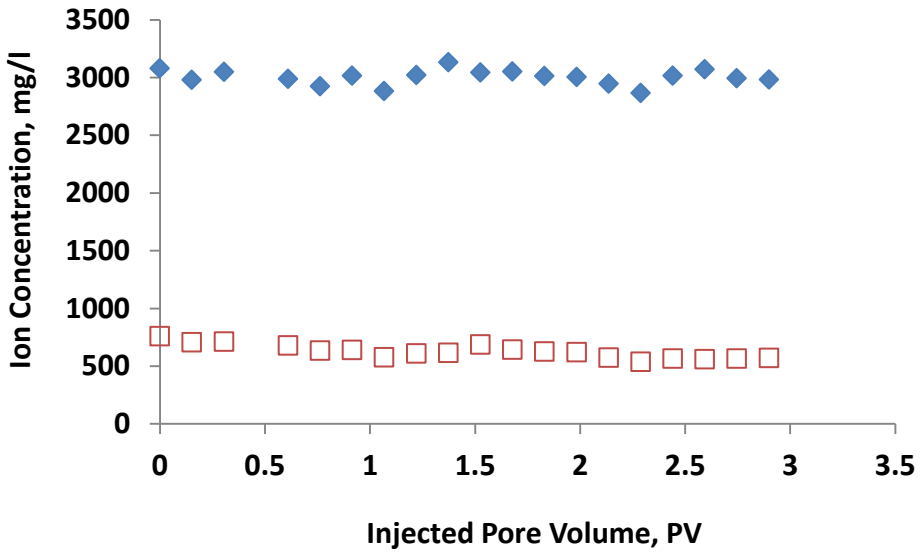

Fig. 33—No precipitation of calcium or magnesium ions during core flooding experiment with the organic alkali.

Case-2 Cores Pre-flushed with Formation Brine

Three core flood experiments were conducted to evaluate the effect of mixing of formation brine with high levels of hard ions (e.g. Ca^{2+} = 29,760 mg/L) with alkali solutions (Na_2CO_3, Na-metaborate, and organic alkali). All alkalis where mixed in softened seawater at alkali concentration of 1 wt%, All alkalis showed reduction in permeability with maximum reduction with Na_2CO_3. The reduction is caused by $CaCO_3$ precipitation due to large quantities of Ca^{2+} available in the formation brine. **Fig. 34** shows a total reduction in permeability of 39% when Na_2CO_3 was used. No precipitate was collected from the effluent during the core flood experiment. This is an indication that carbonate precipitate was entrapped in core.

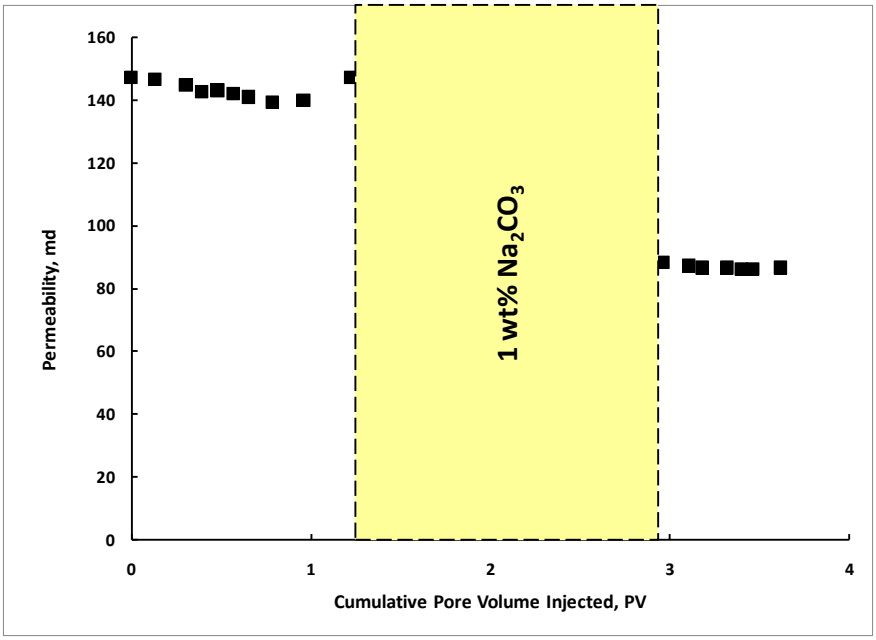

Fig. 34—Reduction in permeability caused by sodium carbonate (1wt%) injection in high salinity formation brine.

Fig. 35 presents the core flood experiment conduct with sodium metaborate. No previous work was represented earlier showing the impact of sodium metaborate interaction with formation brine with this high level of hard ion concentrations. The total reduction in permeability caused by injecting sodium metaborate is 26%.

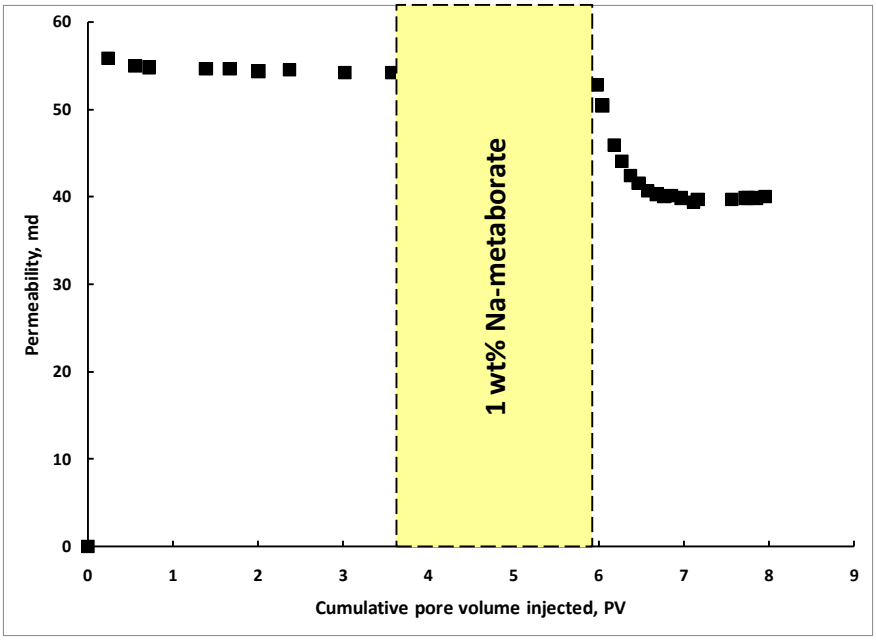

Fig. 35—Reduction in permeability caused by sodium metaborate (1 wt%) alkali injection in high salinity formation brine.

Fig. 36 shows 20% permeability reduction caused by organic alkali at core flood experiment. As can be seen from above discussion sodium metaborate and organic alkali are having the least damage and can be used for brines with high levels of divalent cations.

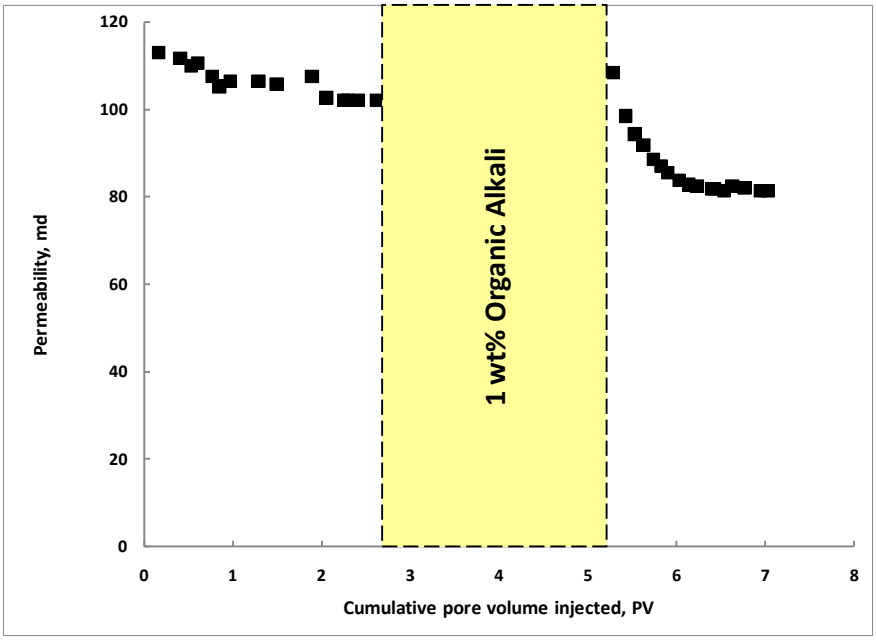

Fig. 36—Reduction in permeability caused by organic alkali (1 wt%) injection in high salinity formation brine.

Conclusions

The impact of four alkalis on injectivity was examined in this paper at two chemical injection scenarios. Based on the results obtained in this study the following conclusions can be drawn:

1. Na_2CO_3, NaOH, and Na-metaborate show precipitation when prepared in seawater and formation brines.
2. Loss in alkalinity was noticed when Na_2CO_3 and NaOH solutions were prepared in seawater and formation brine. Minimum loss was noticed with organic alkali and Na-metaborate.
3. Precipitate for Na_2CO_3 and NaOH are crystalline. For Na-metaborate precipitation was amorphous.
4. Organic alkali is compatible with seawater and formation brine.

5. Sodium carbonate, sodium metaborate and organic alkali did not cause reduction in permeability for carbonate cores saturated with seawater.
6. Organic alkali and sodium metaborate had less permeability reduction when compared to sodium carbonate at cores saturated with formation brine

CHAPTER III
INTERFACIAL TENSION ANALYSIS

Summary

An experimental study was conducted to examine the dynamic interfacial tension in crude oil-alkali-surfactant systems using amphoteric surfactants. In this study 5 amphoteric were screened and extensive experimental study was conducted on the most effective surfactant in reducing minimum and equilibrium IFT values. The surfactant was tested on wide range of parameters. In this study the effect of surfactant concentration, mixing of injection solution with high salinity/high hardness formation brine, effect of two newly introduced alkalis and their concentrations, and the effect of two types of polymers HPAM and AMPS and their concentrations on the generation of transient dynamic minimum IFT.

Mixing of the seawater with high salinity/high hardness formation brine to prepare surfactant solution improved the interfacial behavior of the solution and resulted in lower IFT values with lowest value notice at 75% of seawater with 25% formation brine water.

Addition of of organic alkali or sodium metaborate has several effects on the IFT values it result in lower values, delayed the time for the lower value to happen and was having a continues reduction of the IFT within the time of the experiments.

The experimental results obtained from this study shows that polymer type and concentration causes different effect on the time needed for the minimum IFT to occur. Increasing the concentration of the HPAM caused both delay in the occurrence of the minimum IFT, increased the minimum IFT value and decrease in the equilibrium IFT values. On the other hand increasing the concentration of the AMPS polymer did not cause any change in time the minimum IFT happen, but causes a small increase in the minimum IFT values, Also, no big change was noticed in the equilibrium IFT values when compared to the case when HPAM polymer was used.

Introduction

Reduction of the IFT between the injected fluid and crude oil is one of the main objectives of the chemical flooding processes for this reason alkali and surfactant are added to solution. A three order of magnitude reduction in IFT is required to have an efficient and successful recovery process. In some of the chemical processes alkali and surfactant are added together to have an improvement in the chemical solution performance.

When IFT measurements are conducted they go in several steps which explain the dynamic IFT behavior (**Fig. 37**). The first step is for the diffusion-controlled adsorption from the bulk of the surfactant solution to the oil-water interface. The diffusion rate is affected by the surfactant concentration, salt concentration and aqueous solution viscosity (Taylor and Nasr-El-Din 1996). The diffusion rate, also, affects the time to reach the minimum IFT and the time to reach equilibrium (Aoudia et al. 2010; Ferri and Stebe, 2000). Zhao et al. (2006) showed that the time to reach minimum IFT is a function of surfactant concentration. They reported a decrease in T_{min} with increasing surfactant concentration, this attributed to the change in surfactant adsorption velocity to the oil-water interface. The second factor that affects the adsorption of surfactant to the interface is the salinity and hardness of solution. Increasing the salt concentration in the chemical solution reduces the surfactant solubility in the aqueous phase this enhances the adsorption of surfactant to the interface and causes an accumulation of surfactant molecules and it oil-water contact (Nasr-El-Din and Taylor 1993). Third factor is the viscosity of the aqueous phase, increasing the viscosity of aqueous phase increases the mass transfer resistance that will delay the diffusion process and increase the time to reach to the minimum IFT value (Taylor and Nasr-El-Din 1996). The adsorption to the interface and diffusion into the bulk aqueous or oil of surface-active species (synthetic or in-situ generated by alkali) gives the rise to the dynamic IFT behavior (Nasr-El-Din and Taylor 1993). The objective of the study is to screen different amphoteric surfactants, study effect of surfactant concentration, polymer type and concentration, and alkali type on dynamic IFT behavior.

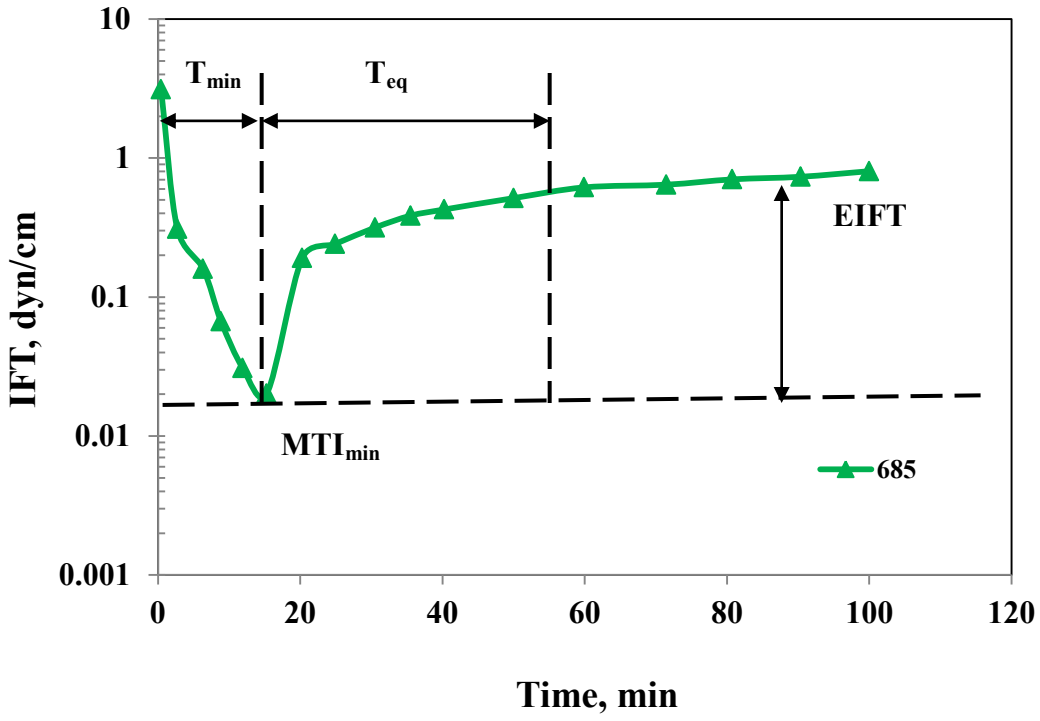

Fig. 37—Dynamic behavior during IFT measurement.

Experimental Studies

Materials

Crude oil was obtained as a well-head sample. The crude oil was first filtered using Berea sandstone cores. The filtered crude was centrifuged to remove any remaining water or solids from the oil. The crude oil density and viscosity were 0.825 g/cm^3 and 20.4 cP at room temperature.

The water used in all experiment was obtained from a water system with resistivity greater than 18 MΩ.cm at 25^{o}C. Sodium chloride, calcium chloride, magnesium chloride, sodium bicarbonate, sodium carbonate and sodium sulfate used to prepare different brine were an analytical grade.

Amphoteric surfactants used are Amphosol LB (Lauryalamidopropyl betaine), Petrostep CG-50 (cocamidopropyl betains), and Amphosol CS-50 (cocamidopropyl

hydroxysultain) were kindly supplied by Stepan Company and used as received. A SS series of amphoteric and GreenSurf series, which is an environmentally friendly surfactant design to lower adsorption behavior were kindly provided by Oil Chem. Technologies, Inc. (Sugar Land , TX) and used as received. Members of both above series have increasing molecular weights and patented. All these samples were screened and selected based on the minimum IFT values achieved between the surfactant solution prepared in seawater and the crude oil

Two kinds of polymers were used in this study, the first polymer (Flopaam 3630S) is HPAM with molecular weight of $18X10^6$ and degree of hydrolysis (DH) of 30%. The second chemical is copolymer of acrylamide and 2-acrylamido 2-methyl propane sulfonate (AMPS) called AN-125 with molecular weight and DH of $6X10^6$ and 20-30%, respectively. Both chemicals were provided by SNF Floerger (Cedex, France) in solid form. The chemicals were used as received.

Two newly proposed alkalis were used in this study. First alkali is organic alkali (OA-100) proposed as an environmentally friendly product to minimize water softening requirement to prepare chemical slug and reduce the potential of precipitation in reservoirs containing high concentrations of multivalent ions in it's formation brine. Sodium Metaborate has been introduced recently as an alternative of conventional alkalis (Flaaten et al. 2008-a, Flaaten et al. 2008-b, Zhang et al. 2008, Hirasaki 2008). Sodium Metaborate sequester divalent ions Ca^{2+} and Mg^{2+} by complex formation, and can tolerate precipitation for divalent ions up to 6,000 ppm (Flaaten et al. 2008-a, Flaaten et al. 2008-b, Zhang et al. 2008). More discussion about these two alkalis can be found in Chapter II.

Methodology

Spinning Drop Method

Dynamic IFT measurements were conducted using the spinning-drop tensiometer (University of Texas, Model 500) and procedure recommended by Cayias et al. (1975)(**Fig.38**). A capillary glass tube is filled with chemical solution to be tested. Oil

drop was transferred to the capillary tube containing chemical solutions using a syringe and Hamilton needle. The tube containing the chemical solutions and oil droplet is placed in to the cylindrical holder in the instrument. The glass tube is secured into the instrument using a threaded cup with o-ring seals to prevent the leak of air bubbles in to the tube. The tube was accelerated to a constant rotational speed and oil droplet shape was observed using an optical microscope. Micrometer attached to the microscope is used to measure the oil droplet width changes with time after introduced to the chemical solution. To assure accurate reading the ration between the droplet length and diameter was maintained greater than 4. In case of very low IFT values the drop stretched longer than the tube and can affect the reading, rotational speed was reduced to lower values so the oil drop shrink to readable size the new speed was recorded and included in IFT calculations. To calculate IFT the following expression is used:

$$\boldsymbol{\sigma = \frac{\Delta\rho\omega^2 r^3}{4}} \quad \text{.....(13)}$$

where σ interfacial tension

Δρ density difference between aqueous solution and the crude oil

ω rotational speed

r radius of the oil droplet

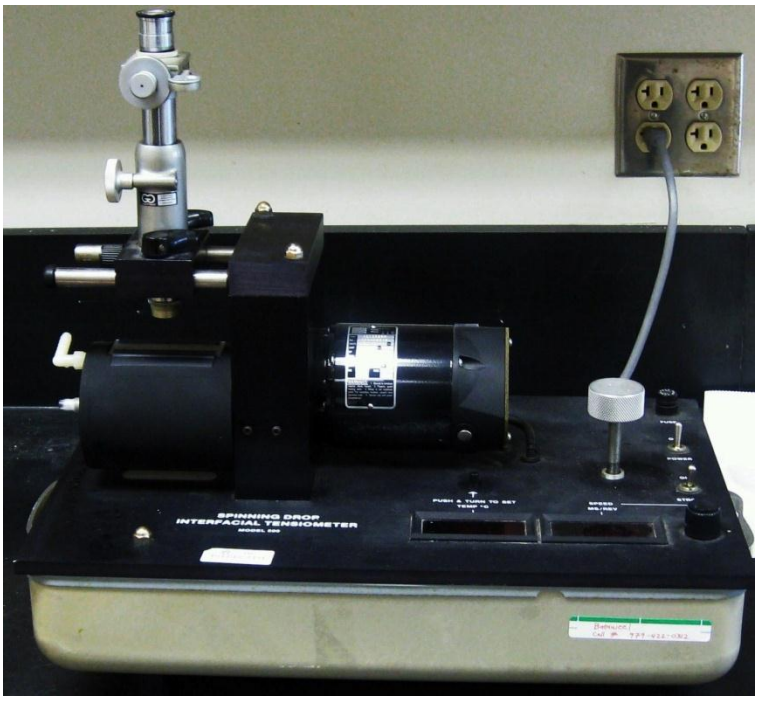

Fig. 38—Spinning-drop tensiometer (University of Texas Model-500).

Result and Discussion

Initial surfactant screening

Several amphoteric surfactants were received for investigation and were initially tested to evaluate it's interaction with crude oil to measure the IFT values generated. In this stage of the study several surfactants were tested at different concentrations ranging from 0.05 to 1 wt% prepared in seawater. The first surfactant tested was AMPHOSOL LB (Lauryalamidopropyl betaine). The lowest IFT achieved was 3.82 when 0.05 wt% surfactant was used the equilibrium IFT ranges between 5.33 and 5.70 dyn/min for surfactant concentrations ranging between 0.05 to 1 wt%. This surfactant did not show enough reduction in IFT values that can be attractive to be used in formulating chemical solution for chemical EOR application. **Fig. 39** shows the IFT values vs. time for

different surfactant concentrations. As seen in in Fig.1 there is no noticeable change in IFT values as the surfactant concentration was varied.

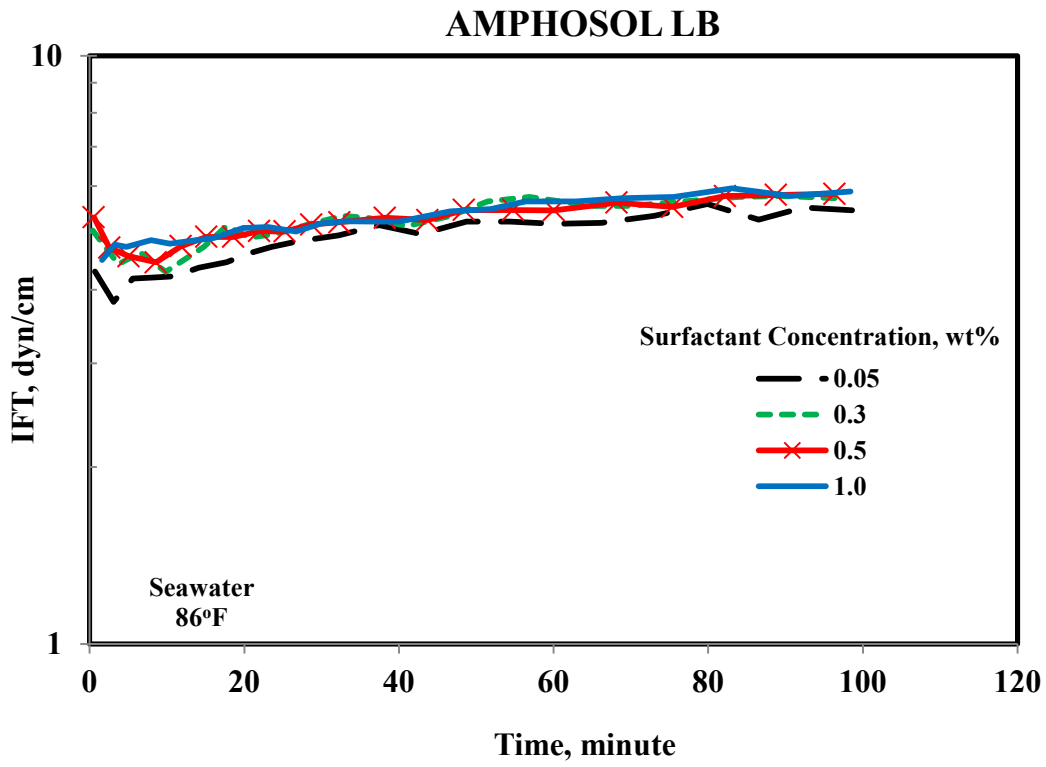

Fig. 39—Effect of Amphosol LB concentration on the IFT value of the surfactant solutions prepared in seawater.

The second surfactant tested was AMPHOSOL CS-50 (cocamidopropyl hydroxysultain). The lowest minimum and equilibrium IFT values achieved with this surfactant were 1.86 and 3.28 dyn/cm, respectively, at concentration of 1 wt%. **Fig. 40** presents the IFT values for this surfactant at different concentrations and the equilibrium IFT values ranged between 3.28 and 5.72 dyn/cm. A wider range of IFT values can be seen in this type of surfactant when surfactant concentration was varied. Still the IFT value is not low enough to increase the capillary number to improve recovery.

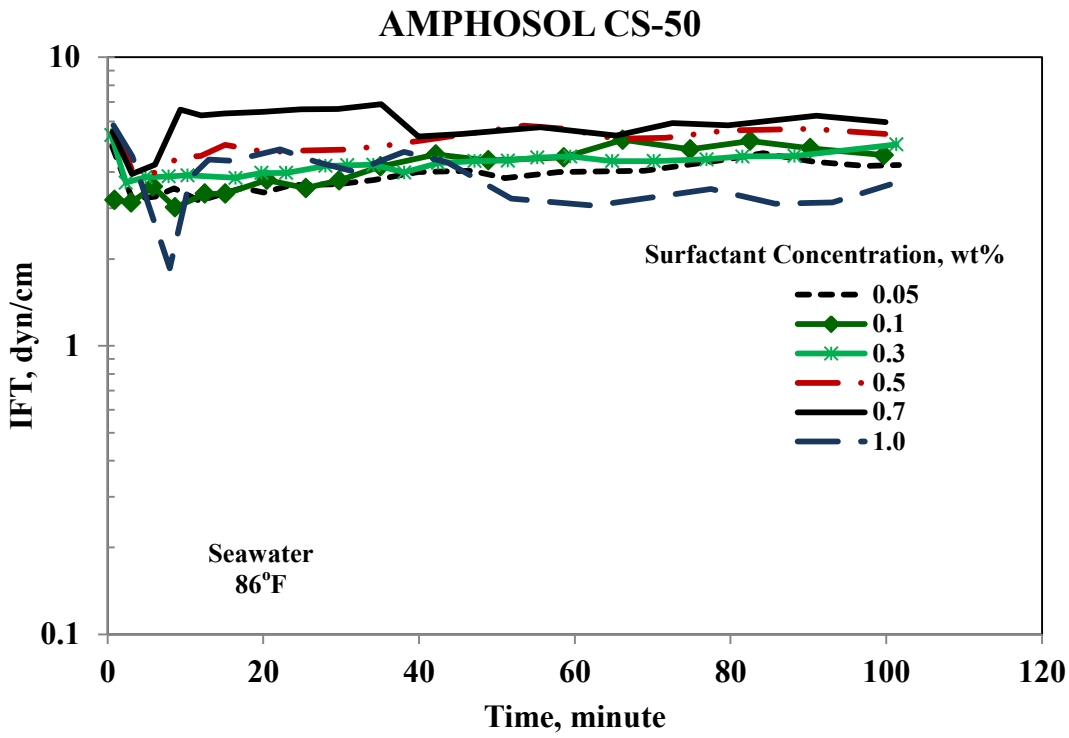

Fig. 40— Effect of Amphosol CS-50 concentration on the IFT value of the surfactant solutions prepared in seawater.

Third surfactant used was PETROSTEP CG-50 (cocamidopropyl betains). The lowest minimum and equilibrium IFT values achieved were 0.38 and 1.46 dyn/cm at surfactant concentration of 0.05 wt%. The equilibrium IFT values ranged from 1.46 to 2.68 dyn/cm when surfactant concentration varies from 0.05 to 1 wt%. **Fig 41** shows the increase of equilibrium IFT values as the concentration was increased.

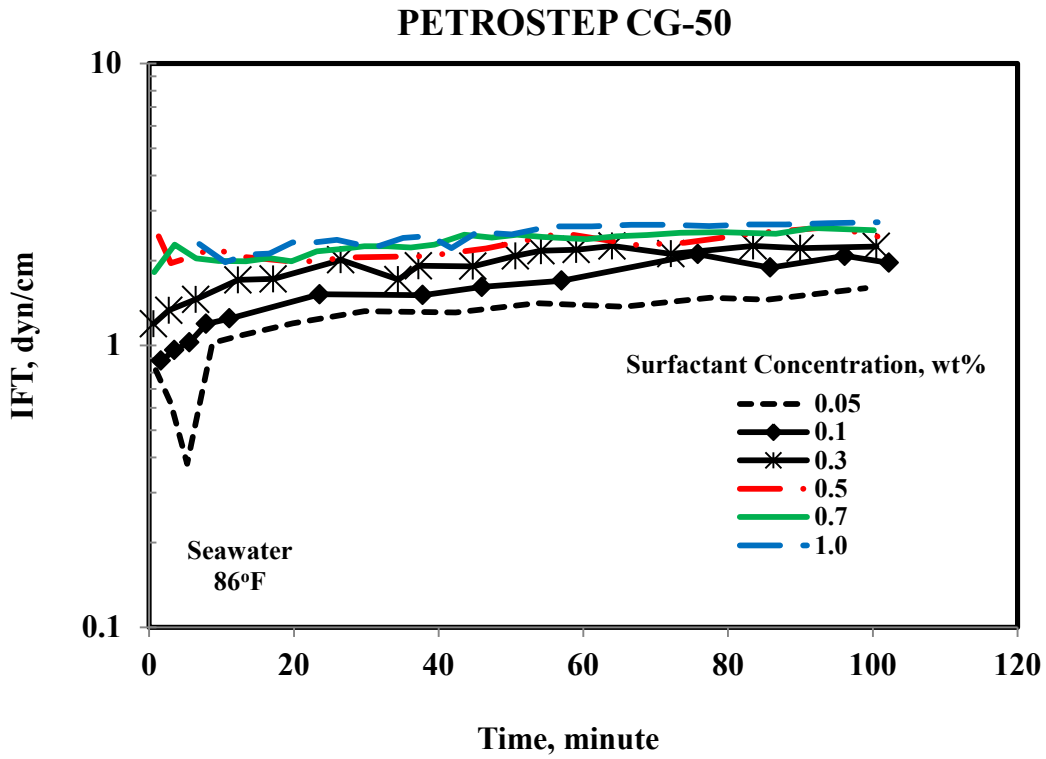

Fig. 41—Effect of Petrostep CG--50 concentration on the IFT value of the surfactant solutions prepared in seawater.

Fig. 42 presents fourth type of surfactant screened in this study SS-885. The IFT values were reducing with time and with surfactant concentration. Ultralow IFT values were achieved using this surfactant and values as low as 0.003 dyn/cm were reached using this surfactant. Due to extremely low IFT values further investigation was continued using this surfactant.

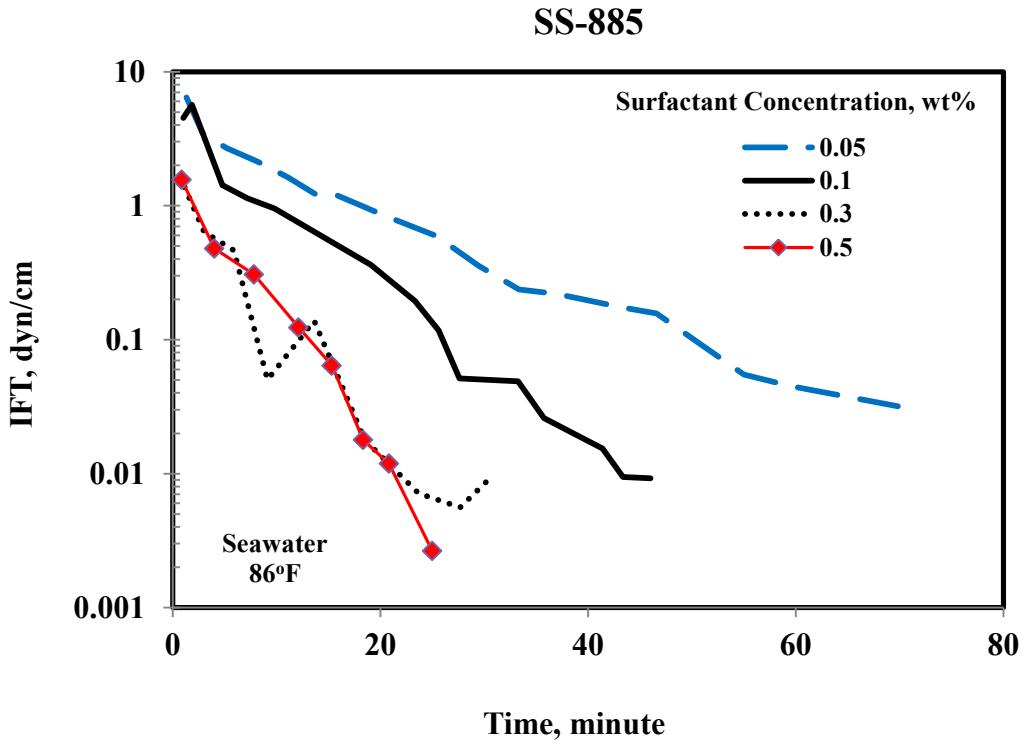

Fig. 42— Effect of SS-885 concentration on the IFT value of the surfactant solutions prepared in seawater.

The last type of surfactant tested was the GreenSurf series. This series of surfactants with an increasing molecular weight design to be environmentally friendly with an improved adsorption characteristics (reduced adsorption to rock surface). Four samples of this series of surfactants were tested to cover range of different molecular weights. The larger number of the surfactant, designated to a larger molecular weight. All samples were prepared using seawater with surfactant concentration of 0.3 wt% and tested using the same protocol used with other experiments. As seen in **Fig. 43**, the minimum and equilibrium IFT values achieved were 0.006 and 0.111 dyn/cm, respectively, at surfactant Greensurf 687, the surfactant with highest molecular weight value. These surfactant showed a general trend with decrease in minimum and equilibrium IFT values, and delay in time of minimum IFT occurs with increasing the molecular weight.

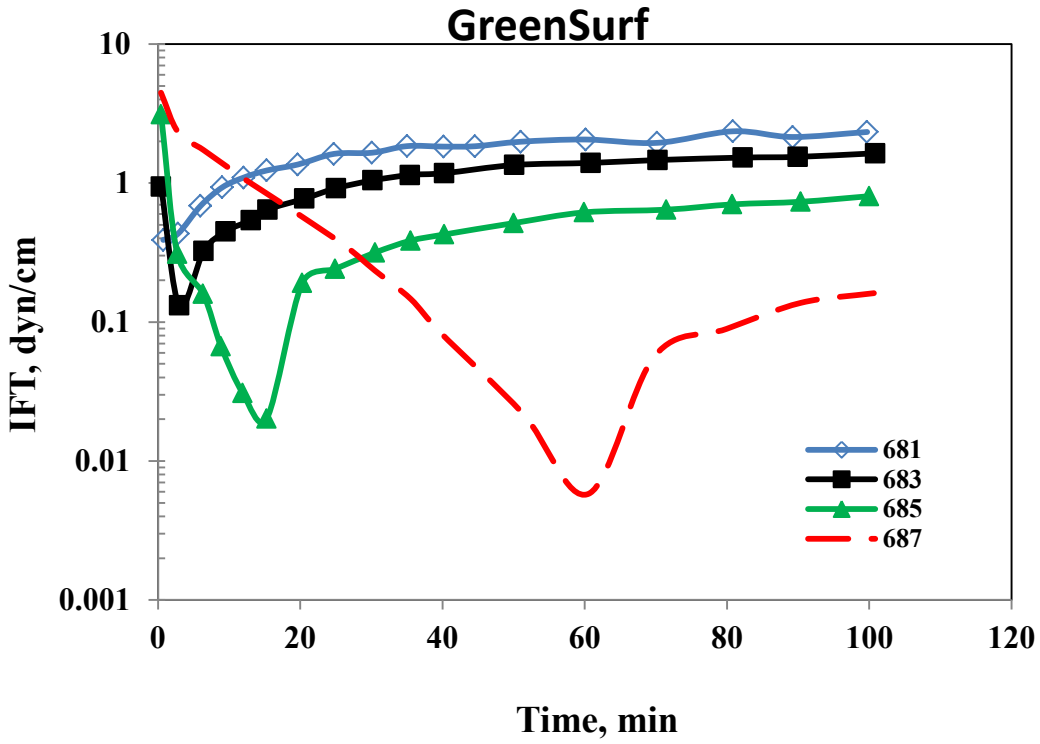

Fig. 43— Effect of GreenSurf molecular weight on the IFT value of the surfactant solutions prepared in seawater.

Effect of surfactant concentration in 6wt% NaCl brine

In these experiments the SS-885 surfactant was prepared in 6 wt% NaCl brine and concentration was varied between 0.1 and 3 wt%. In these experiments two range of surfactant concentration were used intermediate at concentrations of 0.1 and 0.3 wt%, and a higher surfactant concentrations at 1 and 3 wt%. In the intermediate surfactant concentration, minimum IFT values of 0.034 and 0.024 dyn/cm was reached in surfactant concentration of 0.1 and 0.3, respectively. In the higher surfactant concentration no clear transient minimum IFT was noticed, however, the minimum IFT values reached were 0.130 and 0.241 dyn/cm at surfactant concentration of 1 and 3 wt%, respectively. **Fig. 44** shows the IFT values with time at 4 different surfactant concentrations.

Increasing the surfactant concentration increases the solution viscosity as shown in **Fig. 45**.

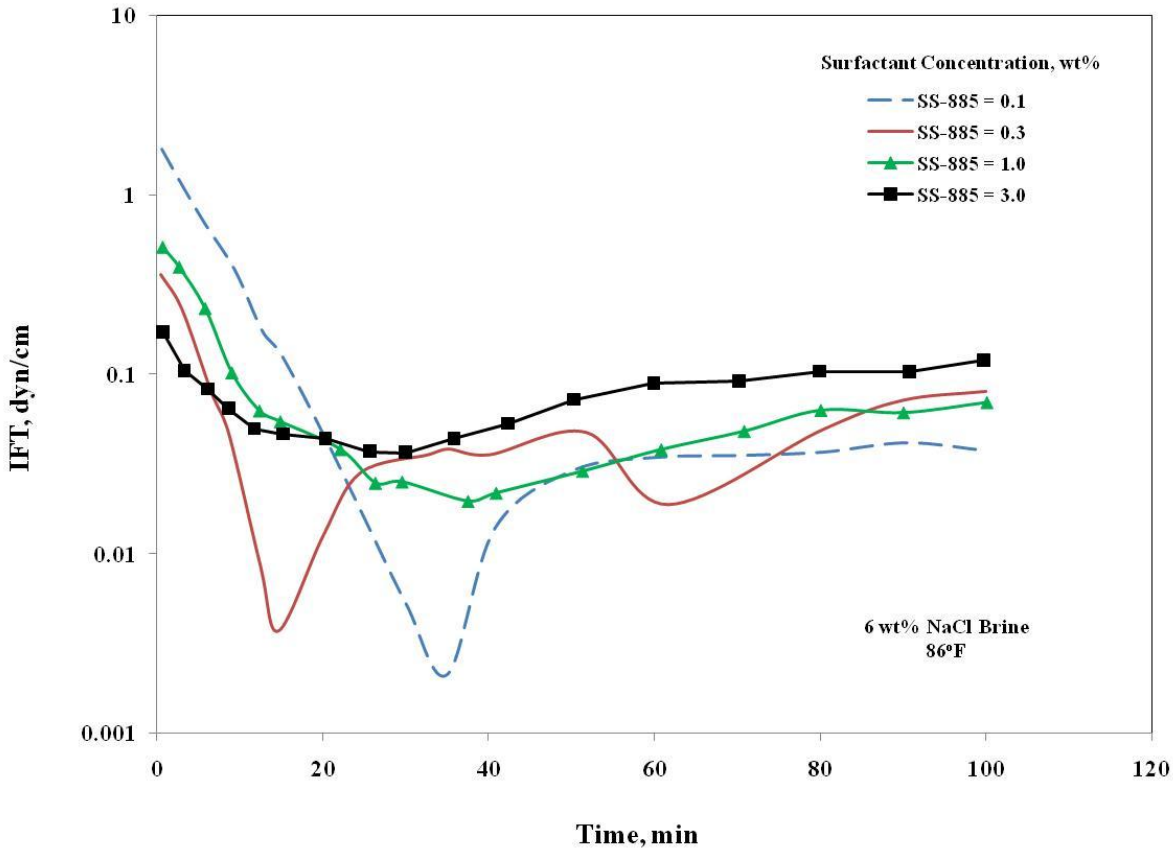

Fig. 44—Effect of surfactant concentration on the dynamic interfacial behavior of the chemical solutions with time.

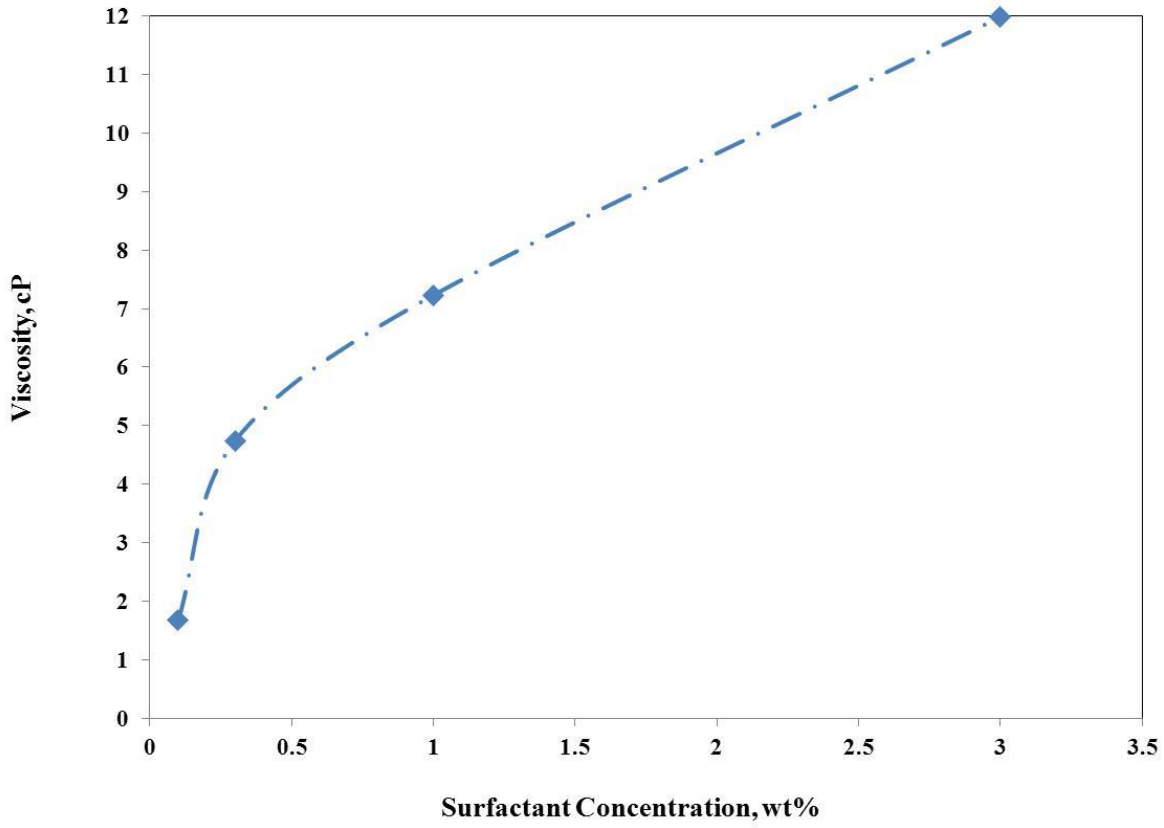

Fig. 45—Effect of surfactant concentration on the solution viscosity prepared in 6 wt% NaCl, where solution viscosity increased with increasing the surfactant concentration.

Effect of seawater and high salinity formation brine mixing

In this set of experiments the effect of seawater with formation brine on IFT values was investigated. Mixed solutions salinity and hardness were increased by mixing different ratios of seawater and brine. Seawater presents the low salinity and hardness compared to formation brine, and high salinity formation brine, which represent high salinity / high hardness. Increasing formation brine volume in the mixed brine from 0 to 25 vol% causes the minimum IFT to drop from 0.0039 to 0.00065 dyn/cm (**Fig. 46**). The increase in the salt concentration causes reduction in the surfactant solvation which drives the surfactant out of the aqueous phase to the interface. Consequently, surfactant

concentration at the oil-aqueous interface increases and results in minimum IFT drops (Nasr-el-din and Taylor, 1992). The reduction in the surfactant solvation by salt increase is caused by the inorganic salt shields charges of the ionic surfactant, this destroys the hydrated shells around the ions and strengthen the hydrophobicity of the surfactant which enhances the adsorption of the surfactant to the oil-aqueous interface. The second effect of high salt concentration is the compress of the double electrical layer, which reduces the repulsion between similar surfactant head groups having the same charges and causes a tighter arrangement of the surfactant at the interface which also causes increase in surfactant concentration and IFT reduction (Zhao and et al. 2006).

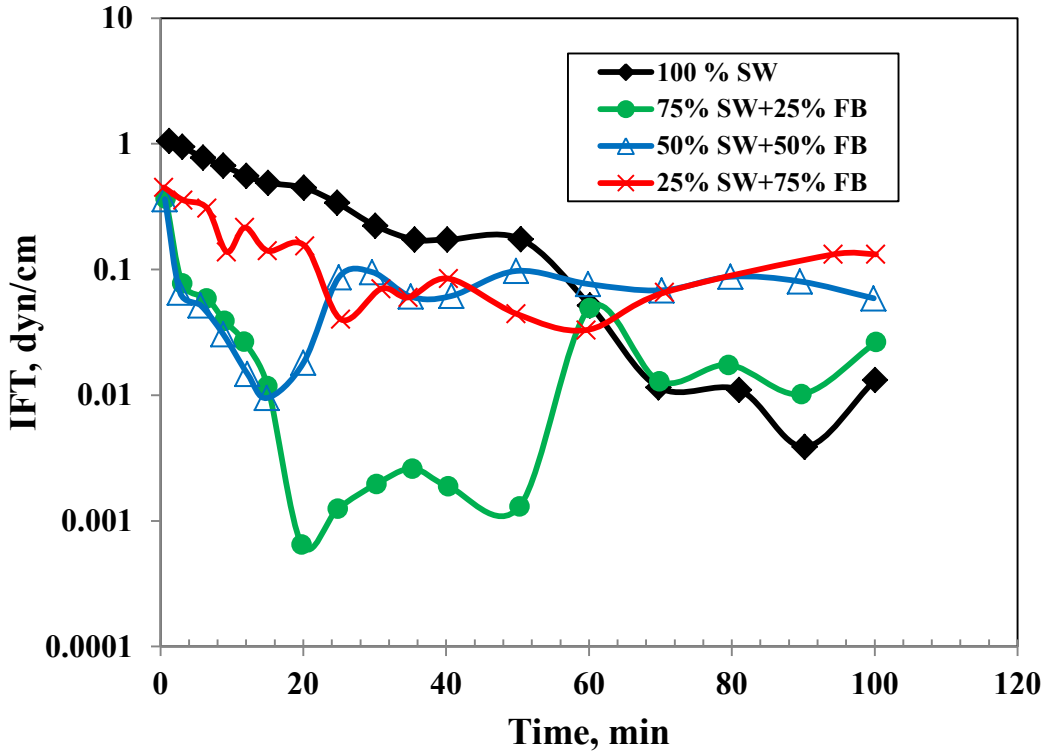

Fig. 46—Effect of seawater-formation brine mixing on the IFT behavior.

Further increase in IFT values were measured when increasing the salinity and hardness by increasing the formation brine concentration. Increasing the formation brine portion in the mixings water to prepare the surfactant solution resulted in more

portioning of the surfactant to the oil phase which reduces the amount of surfactants at the oil-aqueous interface. The reduction of surfactant concentration at the interface causes an increase in the IFT values measured.

Effect of alkali type and concentration

To study the effect of alkali on the interfacial properties of the alkali-surfactant (AS) chemical solution two alkalis were used organic alkali and sodium metaborate (for more information about these alkali see Chapter II). The concentration for both alkalis were varied between 0 and and 1 wt.% with constant surfactant concentration at 0.3 wt%. The chemical solutions were prepared in seawater. When organic alkali (OA-100) was used there was a continuous decrease in IFT values, however, the minimum values were reached in later time. The reduction in IFT values can be explained by increase of salinity or by in-situ generation of the surface active solution. **Fig. 47** shows the IFT behavior versus time when OA-100 was used.

Fig. 48 shows the effect of sodium metaborate concentration on the IFT-time behavior. The IFT values were showing a very gradual decrease with time when sodium metaborate was added to the surfactant solution. In case on 0.1 wt.% sodium metaborate was showing a slow reduction in IFT values until time was 70 minute, after that a more rapid decrease in the IFT values were noticed. The IFT value dropped from 0.1733 to 0.0013 dyn/cm at time from 70 to 99 minutes from start of the experiment. The slow decrease in IFT values was noticed in both solutions and this behavior is an indication of slow diffusion of the surfactant molecules to the oil-solution interface. This can be explained by possible association of the surfactant molecules with the alklais since both of the forms polymeric type molecules no further investigation will be discussed about this behavior since it is out of the scope of this research.

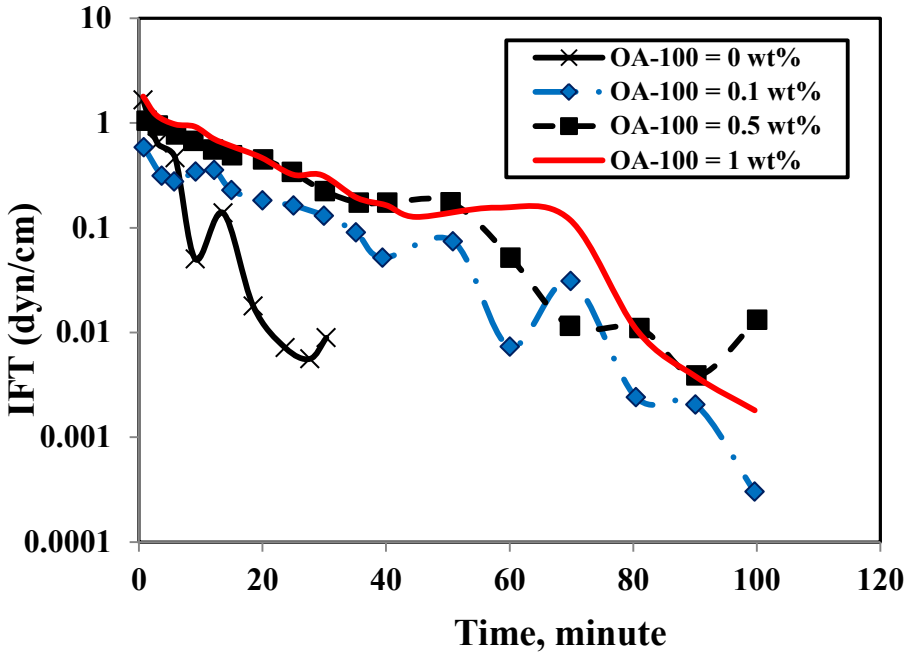

Fig. 47—Effect of organic alkali concentration on the IFT-time behavior.

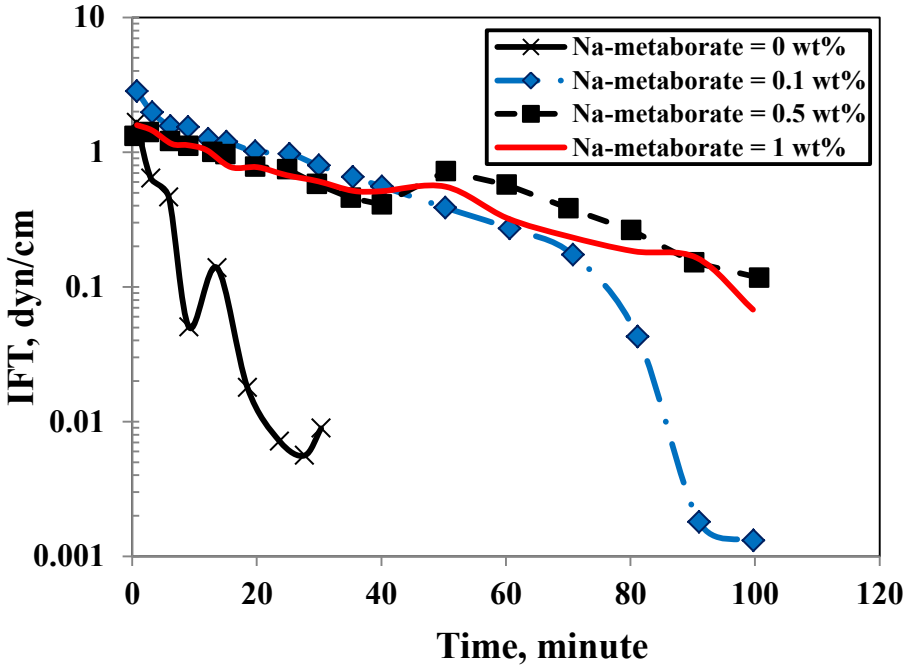

Fig. 48—Effect of sodium metaborate concentration on the IFT-time behavior.

Effect of polymer concentration on IFT-time behavior at organic alkali-surfactant-polymer solution (OASP)

The effect of concentration of two types of polymer on the IFT behavior was evaluated. The OASP solution was prepared in seawater with 0.5 wt% of organic alkali (OA-100) and 0.3 wt% of amphoteric surfactant (SS-885). **Fig. 49** gives the effect of AMPS polymer concentration on the IFT behavior for polymer concentration of 1,000 and 3,000 ppm. Both solutions show dynamic IFT behavior with minimum IFT value achieved 35 minutes for both them and this was followed with gradual increase of IFT values to reach equilibrium at 0.31 and 0.56 dyn/cm. As discussed earlier the minimum IFT values are achieved when maximum concentration of in-situ surfactant, generated by alkali, and synthetic surfactant are on the interface.

Fig. 50 shows the effect of HPAM concentration on the IFT behavior of the OASP solution. A more noticeable effect by this type of polymer on the IFT behavior when compared to AMPS. HPAM has a larger molecule and will have a greater impact on the viscosity of the aqueous phase than the AMPS as will be discussed in the coming sections. Two polymer concentrations were used 1,000 and 3,000 ppm. Both OASP solutions showed dynamic IFT behavior with time. When higher polymer concentration was used a delay in the minimum IFT was measured and higher minimum IFT value was reported. The delay of reaching minimum IFT was reported by Taylor and Nasr-El-Din (1996).

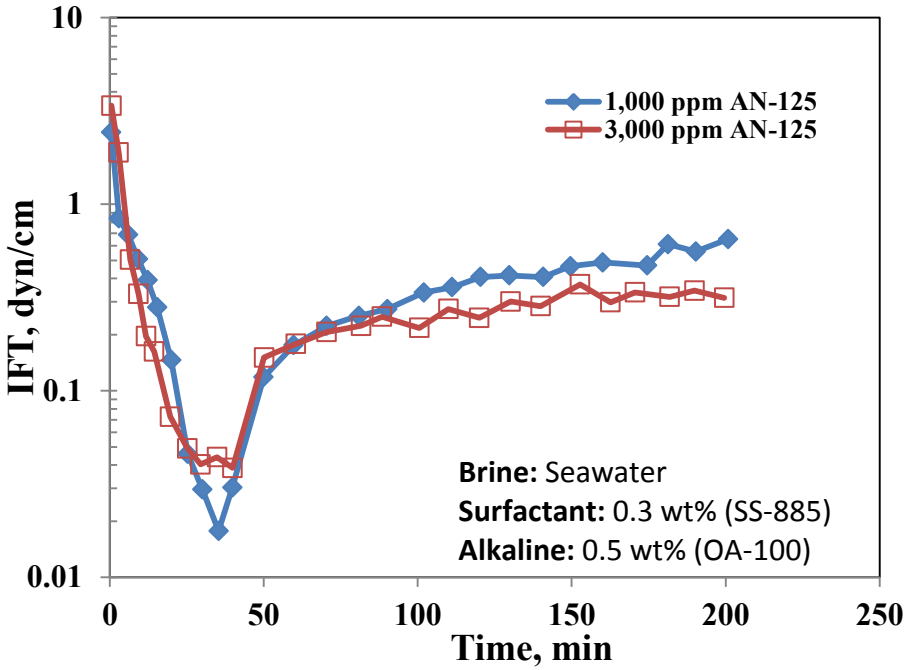

Fig. 49—Effect of AMPS polymer concentration on IFT-time behavior for OASP solution.

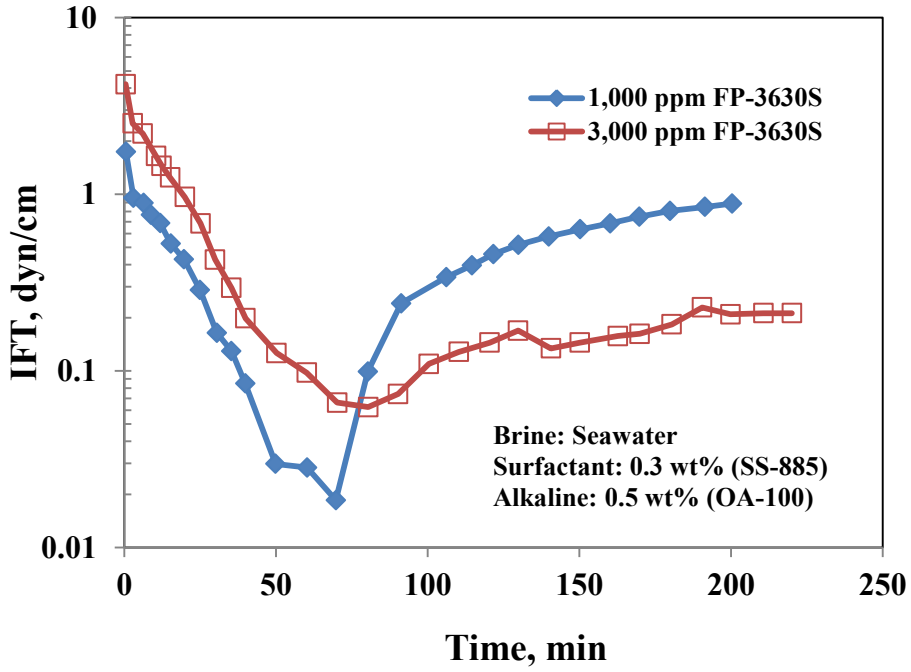

Fig. 50—Effect of HPAM polymer concentration on the IFT-time behavior for OASP solution.

Effect of polymer type on IFT-time behavior at organic alkali-surfactant-polymer solution (OASP) (OA-100)

Effect of polymer type, for two concentrations 1,000 and 3,000 ppm, on IFT behavior was tested. **Fig. 51** shows the effect of AMPS and HPAM at 1,000 ppm on the IFT behavior for OASP solution. Both solutions show dynamic behavior with almost the same minimum and equilibrium IFT. The only difference was the delay caused by the HPAM for the minimum IFT to happen. This can be caused by the larger size of the HPAM molecule that cause a delay for the surfactant molecules to adsorb to the interface.

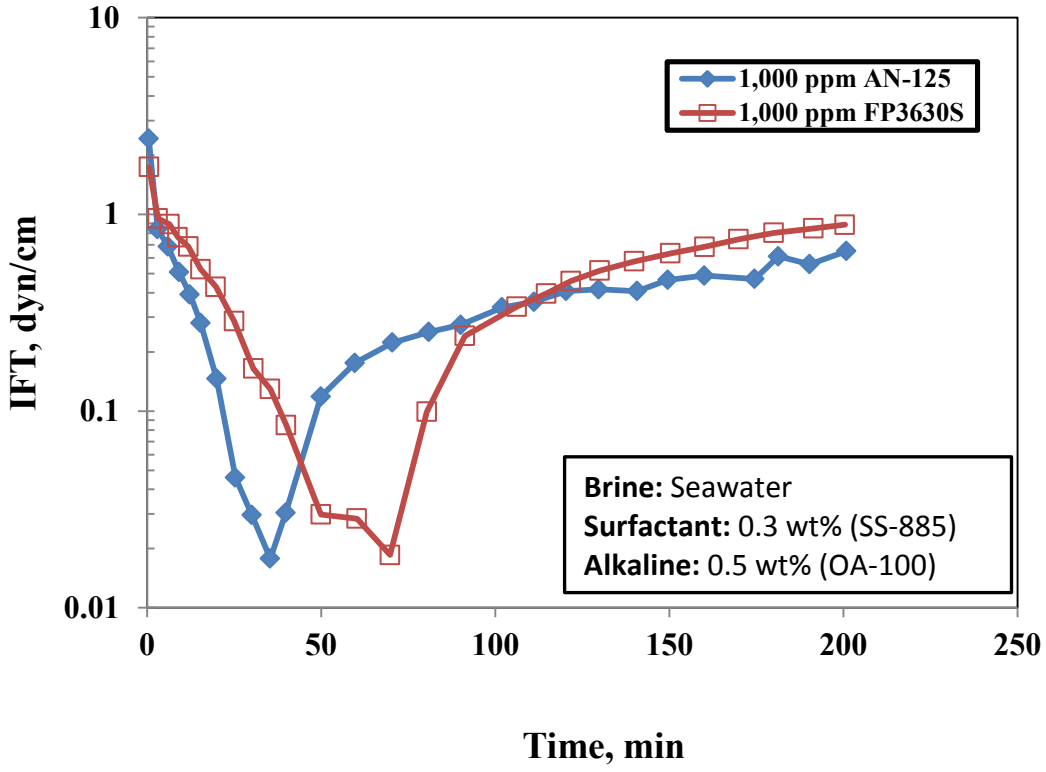

Fig. 51—Effect of polymer type (AMPS & HPAM) on IFT-time behavior for OASP solution at 1,000 ppm polymer concentration.

When polymer concentration was increased to 3,000 ppm the chemical solutions showed similar behavior as in the case of low polymer concentration with an increase in the minimum IFT value for the solution prepared with HPAM. As can be seen in **Fig. 52** gradual decrease for the IFT value until the minimum was reached this was followed with a slow increase to equilibrium IFT values.

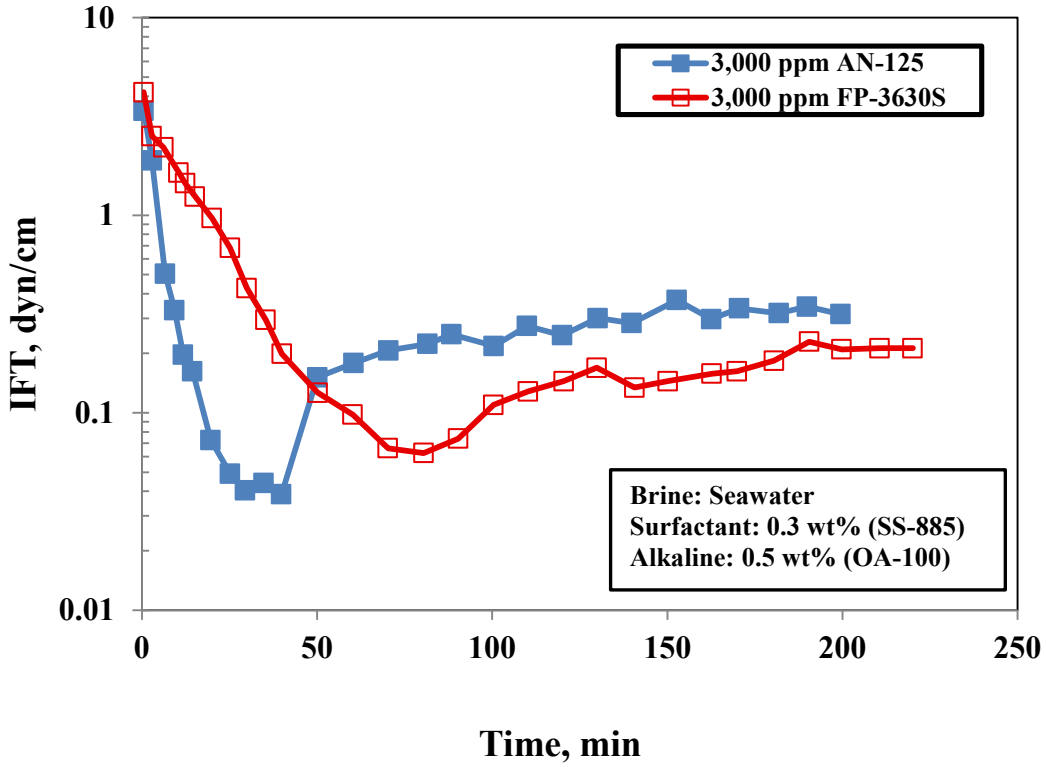

Fig. 52—Effect of polymer type (AMPS & HPAM) on IFT-time behavior for OASP solution at 3,000 ppm polymer concentration.

Effect of polymer concentration on IFT-time behavior at sodium metaborate alkali-surfactant-polymer solution (ASP)

Fig. 53 shows the effect of AMPS polymer concentration in the ASP solution prepared with sodium metaborate. At higher polymer concentration the IFT shows slower reduction in IFT with time and higher minimum IFT. At the low polymer minimum IFT was 0.001 dyn/cm and was reached after 50 minutes.

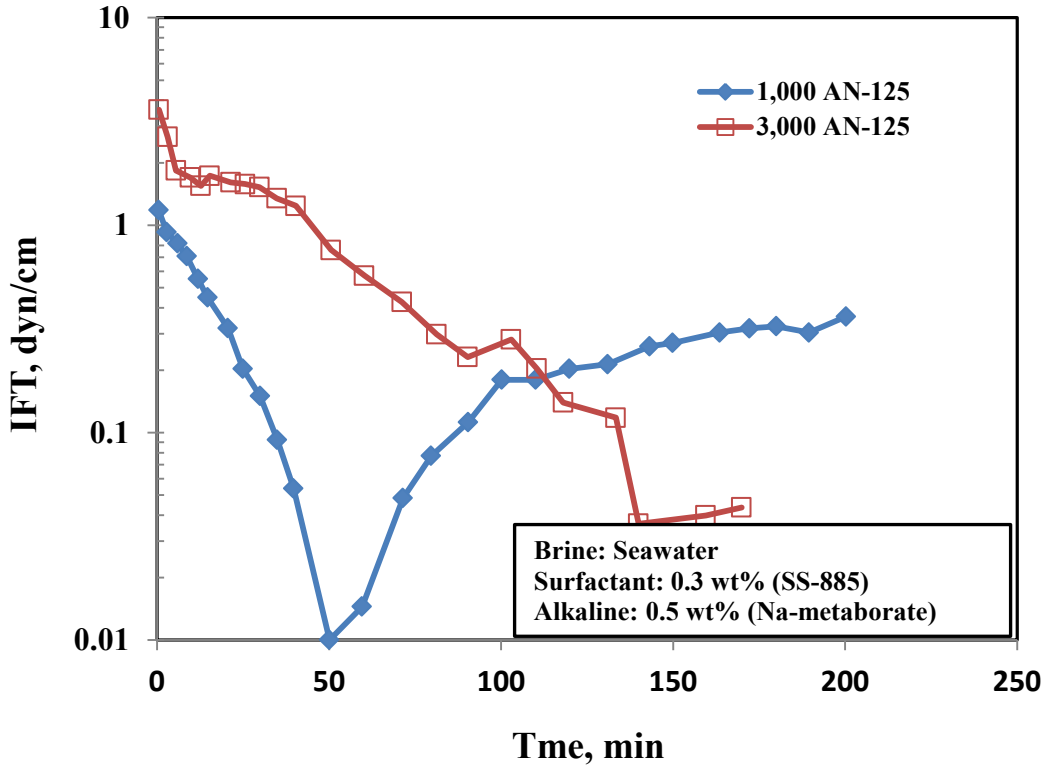

Fig. 53— Effect of AMPS polymer concentration on the IFT-time behavior for ASP solution.

Fig. 54 shows the effect of HPAM polymer concentration on IFT behavior at ASP solution. At low polymer concentration (1,000 ppm) the IFT shows a dynamic behavior with clear sharp minimum at 0.0063 dyn/cm that happen after 53 minutes after solution oil interaction. I the case of higher polymer concentration IFT drop to around 0.07 dyn/cm and stabilized for 147 minutes before it start increasing again.

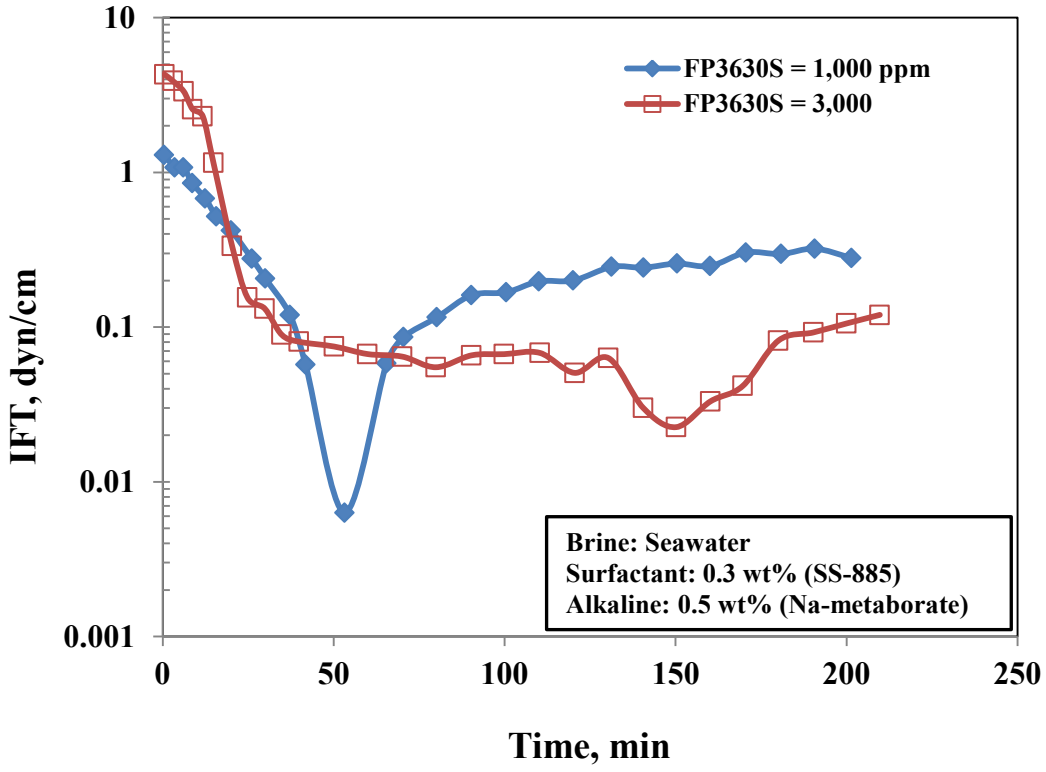

Fig. 54—Effect of HPAM polymer concentration on the IFT-time behavior for ASP solution.

Effect of polymer type on IFT-time behavior at sodium metaborate alkali-surfactant-polymer solution (ASP)

Fig. 55 shows an identical behavior of IFT using 1,000 ppm of HPAM and AMPS. Both solutions show dynamic behavior with minimum and equilibrium IFT around 0.0063 and 0.3 dyn/cm, respectively. Due to high seawater salinity and the added salinity by the sodium metaborate alkali the effect of polymer viscosity was diminished and no difference can be seen in the behavior of the two solutions.

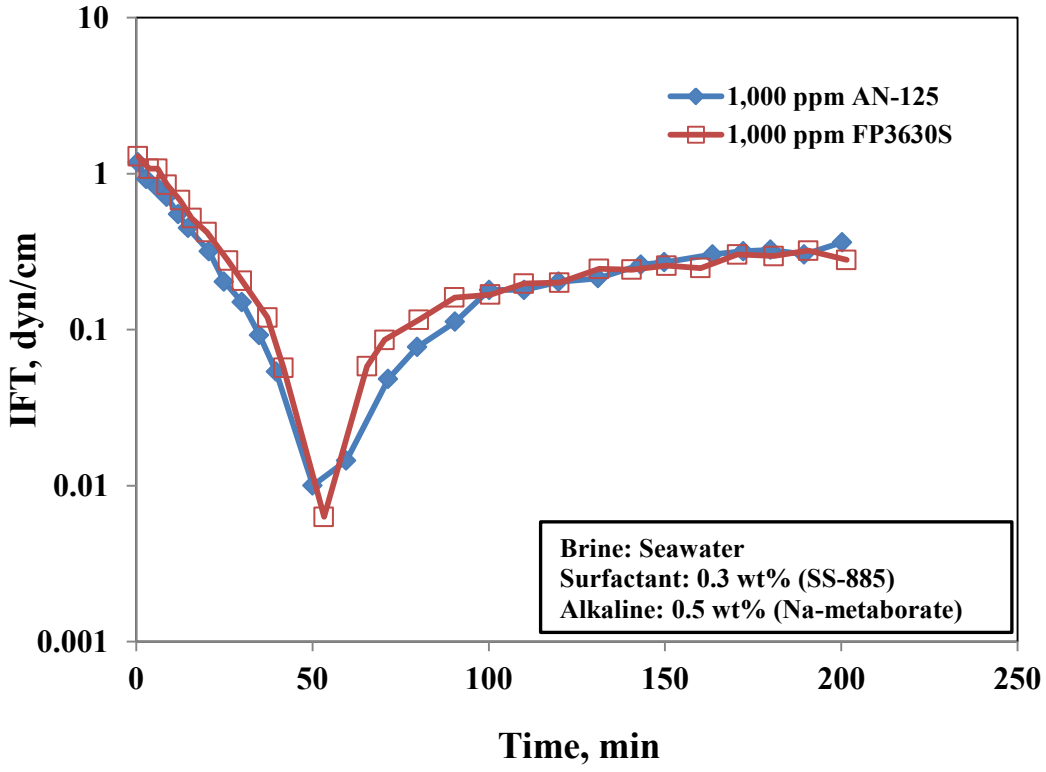

Fig. 55—Effect of polymer type (AMPS & HPAM) on IFT-time behavior for ASP solution at 1,000 ppm polymer concentration.

Fig. 56 shows the IFT behavior for solution with higher polymer concentration 3,000 ppm. With higher polymer concentration the solution will exhibit more viscosity and variation between two types of the polymer on IFT will be more pronounced.

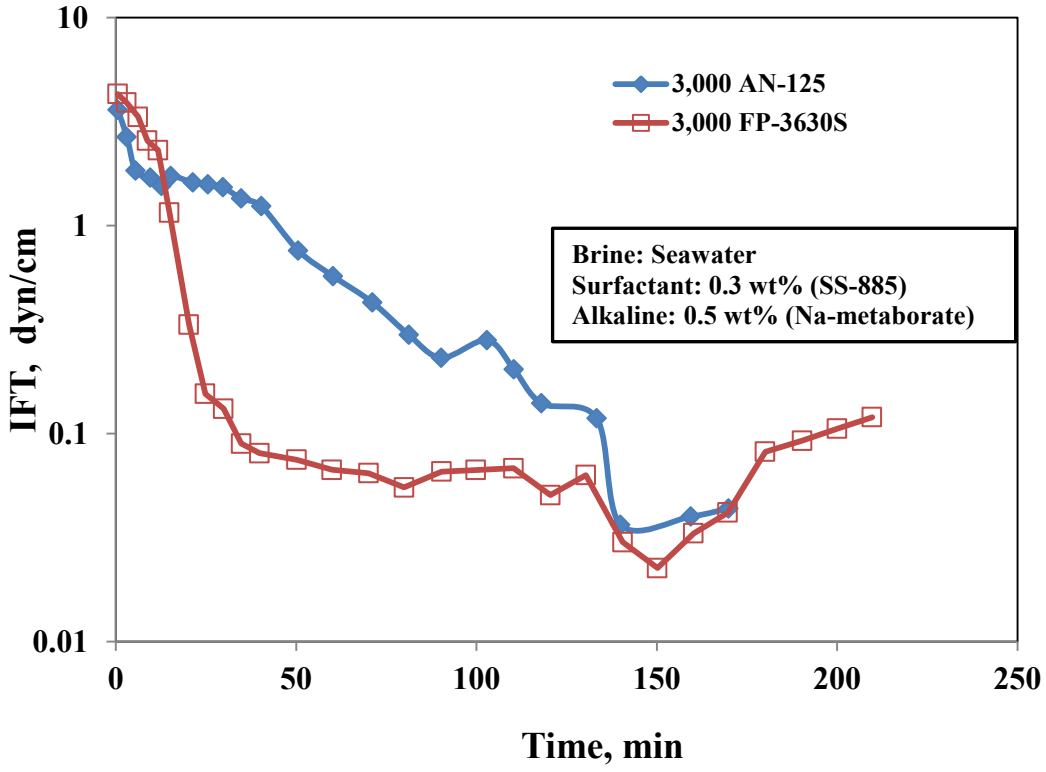

Fig. 56— Effect of polymer type (AMPS & HPAM) on IFT-time behavior for ASP solution at 3,000 ppm polymer concentration.

Conclusion

1. The SS-885 surfactant showed the lowest IFT values in all examined concentrations.
2. Mixing the injected seawater with high salinity high hardness formation brine caused further reduction in IFT.
3. Increasing Alkali concentration result in increase in IFT values.
4. Adding polymer to the formula with organic alkali caused increase in the IFT values with polymer concentration.
5. Reduction in IFT values was noticed when polymer was added to the formula with sodium metaborate.

CHAPTER IV
RHEOLOGICAL PROPERTIES OF SP SOLUTIONS

Summary

Mobility control during chemical flooding is one of the most important factors for enhanced oil recovery using chemical process. Polymers are used to increase the viscosity of the injected fluid to improve the sweep efficiency by having a favorable mobility ratio during chemical flooding. Characterization of rheological properties of the surfactant-polymer (SP) solution is important for understanding the behavior of chemical slug in porous media.

An experimental study was conducted to measure the rheological properties of chemical flooding solution over a wide range of parameters. Effects of temperature, salt type, salt concentration, surfactant type and surfactant concentration on dilute aqueous solution of polymer used for high salinity enhanced oil recovery applications were investigated in details. In some cases the chemical slug was prepared in seawater and viscosity measurement was conducted at 90^{o}C.

Amphoteric surfactant showed compatibility with polymer solution and can be used in chemical flooding. Effect of concentrations of two types of surfactants, anionic and amphotaric on chemical slug viscosity was studied. Amphotaric surfactant was found to have a preferable rheological attributes when compared to anionic surfactant. Amphoteric surfactant can maintain viscosity of chemical solution at high salinity and no reduction in viscosity was noticed when this type of surfactant was added to the solution. On the other hand, reduction in viscosity was measured when anionic surfactant was added to the solution.

Introduction

Water-soluble polymers are used in different chemical flooding methods to improve the volumetric sweep efficiency of the displacement process by reducing the mobility of the aqueous phase (Nasr-El-Din et al. 1991, Lee et al. 2009, Green and Willhite 1998).

Mobility control is discussed in terms if mobility ratio, M, which is given by the following equation:

$$\mathbf{M} = \left(\frac{\mathbf{k_{rw}}}{\mathbf{\mu_w}}\right)_{\mathbf{S_{or}}} \left(\frac{\mathbf{\mu_o}}{\mathbf{k_{ro}}}\right)_{\mathbf{S_{rw}}} \quad \text{.....(14)}$$

where k_{rw} and k_{ro} are the relative permeabilities to water and oil, respectively; μ_w and μ_o are the water and oil viscosity, respectively. Water relative permeability and viscosity are measured at residual oil saturation. Oil relative permeability and viscosity are measured at irreducible water saturation. M affects the stability of the displacement process, when M >1 the flow is unstable and viscous fingering occurs. Favorable mobility is achieved when M<1 (Green and Willhite 1998).

Mobility control is important to maintain the integrity of the chemical slug for other methods of chemical flooding, e.g., alkaline-surfactant-polymer and surfactant-polymer flooding (Green and Willhite 1998). Mobility control is needed in the chemical slug to prevent it from fingering to the oil bank ahead of it (This can cause the chemicals to dissipate by dispersive mixing), between the slug and mobility buffer, and between the water drive and the mobility buffer or to the water bank trailing it.

Types of polymers

Discussion about polymer types used in EOR application were given in Chapter I.

Bulk rheological properties

Shear Viscosity

Fig. 57 (Green and Willhite 1998) shows a typical shear-viscosity behavior of a shear-thinning fluid. Newtonian fluid behavior is shown in low and high shear rates, which are called lower and upper Newtonian flow regions, respectively. Constant bulk viscosity is found in these two Newtonian regions. In between these two regions there is a transition to a shear thinning behavior. Rheological behavior of shear thinning fluid was described

by widely used Carreau model (Green and Willhite 1998; Nasr-El-Din et al. 1991; Lee et al 2008):

$$\frac{\mu-\mu_\infty}{\mu_0-\mu_\infty} = 1 + \gamma\tau^{2}{}^{n-1}{}^{2} \quad \text{.....(15)}$$

where μ is steady shear viscosity, μ_0 is shear viscosity for the lower Newtonian region, μ_∞ is shear viscosity for the upper Newtonian region, τis time constant (inverse of the critical shear rate where lower Newtonian region ends and shear thinning region starts), γ is shear rate, and n is power low index.

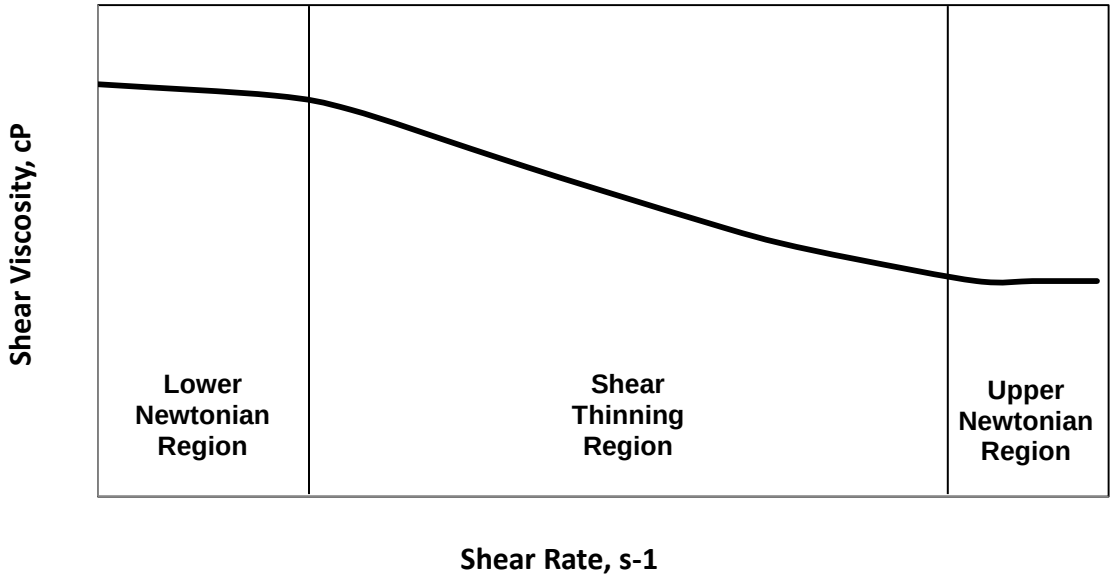

Fig. 57—Rheology of shear-thinning fluids.

Newtonian behavior

A fluid in this region exhibits a viscosity that is independent on shear rate conditions.

Non-Newtonian behavior

A Non-Newtonian fluid is a fluid whose viscosity changes with shear rate. Polymeric solutions at a critical shear rate value show a transition from Newtonian to shear-thinning behavior. In the shear thinning behavior, the viscosity decreases with increasing shear-rate. This is due to uncoiling and aligning of polymer chains when exposed to shearing. The fluid viscosity in the Non-Newtonian region can be fitted using the power-low model:

$$\mu = k\dot{\gamma}^{n-1} \quad \text{.....(16)}$$

where k is flow consistency index.

Interaction between polymer and chemical species in solution

Polymers have several chemical and physical interaction when put in solution with other chemicals such as alkaline, salts, and surfactants. These interactions affect the way polymers solutions behave when flowing in the porous media. Following are some of the interactions that affect polymer performance:

Hydrolysis

Hydrolysis is the process in which a certain molecule is split into two parts by the addition of a molecule of water. Hydrolysis will convert the amide groups (NH_2) to carboxylate groups (COO^-) and ammonia (NH_3) (Green and Willhite 1998, Al-Muntasheri and et al., 2008, Kurenkov et al. 2001). **Fig. 58** shows the hydrolysis process. Hydrolysis can further enhanced by increasing solution temperature (Nasr-El-Din et al. 1991). The increase in solution temperature will increase the negative charges that increase intramolecular repulsions and hence improve viscosity (Muller 1981; Levitt and Pope 2008).

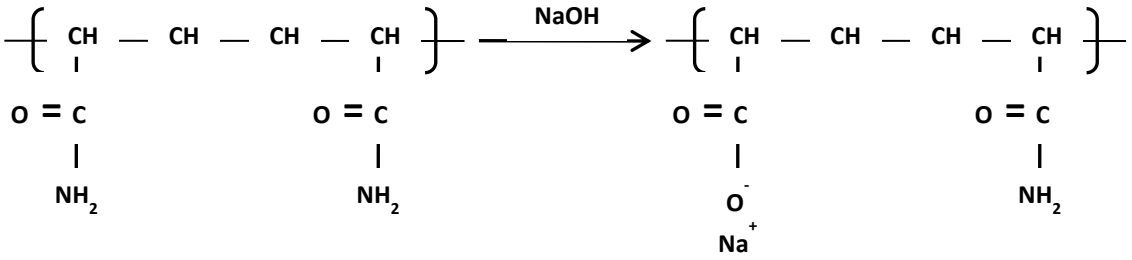

Fig. 58—Hydrolysis of amide groups in polyacrylamide polymer in presence of alkaline.

Charge Shielding

Nasr-El-Din et al. (1991) studied the effect of several chemical species on the shear viscosity behavior of HPAM polymers used in EOR applications. In de-ionized water the polymer solution stretches due to the repulsive forces between the negative charges and hydraulic radius is large. Large hydraulic radius means high viscosity. When salts are introduced to the mixing brine, cations in the solution increases and the repulsive forces in the polymer will decrease, due to charge screening effects. Charge screening effects will cause the polymer to coil-up and reduce the hydraulic radius of the polymer chain, which causes the degree of polymer chain entanglement to diminish. Other effect of the reduction of the polymer chain size caused by charge screening is the increase in the critical shear rate.

Polymer Precipitation and Phase Separation

Zaitoun and Potie (1983) studied the effect of brines containing divalent cations on the stability of the hydrolyzed polyacrylamides. They found that precipitation is possible if excessive concentrations of multivalent cations exists in 33% hydrolyzed polyacrylamide at 80 oC (Zaitoun and Potie 1983; Levitt and Pope 2008). Decrease in temperature and monovalent cation concentration caused a decrease in the critical amount of calcium to precipitate the hydrolyzed polyacrylamide (Levitt et al. 2008). At high degree hydrolysis the precipitation is caused by site fixation phenomena, at low degree of hydrolysis the precipitation is caused by poor salvation (Levitt et al. 2008).

Experimental Studies

Material

Two kinds of polymers were used in this study, the first polymer (Flopaam 3630S) is HPAM with molecular weight of $18X10^6$ and degree of hydrolysis (DH) of 30%. The second chemical is copolymer of acrylamide and 2-acrylamido 2-methyl propane sulfonate (AMPS) called AN-125 with molecular weight and DH of $6X10^6$ and 20-30%, respectively. Both chemicals were provided by SNF Floerger (Cedex, France) in solid form. The chemicals were used as received.

Three surfactants were used in this paper: two betaine-based amphoteric surfactants, supplied by Oil Chem. Technology, and an anionic surfactants of Alpha-olefin sulfonate (Anionic PS C1) by Stepan.

Seawater was used to prepare chemical solutions using compositions shown in Table 1.Sodium chloride, calcium chloride, magnesium chloride, sodium bicarbonate, and sodium sulfate were (ACS) reagent grade and obtained from Mallinckodt Baker, Inc. These salts and deionized water (resistivity = 18 MΩ.cm) were used to prepare seawater solution.

Equipment

Grace Instrument M5600 HPHT Rhometer was used for measuring all the bulk rheological properties (**Fig. 59**). The rheometer uses a bob-and-cup arrangement for rheological property determination. The liquid is placed inside an annulus between the two cylinders (bob and cup), where the cup (outer cylinder) is rotated at a set speed that determines the shear rate. The liquid between the two cylinders exerts a drag force (torque) on the bob (inner cylinder), which is measured and converted to a shear stress.

The M5600's unique frictionless bob shaft construction and advanced sensor design enables the measuring of small changes in shear stress instantly by non-mechanically transmitting a zero friction rotational torque signal from the pressure containment area. The outer cylinder (sample cup) is driven by a stepper motor at speeds from 0.0001 – 1,100 rpm. The thermocouple probe measures the sample temperature at the tip of the

bob shaft. All electronics and other sensitive components are protected from the influences of both the sample fluid and its vapor. (Operation Manual of M5600).

Fig. 59—High-Pressure / High-Temperature Grace Instrument M5600 Rheometer.

Methodology

Shear Viscosity Measurement

The viscosity of various polymer solutions as a function of shear rate was measured over a range of 0.1 to 900 s^{-1}. This range includes shear rates 0.1 – 10 s^{-1} that is encountered in chemical flooding (Nasreldin et al. 1991). The viscosity was measured by increasing the shear rate.

Result and Discussion

Effect of surfactant concentration in 6 wt% Nacl brine on shear-viscosity

In this experience evaluation of four surfactant concentrations has been evaluated at brine salinity of 6 wt% NaCl. The runs were conducted at atmospheric pressure and room temperature (75°F). The effect of adding amphoteric surfactant (SS-885) in saline water was evaluated in at different surfactant concentrations (0.1 – 3 wt%). **Fig.60** shows the increase in solution viscosity with increasing surfactant concentration. Scond observation was that these solutions are showing Newtonian behavior at shear rate between 300 and 900 s^{-1}. This increase in the viscosity will reduce the effect of salt on the polymer chains as discussed in previous discussion.

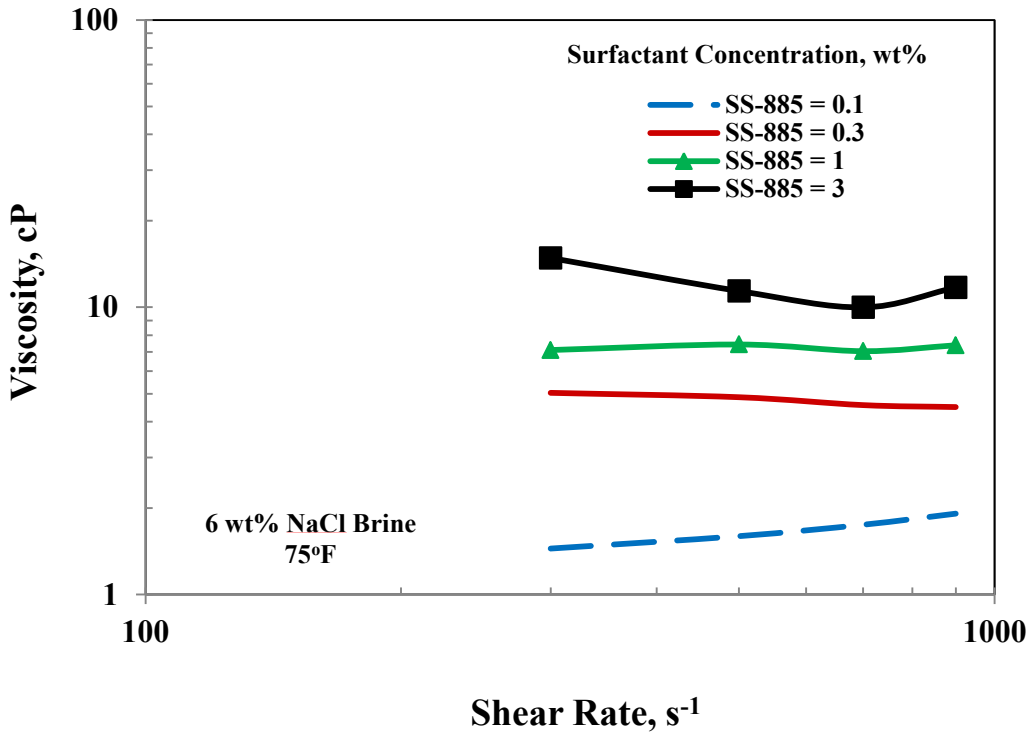

Fig. 60—Effect of surfactant concentration on viscosity of 6 wt% NaCl brine (75°F).

Effect of mixing brine salinity on shear-viscosity

Fig. 61 shows the viscosity-shear rate curve for polymer solutions having 3,000 ppm polymer and 0.3 wt% amphoteric surfactant in various NaCl concentrations at 75^{o}F. Shear thinning behavior was noticed in all the curves and deviation from this behavior was noticed the high shear rates. Viscosity reduced with increasing the NaCl concentration due to the charge shielding mechanism discussed earlier. This will have a practical implantation where high salinity brines are used to prepare the polymer and chemical stage during chemical flooding process. If the gained viscosity will not satisfy the requirement for favorable mobility ratio more surfactant need to be added, which can increase the cost. Other alternative is to use other technology (i.e. emulsion, foam……) or use other type of viscosifying agent. Using fresher mixing water with less salinity can eliminate this problem. **Table 5** gives the power-law parameter for this polymer solution at different salinities (0, 1, and 6 % NaCl). At 1 and 6 % NaCl power-law index was almost independent on the change in salinity. However, in the case of deionized water power-law index shows lower values and indication of more shear-thinning behavior compared to the samples containing more than 1 % NaCl.

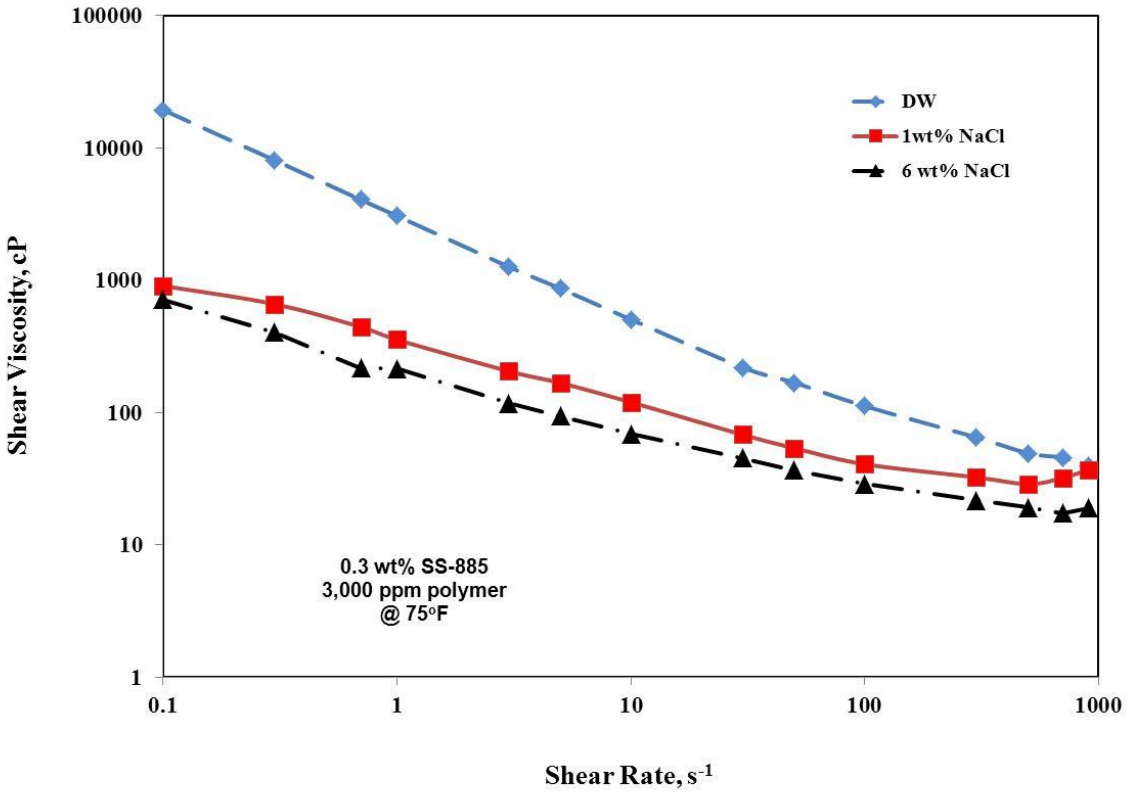

Fig. 61—Effect of salinity on the shear-viscosity with 0.3 wt% surfactant and 3,000 ppm polymer at 75°F.

Table 5—Power-law parameters of 3,000 ppm Flopaam 3630s prepared at different NaCl concentrations.

NaCl, %	K, cp	n	R^2
0	3111.1	0.244	0.9979
1	362.21	0.511	0.9993
6	196.06	0.571	0.9934

Effect of cation type on shear-viscosity

Fig. 62 shows the effect of two brines on the viscosity of the chemical solutions. The experiments were conducted at room temperature with polymer concentration of 3,000 ppm of Flopaam 3630s. Three runs were conducted at this set of experiment with one of the solutions were prepared in deionized water as base case. The second solution was prepared using 0.1% $CaCl_2$ and third with 1% NaCl. The chemical solutions prepared in deionized water and 0.1% $CaCl_2$ show shear thinning behavior on most of the tested shear rate (0.05 – 900 s^{-1}) with part of the upper-Newtonian region at high shear rate values. In case of solution with 1% NaCl shows extension of the low-Newtonian region to shear rate around 0.5 s^{-1} , also the upper-Newtonian region start at earlier than the other two solutions. This resulted in smaller shear thing region for this solution. As can be seen in the figure the three solution show bigger differences in the solution viscosities at low shear rates and viscosity values get closer to each other at high shear rate range. The solution prepared in deionized water shows more reduction in viscosity with increase in shear rate compare the other two solutions that contain salt. **Table 6** gives the power-law parameter for this polymer solution at different brine types CaCl and NaCl.

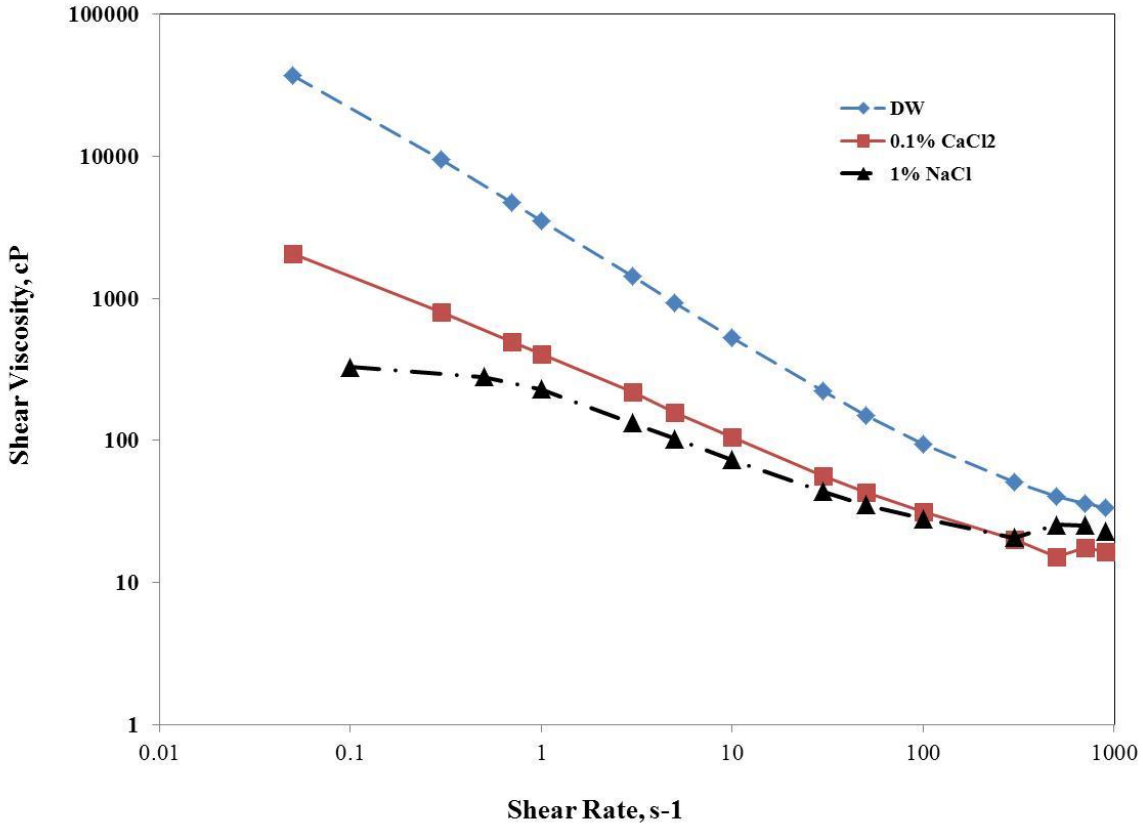

Fig. 62—Effect of cation type on polymer viscosity.

Table 6—Power-law parameters of 3,000 ppm Flopaam 3630s at different cation type.

Mixing Brine	K, cP	n	R^2
Deionized water	3,507.2	0.198	0.9995
0.1% $CaCl_2$	402.24	0.433	0.9994
1.0% NaCl	220.21	0.537	0.9968

Effect of polymer concentration on shear-viscosity on polymer solution

Fig. 63 presents the variation in viscosity of Flopaam 3630S due to shear rate at different surfactant concentrations. All the solutions were prepared in 1 wt% NaCl and polymer concentrations were varied between 1,000 and 3,000 ppm. Increasing the polymer concentration causes an increase in solutions viscosities. All the solutions showed a

shear thinning behavior in most of the tested range. A deviation from the shear thinning behavior was noticed lower and higher shear rate, where Newtonian behavior dominates. **Table 7** gives the power-law parameter for this solution at different polymer concentrations.

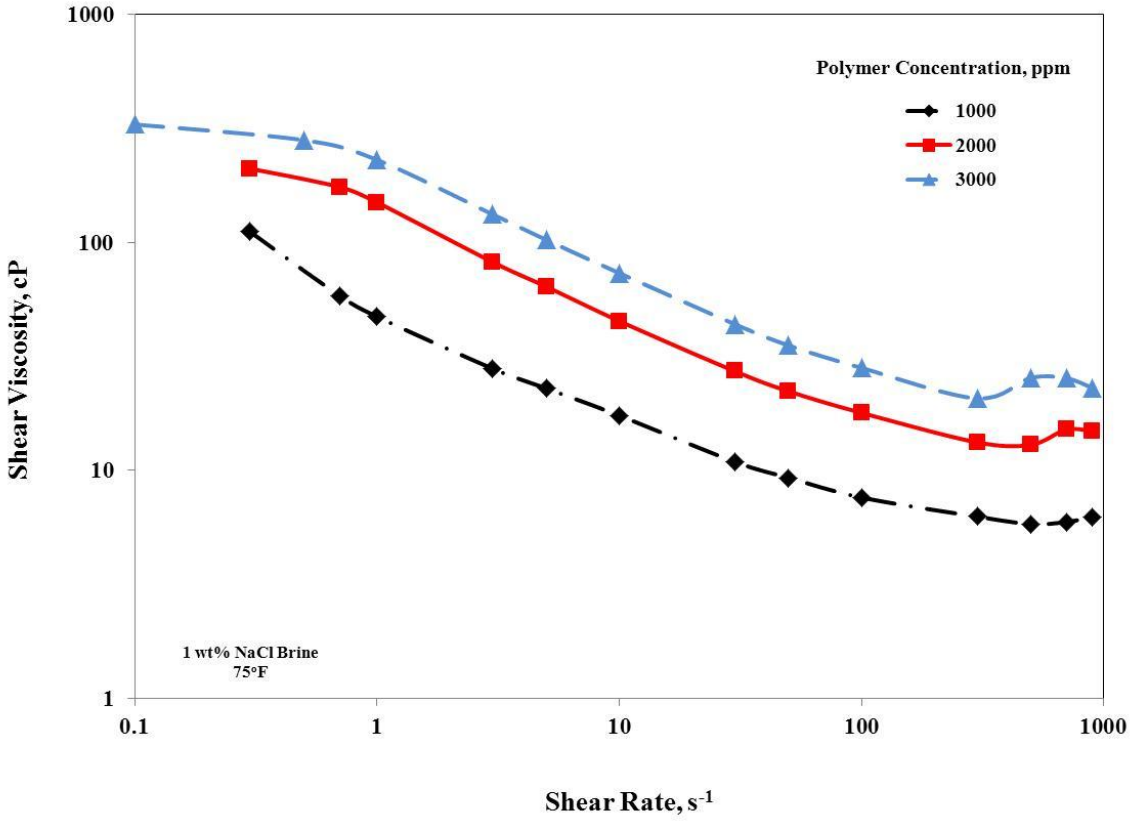

Fig. 63—Effect of polymer concentration on the shear-viscosity of 1 wt% NaCl brine at 75°F.

Table 7—Power-law parameters of Flopaam 3630s prepared in 6% NaCl at different polymer concentrations.

Polymer Concentration, ppm	K, cp	n	R^2
1,000	44.473	0.601	0.9951
2,000	139.05	0.535	0.9943
3,000	220.21	0.537	0.9968

Effect of surfactant on polymer viscosity

In EOR processes, surfactant and polymer are co-injected in the reservoir in SP or ASP flooding. Surfactants are injected to lower the IFT or alter the wettability to mobilize the residual oil.

Nasr-el-din et al. (1991) examined the effect of anionic (Neodol 25-3S) and non-ionic (Triton X-100) on the viscosity of partially hydrolyzed polyacrylamide (Alcoflood 1175L). They found insignificant effect on viscosity when increasing non-ionic surfactant concentration up to 10%. However, a dramatic reduction in polymer viscosity was noticed when it was mixed with anionic surfactant (Nasreldin et al. 1991; Shupe 1981).

In this study the effect of amphoteric surfactant and surfactant concentration was examined in de-ionized water, 1 and 6 wt% NaCl. **Fig. 64** shows no effect in polymer viscosity when surfactant added to it in de-ionized water solvent. Adding NaCl to the solution resulted in two effects; first, the overall viscosity of reduced compared the case where de-ionized water was used due to the charge shielding as discussed earlier. Secondly, the difference in viscosity when amphoteric surfactant was varied.

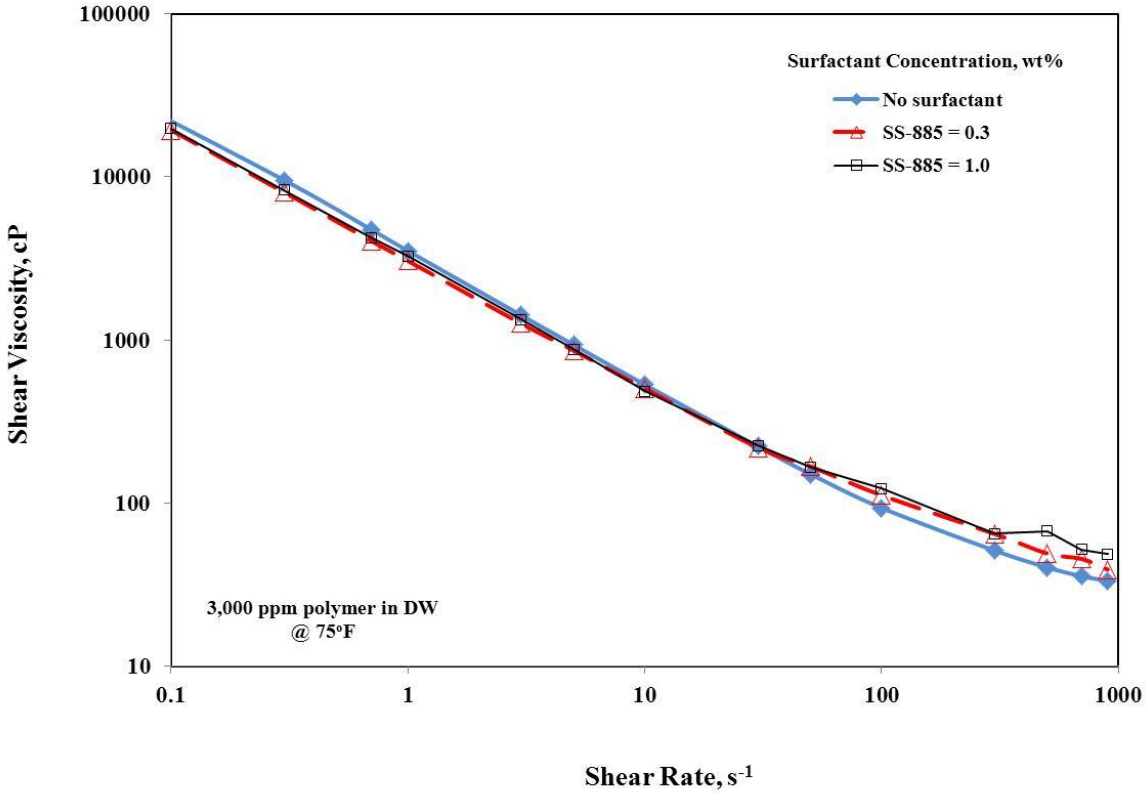

Fig. 64—Effect of amphoteric surfactant concentration on shear-viscosity of polymer solution in deionized water at 75°F (3,000 ppm Flopaam 3630s).

Figs. 65 and 66 show an increase in solution viscosity when surfactant concentration was increased. All shear-viscosity tests show a shear-thinning behavior within the measurement range of the equipment except the case of were no surfactant was used and solution was prepared in 1 wt% NaCl (**Fig. 65**).

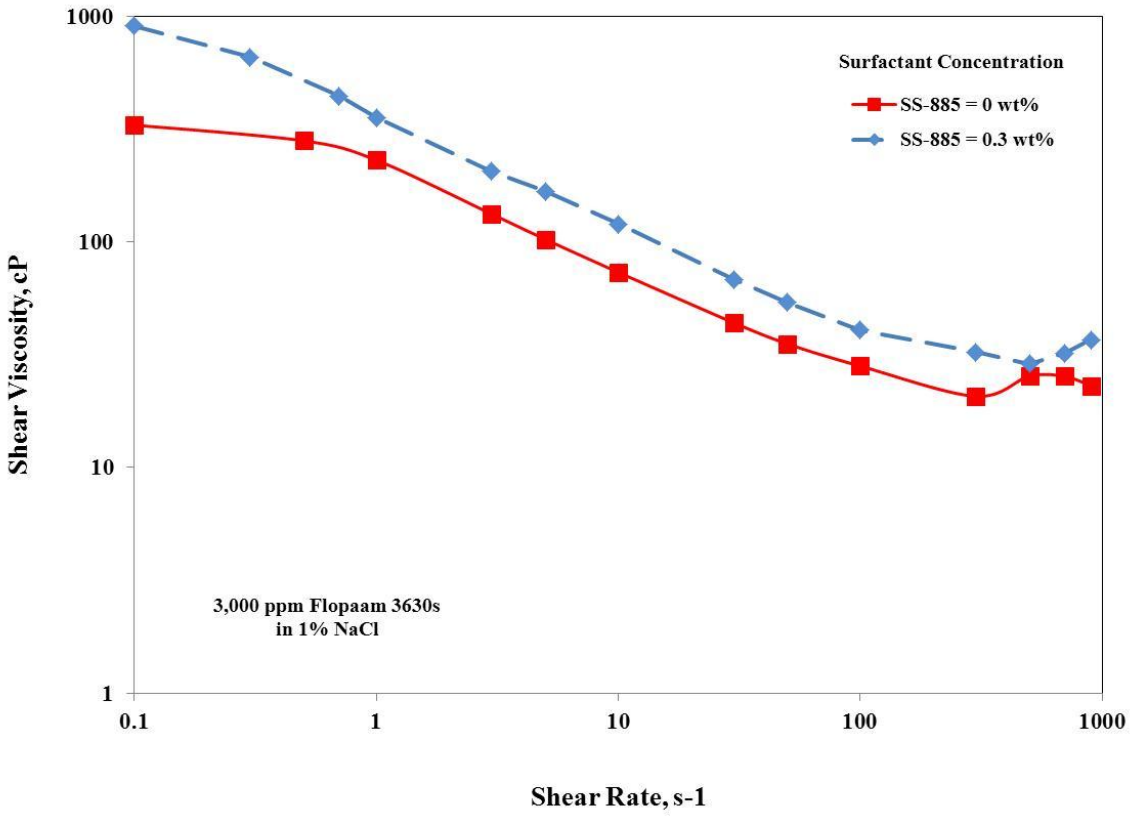

Fig. 65—Effect of surfactant concentration on shear-viscosity in 1 wt% NaCl brine at 75°F.

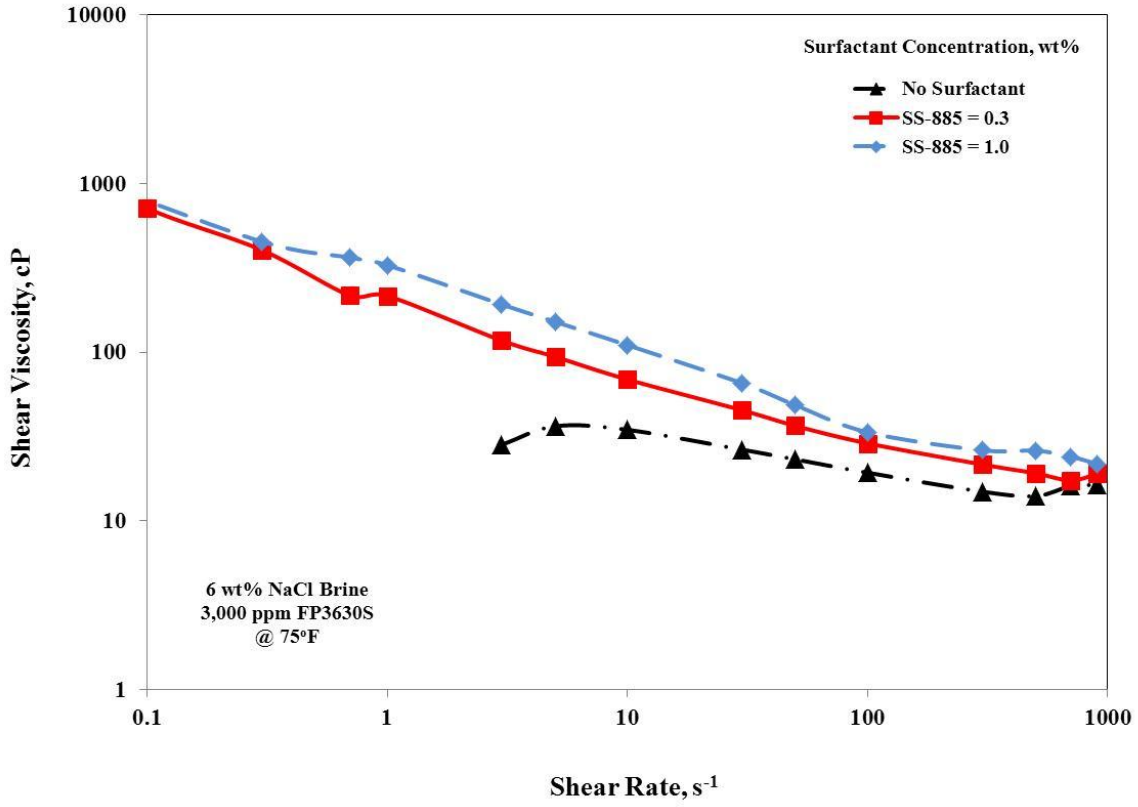

Fig. 66—Effect of surfactant concentration on shear-viscosity in 6 wt% NaCl brine at 75°F.

Viscosity for SP chemical solutions prepared in seawater used for core flooding experiments

To increase the efficiency of chemical flooding, polymers are co-injected with the surfactant slug or after it. In both cases surfactant and polymer mixing is to be expected and effect of mixing should be examined. Several SP solutions were prepared and tested for core flooding experiments using sandstone cores. The viscosity measurements for solutions were tested at 300 psi and 195°F. Two set of samples are prepared with two different polymer types. The first set of samples was prepared from HPAM polymer (Flopaam 3630s) with specific type of amphoteric surfactant (more details about this chemical is given in Chapter IV). These samples were prepared at two polymer

concentrations 1,000 and 3,000 ppm. The second set of samples was prepared from AMPS type polymer (AN-125) with concentration of 3,000 ppm. Three samples were prepared in this set, one with no surfactant and the other two with two type of surfactants amphoteric and anionic. All the samples were prepared in seawater (**Table 3**).

Fig. 67 shows the effect of polymer type and concentration on viscosity of SP solutions used in core flood experiments. Two amphoteric surfactants are used with similar composition. The GS-series surfactant was modified from SS-series to lower adsorption and no significant difference is expected in the way these surfactants will impact the solution viscosity. However, when both solutions were prepared with 3,000 ppm polymer concentrations, the Flopaam 3630s shows higher viscosities compared to AN-125 at all shear rate tested in this experiment. The difference in viscosity is due to the difference in nature and size of the polymer molecules from both types. The Flopaam 3630s (HPAM) have molecular weight of $18X10^6$ Dalton whereas AN-125 (AMPS) have a molecular weight of $6X10^6$ Dalton. Solution prepared with 3,000 ppm Flopaam 3630s shows shear thinning behavior at all shear rates used in this experiment (10-100 s^{-1}). However, solution prepared at lower concentration (1,000 ppm of Flopaam 3630s) shows power-law fluid at low shear rates from 10 up to 50 s^{-1} after that it start showing more Newtonian behavior. Moreover, reducing the polymer concentration from 3,000 to 1,000 ppm caused reduction in viscosity between 75 and 80%.

Solutions prepared with AN-125 in concentrations 3,000 and 4,000 ppm show shear thinning at low shear rates and more Newtonian behaviors at higher shear rates. Increasing the concentration from 3,000 to 4,000 ppm caused a 65-74% increase in solution viscosity.

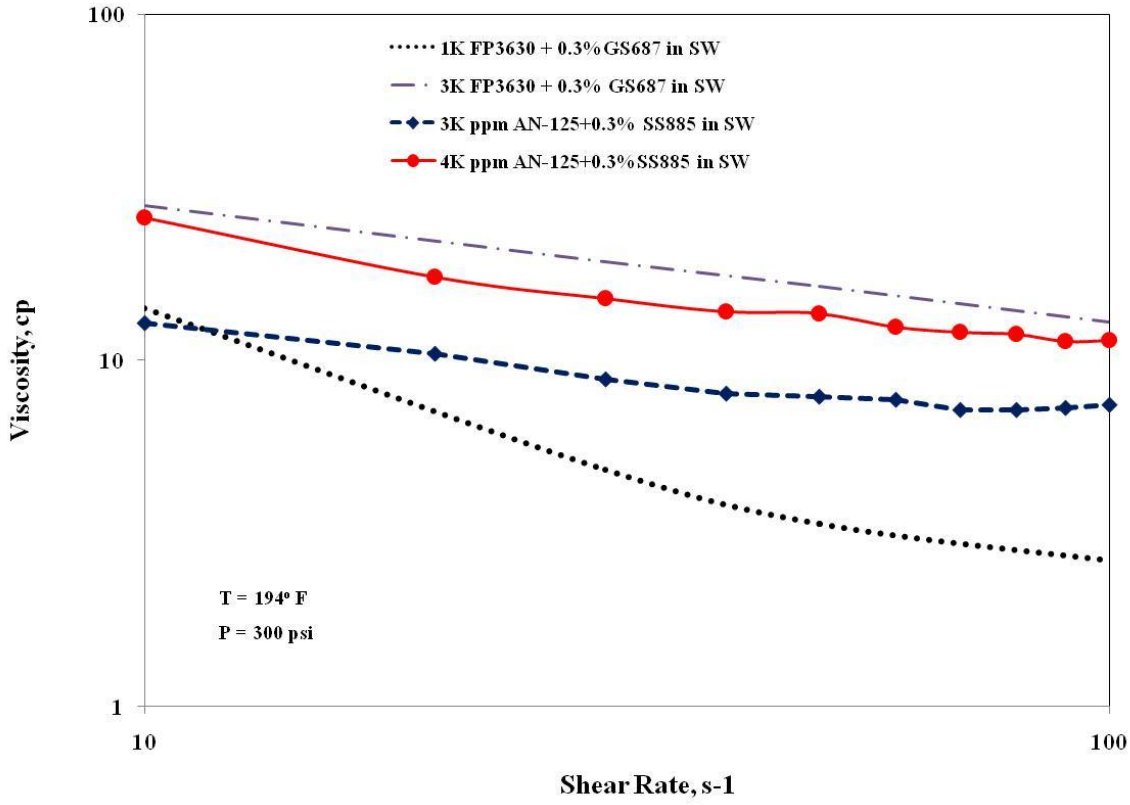

Fig. 67—Effect of polymer concentration and type on viscosity of several SP solutions prepared in seawater.

Fig. 68 shows the viscosity curves of SP solution having 3,000 ppm AMPS polymer and two types of surfactants, amphoteric (SS-885) and anionic (Petrostep C-1), with 0.3 wt% concentrations all prepared in seawater. There no difference between viscosity curve for polymer solution with and without amphoteric surfactant. Both solutions show non-Newtonian behavior (shear thinning). However, when anionic surfactant was added it showed viscosity reduction and Newtonian behavior at the shear rate tested. This finding is with agreement with observation by other researchers (Shup 1981; Nasr-El-Din et al. 1991). The effect of surfactant type on the viscosity of the chemical solution has a direct field implication. Since anionic surfactant cause a decrease in viscosity more polymer need to be added if SP solution is prepared with this type of surfactant. On the

other hand, amphoteric surfactant did not show any negative impact on viscosity at these conditions which give it an advantage when designing chemical slug.

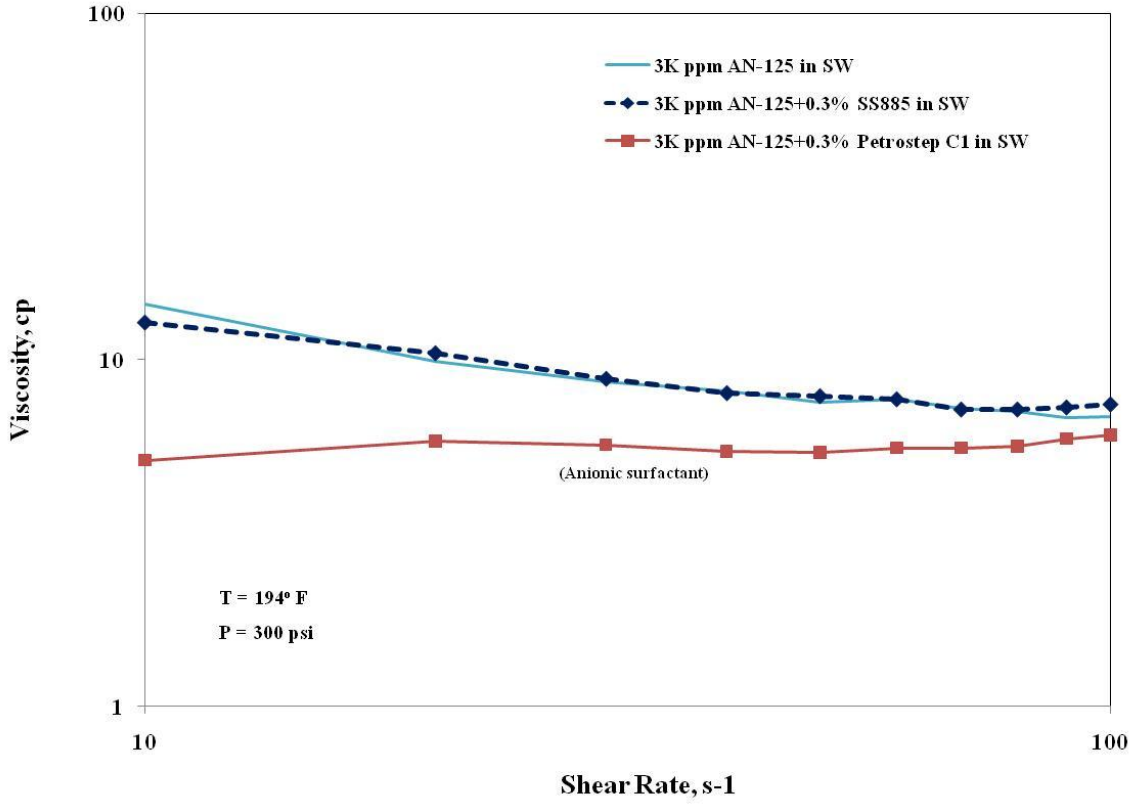

Fig. 68—Effect of surfactant type on the viscosity of the SP solution used for core flood experiments.

Conclusion

Based on the results obtained in this study the following conclusions can be drawn:

1. Adding the amphoteric surfactant improved the solvent viscosity.
2. Amphoteric surfactant did not have any effect on the viscosity of the solution when prepared in DW
3. Amphoteric surfactant increased the solution viscosity when prepared in saline water (1 & 6% NaCl).
4. Increasing salinity caused reduction in solution viscosity.

CHAPTER V
LOW-TENSION POLYMER FLOODING USING AMPHOTERIC SURFACTANT IN HIGH SALINITY/HIGH HARDNESS AND HIGH TEMPERATURE CONDITIONS IN SANDSTONE CORE

Summary

Surfactant-polymer (SP) flooding is one of the chemical EOR processes that is used to recover residual oil saturation. During the 80's BP proposed low-tension polymer flooding (LTPF) method to overcome some of the challenges caused by using high concentration of surfactant during some early SP flooding projects and to reduce the cost of operation. In high salinity/high hardness and high temperature application many chemical flooding methods would not be affective. Amphoteric surfactant shows high thermal and chemical stability in these environments and was evaluated in this study.

An experimental study was conducted to study the effect of two types of amphoteric surfactants, two types of anionic surfactants, and two types of polymers that are suggested to be used for high salinity / high hardness at elevated temperature on the performance of the low-tension polymer flooding (LTPF) process in recovering water flood residual oil. Surface and interfacial tension, zeta potential and core flood experiments were conducted to study the surfactant-polymer interaction at high salinity brine, ability of the solution to lower IFT, surface charge to predict chemical retention, tertiary oil recovery, oil cut and pressure drop during chemical propagation in the porous media. In this study Berea sandstone cores with 1.5 in. diameter and 20 in. length were used to determine the above parameters.

Amphoteric surfactant showed association with two types of polymers, HPAM and AMPS, that caused reduction in surface activity until polymer-free aggregate concentration was reached. Increasing polymer concentration increases the surfactant concentration needed to reach to polymer-free aggregate concentration. When HPAM polymer used in preparing chemical slug, it shows higher injectivity decline compared to

AMPS. Anionic surfactant showed less chemical retention due to the negative surface charge on Berea sandstone particles when this type of surfactant is used. No recovery was obtained during surfactant flooding, which prove that IFT reduction can't improve recovery without the aid of mobility control by polymers.

Introduction

Surfactant-polymer flooding of oil reservoir has been conduct by either using different injection schemes, where surfactant slug is injected and followed by mobility buffer behind the main surfactant slug to maintain its integrity or by mixing the two chemical together to get the synergy of both process. The other approach to vary different surfactant-polymer operation is by varying chemical concentration specially the surfactant. Division of this process due to surfactant concentration result of two types of process: Low-tension polymer flooding (LTPF) with low surfactant concentration and micellar-polymer process for higher surfactant concentration (Shah and Schechter 1977, Austad et al. 1994; Kalpakci et al. 1990).

Usual concentration of surfactant has been used in range of 2-5 wt% with polymer above 1,000 ppm (Austad et al. 1994). In this high chemical concentrations with high salinity environment can increase phase separation possibility, which require high concentrations of alcohol to prevent it (Austad et al. 1994; Kalpakci et al. 1990). In some cases two surfactants were used with these high concentration formulations, which result in high cost complicated system. Kalpakci et al. (1990) suggested a new approach to cost effective chemical flooding process called: low tension polymer flood (LTPF). This method was proposed to overcome some of the issues raised from using usual SP flooding process. The proposed method gains its applicability from its simplicity where low chemical concentration eliminates the phase separation or some of the unfavorable interactions between the surfactant and polymer, which exclude the need for alcohol; this will also reduce the cost. In case of LTPF, surfactant concentration ranges between 0.025 – 1 wt.% (Austad et al. 1994). Advantages of using LTPF are the following: the

process is cost effective, minimize incompatibility between surfactant and polymer, and simplify the process by reducing the chemical required.

One of the concerns when the surfactant-polymer technology is used is the interaction between these two chemicals. Surfactant-polymer interaction (SPI) can sometimes result in an unfavorable condition that diminishes the effectiveness of the process and can cause negative impact on the whole process. The interactions between surfactant molecules and synthetic polymers in aqueous solutions affects the rheological properties of solutions, adsorption characteristics at solid-liquid interfaces, stability of colloidal dispersions, the solubilization capacities in water for separately soluble molecules, and liquid-liquid interfacial tensions (Nagarajan 2001). When polymer and surfactant mutually exist in a solution one or more of the following forms can be found (Nagarajan 2001):

1. Single dispersed polymer molecules.
2. Single dispersed surfactant molecules.
3. Intermolecular complexes between polymer and surfactant molecules.
4. Surfactant aggregates.

When some type of surfactants are introduced to the solution that have polymer, surfactant molecules have the tendency to associate with the polymer molecule, which can affect the adsorption process of the surfactant to the solution-oil interface and diminish its ability to reduce the IFT. One of the methods used to study the surfactant-polymer association is the surface tension at different surfactant and polymer concentrations (Nagarajan, 2001). This method can be used to determine the when polymer free aggregate are formed and solution shows high surface activity, more discussion of this will be given in coming section.

Wang et al (2010) discussed the development and the evaluation 5 group of surfactants to attain an ultra-low IFT values. These surfactants were evaluated to stability at high temperature, high salinity, high hardness and environmental issues. They found that betaine type surfactant showed the best tolerance and ability to improve recovery without the need to include alkalis. Stournas (1984) proposed the use of

amphoteric surfactant for enhanced oil recovery and used Arabian medium crude oil in his study. The surfactant was tested at salinity of 200,000 ppm of totaled dissolved salts with cation ratio of Na^{+}:Ca^{2+}:Mg^{2+} = 10:2:1.

Polymers are added to viscosify the displacing fluid to improve mobility ratio to favorable values (Sorbie 1991; Green and Willhite 1998). During transport of chemicals in porous media chemicals interact with reservoir component including polymer. These interactions will cause retention of the polymer solution that result in lower viscosity than the injected fluids (Sorbie 1991). Polymer retention reduces permeability that result in injectivity decline. Researchers observed three types of retention mechanisms: adsorption, mechanical entrapment, and hydrodynamic retention (Sorbie 1991).

Szabo (1979) conducted extensive work on adsorption and retention measurement on AMPS, HPAM, xanthan, and other types of polymer using Berea cores. He found a uniform retention of AMPS that indicate adsorption as the main retention mechanism; however, the dominant retention mechanism with HPAM was mechanical entrapment. He also, found that adsorption of HPAM at 2% NaCl was 3 times higher than AMPS, which was not sensitive to salinity.

Core flood analysis and calculation (Flaaten et al. 2008)

Chemical flood experiments were analyzed using the core parameter and measured pressure drops during the water flooding part of the experiment. The estimated values that were calculated are the viscosity of the chemical slug for better mobility control and to predict the pressure drop due to the permeability reduction by polymer. Fluid mobility (λi) is the ratio between effective permeability (Ki) and it's viscosity and is given by the following equation:

$$\boldsymbol{\lambda i} = \frac{\boldsymbol{Ki}}{\boldsymbol{\mu i}} \quad \text{.....(17)}$$

Mobility ratio (M) between displacing and displaced fluid for effective displacement should satisfy the following criteria M ≤ 1. Mobility ratio is given by the following equation:

$$\boldsymbol{M} = \frac{\boldsymbol{\lambda_{displacing}}}{\boldsymbol{\lambda_{displaced}}} \quad \text{.....(18)}$$

The mobility values were calculated from the water flooding stage of the core flood was determined using the end-point relative permeability at residual oil saturation (S_{orw}). The above calculation was used to estimate the apparent viscosity (μ_{app}) of the injected fluid. μ_{app} is estimated by the following equation:

$$\boldsymbol{\mu_{app}} = \frac{\mathbf{1}}{\boldsymbol{\lambda_{rel}}} = \frac{\mathbf{1}}{\boldsymbol{\lambda_o + \lambda_{aq}}} \quad \text{.....(19)}$$

To predict the pressure drop during chemical injection (ΔP_{slug}), a pressure drop ratio between estimated chemical flood and actual water flood (ΔP_{wf}) is given by the following equation:

$$\frac{\boldsymbol{\Delta P_{slug}}}{\boldsymbol{\Delta P_{wf}}} = \frac{\boldsymbol{k_{wf}/\mu_{wf}}}{\boldsymbol{k_{slug}/\mu_{slug}}} = \frac{\boldsymbol{k_{rw} R_k \mu_{slug}}}{\boldsymbol{\mu_{wf}}} \quad \text{.....(20)}$$

Chemical and polymer solutions injected during chemical flooding are non-Newtonian fluids that exhibit shear thinning behavior. Viscosity of the injected fluid is affected by the shear rate that is caused by fluid flow in the porous media. Shear rate (γ) of chemical solutions flowing in porous media is calculated using the following equation (Rojas et al. 2008, Gomaa and Nasr-El-Din):

$$\boldsymbol{\gamma} = \frac{\boldsymbol{v}}{\boldsymbol{\phi L}} \quad \text{.....(21)}$$

where ν is the Darcy velocity, m/s; ϕ is porosity, fraction; L is a characteristic length representative of the pore-scale velocity gradient, which can be calculated using the following equation

$$\boldsymbol{L = 0.05\, D} \quad \text{.....(22)}$$

where D is the average pore diameter; microns and can be estimated by taking the square root of the permeability in (in milliDarcy).

Resistivity factor (F_r), is given by the following equation (Nasr-El-Din et al. 1992, Pye 1964)):

$$\boldsymbol{F_r = \frac{(q/\Delta p)initial}{q/\Delta p}} \quad \text{.....(23)}$$

where q is injection rate cm^3/min and Δp are pressure drop along the core sample.

Experimental Studies

Materials

Berea sandstone cores were used to conduct this study. The core samples were cut in cynical shape with 1.5 in. diameter and length ranges between 17 to 20 in.

Formation brine and seawater were used in this study for injection into the core and aqueous solution preparation. Synthetic formation brine and seawater were prepared using compositions shown in **Table 8**. Sodium chloride, calcium chloride, magnesium chloride, sodium bicarbonate, and sodium sulfate were (ACS) reagent grade and obtained from Mallinckodt Baker, Inc. These salts and deionized water (resistivity = 18 MΩ□cm) were used to prepare seawater solution. Crude oil samples were used in this study. Crude oil samples were filtered using Berea sandstone and centrifuged before injected to the core sample.

Table 8—Sandstone Brine & seawater composition.

	Concentration, mg/L	
Ions	**SS Formation Brine**	**Seawater**
Na^{+}	54,400	16,877
Ca^{2+}	10,600	664
Mg^{2+}	1,610	2,279
Ba^{2+}	–	–
Sr^{2+}	–	–
HCO_3^{-}	176	193
Cl^{-}	107,000	31,107
SO_4^{2-}	370	3,560
CO_3^{-}	–	–
TDS	174,156	54,680
Viscosity (mPa.s)*	1.4022	1.1429
Density (g/cm^3)*	1.1151	1.0354

Four surfactants were used in this paper: two betaine-based amphoteric surfactants, supplied by Oil Chem. Technology, and two anionic surfactants one (Anionic ORS) (Oil Chem. Technology) second was Alpha-olefin sulfonate (Anionic PS C1) (Stepan). Two polymers were used in this study: partially hydrolyzed polyacrylamide (HPAM) and a copolymer of 2-acrylamido-2methyl propane sulfonate and acrylamide (AMPS) where both polymers were obtained from SNF. Description of each of the above chemicals is given in **Table 9**.

Table 9—Chemicals information used for low-tension polymer flooding in Berea sandstone cores.

	Chemical	Description
1	**Amph-GS**	Betaine based amphoteric surfactants that are formulated to give extremely low CMC values in order to reduce the amount of monomer surfactant present in the aqueous phase since monomers shows more adsorption than micelles. TDS >200,000 ppm, hardness > 2000 ppm, Temperature > 100°C.
2	**Amph-SS**	Betain based amphoteric surfactant, TDS >100,000 ppm, hardness > 1000 ppm, Temperature > 100°C.
3	**Anionic-PS C1**	Alpha-olefin sulfonate.
4	**Anionic-ORS**	alkyl aryl sulfonic acid, TDS < 30,000 ppm, hardness < 400 ppm, Temperature > 100°C.
5	**HPAM**	Flopaam 3630S , medium hydrolysis , high MW, standard polyacrylamide, 30 % anionic , MW : 18 millions.
6	**AMPS**	Flopaam AN125 Copolymer of acrylamide and 2-acrylamido 2-methyl propane sulfonate, 25 % anionic , MW : 6 millions (25 % sulfonated).

Surface tension

Surface tension measurements were done using the Wilhelmy plate technique at room temperature. Chemical solutions with different surfactant concentrations were evaluated.

Interfacial tension measurements

Details of dynamic IFT measurements were discussed in Chapter III.

Core flood studies

Experimental Set-up

A coreflood apparatus was designed and built to simulate fluid flow in porous media in the reservoir. The schematic diagram of the coreflood apparatus is shown in **Fig. 69**. Positive displacement pump, (ISCO 500 D syringe pump) equipped with a programmable controller, was used deliver fluids at constant flow rates at variable speeds up to 400 cm^3/min and pressure up to 2,000 psi. The pump is connected to three accumulators to deliver brine, oil or chemical solutions. Accumulators with floating pistons rated up to 3,000 psi. and 250^oF were used to store and deliver fluids. A set of valves were used to control the inject fluid into the core sample. The coreholder can accommodate a core plug with diameter of 1.5 inches and length up to 20 inches. Pressure transducers were used to measure the pressure drop across the core. The flow was upward to eliminate gravity segregation effects. Back pressure regulator was used to control the flowing pressure downstream of the core. A second back pressure regulator was used control the confining pressure on the core plug. Convection oven was used to provide temperature controlled environment. Data acquisition system was used to collect data from the pressure transducer.

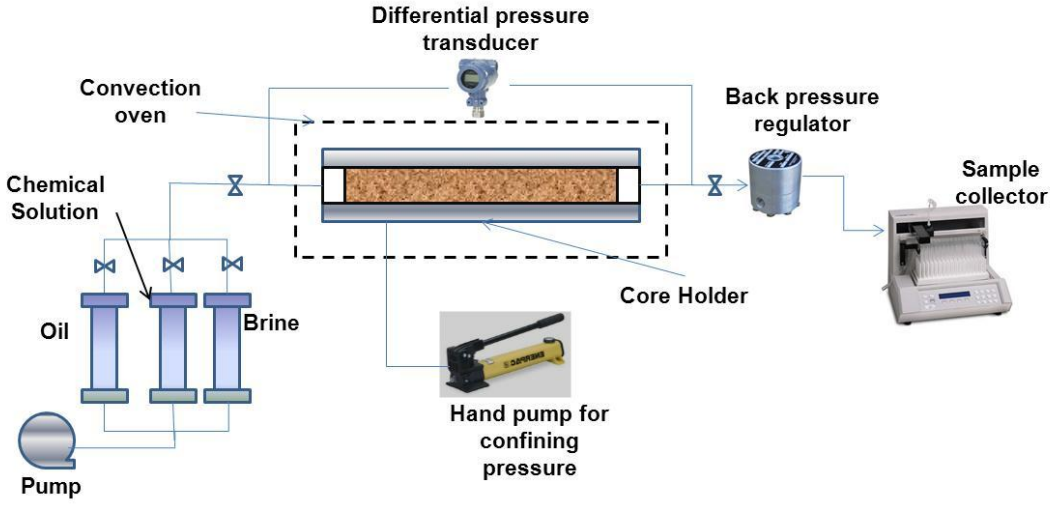

Fig. 69—Schematic for core flood set-up.

Procedure

Following are the steps for core preparation and core-flow experiments:

- Core samples were dried overnight in 100 ^{o}C oven.
- Core samples were vacuum saturated for 8 hours.
- Core sample was loaded to the core-holder and confining pressure was applied.
- From 5 to 10 PV of brine was injected to the core to establish 100% water saturation.
- Base permeability to water was measured using different flow rates (0.5, 1, 2, 4 and 8 cm^3/min).
- Crude oil flood to displace movable water and establish irreducible water saturation (S_{wir}).
- Determine relative permeability to oil at S_{wir}.
- Water flooding started as a secondary recovery and 2 pore volumes were injected to establish residual oil saturation.
- Chemical flooding started as a tertiary recovery and 0.5 to 2 pore volumes were injected.

- One pore volume of polymer buffer was injected behind the chemical slug to maintain its integrity.
- This was followed with chase brine injection.

Result and Discussion

Surfactant-polymer interaction

Surface tension measurement was used to study the amphoteric surfactant interaction with two types of polymers used in this study HPAM and AMPS. Two concentrations were used for each polymer type 1,000 and 3,000 ppm and surfactant concentration was varied between 0.0001 and 1 wt% in seawater. The objective of this experiment was to find the surfactant concentration range where the surface activity was diminished due to the adsorption or association of surfactant at the polymer molecules. When surfactant is associated or adsorbed to the polymer, it is not free in the solution so it loses its ability to adsorb to the interface and diminish the surface activity of the chemical solution. **Figs. 70 and 71** show effect of polymer concentration and type on the surface activity of the solution. When no polymer was used increasing surfactant concentration from 0.0001 to 0.005 wt% caused the surface tension to drop from 66 to 34.5 dyn/cm and stays close to this value for the rest of concentrations. The surfactant concentration where surface tension starts leveling is the critical micelle concentration (CMC). When 1,000 ppm polymer was added surface tension was higher since the surfactant was associated with the polymer and not active any more, until all polymer molecules are saturated and any increase in surfactant concentration start forming free aggregate in the solution (this is called polymer-free aggregates) and as a result low surface tension values was observed close to the values when CMC was reached. Further increase polymer concentration to 3,000 ppm caused an increase polymer-free aggregate concentration to higher value. Increasing the polymer concentration, increases the amount of molecules that associate with the surfactant and increase the amount of surfactant needed to saturate all the polymer molecules. This increases the amount of surfactant needed exceed the polymer-free aggregate concentration. In both solutions with different polymer type and

concentration of 3,000 ppm was used in seawater the polymer-free aggregate concentration was less than 0.1 wt.% of surfactant. For design reason surfactant concentration should be more than this value. In this study the surfactant concentration of 0.3wt% was used to be away from the polymer-surfactant association.

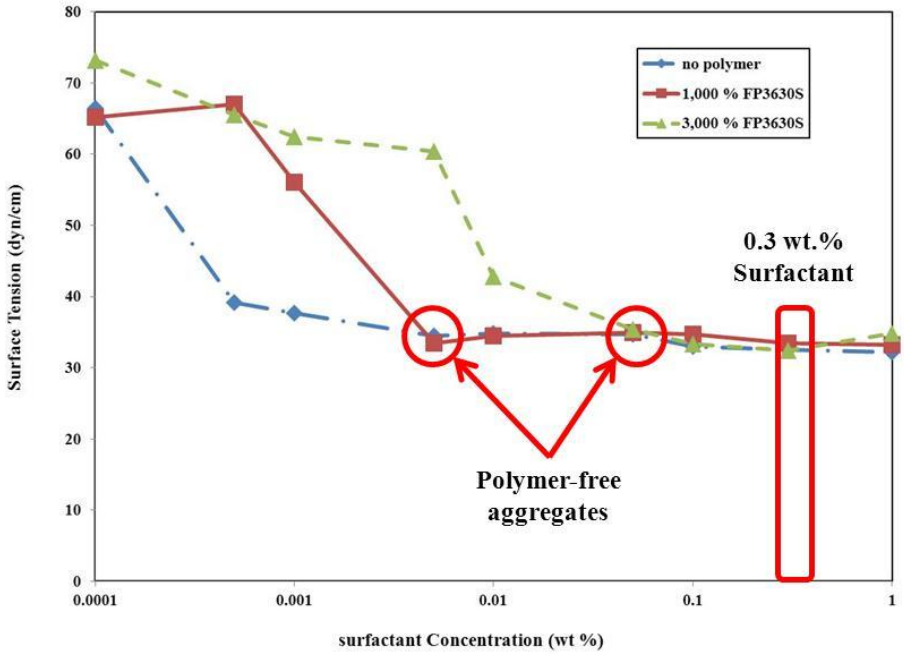

Fig. 70—Effect of polymer concentration on surface activity of amphoteric surfactant (Amph-SS).

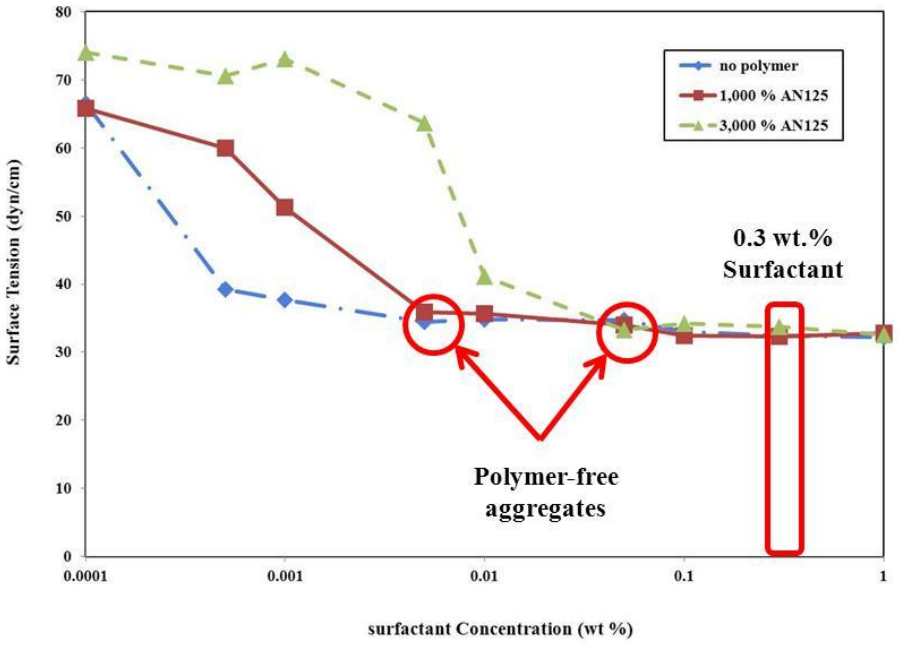

Fig. 71—Effect of polymer type on surface activity of amphoteric surfactant (Amph-SS).

Interfacial tension experiments

Interfacial tension experiments were conducted for the two amphoteric surfactant and two polymer types HPAM and AMPS. Two solutions with different HPAM polymer concentrations were prepared and tested with Amph-GS surfactant. **Fig. 72** shows the IFT as a function of time of crude oil against various solutions with 0.3 wt% Amph-GS surfactant in seawater, and from 0 to 3,000 ppm HPAM polymer. At no polymer added to the solution it shows a dynamic IFT behavior with minimum IFT value at 0.0008879 dyn/cm then IFT increased to equilibrium at 0.02056 dyn/cm. As can be seen in the figure there is no big change in the final equilibrium IFT, however, there is difference in the IFT values with time. Increasing solution viscosity by increasing polymer concentration caused the minimum IFT values to increase and the time to reach to equilibrium IFT becomes longer. Increasing the aqueous phase viscosity increases the mass transfer resistance, which controls the diffusion process and affects the adsorption

and desorption rate of the surfactant to and from the solution-oil interface (Taylor and Nasr-El-Din 1996). The equilibrium IFT did not show significant difference and ranged between 0.022 and 0.045 dyn/cm.

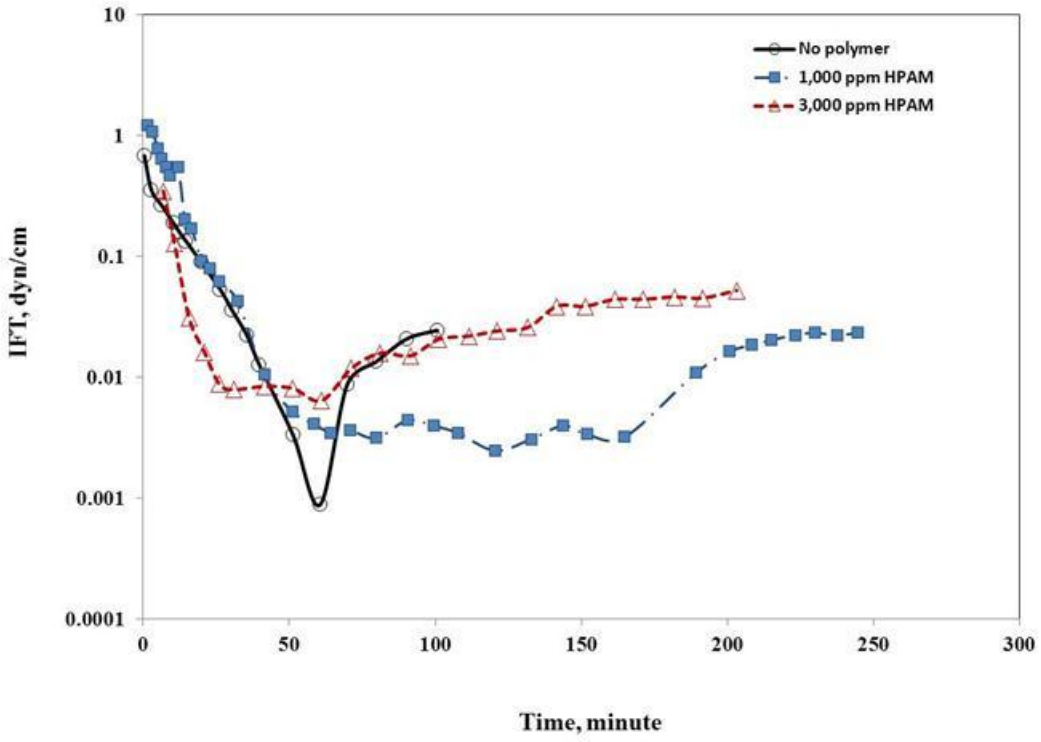

Fig. 72—Effect of HPAM polymer concentration on interfacial tension. The solution contains 0.3 wt.% of Amph-GS surfactant prepared in seawater.

Fig. 73 shows the effect of polymer type on the IFT behavior when Amph-GS is used to prepare solution. Two polymers are used in this study AMPS and HPAM. These polymers have different molecular weight and when added to solution they will give difference in solution viscosity. HPAM has MW of $18X10^6$ and AMPS has MS of $6X10^6$. HPAM gives higher viscosity than the AMPS when same concentrations are used to prepare the solution. In the figure the increase in viscosity caused increase in the minimum IFT and gradual increase in IFT with time to reach equilibrium when polymer

was added to the solution. On the other hand, solution without polymer shows a more rapid increase in the IFT values since it has less viscose solution. The equilibrium values for this set of solutions ranges between 0.025 and 0.046 dyn/cm.

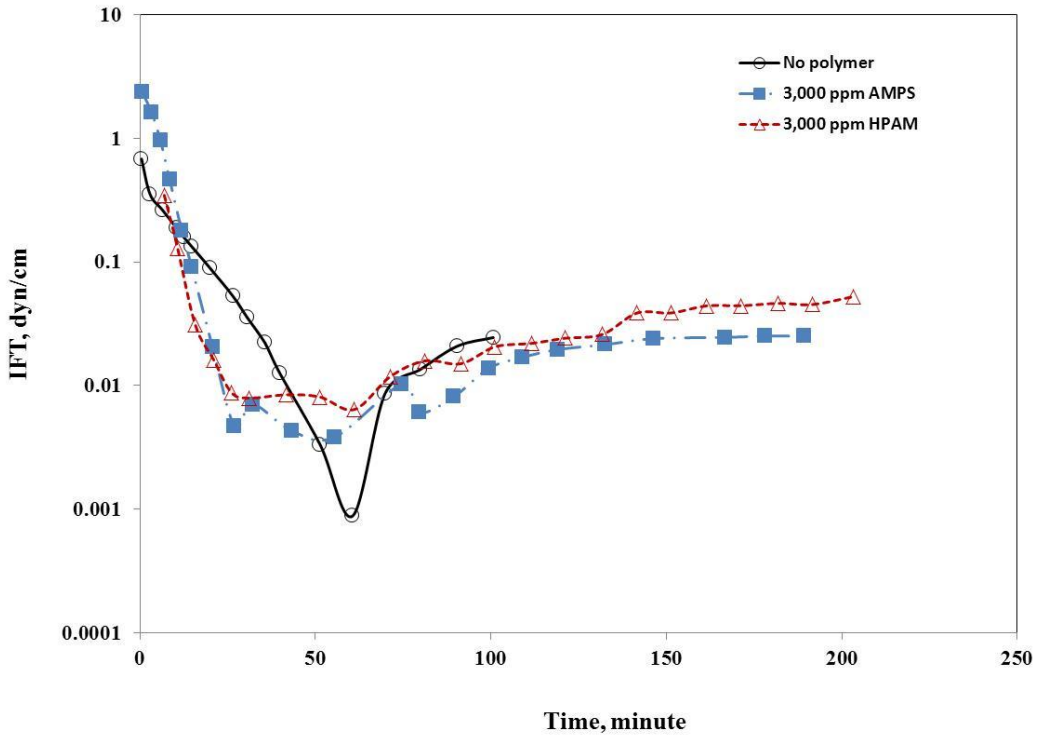

Fig. 73— Effect of polymer type (HPAM & AMPS) on interfacial tension. The solution contains 0.3 wt.% of AMPH-GS prepared in seawater.

Fig. 74 shows the IFT for solutions prepared with 0.3 wt% Amph-SS surfactant prepared in two polymer types with concentration of 3,000 ppm of polymer and no polymer solution. All three solutions showed dynamic IFT with most clear one when no polymer was added. The equilibrium IFT values ranged between 0.051 to 0.072 dyn/cm.

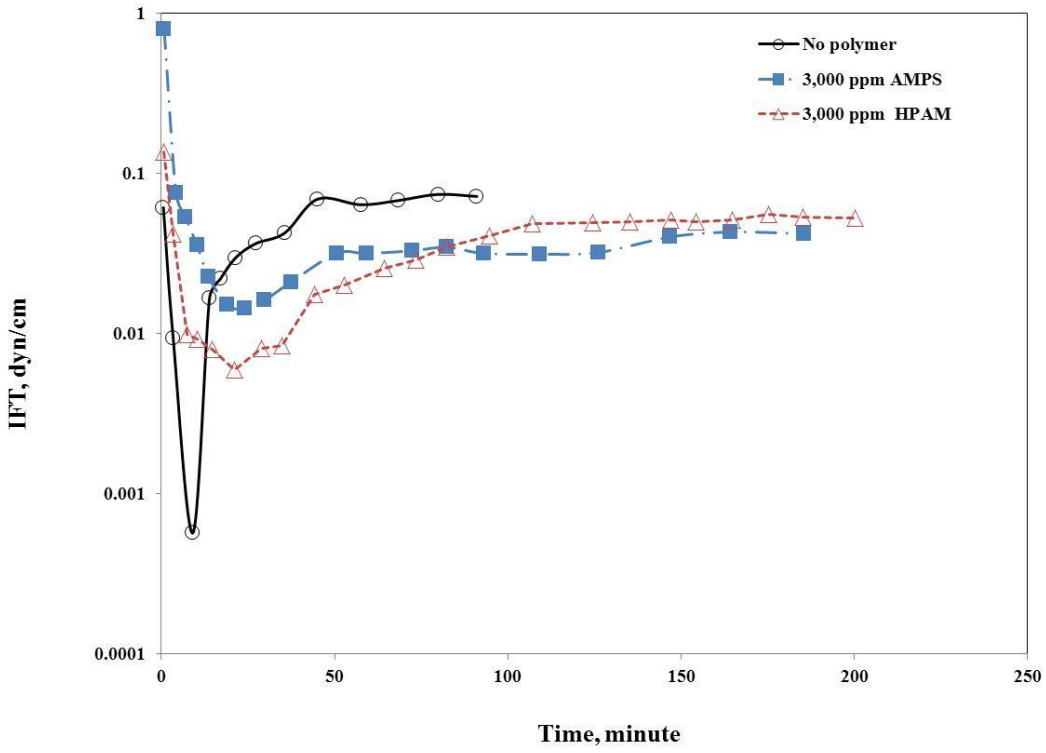

Fig. 74—Effect of polymer type (HPAM & AMPS) on interfacial tension. The solution contains 0.3 wt.% of AMPH-SS prepared in seawater.

Core flood studies

In this study 7 chemical flooding experiments were conducted to study LTPF in recovering oil for residual oil after water flooding. All chemical flooding experiments were conducted in tertiary mode at residual oil saturation (S_{or}). Cores information used in this study are given in **Table 10**. Chemical formulations for core flood experiments 1 to 5 are given in **Table 11**.

Table 10—Berea sandstone core information used for low-tension polymer flooding.

Core number	BSS-20	BSS-18	BSS-16	BSS-9	BSS-8	BSS-11	BSS-12
Core flood #	1	2	3	4	5	Ext-1	Ext-2
Length (cm)	50.8	50.8	50.8	50.8	50.8	50.8	43.18
Diameter (cm)	3.718	3.718	3.718	3.713	3.71	3.635	3.658
Porosity (%)	18.4	18.1	18.4	19.0	18.5	19.5	19.6
Permeability (md)	113.5	77.7	96.9	112	77.0	120.1	91.3

Table 11—Chemical formulation for low-tension polymer flooding in Berea sandstone cores (1-5).

Core flood	Stage	Alkali Type	Alkali Conc., Wt.%	Surfactant Type	Surfactant Conc., Wt.%	Polymer Type	Polymer Conc., ppm	Mixing Brine Type
1	**Chemical Slug**			Amph-GS	0.3	HPAM	1,000	Seawater
	Polymer Slug					HPAM	1,000	Seawater
2	**Chemical Slug**			Amph-GS	0.3	HPAM	3,000	Seawater
	Polymer Slug					HPAM	3,000	Seawater
3	**Chemical Slug**			Amph-SS	0.3	HPAM	3,000	Seawater
	Polymer Slug					HPAM	3,000	Seawater
4	**Chemical Slug**			Amph-SS	0.3	AMPS	3,000	Seawater
	Polymer Slug					AMPS	3,000	Seawater
5	**Chemical Slug**			Anionic-PS	0.3	AMPS	3,000	50% Seawater
	Polymer Slug					AMPS	3,000	50% Seawater

Core Flood-1

This experiment was conducted to study the performance of new class of amphoteric surfactant to recover oil from Berea sandstone cores at high salinity high temperature conditions. First, 2.15 pore volume (PV) of formation brine was injected during the secondary recovery stage at constant flow rate of 0.3 ml/min. Oil recovery start stabilizing at 1.17 PV and total oil recovery at this stage was 34% OOIP. This was followed with 0.5 PV of chemical slug stage that consist of 0.3 wt% AMPSurf#1 and 1,000 ppm of HPAM polymer prepared in seawater. One pore volume of polymer drive of 1,000 ppm HPAM was injected behind the chemical slug to maintain the integrity of the chemical stage ahead of it.

Fig. 75 shows the oil cut and cumulative oil recovery as a function of core cumulative effluent value during different injection stages. Oil cut was high during the early stage of water flooding then dropped to zero with small oil pockets coming in late stages. No extra oil was recovered in the later stages of the water flood indicating that all mobile oil was recovered and residual oil saturation was reached. During SP injection the oil cut was zero. However, oil cut between 0 and 7.2% started during polymer injection and continuous during the chase brine stage. The discontinuous production of the oil bank indicates that no clear and sharp oil bank was formed. Three things should be noticed during recovery related to oil bank formation; first when the oil production was initiate in reference to chemical injection initiation. Second thing that should be observed is the oil cut percentage. Last thing to be observed is the period it takes for the oil production from beginning to end. Tailing of oil production can be a result of bad displacement or early water breakthrough. An indication of a favorable displacement should be sharp increase oil cut that start as soon chemical injection started. Bataweel et al. (2011b) studied the formation and propagation of oil bank in Berea sandstone using different chemical flooding processes with similar formulation and chemicals used in this study. They found that in this type of rock with similar permeability range used in this study that recovery was dominated with the fluid flow in the porous media and that the formation of flow channels will result in limited recovery and will affect the formation a sharp oil bank.

Oil production in this experiment started at 2.75 PV, which is 0.60 PV after chemical flood was initiated. Oil production seized at 4.19 PV with total oil recovery of 39.22% during this experiment. Oil recovered during tertiary mode was 7.74% of remaining oil after water flooding.

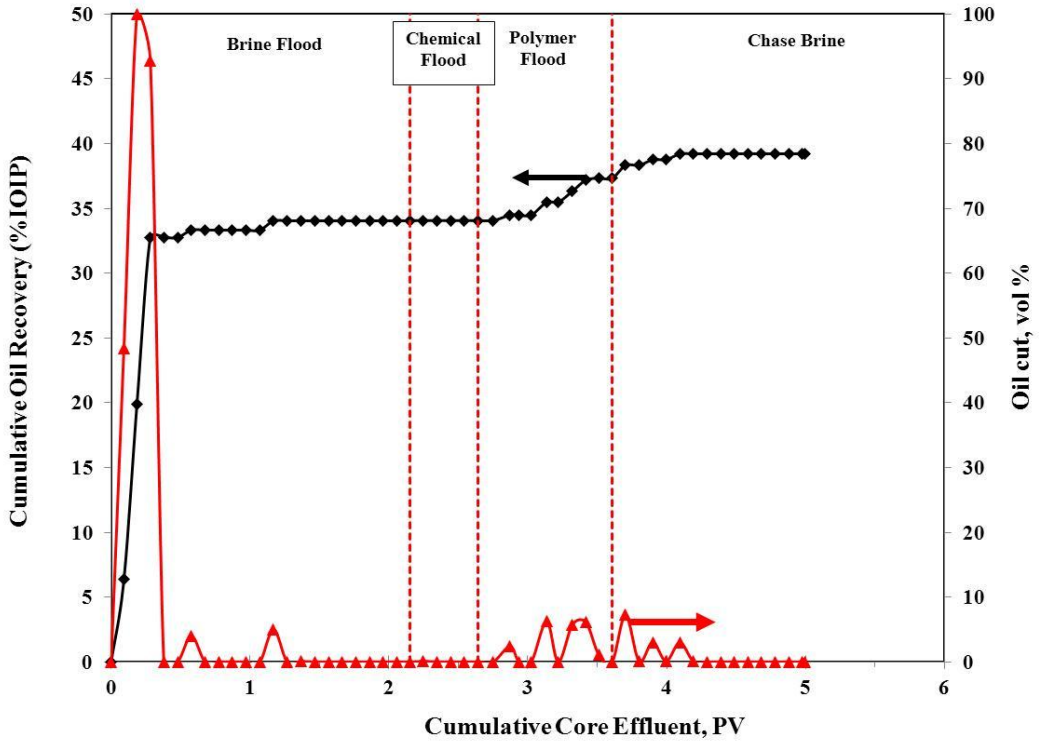

Fig. 75—Core flood-1 history for slug having 1,000 ppm HPAM polymer, 0.3 wt.% Amph-GS surfactant in seawater.

Core Flood-2

In this experiment the amount of polymer was increased to 3,000 ppm to improve the oil displacement by improving the mobility. Polymer losses a lot of its viscosity when prepared in seawater due to high salinity and high divalent cations this require more polymer to be added to the chemical formulation to increase the viscosity. The same formulation and injection scheme used in the first experiment except the change in the polymer concentration. Oil recovery of 34.14% OOIP was achieved after injecting 1.914 PV of formation brine during the water flooding phase (**Fig. 76**).

Fig. 76 depicts the flood history for chemical flood process for the second experiment. Chemical injection started at 1.914 PV with slug size of 0.5 PV. First oil cut started 0.38 PV after chemical slug was initiated at 2.295 PV during SP injection and continuous during polymer and chase-brine injection. A more distinct oil bank was produced in this experiment compare to the first one with oil cut ranging between 4 and 11.9%. Total oil recovered during this experiment was 48.4% OOIP. The oil recovery during the tertiary mode was 21.58% of remaining oil after water flooding. Increasing the polymer concentration improved the chemical invasion to the core and helped to increase the amount of oil contacted by the chemical solution and resulted in improvement in the recovery during the tertiary phase. However, higher pressure was needed to inject this formulation more discussion about the pressure profile for the two first experiments will be discussed in the coming section. **Fig. 77** shows the effect of increasing polymer concentration on the oil recovery. HPAM concentration was increased from 1,000 to 3,000 ppm, which reflected on an increase in recovery from 7.8 to 21.6 % of residual oil saturation. The enhancement in recovery can be explained by an increase in the pressure gradient during chemical injection caused by higher viscosity of the chemical slug. Discussion of pressure profile of the two experiments are given in the following section.

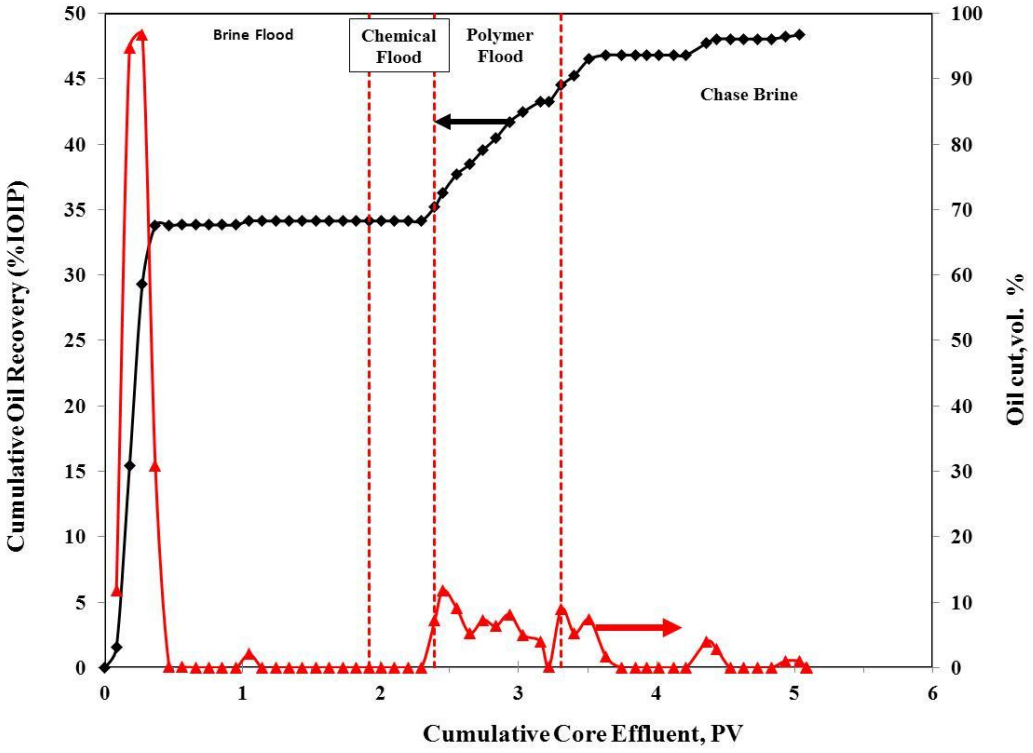

Fig. 76—Core flood-2 history for slug having 3,000 ppm HPAM polymer, 0.3 wt.% Amph-GS surfactant in seawater.

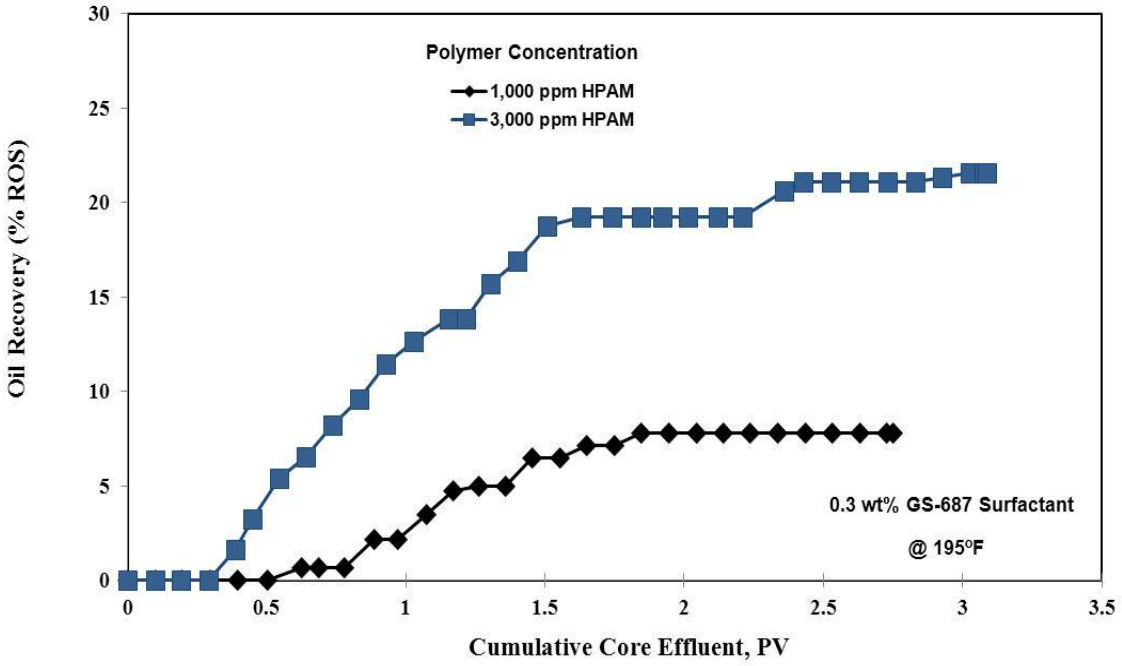

Fig. 77—Improvement in oil production during tertiary recovery mode by increasing polymer concentration .

Effect of polymer concentration on pressure drop

Fig. 78 shows the pressure profile of the experiment 1 and 2 were polymer concentration of HPAM (Flopaam-3630s) was changed from 1,000 to 3,000 ppm. In this figure the pressure is normalized to the stable pressure drop during water flooding as a function of core cumulative effluent. In analyzing this figure two pressure behaviors should be noticed; pressure during chemical injection (surfactant-polymer and polymer) and pressure drop during initial and final brine injection. Pressure during chemical injection is important since the success of any flooding operation should guaranty the ability to inject chemical solution into the reservoir. Loss on injectivity resulted in chemical EOR failure and termination of some of the field pilot tests (Austad et al 1994). The increase in pressure drop in the final brine injection gives an indication of the chemical entrapment in the cores either by size exclusion or adsorption. Residual pressure drop was 7.3 and 4.0 times the initial water flooding stage for high and low polymer

concentrations, respectively. AMPS shows better chemical stability at high salinity/high hardness brine at elevated temperature (Doe et al.1987; Moradi-Araghi et al. 1987; Seright et al. 2010).

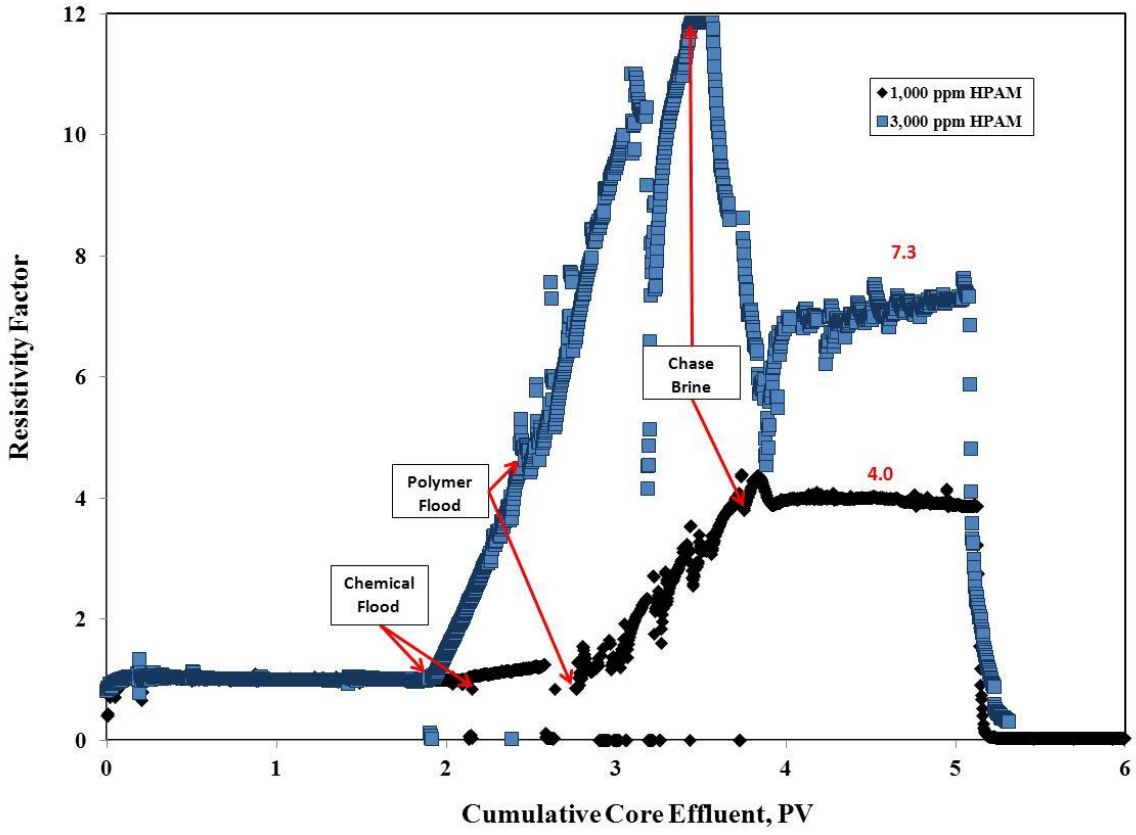

Fig. 78—Increase of polymer concentration caused an increase in the pressure profile during chemical and chase brine injection.

Core Flood-3

In this experiment different type of amphoteric surfactant was evaluated with HPAM polymer. The chemical solution composed of 0.3 wt% AMPSurf#2 and 3,000 ppm HPAM polymer. Same injection scheme was followed as previous experiments. **Fig. 79** shows the core flood history for the third experiment, during secondary recovery phase 25.7% of oil was produced after injecting 1.92 PV of formation brine. Chemical flood

was started and some oil was produced in this stage, however the oil bank was initiated at 2.4 PV and continued until 3.8 PV. The oil cut during oil production varied between 3.0 and 12.6% with an average value 5.22%. Total oil produced in this experiment was 37.4% . The recovered oil during the chemical EOR process was 16% which is less than the first surfactant. The figure in page 131 depicts the pressure profile of this experiment and shows similar behavior as the second experiment with same polymer type and same concentration, more discussion about the pressure performance will be given in coming section.

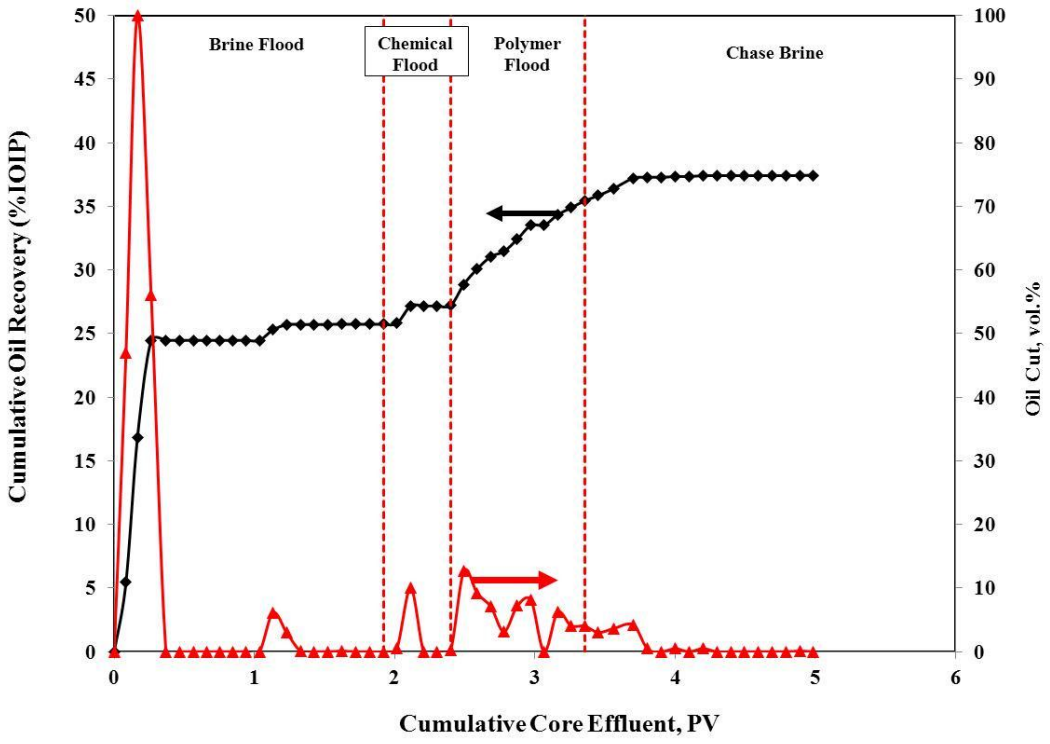

Fig. 79—Core flood-3 history for slug having 3,000 ppm HPAM polymer, 0.3 wt.% Amph-SS surfactant in seawater.

Effect of surfactant type on oil recovery

Fig. 80 shows the improvement in recovery by using the modified amphoteric surfactant (Amph-GS) compared to (Amph-SS) surfactant. This indicates that reducing surfactant adsorption will improve chemical propagation in the core that reflects on higher recovery. Recovery improved from 16.1 to 21.6 % by this improved surfactant.

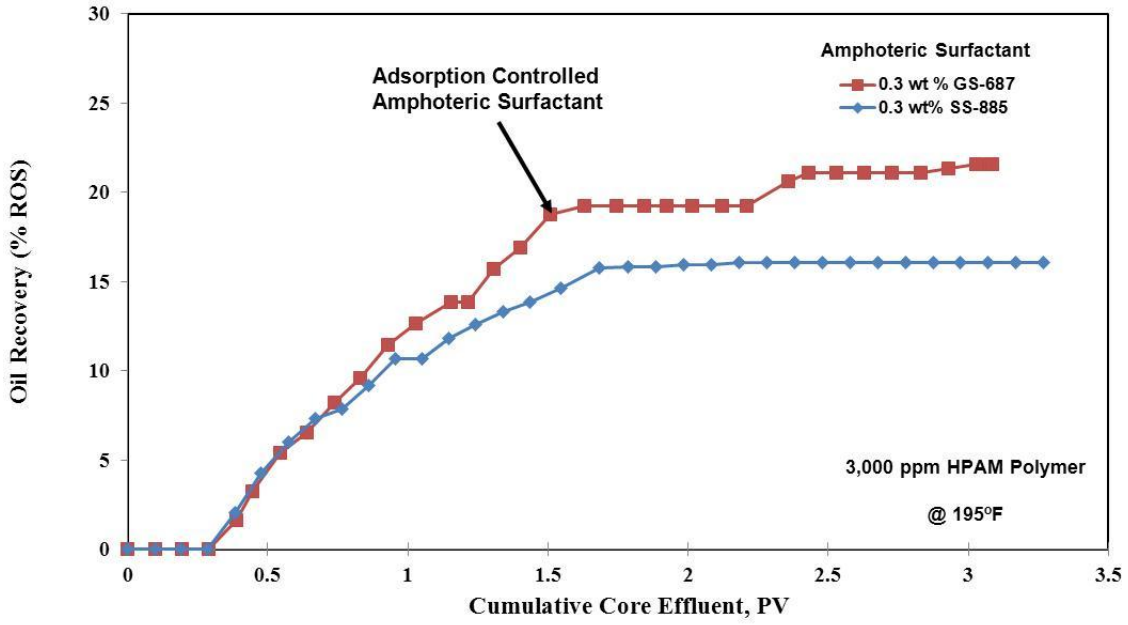

Fig. 80—Improved amphoteric surfactant shows higher oil production during tertiary recovery mode compared to standard amphoteric surfactant using HPAM polymer in both solutions.

Core Flood-4

In this core flood 3,000 ppm of AMPS polymer was used to replace the HPAM. Similar injection scheme was followed in core flood-3. **Fig. 81** shows the oil recovery and oil bank at different flooding stages. Chemical injection was initiated at 1.80 PV and first oil production started by chemical flooding was at 2.16 PV. The oil bank flowed for 0.73 PV with an average oil cut of 7.78%. The oil cut ranged between 1 and 20 during oil bank production. Total oil recovered during secondary and tertiary phase was 41.6%

with 32.1% by water flooding. The incremental oil recovered during the EOR process was 14 %, which is close to the oil produced with formulation using HPAM. One observation worth noticing is that the oil bank in the fourth experiment was produced in shorter time with higher concentration. This is favorable production mode from economical point of view. Pressure profile for this experiment and previous one will be discussed in the coming section.

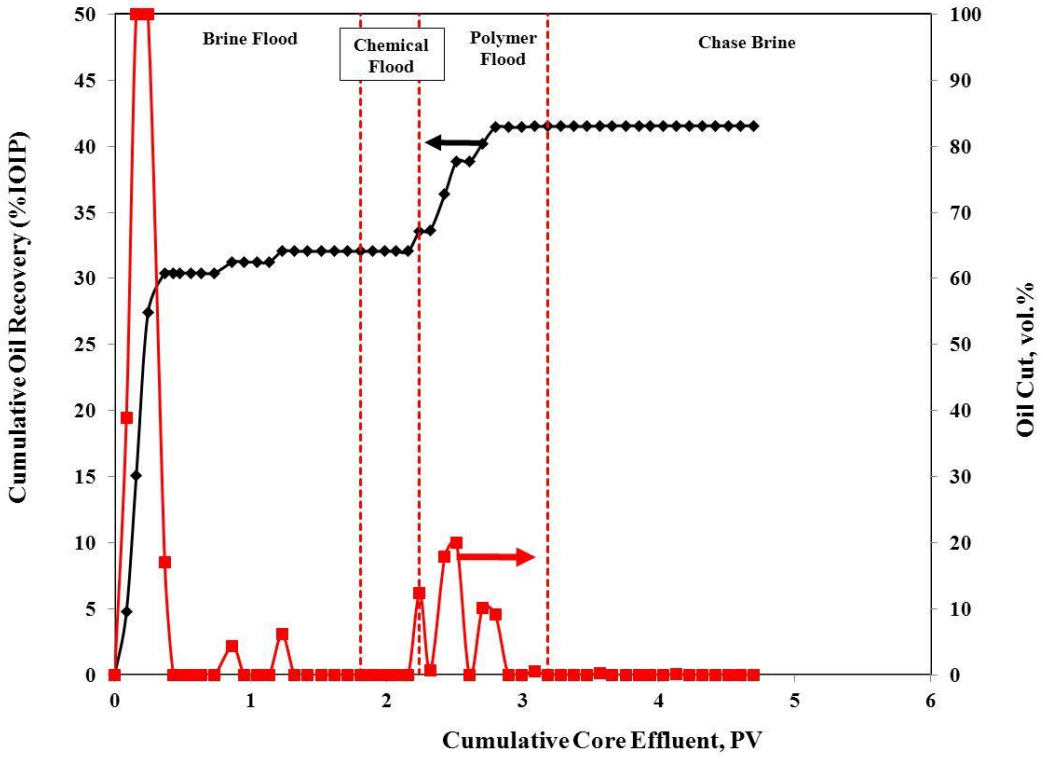

Fig. 81—Core flood-4 history for slug having 3,000 ppm AMPS polymer, 0.3 wt.% Amph-SS surfactant in seawater.

Effect of polymer type on pressure drop

In this work two types of polymer were used with different molecular weights (MW). First polymer was HPAM with 18 M Dalton and AMPS with 6 M Dalton. **Fig. 82** plots the pressure profile during water, chemical and chase flooding with same surfactant

formulation with change in the polymer type. Polymer concentration was 3,000 ppm for the two core flood experiments. As can been seen the two polymers showed similar pressure profile during chemical flooding. However, the AMPS with smaller MW showed less residual damage with an increase in pressure drop by 2.5 times compare to 7.5 when HPAM was used. The above discussion shows that AMPS have better injectivity characteristics that will allow more chemicals to be injected to the reservoir and more successful operation.

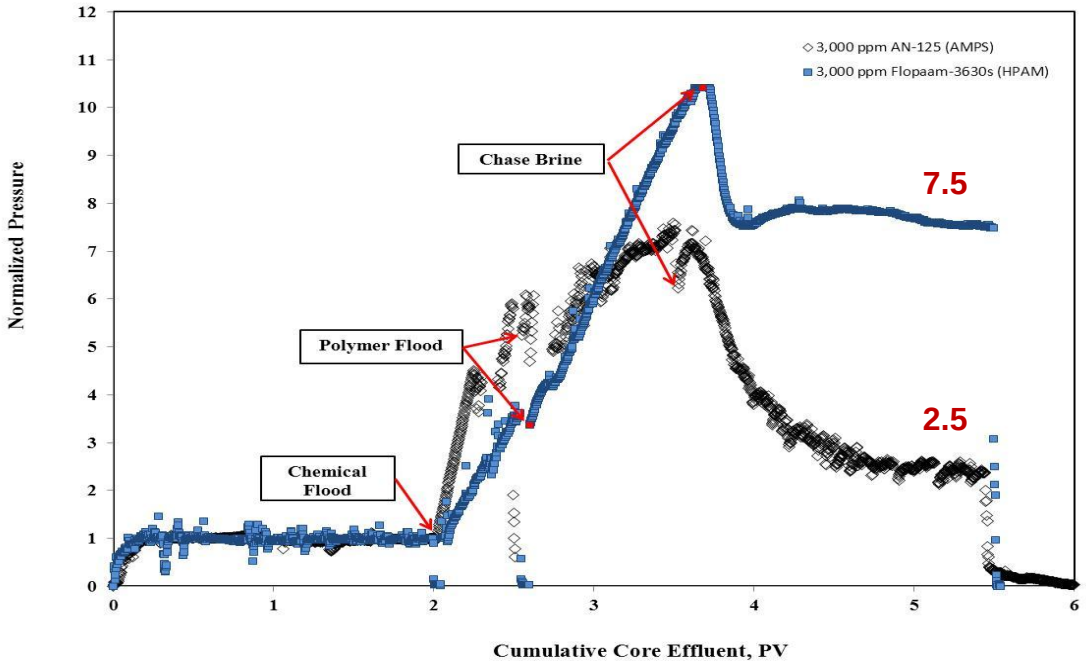

Fig. 82—Polymer with larger molecule size (HPAM) did not affect significantly the pressure profile during chemical injection but resulted in more pressure drop during chase brine injection as an indication of polymer trapping by either size exclusion or adsorption.

Core Flood-5

In this experiment anionic surfactant was used as a replacement amphoteric in the previous core floods. Surfactant concentration was 0.3wt% with 3,000 ppm of AMPS polymer. In this experiment seawater was used in water flooding stage instead of

formation brine as in previous experiment. This precaution is taken to avoid any surfactant precipitation when it get mixed with high salinity formation brine also 50% diluted seawater was used to mix chemical slug to avoid any negative interaction. Anionic surfactant used in this experiment to compare it with amphoteric surfactant, since anionics are the most used surfactants in chemical injection studies and field cases.

Fig. 83 depicts the history of the core flood experiment. Oil recovery during the water flooding stage was 28.3%. Chemcal injection started at 1.95 PV and total of 2 PV of SP chemical stage was injected. Oil bank start form at 2.13 PV and continued to flow until 3.14 PV with an average oil cut of 8.85%. The total produced oil with secondary and tertiary recovery was 43.1% with 20.6% recovered by EOR from remaining oil.

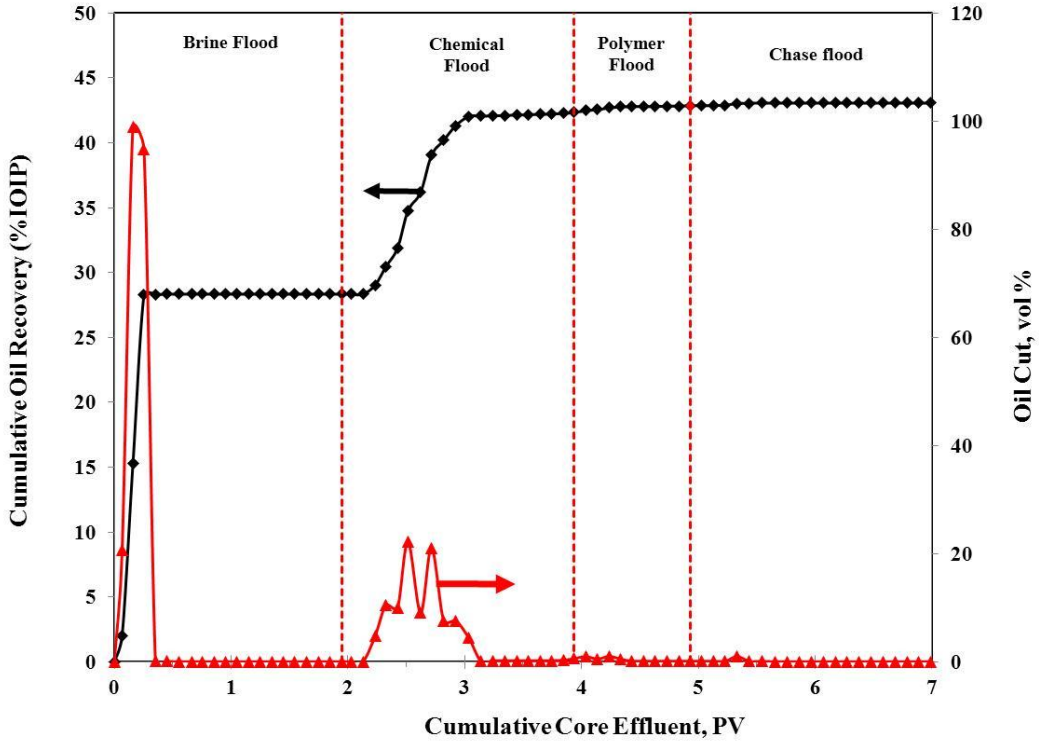

Fig. 83—Core flood-5 history for slug having 3,000 ppm AMPS polymer, 0.3 wt.% Anionic-PS surfactant in seawater.

Fig. 84 shows the pressure profile during different stages of core flooding experiment. The pressure profile in this experiment shows different profile compared to other experiment since 2 pore volumes of the chemical solution was injected into the core compare to 0.5 PV on the previous experiment. In this experiment the initiation, propagation and end of the oil bank happened during the chemical injection stage, not like other experiment where the oil bank starts at the end of the chemical slug and continues during the polymer and chase flood stage. The most important observation in this run is the final residual pressure during chase fluid injection, pressure values was close to the pressure drop during the water flooding stage with value of 1.13 normalized pressure. This can be explained by the low adsorption of the surfactant in the chemical solution in this experiment since anionic surfactant is negatively charged which is similar to the charge on the sandstone cores used in this experiment. On the other hand, amphoteric surfactant have positive and negative charge which is less negative when compared to the anionic surfactant, this can result to higher adsorption on the sandstone rock (Schramm et al. 1991). To study the charges on the Berea sandstone particles at seawater and in expectance of surfactant, zeta potential was measured using anionic and amphoteric surfactant prepared in seawater. **Table 12** shows that Berea sandstone particles were negatively charged when was submersed in anionic surfactant solution, and was positively charged at amphoteric surfactant solution.

Table 12—Zeta potenial for Berea sandstone particles at different surfactant solutions prepared in seawater.

Solution	Zeta potential
Seawater	-14.3
0.3 wt% AMPSur-2 in seawater	10.2
0.3 wt% Anionic-1 in seawter	-21.5

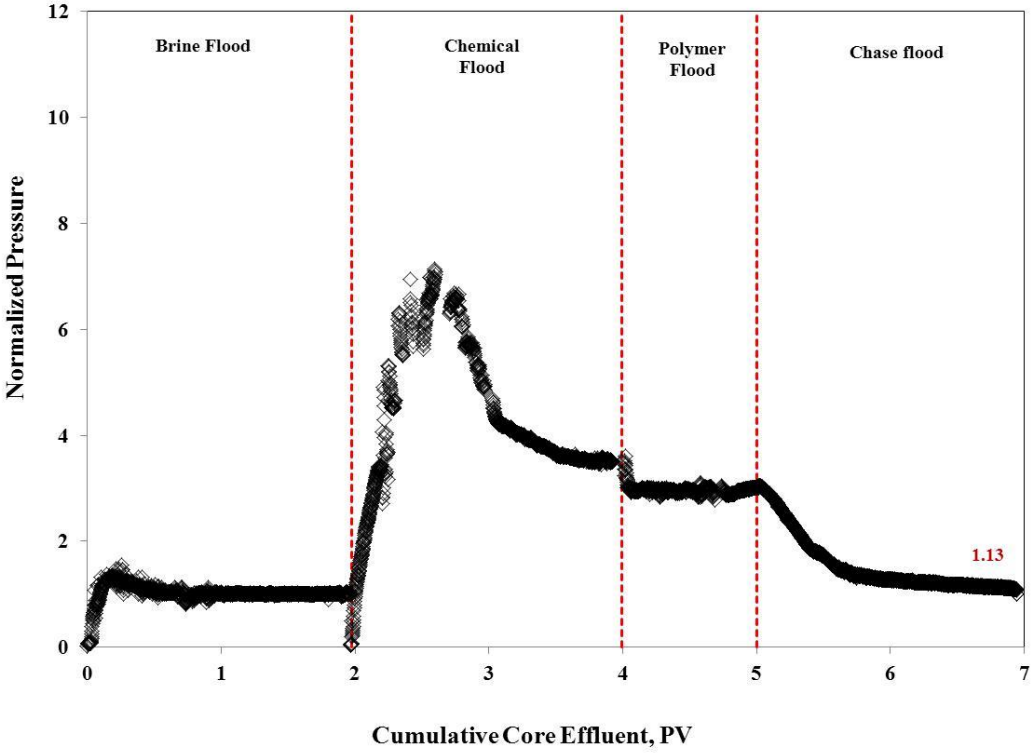

Fig. 84—Normalized pressure profile during different stages of Core Flood-5. The solution contain 0.3 wt.% Anionic-PS, and 3,000 ppm AMPS polymer prepared at 50% seawater. Relative injectivity reached close to original value.

Extended core flood experiments

Two extended core flood experiments were conducted to study the effect of different chemical flooding schemes on the recovery enhancement. Different chemical recipes were used in these experiments to evaluate the total recovery process and the impact by each formulation.

Core Flood-Ext-1

Table 13 gives the experiments steps and chemical solution used in each step. In this core flood experiment, 9 injection stages were pumped into the core. These stages were divided to 4 main injection periods: water flooding, 1st chemical flood that include main

SP slug with amphoteric surfactant followed by polymer then chase brine, 2nd chemical S slug with higher amphoteric surfactant concentration followed with lower polymer concentration injection 2,000 ppm, 3rd chemical injection period that start with injecting the core with 3 wt% NaCl to recondition the porous media by lowering the salinity and get rid of divalent cations, because the injected SP stage contain anionic surfactant that have low tolerance to salinity and hardness.

Table 13—First extended core flood experiment (Ext-1).

#	Stage	Formulation	Injected PV
1	**Water flooding**	SS brine	2
2	**Chemical Flood-1 (SP)**	0.3 wt% SS-885(S); 3,000 ppm AN-125 (P) in Seawater	1
3	**Polymer Flood-1 (P)**	3,000 ppm AN-125 (P) in Seawater	1
4	**Chase Flood-1**	SS-Brine	1
5	**Chemical Flood-2 (S)**	0.6 wt% SS-885 (S)	0.3
6	**Polymer Flood-2 (P)**	2,000 ppm AN-125 (P) in Seawater	1.5
7	**Chase Flood-2**	3 wt% NaCl brine	2.3
8	**Chemical Flood-3 (SP)**	0.5 wt% ORS-43 (S); 3,000 ppm AN-125 (P) in 3 wt% NaCl Brine	1.9
9	**Chase Flood-3**	3 wt% NaCl brine	0.9

Fig. 85 gives the injection history of the experiment and cumulative oil produced with each injection stage. Recovered oil during water flooding stage was 35.9% after injecting 2.07 PV of formation brine. Total oil recovery increased to 42.3% after 1st chemical set was injected to the core. No oil was produced when 0.6 wt% amphoteric surfactant was injected. This is with an agreement with Bataweel et al. (2011b) using the same surfactant at room temperature. In their work they visualize the surfactant flood using CT scan technology and found that the injected surfactant did not form an oil bank. The surfactant flood was followed by 1.5 PV of 2,000 ppm AMPS polymer with no oil recovered. Last set of chemical flooding was started with reconditioning the core

by injecting 3% NaCl, this was necessary since the SP flood that was planned to follow was containing surfactant that have low tolerance to salinity and hardness. The SP slug was prepared in 3% NaCl to avoid surfactant complexation with divalent cations that can cause surfactant precipitation. Oil recovery improved significantly when this formulation was used and reached to 70.7% with recovery of 44.3% of remaining oil after water flooding due to chemical EOR process. A total of 1.9 PV of SP solution was injected in this stage and was followed with chase brine injection using 3%NaCl. Although this formulation showed a high potential but has two disadvantages: first, using this surfactant in high salinity/high hardness environment requires removing the divalent cations from the formation by extensive injection proper brine composition which adds more operation and capital cost to the project, and the inefficiency of divalent cations removal in reservoir scale (Murtada and Marx 1982; Hamaker and Franzier 1978). Second, the surfactant-polymer solution showed separation with the upper phase showing formation of viscous phase (**Fig. 86**). This chemical recipe was not pursued any further since it was showing some separation when kept for several days. The separated solution was having a high viscosity and can cause retention of chemicals and that can result in loss of injectivity.

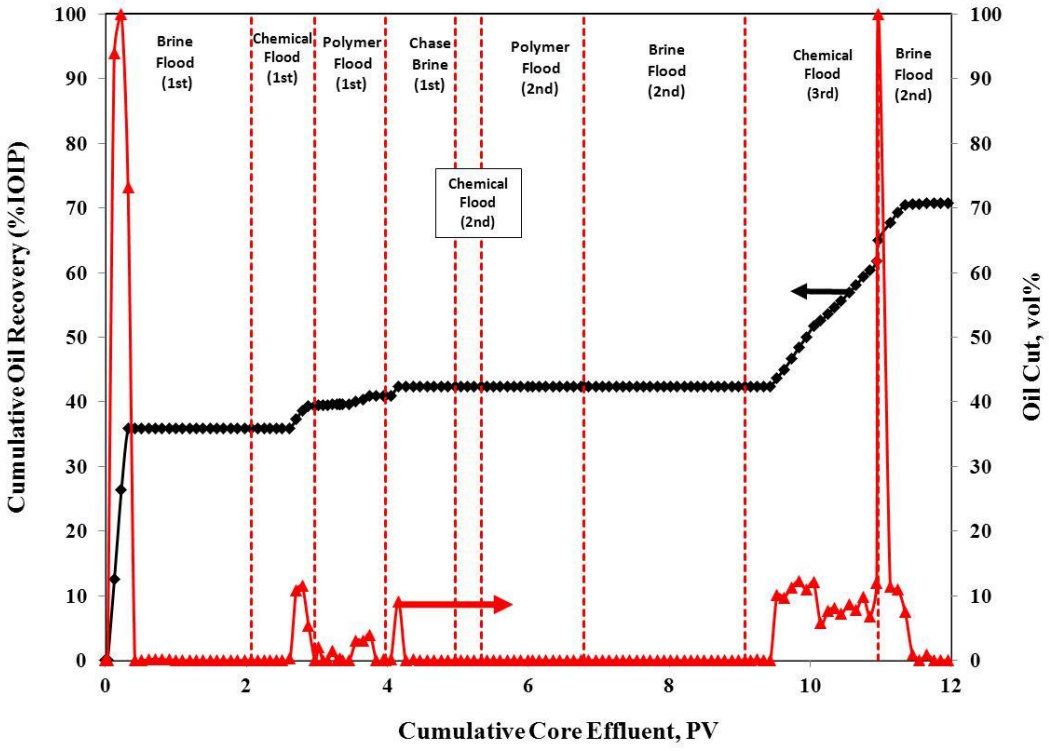

Fig. 85—Flood history for First extended core flood (Ext-1).

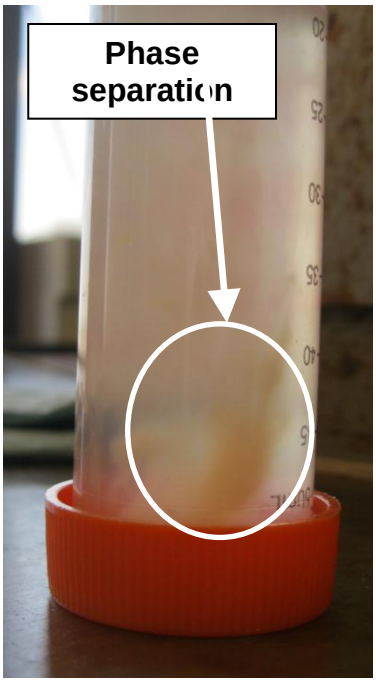

Fig. 86—Surfactant-polymer phase separation due to incompatibility in 3wt% NaCl brine.

Core Flood-Ext-2

Fig. 87 the second extended core flood experiment was conducted to study the injection of more tolerant anionic surfactant at high salinity/high hardness brine in the formation and while mixing. In this experiment two set of chemical flooding was injected to the core; first one SP solution prepared with amphoteric surfactant prepared in 50% diluted seawater followed with polymer flood prepare in 50% seawater. The second set more tolerant anionic surfactant was used and prepared with 50% seawater. Seawater was used during water injection in this experiment a total of 1.84 PV was injected with oil recovery of 37.5%. **Table 14** shows the chemical formulation for different chemical injection stages.

Chemical flood using the amphoteric surfactant increased the recovery to 41.4% after injecting 1.4 PV oil bank formed and propagate during chemical injection. No oil was recovered during polymer and chase fluid flooding. Insignificant improvement in

recover was gained when 1.5 PV of the second chemical formulation was injected and recovery increased to 45%.

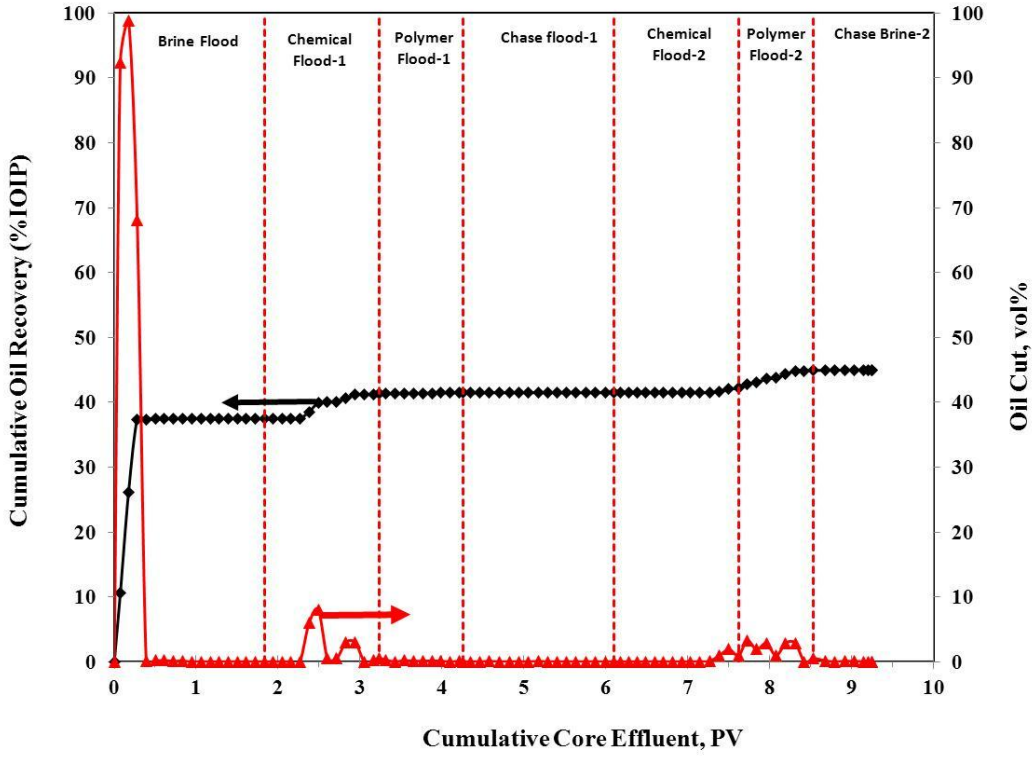

Fig. 87—Flood history for second extended core flood (Ext-2).

Table 14—Second extended core flood experiment (Ext-2).

#	Stage	Formulation	Injected PV
1	**Chemical Flood-1 (SP)**	0.3 wt% SS-885(S); 3,000 ppm AN-125 (P) in 50% Seawater	
2	**Polymer Flood-1 (P)**	3,000 ppm AN-125 (P) in 50% Seawater	
3	**Chase Flood-1**	Seawater	
4	**Chemical Flood-2 (SP)**	0.3 wt% Petrostep C-1 (S); 3,000 ppm AN-125 (P) in 50% Seawater	
5	**Polymer Flood-2 (P)**	3,000 ppm AN-125 (P) in 50% Seawater	
6	**Chase Flood-2**	Seawater	

Conclusions

Based on the results obtained in this study the following conclusions can be drawn:

1. .Amphoteric surfactant shows association with the two types of polymers used in chemical flooding HPAM and AMPS that result in reduction surface activity in low surfactant concentration.
2. Increasing the polymer concentration increased the polymer-free aggregate concentration.
3. Increasing the HPAM polymer concentration from 1,000 to 3,000 ppm resulted in improving oil recovery this was reflected on better oil bank formation.
4. Increasing polymer concentration resulted in higher pressure drop during chemical injection and permanent reduction in injectivity when formation brine was initiated as chase flooding.
5. AMPS polymer shows less injectivity loses compared to HPAM.
6. Surfactant-polymer solution prepared with anionic surfactant showed better injectivity characteristics with less chemical retention compared to SP solution prepared with amphoteric.
7. Zeta potential measurement shows that anionic surfactant increased Berea sandstone particle negative charge in seawater, which means less chemical

adsorption. Compared to amphoteric surfactant which shows positive values indicating more chemical adsorption at rock surface.

8. Amphoteric surfactant flooding without polymer did not show any oil recovery.
9. Alkyl aryl sulfonate anionic surfactant showed higher recovery but need to get rid of divalent cations in the formation and during chemical solution preparation. It showed surfactant-polymer complexation that can cause

CHAPTER VI
ASP VS. SP FLOODING IN HIGH SALINITY/HARDNESS AND TEMPERATURE IN SANDSTONE CORES

Summary

Chemical flooding methods are used to recover residual oil left after water flooding. Several chemical flooding processes has been used to improve recovery: surfactant-polymer (SP), low-tension polymer flooding (LTPF), and alkaline-surfactant-polymer flooding (ASP). When working high salinity/ high hardness reservoirs each of above processes will interact differently with reservoir component and will give different recovery results.

An experimental study was conducted to examine different type of chemical flooding technologies on the oil recovery of the water flooded residual oil, formation and injectivity decline of each technology. Two Anionic, two amphoteric surfactant, two alkalis and two types of polymers were used in this work to formulate the different chemical solutions.

ASP formulation prepared with anionic surfactant showed the best oil recovery compared to other chemical flooding processes. Although solutions prepared with amphoteric surfactant shows the least IFT values they did not give the highest recovery. ASP solution prepared using organic alkali showed similar recovery when compared to high concentration surfactant formulation.

Introduction

Chemical flooding is one of the processes used in enhanced oil recovery (EOR). It involves injection of a specific chemical formulation that will effectively displace remaining oil. Chemical EOR is used to achieve one or more of the following microscopic displacement mechanisms: interfacial tension (IFT) reduction, wettability alteration, and mobility control (Zhang. 2005; Green and Willhite. 1998; Taber et al. 1997). Surfactant-polymer (SP) and alkali-surfactant-polymer (ASP) are among the

chemical flooding processes that show potential in recovering residual oil after water flooding. Residual oil saturation can reach up to 60% of the original oil in place after water flooding (Thomas and Ali 2001). Significant recoveries were reported in some of the field cases using SP (Kalpakci et al. 1990; Bragg et al. 1982; Ferrel et al. 1987) and ASP process. For successful displacement of trapped oil by chemical flooding, chemical slug should achieve the following (Hirasaki et al. 2008; Levitt et al. 2009; Flaaten et al. 2010):

1. Achieve and maintain the ultra-low IFT during the displacement process.
2. Improve mobility control for microscopic and macroscopic displacement.
3. Compatibility with mixing and formation brine to prevent surfactant precipitation or separation in presence of high concentration of divalent cations.
4. Low surfactant adsorption at the reservoir rock.
5. Compatibility between surfactant and polymer to minimize separation, complexation and retention.

Poor field performance of alkali flooding is caused by: consumption of the alkali in the reservoir that prevents deep propagation, low acid content in some oils that will not cause enough reduction in the IFT due to lack of in-situ generated soap, and lack of mobility control in viscous oil or heterogeneous reservoirs (Nasreldin et al. 1994). ASP is a modification on the alkaline flooding process by adding synthetic surfactant to the chemical solution to raise the optimum salinity where middle phase emulsion or micro-emulsion forms and to compensate for the shortage of in-situ generated soap in low-acid content oil (Nelson et al. 1984; Nasr-el-Din et al. 1992; Arihara et al. 1999). The solution resulted from this modification showed a significant improvement in oil recovery and the introduction of the ASP process (Nelson et al. 1984; Nasr-el-Din et al. 1992). In ASP, co-injection of synthetic surfactant with in-situ generated soap, by interaction of alkali with natural acids in the oil, results in low IFT values (Li et al. 2003). The generated and synthetic surfactant adsorbs to the oil-solution interface forming mixed micelle that result in ultra-low IFT. Ultra-low IFT at the oil-solution interface emulsifies and mobilized residual oil in the reservoir (Li et al. 2003). Second

contribution to alkali to the flooding process is the introduction to higher OH^- concentration that adsorbs to rock surface and increases the negative charges. The negatively charged surface reduces the adsorption of anionic surfactants (Liu et al. 2008) used in chemical flooding and affect the wettability by increasing the double layer (Nasralla et al. 2011; Zhang 2005). Alkali helps to cut chemical cost by introducing in-situ surfactant and lowering surfactant consumption by adsorption.

Shen et al. (2009) conducted an ASP flooding experiment using 3-D physical model of a vertical heterogeneous reservoir. They conclude that physio-chemical interaction such as adsorption, retention, and emulsion of ASP solution caused flow resistance and pressure increase. This increase in pressure caused fluid flow to change direction from high-permeability zone to low and middle-permeability layers.

The scaling problem caused by ASP injection in the Daqing pilot site was discussed by Wang et al. (2004). In the pilot test production wells in Daqing, scale was found in the wellbores and pumps, which resulted in a shutdown period of 114 days to replace and check the affected pumps, after that frequent pump malfunctions occurred from scale accumulations. Serious scale problems were found on the ground collecting and gathering system such as ground pipe walls, oil transferring stations, multipurpose stations, oil/water separating system, produced water disposal system, valves, pump heads, and flowmeters. Flateen et al. (2008) proposed sodium metaborate as a weaker alkali to avoid problems caused by strong alkalis in the ASP floods. The sodium metaborate shows a promising result and more tolerance to hard ions. Berger and Lee (2006) evaluated organic alkalis to replace inorganic alkalis and found that they can be mixed with similar chemicals used to formulate ASP with more tolerance for high-salinity and high-divalent cations concentrations. In our work we will investigate using these alkalis to reduce the negative impacts caused by interactions by strong alkalis. For detailed discussion about SP flooding see Chapter V.

Experimental Studies

Materials

Berea sandstone cores were used to conduct this study. The core samples were cut in cynical shape with 1.5 in. diameter and length ranges between 15 to 20 in.

Formation brine and seawater were used in this study for injection into the core and aqueous solution preparation. Synthetic formation brine and seawater were prepared using compositions shown in **Table 1 (Chapter V)**. Sodium chloride, calcium chloride, magnesium chloride, sodium bicarbonate, and sodium sulfate were (ACS) reagent grade and obtained from Mallinckodt Baker, Inc. These salts and deionized water (resistivity = 18 MΩ□cm) were used to prepare seawater solution. Crude oil samples were used in this study. Crude oil samples were filtered using Berea sandstone and centrifuged before injected to the core sample.

Four surfactants were used in this paper: two betaine-based amphoteric surfactants, supplied by Oil Chem. Technology, and two anionic surfactants one (Oil Chem. Technology) second was Alpha-olefin sulfonate (Stepan). Two polymers were used in this study: partially hydrolyzed polyacrylamide (HPAM) and a copolymer of 2-acrylamido-2methyl propane sulfonate and acrylamide (AMPS) were both polymer were obtained from SNF. Description of each of the above chemicals is given in **Table 15**.

Table 15—Chemicals information used for ASP and SP flooding in Berea sandstone cores.

	Chemical	Description
1	**Amph-GS**	**GreenSurf-687**. Betaine based amphoteric surfactants that are formulated to give extremely low CMC values in order to reduce the amount of monomer surfactant present in the aqueous phase since monomers shows more adsorption than micelles. TDS >200,000 ppm, hardness > 2000 ppm, Temperature > 100°C.
2	**Amph-SS**	**SS-885**. Betain based amphoteric surfactant, TDS >100,000 ppm, hardness > 1000 ppm, Temperature > 100°C.
3	**Anionic-C1**	**Petrostep C-1**. Alpha-olefin sulfonate.
4	**Anionic-S2**	**Petrostep S-2**. Light internal olefin sulfonate.
5	**HPAM**	**Flopaam 3630S** , medium hydrolysis , high MW, standard polyacrylamide, 30 % anionic , MW : 18 millions.
6	**AMPS**	Flopaam **AN-125** Copolymer of acrylamide and 2-acrylamido 2-methyl propane sulfonate, 25 % anionic , MW : 6 millions (25 % sulfonated).
7	**Na_2CO_3**	Sodium carbonate
8	**Organic alkali**	**OA-100**, sodium salt of polyaspertic acid

Interfacial Tension Measurements.

For more details of this measurements see Chapter V.

Core Flood Studies.

For more information about core flood studies see Chapter V.

Result and Discussion

Interfacial tension measurement

Fig. 88 shows the IFT measurement for different solutions used for the core flood experiments. As can been seen there is two group of IFT curves. One with higher IFT values and these samples are prepared using anionic surfactant. The other group, which is showing lower IFT values are prepared using amphoteric surfactant. The two curves

that are showing the least IFT values are ASP samples prepared with Na_2CO_3 and organic alkali. The two alkalis helped reduce IFT values.

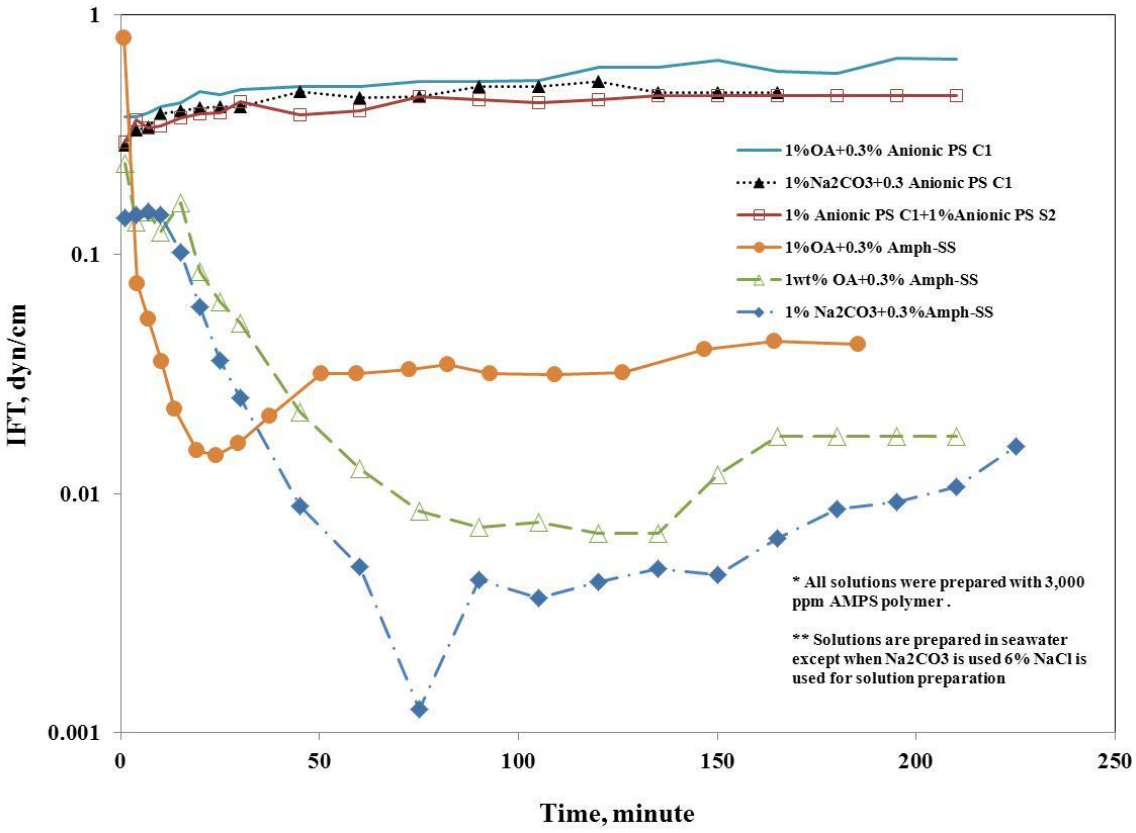

Fig. 88—IFT measurement for chemical solution used in core flood experiments.

Core flood studies

In this study 7 chemical flooding experiments were conducted to study SP and ASP flooding to recover oil from residual oil after water flooding. The first three experiments were discussed in Chapter V and discussed again for easier comparison with new core flood experiments. All chemical flooding experiments were conducted in tertiary mode at residual oil saturation (S_{or}). Cores information used in this study are given in **Table 16**. Chemical formulations for core flood experiments are given in **Table 17**.

Table 16—Berea sandstone core information used for ASP and SP flooding.

Core number	BSS-18	BSS-9	BSS-8	BSS-10	BSS-13	BSS-19	BSS-17
Core flood #	2	4	5	9	10	11	12
Length (cm)	50.8	50.8	50.8	50.8	39.1	40.3	39.1
Diameter (cm)	3.718	3.713	3.71	3.66	3.71	3.73	3.64
Porosity (%)	18.1	19.0	18.5	19.3	18.7	18.3	19.6
Permeability (md)	108.9	157	108.0	166	124.6	133.7	202.0

Table 17—Chemical formulation for ASP and SP flooding in Berea sandstone cores.

Core flood	**Stage**	**Alkali**		**Surfactant**		**Polymer**		**Mixing**
		Type	**Conc., Wt.%**	**Type**	**Conc., Wt.%**	**Type**	**Conc., ppm**	**Brine Type**
2	**Chemical Slug**			Amph-GS	0.3	HPAM	3,000	Seawater
	Polymer Slug					HPAM	3,000	Seawater
4	**Chemical Slug**			Amph-SS	0.3	AMPS	3,000	Seawater
	Polymer Slug					AMPS	3,000	Seawater
5	**Chemical Slug**			Anionic-C1	0.3	AMPS	3,000	50% Seawater
	Polymer Slug					AMPS	3,000	50% Seawater
9	**Chemical Slug**			Anionic-C1 Anionic-S2	1 1	AMPS	3,000	Seawater
	Polymer Slug					AMPS	3,000	Seawater
10	**Chemical Slug**	OA-100	1	Anionic-C1	0.3	AMPS	3,000	Seawater
	Polymer Slug					AMPS	3,000	Seawater
11	**Chemical Slug**	Na_2CO_3	1	Anionic-C1	0.3	AMPS	3,000	Seawater
	Polymer Slug					AMPS	3,000	Seawater
12	**Chemical Slug**	OA-100	1	Amph-SS	0.3	AMPS	3,000	Seawater
	Polymer Slug					AMPS	3,000	Seawater

Core Flood-2 (BSS-18)

This experiment was conducted to evaluate new betaine based amphoteric surfactant designed to lower adsorption by reducing the amount of monomer of the surfactant in the solution by forming micelles in extremely low CMC values. The flooding sequence in this experiment was as follows: starts with injection of 1.914 PV of formation brine, 0.5 PV of chemical slug (SP), followed with 1 PV of polymer stage, the flood was ended with 1.5 PV of chase flooding using formation brine. The same sequence was followed in all experiments with some modification with chemical solution or injected volume. The chemical slug consist of 0.3 wt% of Amph-GS (surfactant), and 3,000 ppm HPAM (polymer) prepared in seawater. The polymer stage composed of 3,000 ppm HPAM polymer in seawater.

Fig. 89 shows the cumulative oil recovery and oil cut as a function of the core cumulative effluent. During water flooding (secondary recovery mode) oil recovery reached to 34.1% of original oil in place (OOIP) that increased to total recovery of 48.3% after chemical and polymer flooding. The oil recovery during the tertiary recovery mode was 21.6% of remaining oil after the water flooding stage. Oil cut was high during early stages of water injection and dropped to zero at 0.467 PV and continued at zero for the rest of the water flooding stage. This indicates that all movable oil was produced and oil saturation in the core reached to irreducible oil saturation. When the chemical slug started oil cut was zero and started increasing after 0.381 PV of initiating the chemical injection stage and reached to a maximum of 11.9%. Oil bank continued during the polymer flood and ended during the chase flood stage. The oil bank continued producing for 1.452 PV.

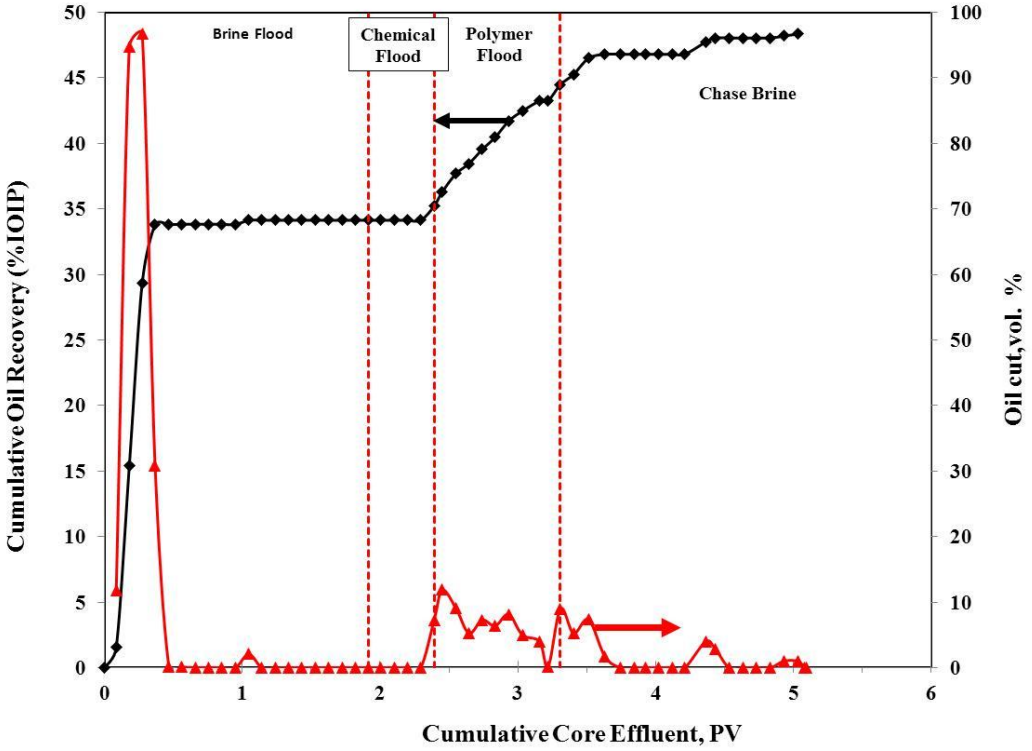

Fig. 89— Core flood-2 (BSS-18) history for slug having 3,000 ppm HPAM polymer, 0.3 wt.% Amph-GS surfactant in

Fig. 90 depict the pressure drop profile during the core flooding experiment. Pressure drop stabilized during the water flooding stage. Upon chemical and polymer injection stage a continues increase of pressure drop in the core was noticed. A sudden drop in pressure that was followed with quick increase in pressure, this can be explained by the breakthrough of the chemical due to the size exclusion that result due the large size of the polymer molecules. When chase flooding started pressure continued high for some time then start decreasing rapidly and stabilizing at 7.5 times the pressure during the water flooding stage.

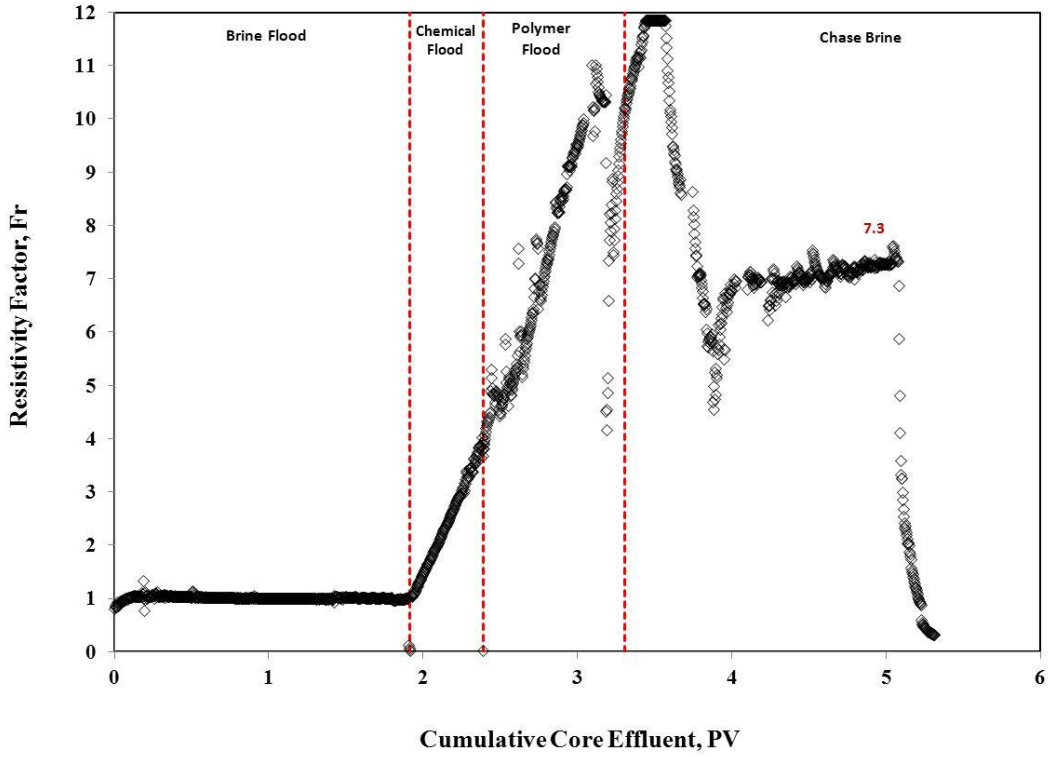

Fig. 90— Resistivity factor during different stages of Core Flood-2. The solution contain 0.3 wt.% Amph-GS, and 3,000 ppm HPAM polymer prepared in seawater. Residual resistivity factor was 7.3 due to large polymer molecular.

Core Flood-4 (BSS-9)

Second betaine based amphoteric surfactant was used with no modification to lower adsorption as the previous surfactant type Amph-SS. Same flooding sequence was followed as the previous experiment. In this experiment the polymer concentration was the same but type was changed to AMPS to reduce the impact of polymer trapping in the core which caused an increase in the pressure drop after injecting the chemical and polymer slug.

Fig. 91 shows the flood history with secondary, tertiary, polymer, and chase flood stages. Same as the previous experiment high oil cut was noticed during the first stages with some separate oil produced during the water flooding stage. No oil was produced during the SP stage but some initial oil production was showing when polymer flooding was started. No clear oil bank was formed and oil production during this experiment was

wiggling between some and zero production. The maximum oil cut reached was 20% for short period of time. Oil recovery during water flooding 32.1% and increased to 41.5% of OOIP. The oil recovered during chemical flooding was 14% of residual oil after water flooding. The reduction in recovery can be explained to higher surfactant retention when compared to Amph-GS. Schramm (2000) shows that standard amphoteric surfactant can show higher adsorption values on sandstone when compared to anionic. As discussed earlier zeta potential of Amph-SS on Berea sandstone particles in seawater and found positive values compared to negative zeta values when particles were evaluated in seawater (**Table 12**). **Fig. 92** depicts the change in resistivity factor during initial, and final water flooding, and during chemical injection. As noticed in the figure an increase in the residual resistivity factor to 2.5 times.

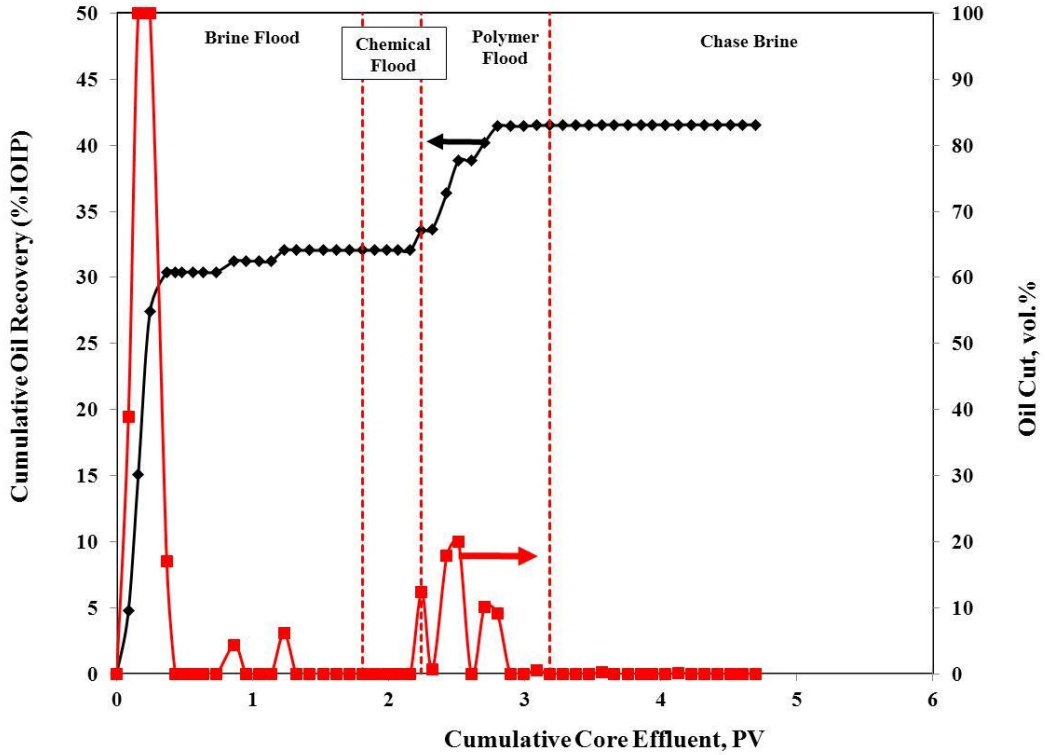

Fig. 91— Core flood-4 (BSS-9) history for slug having 3,000 ppm AMPS polymer, 0.3 wt.% Amph-SS surfactant in seawater.

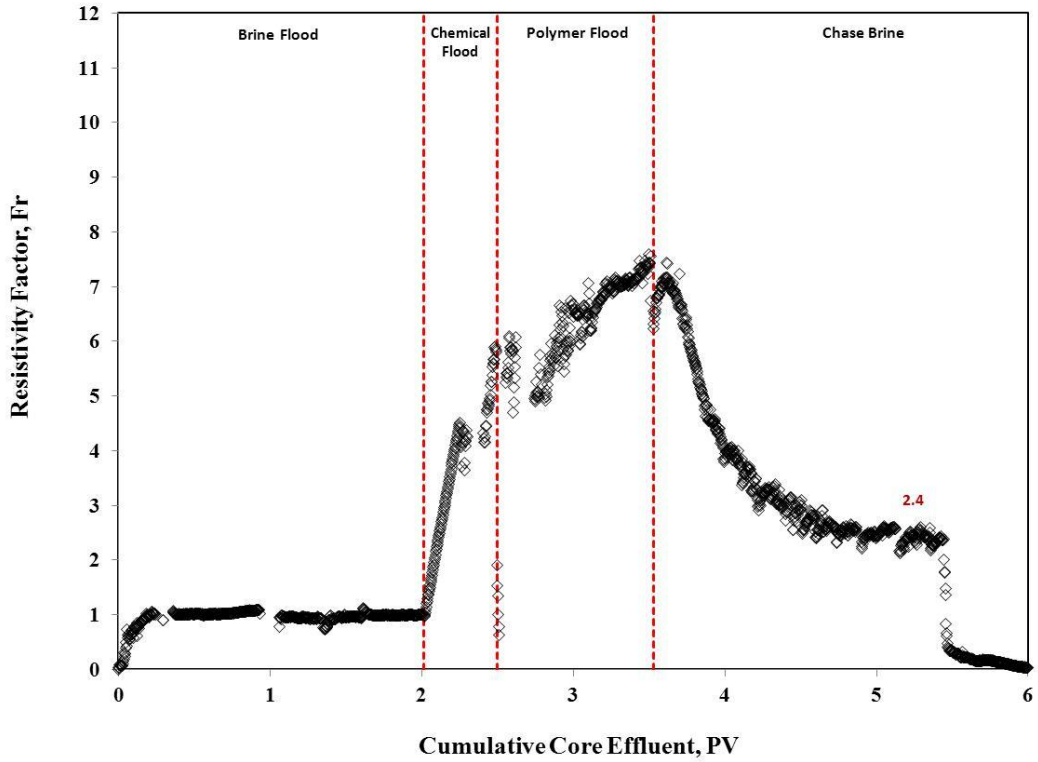

Fig. 92— Resistivity factor during different stages of Core Flood-4. The solution contain 0.3 wt.% Amph-SS surfactant, and 3,000 ppm AMPS polymer prepared in seawater. Residual resistivity factor reached 2.4 indicating loss of injectivity.

Core Flood-12 (BSS-17)

In this core flood test ASP flood was evaluated to study the performance of this method compared to the LTPF used in the previous experiment and discussed in more details in Chapter V. In this work Amph-SS with organic alkali was used as an alternative. To our knowledge this is the first time amphoteric surfactant is used with organic alkali and tested in core flood experiment. Organic alkali was selected to minimize operation requirement by eliminating the need to water softening (Bataweel and Nasr-El-Din 2011a; Berger and Lee 2006; Guerra et al. 2007). The chemical formulation for this experiment was the following 1 wt.% OA-100 (alkali), 0.3 wt.% Amph-SS (surfactant), and 3,000 AMPS (polymer). Same injection scheme was followed in this experiment as previous floods.

Fig. 93 show the flood history, oil recovery during the water flooding phase was 29.1% of OOIP. Total recovery increased to 38.8% after chemical injection. With oil recovery of 13.8% of residual oil caused by EOR process. As can be seen, that addition of organic alkali did not result in recovery increase when compared to same chemical formulation without organic alkali. Although, adding organic alkali resulted in lower IFT values it did not yield higher oil recovery, chemical solution flow in the core was dominated with the surfactant adsorption in the sandstone rock. It appears that organic alkali did help to reduce the surfactant adsorption level. The oil bank in this run was instable similar to the pervious experiment. Two distinctive peaks of produced of oil is shown. The first peak was at 12.4% then dropped to zero and increased again to 16.7%. This is in agreement with observation by Bataweel et al. (2011b) during monitoring the core flood experiment using CT scan were chemical front start shIFTing from piston-like displacement and was dominated with flow through channels.

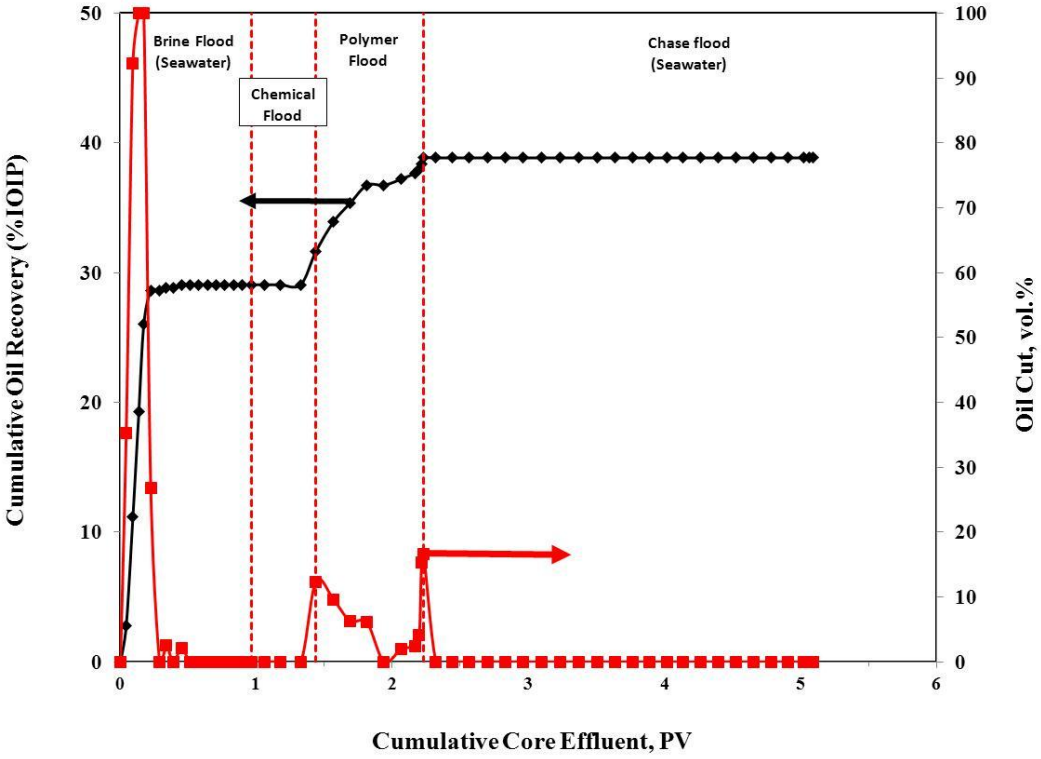

Fig. 93— Core flood-12 (BSS-17) history for slug having 1 wt% OA-100, 3,000 ppm AMPS polymer, 0.3 wt.% Amph-SS surfactant in seawater.

Effect of chemical flooding type

The following set of experiment studied the effect of four different types of chemical flooding used in the industry using anionic surfactant. The chemical types either differed by type of chemicals used or concentration of chemical used. ASP, organic alkali-surfactant-polymer (OASP) and two SP techniques were used: LTPF and high surfactant concentration (micellar) flooding. The impact on oil recovery, formation of oil bank and pressure response was analyzed. First each core flood experiment was discussed separately then comparison of these different processes were made.

Core Flood-5 (BSS-8)

In this run anionic surfactant was used in preparing the chemical solution. LTPF method was used in this experiment. The surfactant concentration was in the low range side with value of 0.3 wt% of Anionic-C1, and 3,000 ppm AMPS polymer. The same flooding stages were followed as previous experiments but with an increase in pore volume injected during the chemical flood stage, where 2 PV of chemical solution were injected instead of 0.5 PV.

Fig. 94 gives the recovery and oil cut during all stages of injection as a function of pore volume injected. Oil recovery during the secondary stage was 28.3% of OOIP this increased to 43.1% after injection 2 PV of chemical slug followed with 1 PV of polymer stage. Most of tertiary recovery was produced during the chemical stage with marginal (around 1%) during the polymer and chase flooding stage due to the large size of the injected chemical slug. Tertiary recovery was 20.6% of residual oil after water flooding. It was observed that the oil production started 0.18 PV after the chemical stage was initiated. Also, the oil production showed a rapid increase in recovery as an indication of more like piston displacement. An oil bank flowed continuously for around 1.1 PV with maximum water cut of 22.2%. The anionic surfactant showed and improved better displacement characteristics due to less adsorption at the sand stone rock.

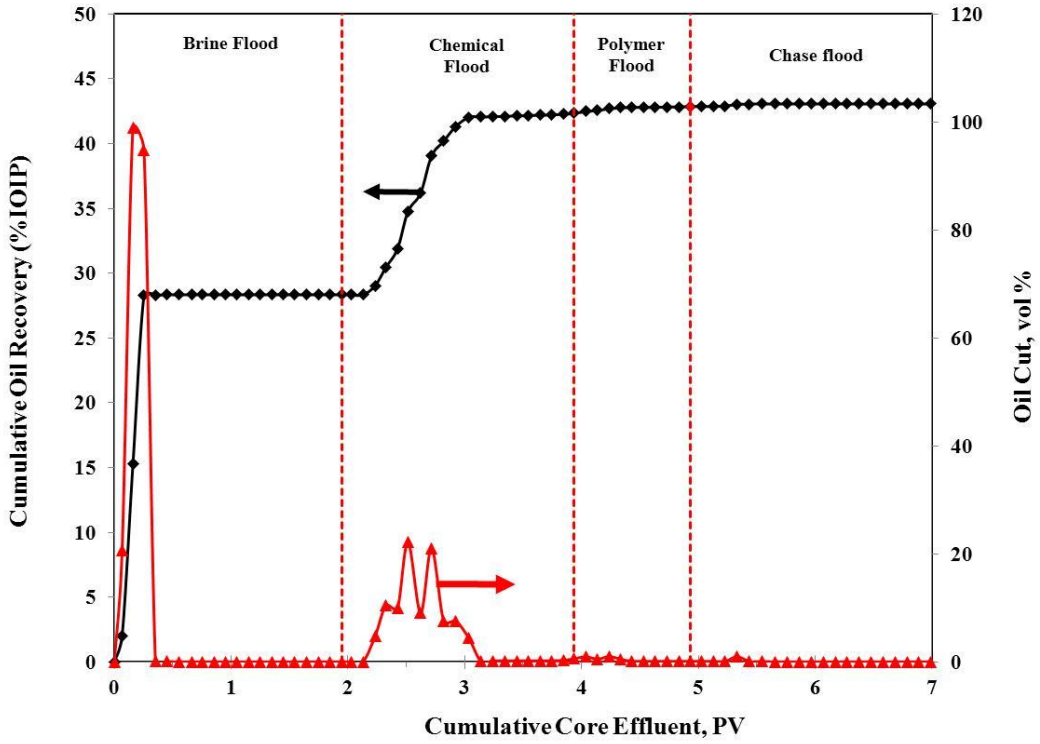

Fig. 94— Core flood-5 (BSS-8) history for slug having 3,000 ppm AMPS polymer, 0.3 wt.% Petrostep C-1 surfactant in 50% seawater.

Fig. 95—Resistivity factor profile during different stages of core flooding experiment. The pressure profile in this experiment shows different profile compared to other experiment since 2 pore volumes of the chemical solution was injected into the core compare to 0.5 PV on the previous experiment. In this experiment the initiation, propagation and end of the oil bank happened during the chemical injection stage, not like other experiment where the oil bank starts at the end of the chemical slug and continues during the polymer and chase flood stage. The most important observation in this run is the final residual pressure during chase fluid injection, pressure values was close to the pressure drop during the water flooding stage with value of 1.13 normalized pressure. This can be explained by the low adsorption of the surfactant in the chemical solution in this experiment since anionic surfactant is negatively charged which is similar to the charge on the sandstone cores used in this experiment. On the other hand, amphoteric surfactant have positive and negative charge which is less negative when

compared to the anionic surfactant, this can result to higher adsorption on the sandstone rock (Schramm et al. 1991). To study the charges on the Berea sandstone particles at seawater and in expectance of surfactant, zeta potential was measured using anionic and amphoteric surfactant prepared in seawater.

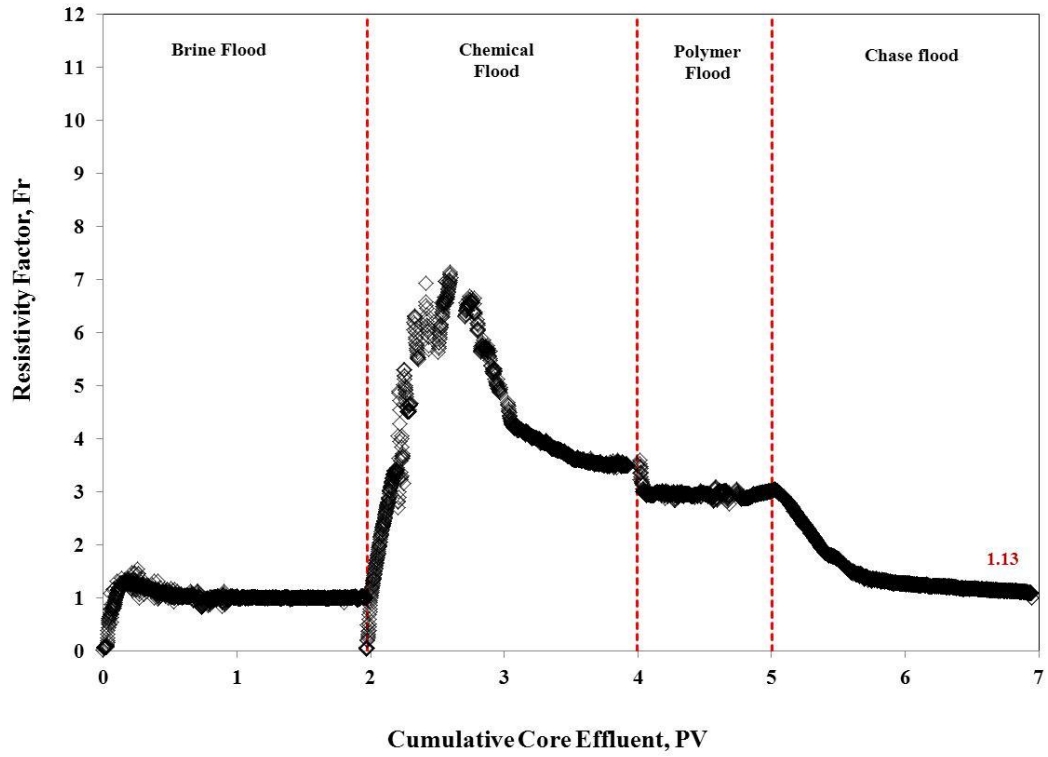

Fig. 95— Resistivity factor during different stages of Core Flood-5. The solution contain 0.3 wt.% Anionic-PS, and 3,000 ppm AMPS polymer prepared at 50% seawater. Residual resistivity factor reached close to original value, indication of less chemical retention.

Core Flood-9 (BSS-10)

In this core flood run higher surfactant concentration was used with total of 2 wt.% at ratio of 1:1. A mixture of two anionic surfactant was used to formulate this solution. We increase the Anionic-C1 concentration from 0.3 to 1 wt % and added to it a co-surfactant with 1 wt% concentration (Anionic-S2). The objective of this experiment was to compare the performance of SP flooding with high surfactant concentration that is recommended in many studies with other type chemical flooding methods. The injection scheme of this experiment is similar to all other core floods with 0.5 PV of chemical solution injected during the chemical flood.

Fig. 96 shows the oil recovery and oil cut as function of pore volume injected. Recovered oil during the water flooding stage was 30.2% of OOIP. Total oil recovered after completing all injection stages was 46.% with 22.7% recovery from residual oil remaining after water flooding. Oil cut increased rapidly after chemical injection and oil production started during this stage. The quick start of oil production after initiating the chemical flooding is an indication of good chemical propagation in the core. This quick response was noticed in the last two experiments and in both of them anionic surfactant was used this is different than the general response noticed when SP solution was prepared using amphoteric surfactant, where little delay in oil production response after initiating chemical flooding. This is a sign of potential chemical retention when amphoteric surfactant is flowing in sandstone rock.

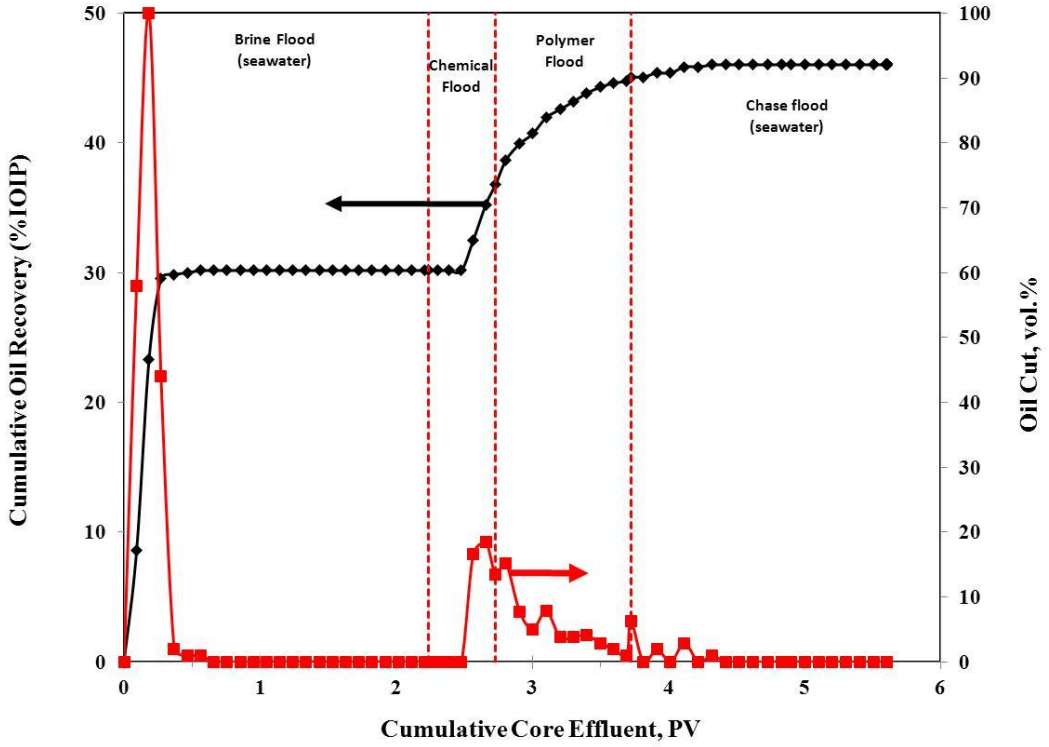

Fig. 96— Core flood-9 (BSS-10) history for slug having 3,000 ppm AMPS polymer, 1 wt.% Petrstep C-1, and 1 wt.% Petrstep S-2 surfactant in seawater.

Fig. 97 depicts the pressure profile during flooding process. Pressure increased to 3 times the chemical slug injection then stabilize when polymer flooding started at the same pressure reached during the chemical injection. When Chase flooding started pressure drop decreased until it reached 1.15 the original pressure. Flow rate was increased to 1 cm^3/min and the residual resistance factor was 1.15. This experiment showed low residual resistance factor similar to the previous experiment when anionic surfactant was used. Low residual resistance factor is an indication of less chemical entrapment when compared to solutions prepared with amphoteric surfactant, which shows higher residual resistance factors.

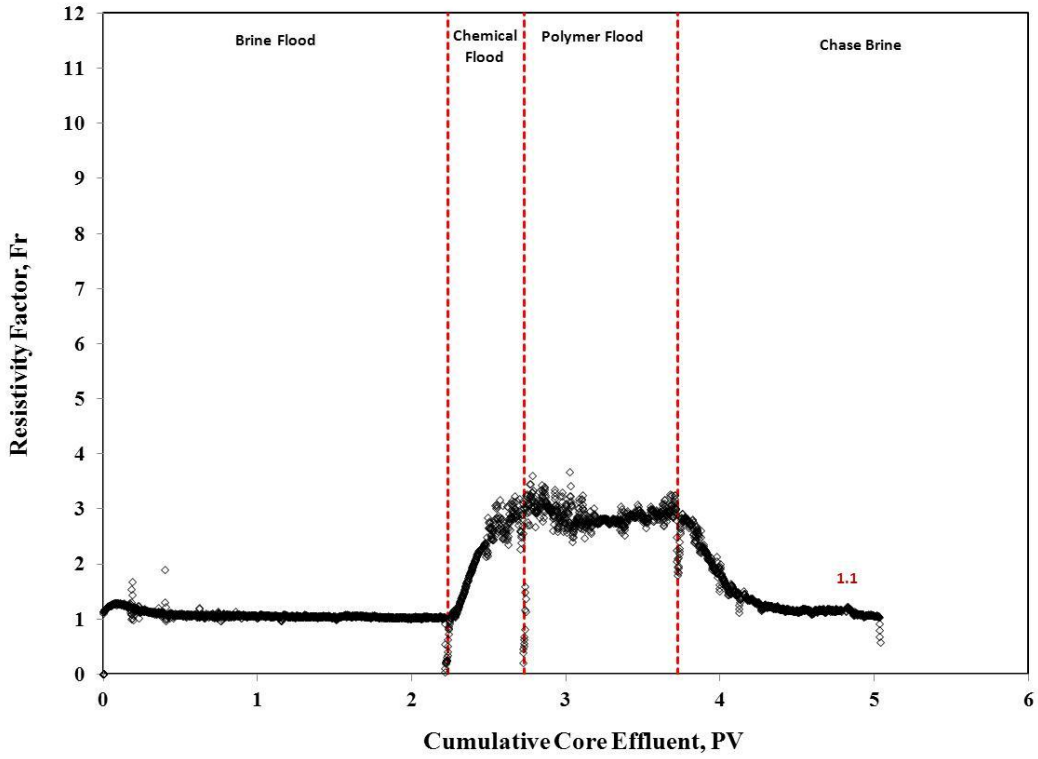

Fig. 97—Resistivity factor during different stages of Core Flood-9. The solution contain 1 wt.% Anionic-PS-C1, and 1 wt% Anionic-PS-S2 surfactant, and 3,000 ppm AMPS polymer prepared in seawater. Residual resistivity factor reached close to original value, indication of less chemical retention.

Core Flood-11 (BSS-19)

In this core flood an ASP method was evaluated and compared with previous techniques used. Alkali used in this run was 1 wt% Na2CO3 with 0.3 wt.% Anionic-C1 surfactant and 3,000 ppm AMPS polymer. After initial water flooding stage, 0.5 PV of chemical solution was injected. This was followed with mobility buffer (1 PV) then with chase flooding using seawater. During experiment oil recovery, oil cut, and pressure profile were monitored and recorded.

Fig. 98 shows the flood history for the ASP experiment. Oil recovery during the water flooding was 35.2% of OOIP this increased to 55.6% after injecting chemical, polymer and chase stages. The oil recovered at ROS was 31.5% after water flooding. Rapid increase in oil production was observed after initiating the chemical flood. Oil

production started during the chemical slug injection and continued producing during polymer flood and reached ultimate production before chase flooding was initiated. Oil cut started 0.23 PV after injection of chemical slug was initiated and continued for 1.265 PV with maximum value at 30.6%. The oil bank observed from the oil cut values shows an initial sharp oil bank with most of the oil produced in this stage followed with smaller volume of produced oil that extend for some time. Sharp oil bank with high oil cut is preferred from production and economical point of view. This core flood run shows the highest total and incremental recovery compare to all other runs.

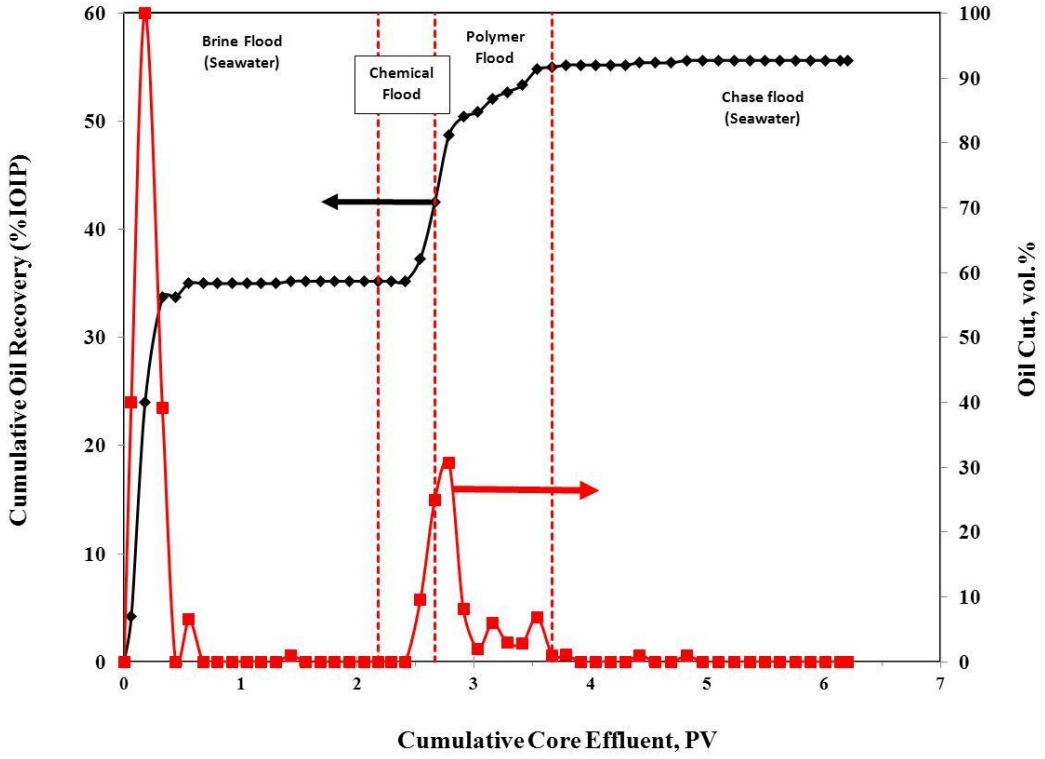

Fig. 98— Core flood-11x (BSS-19) history for slug having 1 wt% Na_2CO_3, 3,000 ppm AMPS polymer, 0.3 wt.% Petrostep C-1 surfactant in seawater.

Pressure profile as function of pore volume injected during the flooding process was shown in **Fig. 99**. The pressure profile shows continues increase in the pressure drop during chemical and polymer flooding. Gradual decrease in pressure drop was noticed

when seawater was injected during the chase flooding process. Residual resistance factor was 2.22 at the end of the chase flooding was completed. When compared to the previous two experiments using same type of surfactant and polymer this shows more decline in injectivity of the core. This can be explained due to the incompatibility of the water saturating the core (seawater) that contain divalent cations that shows incombustibility with chemical slug containing sodium carbonate. Precipitation of $CaCO_3$ and $MgCO_3$ can be potential cause of higher residual resistance factor (ref.).

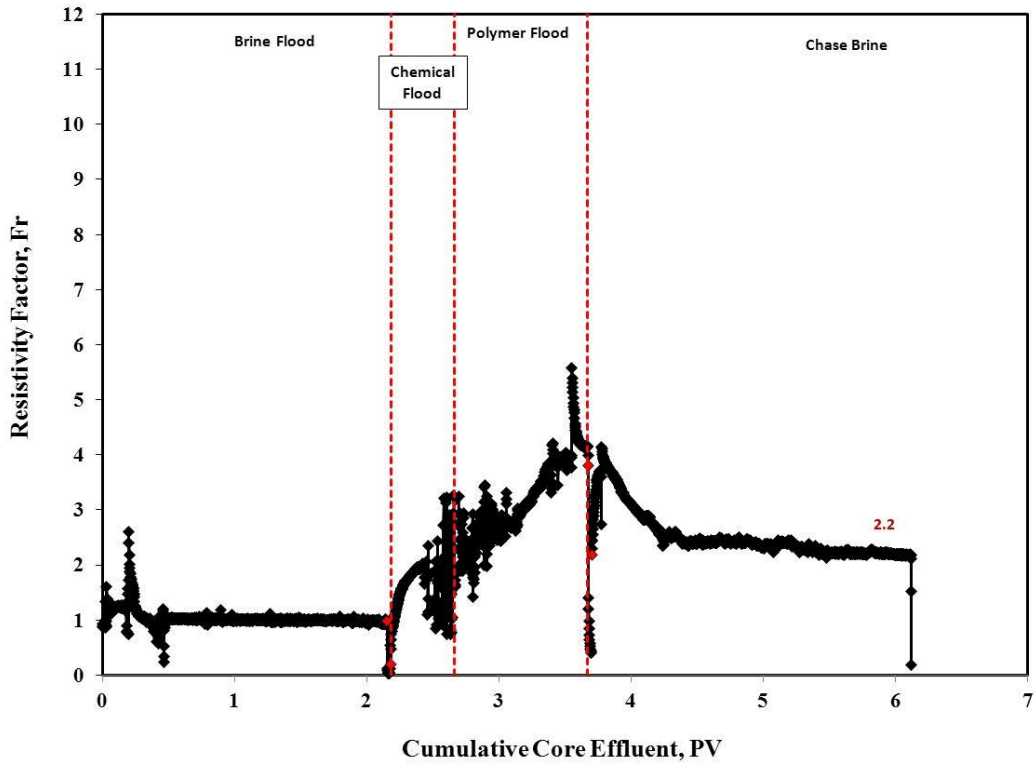

Fig. 99— Resistivity factor during different stages of core flood-11. The solution contain 1 wt.% Na_2CO_3, 3,000 ppm AMPS polymer, 0.3 wt.% Anionic-PS-C1 surfactant in seawater.

Core Flood-10 (BSS-13)

A second ASP flood was conducted using organic alkali as replacement for the sodium carbonate. Organic alkali showed no precipitation when mixed with brines containing

high concentration of divalent cations (Bataweel and Nasr-El-Din 2011a). This type of alkali eliminates the water softening requirement and has high tolerance to salinity and hardness.

Fig. 100 gives the oil recovery and oil cut as function of pore volume injected. Seawater was injected during the water flooding phase and total of 33.3% of OOIP was produced. Total oil production after completing all injection stages was 49.2%. The oil produced during the EOR stage was 23.8% of residual oil after water flooding. A rapid increase in oil production was seen after chemical slug was injected. The oil bank shows an initial stable bank with a maximum oil cut of 21.4% that flowed for a while. Then smaller bank with oil cut values of 5% followed after the main bank.

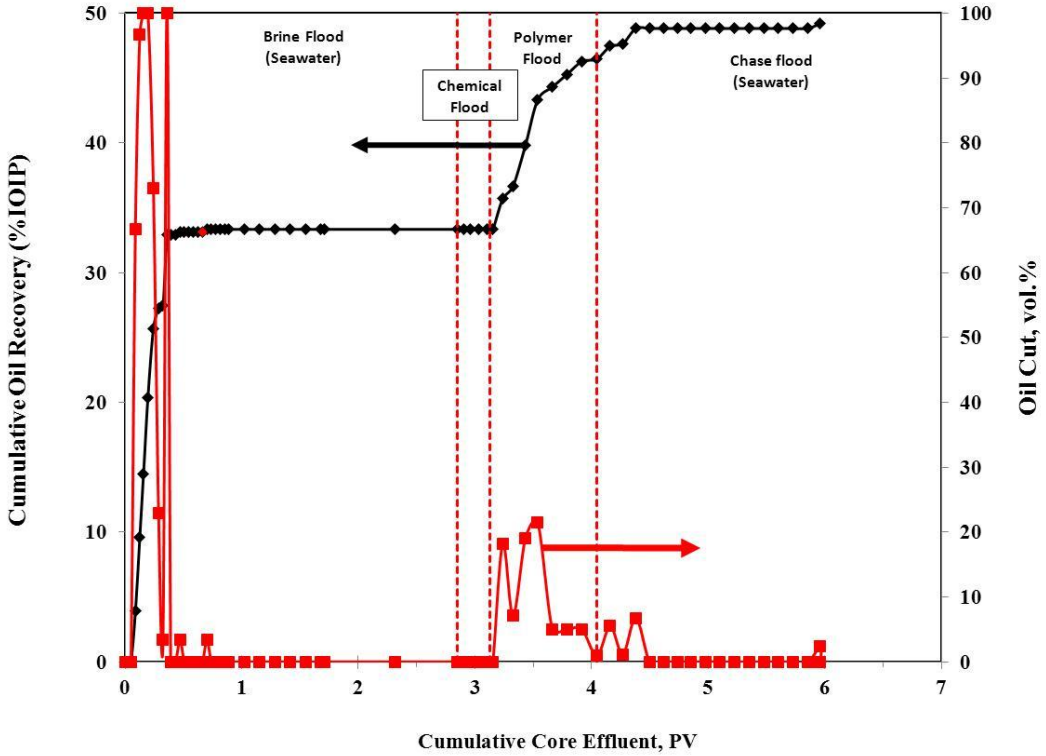

Fig. 100— Core flood-10 (BSS-13) history for slug having 1 wt% OA-100, 3,000 ppm AMPS polymer, 0.3 wt.% Petrostep C-1 surfactant in seawater.

Fig. 101 illustrates the pressure profile during flooding stages. Pressure showed similar pressure behavior as in ASP flood-11. Pressure increased during chemical and polymer flooding to higher values when compared to ASP with Na_2CO_3. The residual resistance factor at end of the experiment was 2.4. Using organic alkali was expected to show less pressure drop but was not the case.

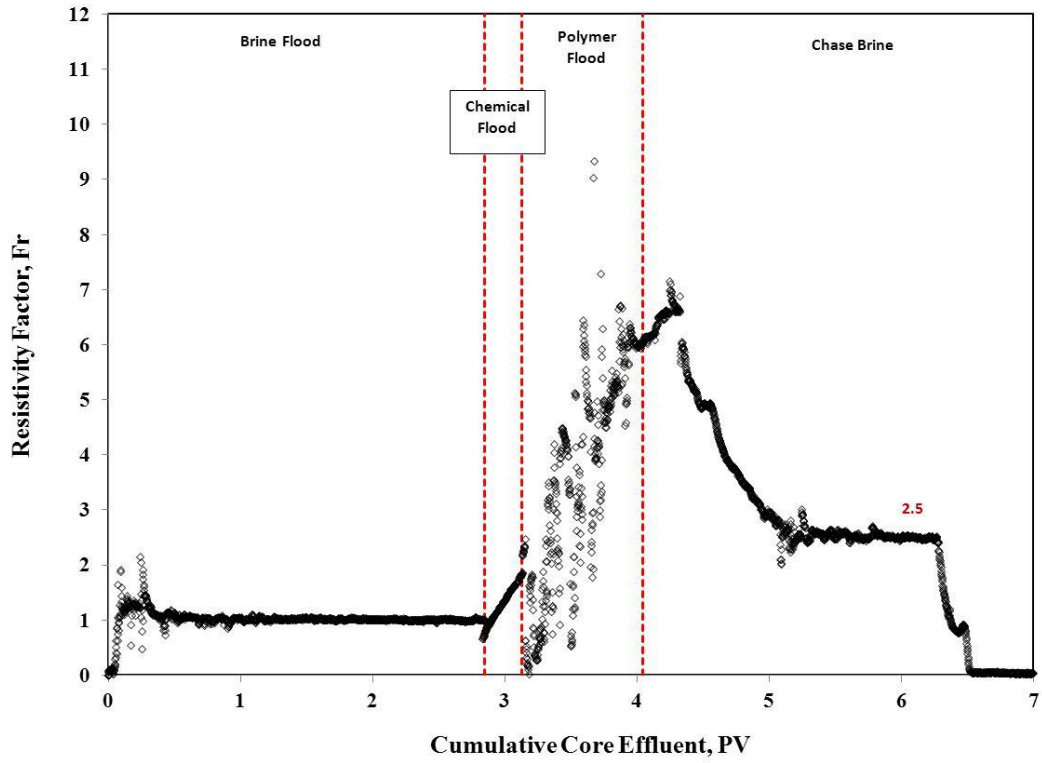

Fig. 101— Resistivity factor during different stages of core flood-10. The solution contain 1 wt.% OA-100, 3,000 ppm AMPS polymer, 0.3 wt.% Anionic-PS-C1 surfactant in seawater.

Oil recovery at different chemical flooding processes

Fig. 102 shows comparison for different chemical flooding processes and recovery during tertiary mode. As seen the ASP flooding is showing the highest recovery at 32%. The lowest is the LTPF process. The high concentration surfactant and OASP shows intermediate recovery with similar recovery values.

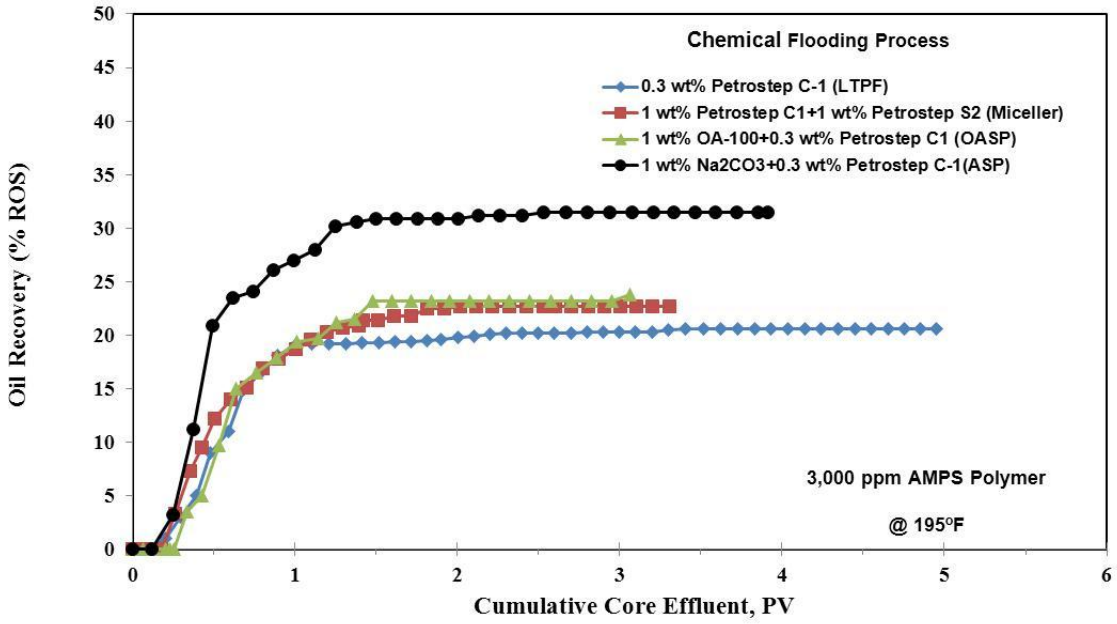

Fig. 102—Oil recovery during different chemical flooding processes.

Conclusions

Based on the results obtained in this study the following conclusions can be drawn:

1. ASP showed higher tertiary recovery when compared with SP flooding.
2. 1 wt.% Na_2CO_3 with anionic surfactant showed higher oil recovery when compared to other formulations.
3. ASP gives higher pressure drop values when compared to SP.
4. Amphoteric surfactant showed lower IFT values but did not show higher recovery values.
5. Method to lower adsorption by lowering CMC values helped improve the chemical propagation through the core sample.

CHAPTER VII
CHEMICAL FLOODING OF DOLOMITE RESERVOIR

Summary

Chemical flooding methods are used to recover residual oil left after water flooding. Most of the chemical flooding studies and pilot tests use anionic surfactants. In carbonate reservoirs consumption of this type of surfactant is very high. This due the to the electrostatic attraction between the negatively charged surfactant and positively charged carbonate rock surface. Sodium carbonate was recommended to be added to the chemical solution to change the charge on the rock surface to negative value and reduce the adsorption. This strategy was successful in lab work but was not reported for any field case to our knowledge.

In this part we will investigate the ability of amphoteric surfactant to recover oil from dolomite cores during tertiary mode after water flooding. This was compared with anionic surfactant and was tested using dolomite core samples with dimensions of 1.5 in. diameter and 20 in. length. The same injection scheme was followed in all experiments.

Chemical solution prepared with amphoteric surfactant showed better recovery when compared with anionic surfactant. Unlike the sandstone cores no injectivity decline was observed and residual resistance was showing lower values due to change of the saturation inside the core samples.

Introduction

Carbonate reservoirs had less attention related to chemical flooding pilot compared with sandstone reservoirs. Enhanced oil recovery (EOR) methods known as surfactant-polymer (SP) and alkali-surfactant-polymer (ASP) shown to be effective in recovering remaining oil in sandstone reservoirs (Bragg et al. 1982; Wang 1999). One of the most factors of chemical flooding success is the ability to propagate the chemicals (surfactant and polymer) in the reservoir without getting consumed by adsorption, precipitation or partitioning to the oil phase. Alkali is added to the chemical solution to aid the surfactant by introducing in-situ surfactant and reducing the surfactant adsorption. Adding the alkali will have some positive impact as discussed by some researchers. Johnson (1975) suggested four recovery mechanisms by alkaline flooding:

1. Emulsification and entrainment where the crude oil is emulsified in-situ and entrained by the flowing aqueous alkaline.
2. Wettability reversal (oil-wet to water-wet) in which oil production increases due to favorable changes in permeabilities accompanying the change in wettability.
3. Wettability reversal (water-wet to oil-wet) in which low residual oil saturation is attained through low interfacial tension and viscous water-in-oil emulsion working together to produce high viscous/capillary number.
4. Emulsification and entrapment in which sweep efficiency is improved by the action of emulsified oil droplets blocking the smaller pore throats.

Fifth mechanism was proposed by Castor et al. (1981) emulsification and coalesces in which the unstable water-in-oil emulsions form spontaneously in the alkaline solution,

Experimental Studies

Materials

Materials are given in Chapters V and VI. **Table 18** gives the composition for brine and seawater. **Table 19** gives the chemicals used in this study and information about these chemicals.

Table 18—Dolomite brine & seawater composition.

	Concentration, mg/L	
Ions	**H Formation Brine**	**Seawater**
Na^{+}	51,187	16,877
Ca^{2+}	29,760	664
Mg^{2+}	4,264	2,279
Ba^{2+}	10	_
Sr^{2+}	1,035	_
HCO_3^{-}	351	193
Cl^{-}	143,285	31,107
SO_4^{2-}	108	3,560
CO_3^{-}	0	_
TDS	230,000	54,680
Viscosity (mPa.s)*	1.851	1.1429
Density (g/cm^3)*	1.15	1.0354

Table 19—Chemicals information used for dolomite flooding.

	Chemical	Description
1	**Amph-SS**	**SS-885**. Betain based amphoteric surfactant, TDS >100,000 ppm, hardness > 1000 ppm, Temperature > 100°C.
2	**Anionic-C1**	**Petrostep C-1**. Alpha-olefin sulfonate.
3	**Anionic-S2**	
4	**AMPS**	Flopaam **AN-125** Copolymer of acrylamide and 2-acrylamido 2-methyl propane sulfonate, 25 % anionic , MW : 6 millions (25 % sulfonated).
5	**Na_2CO_3**	Sodium carbonate
6	**Organic alkali**	**OA-100**, sodium salt of polyaspartic acid

Interfacial Tension Measurements and Core Flood Studies

Interfacial tension measurements are shown in Chapter VI and Core flood studies are given in Chapter V.

Result and Discussion

Core flood studies

In this study 6 chemical flooding experiments were conducted to study LTPF in recovering oil for residual oil after water flooding. All chemical flooding experiments were conducted in tertiary mode at residual oil saturation (S_{or}). Cores information used in this study are given in **Table 20**. Chemical formulations for core flood experiments are given in **Table 21**.

Table 20—Dolomite core information used in flooding experiments.

Core number	MAB-5	MAB-3	MAB-4	MAB-12	MAB-18	MAB-11
Core flood #	1	2	3	4	5	6
Length (cm)	37.62	50.8	43.18	50.8	48.26	43.18
Diameter (cm)	3.80	3.76	3.77	3.77	3.77	3.77
Porosity (%)	18.04	12.60	17.42	16.95	15.45	11.97
Permeability (md)	133.3	_	442.4	328.3	318.8	79.41

Table 21—Chemical formulation for dolomite core flood experiments.

Core flood	Stage	Alkali		Surfactant		Polymer		Mixing Brine
		Type	Conc., Wt.%	Type	Conc., Wt.%	Type	Conc., ppm	Type
1	Chemical Slug			Amph-SS	0.3	AMPS	4,000	Seawater
	Polymer Slug					AMPS	4,000	Seawater
2	Chemical Slug			Amph-SS	0.3	AMPS	3,000	50% Seawater
	Polymer Slug					AMPS	3,000	50% Seawater
3	Chemical Slug			Amph-SS	0.3	AMPS	3,000	Seawater
	Polymer Slug					AMPS	3,000	Seawater
4	Chemical Slug	OA-100	1	Amph-SS	0.3	AMPS	3,000	Seawater
	Polymer Slug					AMPS	3,000	Seawater
5	Chemical Slug	Na2CO3	1	Amph-SS	0.3	AMPS	3,000	6%NaCl
	Polymer Slug					AMPS	3,000	6%NaCl
6		OA-100	1	Anionic – C1	0.3	AMPS	3,000	Seawater
						AMPS	3,000	Seawater

Core Flood-1 (MAB-5)

In this experiment SP flooding was evaluated for dolomite core using amphoteric surfactant solution at iso-salinity condition. The injection scheme for this experiment was as follows: water flooding using seawater, 2 PV of SP slug, 1.2 PV polymer slug, and end the experiment with chase flooding with seawater. The main chemical slug composed from 0.3 wt% Amph-SS (Surfactant), 4,000 ppm AMPS (polymer) prepared in seawater. The polymer buffer consist of 4,000 ppm AMPS in seawater.

Fig. 103 shows the cumulative oil recovery and oil cut as function of cumulative core effluent. The core flood started with injecting 2.70 PV of seawater as water flooding, a total of 53.37% of OOIP was recovered during this phase. Oil production

stopped at 1.2 PV and no more recovery was noticed. Chemical stage started and 2PV of main slug was injected, oil bank start forming at 0.24 PV after chemical stage was initiated. Oil bank continued flowing for around 2 PV with maximum oil cut at 12.87%. Most of the oil recover was during chemical stage and no more recovery was gained during polymer and chase flooding stage. Incremental recovery during chemical flooding was 19.07% OOIP with EOR recovery of 40.9% of residual oil after water flooding.

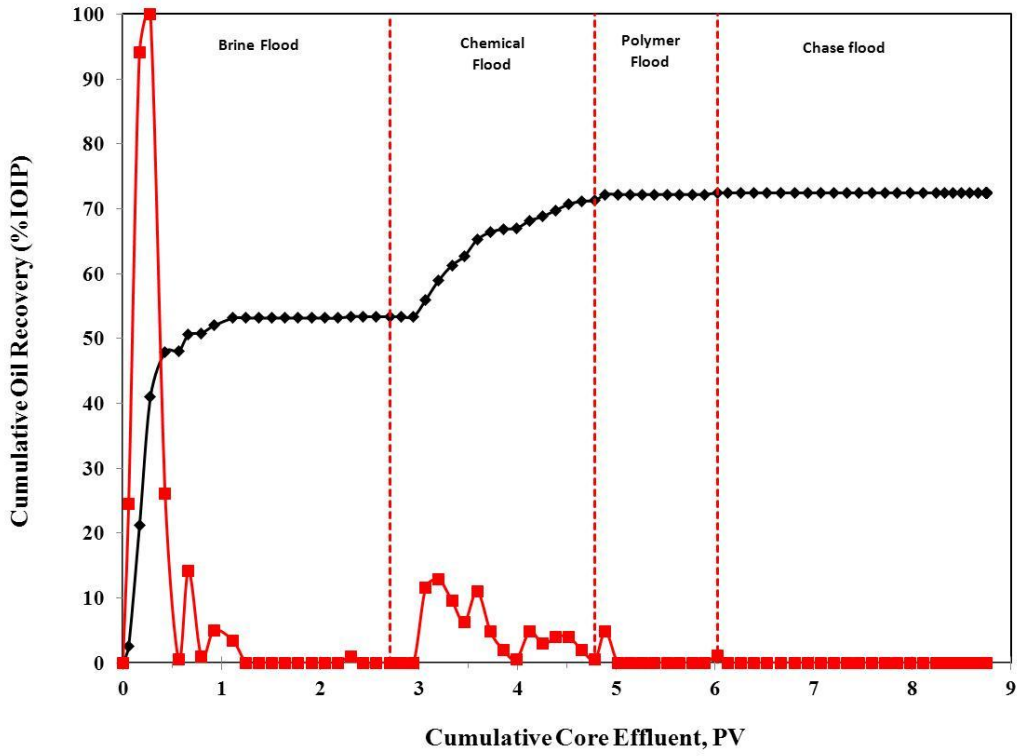

Fig. 103—Core flood-1 (MAB-5) history for slug having 4,000 ppm AMPS polymer, 0.3 wt.% Amph-SS surfactant in seawater.

Fig. 104 shows the resistivity factor (Fr) during the flooding experiment as a function of cumulative injected fluids. Resistivity factor is a normalized pressure taking in to account the flow rate. The initial pressure used for resistivity factor calculation was the stable pressure reached during water flooding stage at residual oil saturation ROS. Resistivity factor increased in early stage of water flooding process to maximum value

of 2. Then Fr started to decline until oil was produced from the core. The increase in Fr was in agreement with formation and progression of an oil bank in the core. When chemical stage was initiated a rapid increase in Fr was depicted which caused by high viscosity and formation of oil bank. Fr reached a maximum at 5.8 then start decreasing gradually when oil bank started flowing out of the core. The Fr stabilized at 2.7 when most of the oil bank was produced. When shIFTed to polymer injection it showed constant value at 1.9 since polymer solution viscosity was less than main slug. Residual flow resistivity was 0.33 which indicates that no significant chemical retention was noticed. The resistivity behavior was different when compared to flowing same solution formulation in sandstone cores. In the sandstone core the residual resistivity was more than 1indicating chemical retention and injectivity decline.

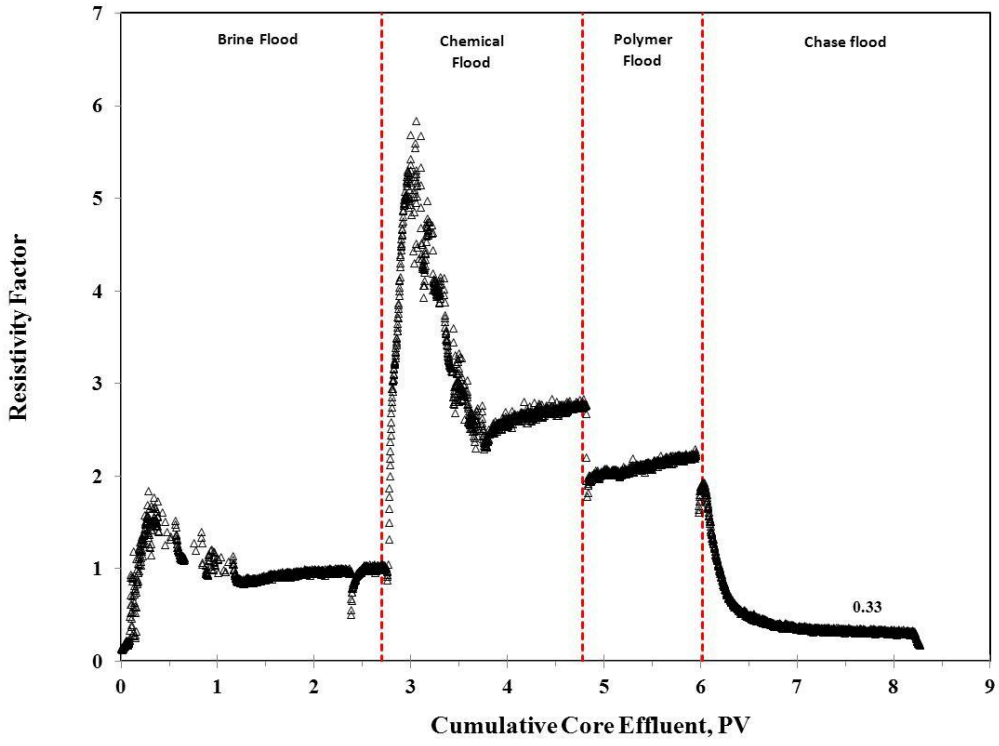

Fig. 104— Resistivity factor during different stages of Core Flood-1. The solution contain 0.3 wt.% Amph-SS, and 4,000 ppm AMPS polymer prepared in seawater. Residual resistivity factor less than original.

Core Flood-2 (MAB-3)

In this core flood chemical formulation is similar to first one with difference in polymer concentration, which was reduced to 3,000 ppm. The same injection scheme was used with same pore volume of chemical and polymer slug were injected.

Fig. 105 presents the core flood history for recovery experiment. When water flood started high oil recovery was produced in the first 0.5 PV. This was followed with much less production with 10% oil cut until 1.5 PV. Oil recovery was 50.36% and no oil was produced after that during water flooding stage. Main chemical slug was initiated at 3.44 PV and oil production started at 3.714 PV. Oil bank start forming and maximum oil cut was 20% the oil production seized at 5.3 PV, where total oil recovery reached to 74.45% of OOIP during the main chemical slug. No oil was produced during polymer and chase flooding stage and incremental oil produced was 24.2% OOIP with EOR recovery of 48.7% of ROS.

Fig. 106 depicts the variation in resistivity factor during different injection stages. It shows similar behavior as the first experiment with less increase in resistivity at different stages were the maximum in this experiment was 4, stable value after oil bank production was 1.9 during chemical stage, and stabilized at 1.2 during polymer flood. Then residual resistivity factor was 0.26 as indication of no significant chemical retention and improvement in aqueous relative permeability due to reduction in oil saturation to 25.46%.

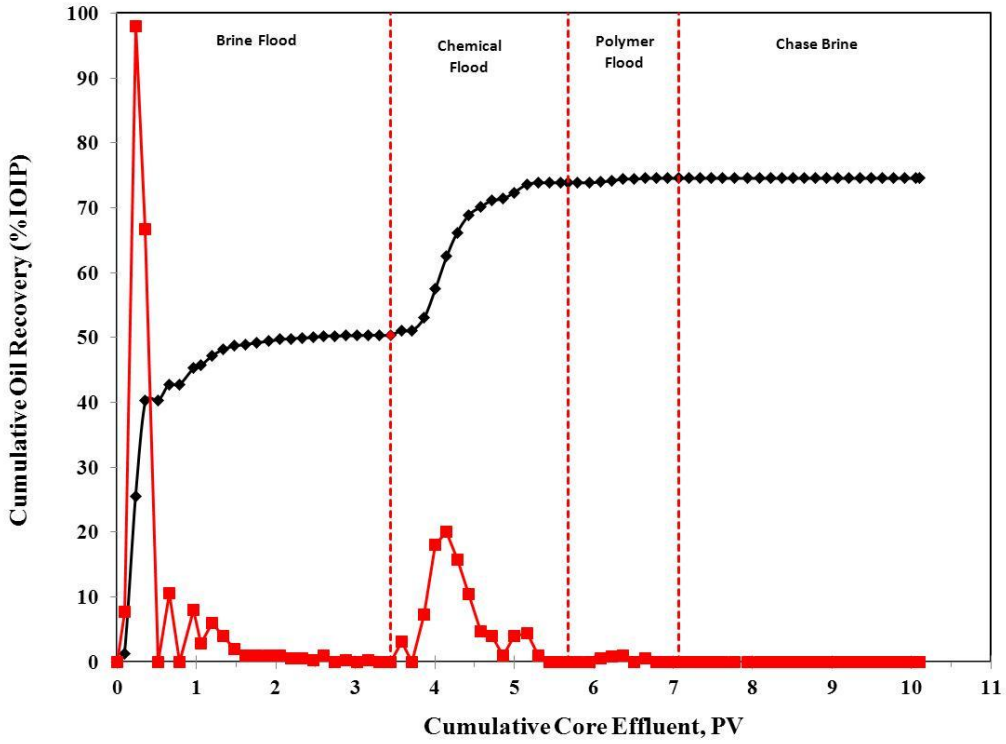

Fig. 105—Core flood-2 (MAB-3) history for slug having 3,000 ppm AMPS polymer, 0.3 wt.% Amph-SS surfactant in 50% seawater.

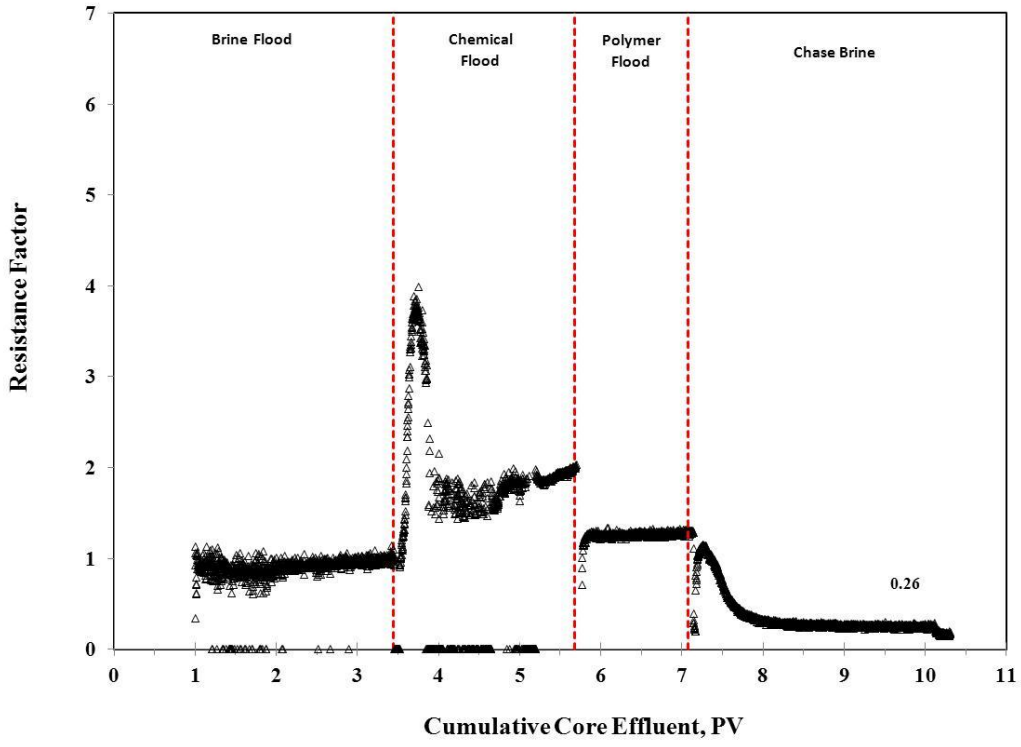

Fig. 106— Resistivity factor during different stages of Core Flood-2. The solution contain 0.3 wt.% Amph-SS, and 3,000 ppm AMPS polymer prepared in 50% seawater. Residual resistivity factor less than original.

Core Flood-3 (MAB-4)

This run is similar to the core flood-2 with difference in the preparation brine where seawater was used. Also, same injection scheme as the previous experiment was followed were 2 PV of the main slug was injected followed with 1 PV of mobility buffer (polymer slug).

Shown in **Fig. 107** is the recovery experiment where oil recovery during the water flooding reached to 59.57% of OOIP and increased to total oil recovery of 89.89% OOIP. The oil produced from the remaining oil in the core was 74.47% of ROS. Oil bank developed when the chemical flooding was commenced and flowed for around 1.5 PV. The maximum oil cut during this stage reached to 20%. Whole the oil bank flowed

during the chemical stage phase and no extra oil production was seen during polymer and chase flooding.

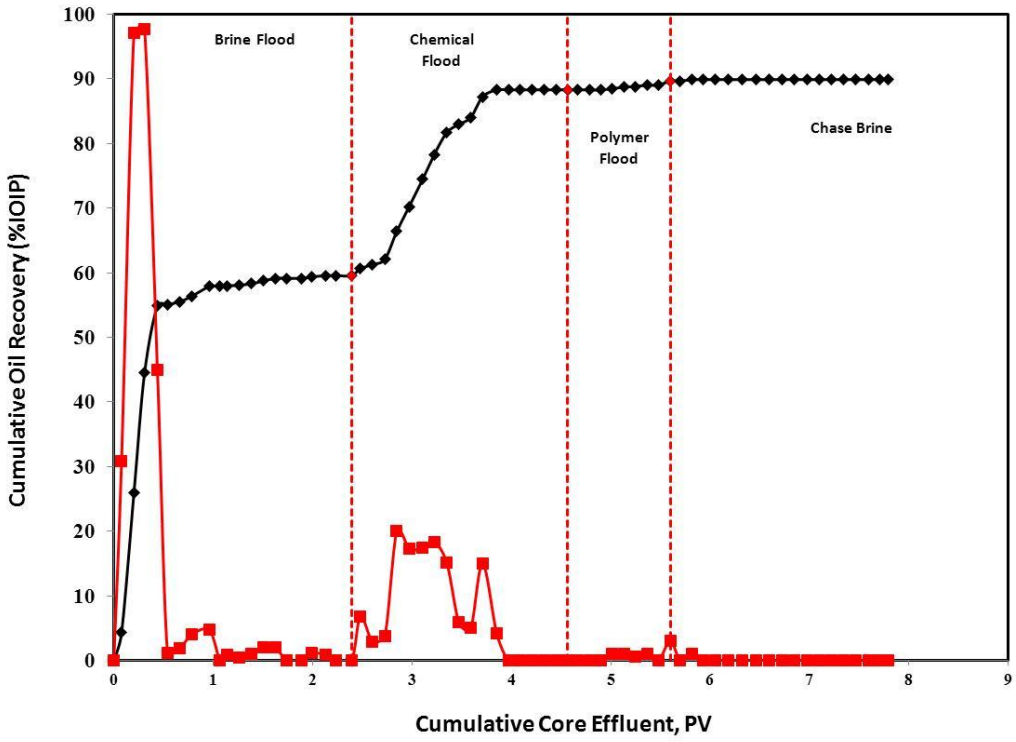

Fig. 107—Core flood-3 (MAB-4) history for slug having 3,000 ppm AMPS polymer, 0.3 wt.% Amph-SS surfactant in seawater.

Depicted in **Fig. 108** is the flow resistivity factor as a function of cumulative fluid injected into the core. The resistivity profile is similar to the previous two experiments with rapid increase in pressure when chemical injected to the core reach to a maximum 4.2 then reduction in pressure starts when oil bank start flowing out of the core. This is followed with constant resistivity at 1.9 with no oil production from the core. Constant pressure during polymer flooding with less value with compared with chemical stage followed with low resistivity during the chase flooding stage 0.37.

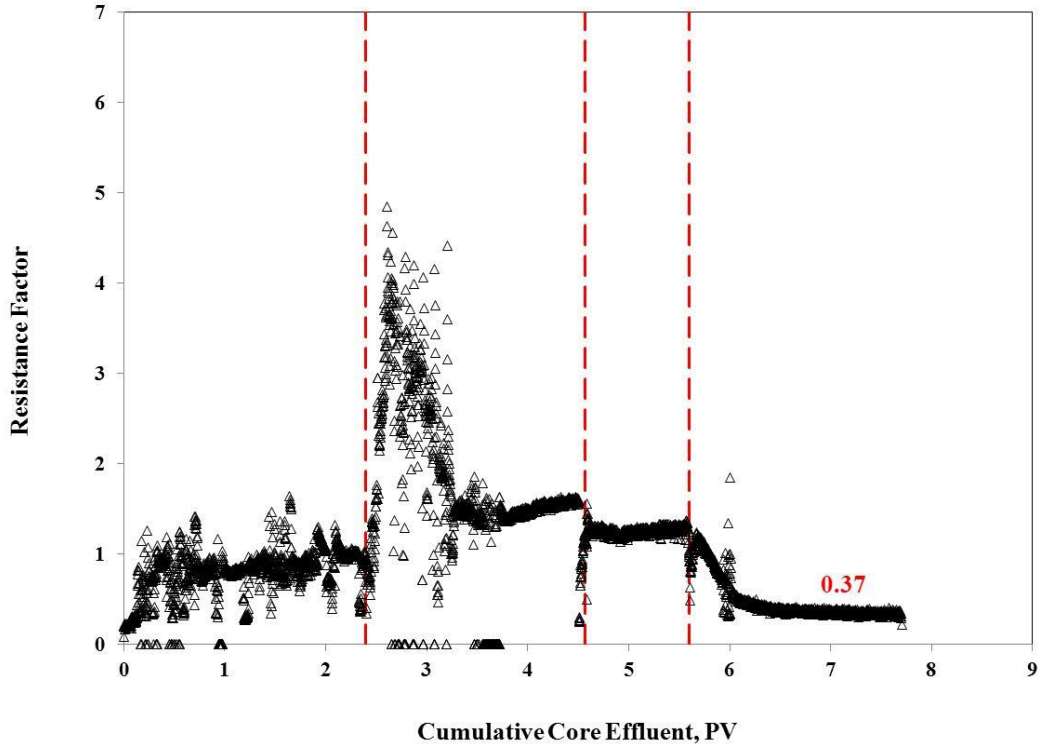

Fig. 108— Resistivity factor during different stages of Core Flood-3. The solution contain 0.3 wt.% Amph-SS, and 3,000 ppm AMPS polymer prepared in seawater. Residual resistivity factor less than original.

Alkali injection into dolomite cores

Core Flood-4 (MAB-12)

This run involves injecting ASP as main chemical slug followed with extended polymer injection stage and no chase flooding. Regarding the injection scheme a smaller chemical slug was injected (0.5 PV) when compared to previous experiments. The chemical slug consists of 1 wt% organic alkali, 0.3 wt% Amph-SS (surfactant), and 3,000 ppm AMPS (polymer) prepared in seawater.

Fig. 109 shows the recovery history of core flood-4 and oil cut in this experiment. During water flooding 74 % of OOIP was produced after injecting 2.36 PV of seawater. This high recovery of this core can be interpreted to the high permeability of this core

compare to other cores. Chemical EOR stage was initiated with chemical solution containing OASP. The recovery from this process was 55.1% of residual oil after water flooding. The chemical slug in this experiment was followed with polymer flooding and no chase flooding followed this stage. No extra oil recovery was observed even with more PV of polymer flooding was injected. A sharp oil bank was formed and flowed for 0.94 with an average oil cut 12.7%.

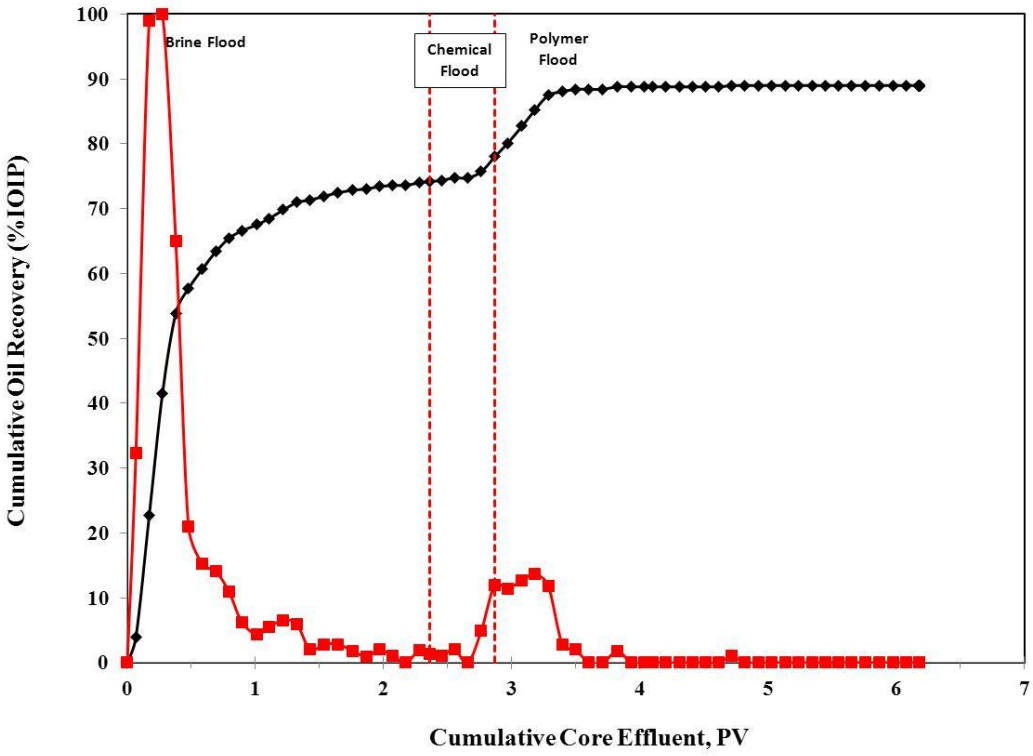

Fig. 109—Core flood-4 (MAB-12) history for slug having 1% OA-100; 3,000 ppm AMPS polymer; 0.3 wt.% Amph-SS surfactant in seawater.

Fig. 110 shows the resistivity factor profile during water flooding, chemical flooding and polymer flooding. Shows similar behavior like pervious core flood experiments with increase in resistance due to bigger volume of polymer injected in the core sample.

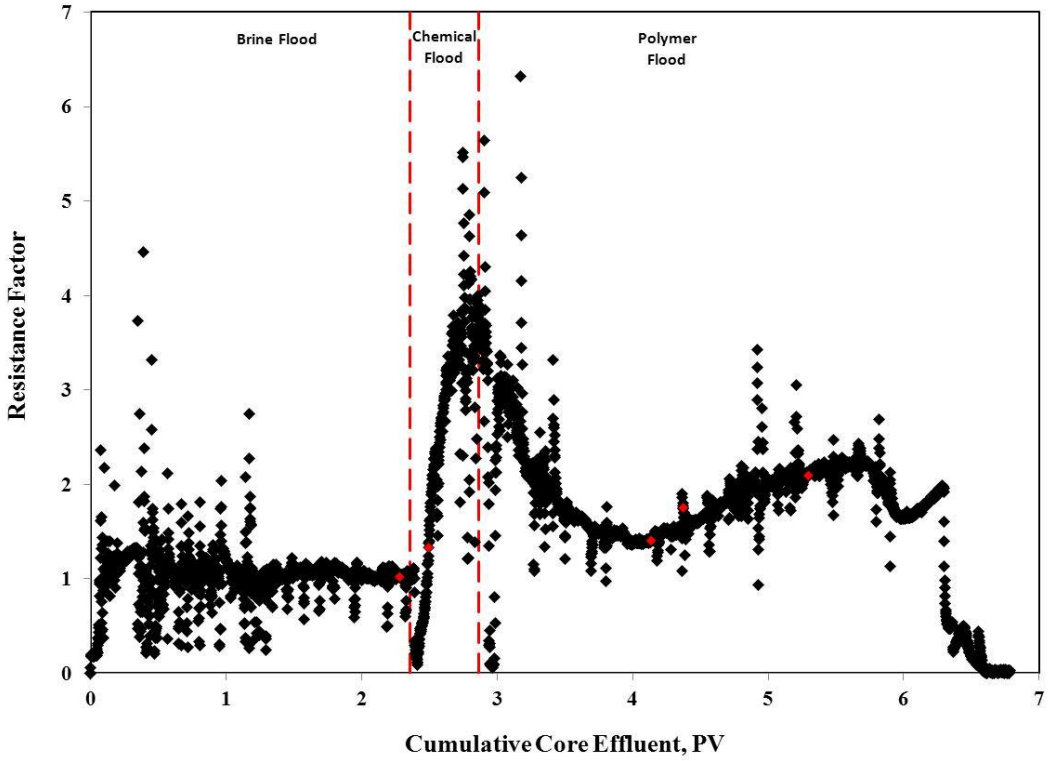

Fig. 110— Resistivity factor during different stages of Core Flood-4. The solution contain 1% OA-100; 3,000 ppm AMPS polymer; 0.3 wt.% Amph-SS surfactant in seawater. Residual resistivity factor less than original.

Core Flood-5 (MAB-18)

This experiment was similar to previous run with different in the type of alkali used which is sodium carbonate in (Na_2CO_3) this experiment and change in the injection scheme where main slug was followed with 1 PV of surfactant stage then chase flooding with seawater.

Shown in **Fig. 111** is the oil recovery and oil cut during water and chemical flooding mode as function of cumulative effluent from the core. Oil production started

immediately when the water flooding started and stopped at 1.3 PV. Water flooding continued until 2.08 PV was injected. Total oil recovery during the water flooding stage was 62.17 % of OOIP. Chemical flooding started and oil production started again after 0.24 PV of the slug was injected. Oil bank start flowing and maximum oil cut reached at 30.48%. Oil bank flowed for 1.49 PV and ultimate oil recovery from both water and chemical flooding reached 98.04% of OOIP with 94.86% of oil produced from residual oil during the tertiary mode. As can be seen in the **Fig. 111** the oil production started during chemical stage and showed rapid increase in recovery and continued and seized during the polymer flooding phase. This ASP formulation showed the maximum recovery compared to all other flooding runs.

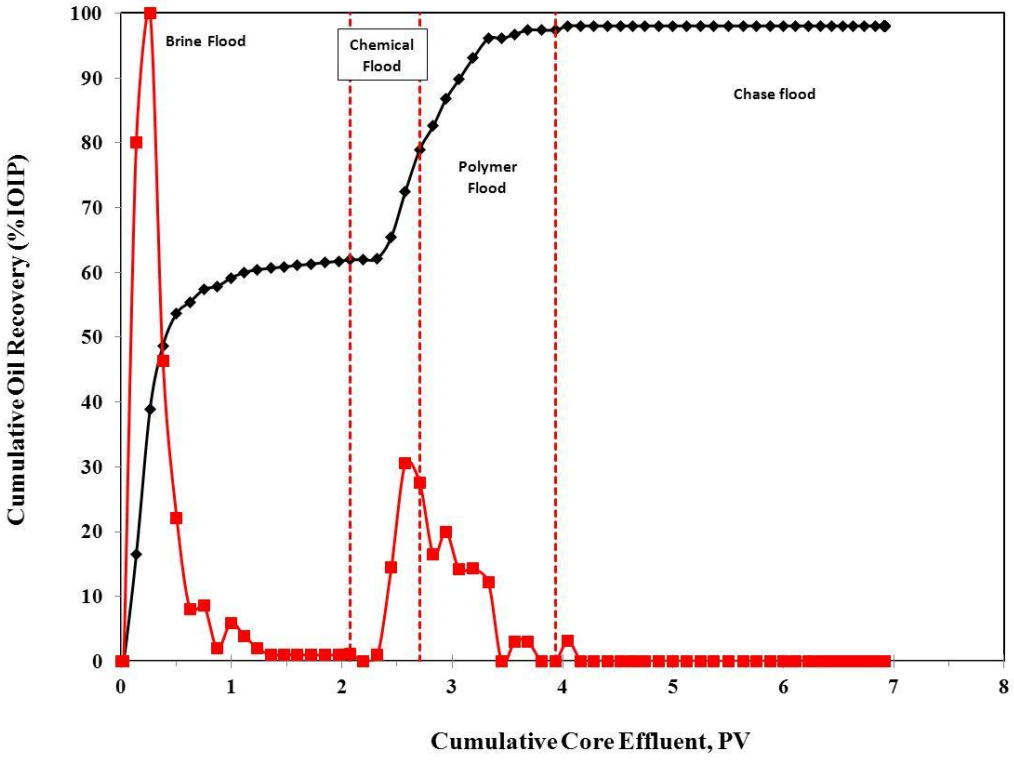

Fig. 111—Core flood-5 (MAB-18) history for slug having 1% Na_2CO_3; 3,000 ppm AMPS polymer; 0.3 wt.% Amph-SS surfactant in 6% NaCl.

Fig. 112 shows a rapid flow resistivity increase when chemical injection started, this was followed with unstable period during the initial polymer injection stage. Resistivity profile was more stable during the last part of the polymer flooding around 2.3. Prompt reduction in resistivity factor was observed when shifting from polymer injection to seawater; the second observation was the low residual resistivity factor of 0.21compared to resistivity during water flooding at ROS, which indicates the no significant chemical retention and favorable relative permeability to aqueous phase due to significant reduction of the oil saturation to 2%. The low chemical retention

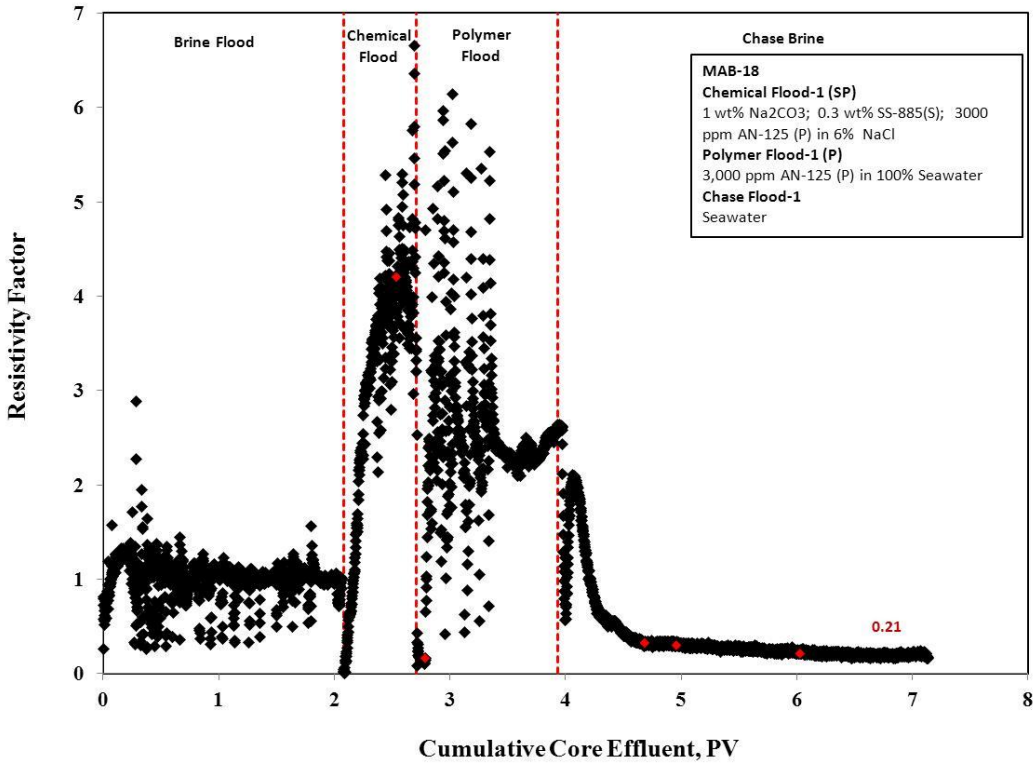

Fig. 112—Resistivity factor during different stages of Core Flood-5. The solution contain 1% Na2CO3, 0.3 wt.% Amph-SS, and 3,000 ppm AMPS polymer prepared in seawater. Residual resistivity factor was 0.21.

Core Flood-6 (MAB-11)

This run is similar to core flood-4 with change in chemical formulation by replacing the amphoteric with anionic surfactant. The same injection scheme was followed with same pore volume injected of main chemical slug and polymer stage.

Fig. 113 presents the oil recovery for this experiment were produced oil during water flooding reached 60.77% and ultimate recovery with tertiary phase reached to 73.08%. The oil bank started 0.475 after initiation of chemical flooding. In this run a delay in oil production was observed when compared to previous experiment. This delay can be explained by the retention in the chemical solution that can be explained by the opposite charge between the dolomite surface and anionic surfactant with negative charge.

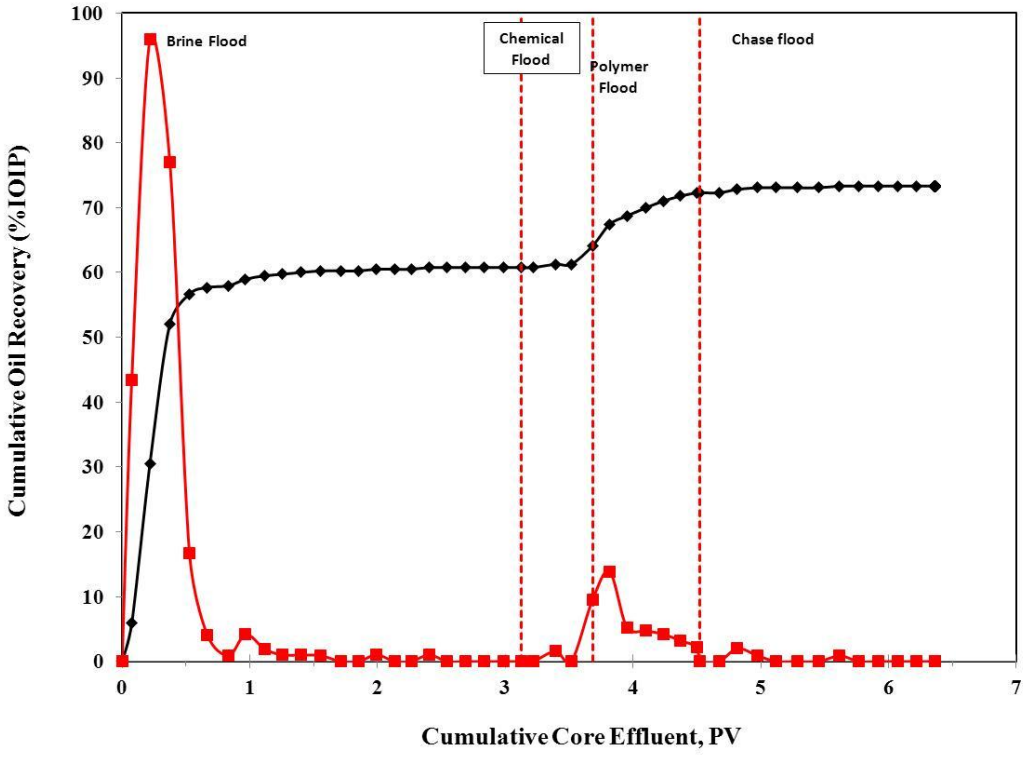

Fig. 113—Core flood-6 (MAB-11) history for slug having 1% OA-100; 3,000 ppm AMPS polymer; 0.3 wt.% Anionic-PS C1 surfactant in seawater.

Shown in **Fig. 114** the resistivity profile for the experiment with an increase in the resistivity during the chemical injection followed with decrease during oil bank production. A second increase in resistivity was noticed when polymer stage was started. The residual resistivity factor for this experiment was 0.64 which is higher than reported values in the previous runs. The resistivity behavior during chemical injection and the higher residual resistance value indicates some chemical retention compare to the previous flood experiment where the surfactant solution contain amphoteric surfactant which is expected to show less chemical retention at dolomite cores.

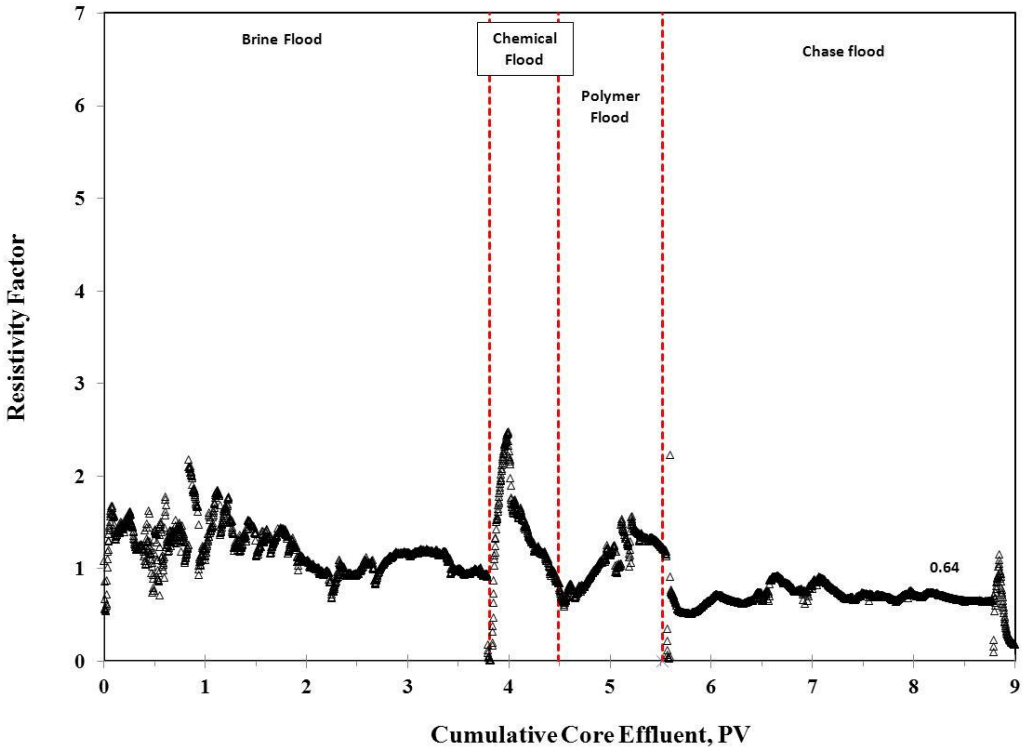

Fig. 114—Normalized pressure profile during different stages of Core Flood-6. The solution contain 1%OA-100; 0.3 wt.% Anionic-PS C1; and 3,000 ppm AMPS polymer prepared in seawater. Residual resistivity factor less than original.

Conclusions

Based on the results obtained in this study the following conclusions can be drawn:

1. Solutions based on amphoteric surfactant shows better recovery and less residual resistance when compared with solutions formulated by anionic surfactants.
2. ASP shows higher recoveries compared to LTPF processes.
3. ASP formulation prepared with sodium carbonate as an alkali shows higher recoveries and injection performance with solution prepared with organic alkali.
4. Organic alkali requires less operational conditions when compared with sodium carbonate. Organic alkali can be prepared in seawater without the need of water softening.
5. Indication of less chemical retention can be seen with solutions prepared using amphoteric surfactant compared to anionic ones.

CHAPTER VIII
FLUID FLOW CHARACTERIZATION OF CHEMICAL EOR FLOODING: A COMPUTERIZED TOMOGRAPHY (CT) SCAN STUDY*

Summary

Chemical flooding methods are used to recover residual oil left after water flooding. Several recovery mechanisms were suggested to improve the displacement effectiveness of the trapped oil. Reducing IFT, mobility control and wettability alteration are the main recovery mechanisms during chemical flooding. Understanding which recovery mechanism that dominate during recovery process helps selecting and optimizing which chemical process to be used.

An experimental study of 4 chemical flood experiments were visualized with computed tomography (CT) in sandstone cores at room temperature. The experiments were conducted to study four different chemical flooding processes: polymer, surfactant, surfactant-polymer (SP), and alkali-surfactant-polymer (ASP). Recovery and oil distribution in the cores were evaluated after the chemical flood.

The experimental results obtained from the core flooding experiment shows best recovery was during ASP and SP flooding with some residual reduction in permeability caused by using polymers. The lowest recovery was obtained during surfactant flooding, which prove that IFT reduction can't improve recovery without the aid of mobility control by polymers.

*Reprinted with permission from "Fluid Flow Characterization of Chemical EOR Flooding: A Computerized Tomography (CT) Scan Study" by Bataweel, M.A., and Nasr-El-Din, H.A.2011, Paper SPE 149066 presented at SPE/DGS Saudi Arabia Section Technical Symposium and Exhibition.

Introduction

Enhanced oil recovery (EOR) involves injection of fluids to displace the hydrocarbon in the porous media. Chemical flooding is one of these processes that are used for recovery enhancement. Surfactants, polymers and alkalis were evaluated separately and in combination by several researchers. Core flood studies are performed to simulate the immiscible displacement in porous media and cores are flooded with chemical at residual oil saturation S_{orw}. During chemical flooding process four flow regions are established which can be seen from the core effluent. The four regions starting from the core outlet are (i) initial two-phase flow at S_{orw}, (ii) oil bank in with increase in saturation, (iii) two or three phase flow of oil, water and microemulsion, and (iv) single-phase flow of the chasing fluid (Austad and Taugbol 1995). Understanding the flow behavior inside the porous media and it's effect on the recovery can explain the different recovery values for each chemical method.

Core flood experiments are used to determine the oil recovery during secondary and tertiary mode. One of the most important output of this experiment is the recovery curve which is used to predict the performance of different flooding processes. This curve is generated by collecting the effluent coming out of the sample without knowing the bath or the displacement mechanism that resulted in this recovery. For this reason the ability to observe the in-situ displacement and saturation distribution at different displacement stages will help better understanding the process.

Peters and Hardham (1990) used X-ray computed tomography (CT) imaging to observe the in-situ displacement processes in number of core flood experiments. They were able to see three displacement mechanisms for unstable miscible flooding; 1) displacement from the fresh area of the core not contacted by initial finger, 2) displacement of the areas of the core contacted by the initial finger, and 3) displacement from the edge of the initial finger due to the lateral growth by dispersion. However in the case of unstable immiscible displacement, only the second displacement mechanism take place which results in slight increase in recovery after breakthrough.

Chakravarthy *et al.* (2004) used CT scan to measure saturation and porosity during CO_2 injection in homogenous and fractured core. They found improvement in recovery when injected viscosified water to reduce the mobility of CO_2. A good agreement in saturation values was found when determined using CT scan and effluent data.

Chen *et al*. (2001) used the CT-scan to investigate the significance of redial countercurrent movement caused by capillary forces and vertical cocurrent movement caused by gravity during surfactant static imbibition. They found that dilute surfactant showed a higher rate of radial penetration compared to water imbibitions, which resulted in higher recovery.

Hou *et al*. (2009) studied the microscopic flow mechanism of polymer flooding using CT. They found that improvement in recovery resulted from flow redirection and viscoelastic effect of polymer flooding.

Computerized tomography

CT is non-destructive imaging technique that uses X-ray technology and mathematical reconstruction algorithms to view cross-sectional slices of an object (Siddiqui and Khamees 2004; Vinegar 1986). In petroleum industry CT scan technology is used in two main application areas: core description and fluid flow characterization.

Several researchers used CT scanning to study variety of EOR techniques including different chemical processes. During these studies, researchers used radiopaque (dopants) to monitor fluid movement and saturation changes inside the cores during fluid flow using different chemical agents. The dopants enhance contrast between aqueous and oil during two phase flowing inside the core. This helps view and quantifies saturation distribution and changes during the flow process.

CT scan principles

CT scan technique is based on the attenuation of the X-ray beams penetrating the scanned object at different angles as the X-ray source rotate around the object. Series of detectors records the transmitted X-ray intensity data. From these projections, a cross

sectional slice is generated through the core by reconstruction by the computer. A three dimensional image can be reconstructed from the cross-sectional slices taken a cross the sample.

The basic quantity measured in CT is the linear attenuation coefficient μ. . This is define from Beer's law:

$$\frac{I}{I_o} = exp^{-\mu h} \quad \text{.....(24)}$$

where I_o is the incident X-ray intensity, I is the intensity remaining after passing through a thickness h of homogeneous sample (Vinegar and Wellington 1987; Akin and Kovscek 2003; Al-Muntasheri et al. 2010).

CT scan application

Withjack et al.(2003) presented a comprehensive list applications of CT in oil industry. They grouped these applications and give examples for each application, following are the suggested categories: core description, desaturation studies, improve recovery, hydrate studies, recovery of viscous oil, formation damage, and perforation analysis.

CT scan in EOR and fluid flow characterization

Fluid flow visualization during core flooding is one of established techniques to study displacement efficiency and saturation changes using different EOR processes. Researchers used CT to understand the effects of viscous, gravity, trapping, bypassing, and heterogeneity on flow inside the rock (Siddiqui and Khamees 2004; Withjack et al. 2003). More description to the saturation determination will be given in coming section.

Porosity determination and core characterization

Porosity and porosity distribution through the core can be determined using CT scan with high agreement (± 1 porosity %) as stated by Akin and Kovscek (2003). The following equation is used to determine the porosity for each volume element

$$\emptyset = \frac{CT_{wsat} - CT_{dry}}{CT_w - CT_A} \quad \text{.....(25)}$$

where ϕ is porosity (frac.), CT_{wsat} is the CT-number of 100% water saturated core inside core-holder, CT_{dry} is the CT-number for dry core inside core-holder, CT_w is the CT-number for water inside core-holder, and CT_A is the CT-number for air inside core-holder.

CT scan applications in core characterization involve whole cores and plugs (Siddiqui and Khamees 2004). In qualitative CT analysis information about heterogeneities, vugs, fractures, bedding planes (lamination), and lithology can by collected (Siddiqui and Khamees 2004). Using information from the CT scan can be useful to predict the flow behavior in the porous medium. Quantitatively, CT data can be used to measure the bulk density and porosity; to quantify heterogeneity, to make core to log comparison for depth matching and log calibration (Siddiqui and Khamees 2004).

Determination of the two-phase saturation

A single energy scan is sufficient to determine two phase saturation. Linear interpolation between the pure states is used for determining the saturation. For porous media containing oil and brine, a scan gives the following (Akin and Kovscek 2003):

$$CT_{owr} = (1-\phi)\mu_r + \phi S_o \mu_o + \phi S_w \mu_w \quad \text{.....(26)}$$

where C_{owr} is the CT-number of porous media saturated with oil and brine, μ_r, , μ_w, and μ_o are the attenuation coefficients for rock, core fully saturated with water and oil, S_o is the oil saturation and S_w is the water saturation.

$$S_w + S_o = 1 \quad \text{.....(27)}$$

The water saturation (Sw) can be calculated using the following equation (Alvestad et al. 1992; Al-Muntasheri et al. 2010):

$$\boldsymbol{S_w = \frac{CTx - CT_{or}}{CT_{wr} - CT_{or}}} \quad \text{.....(28)}$$

where CTx is the CT-number for image in question, CT_{wr} and CT_{or} are 100% water saturated core and 100% oil saturated core. One way to obtain CT_{wr} and CT_{or} is by scanning the 100% water saturated core. Then cleaning the core and totally saturating it by oil and take second scan to determine CT_{or}.

Another way to obtain the value CT_{or} was reported by Alvestad et al. (1992). The CT value of the rock completely saturated with oil is interpolated from the CT images of dry and water saturated sample using the following equation:

$$\boldsymbol{CT_{or} = CT_{dry} + \frac{CT_o - CT_A}{CT_w - CT_A}\left(CT_{wr} - CT_{dry}\right)} \quad \text{.....(29)}$$

In this study, we focus on the change of the saturation across the core sample and development of the oil bank during different chemical flooding processes using X-ray CT scanning and how it can effects oil recovery.

Experimental Studies

Materials

Berea sandstone cores were used to conduct this study. The core samples were cut in cynical shape with 1 in. diameter and length ranges between 8 to 12 in.

Surfactant used was betaine-based amphoteric surfactant. Polymer used was a copolymer of 2-acrylamido-2methyl propane sulfonate and acrylamide (AMPS). Oleic tracer was 1-Iodohexadecane (98%) and obtained from Alfa Aesar. Organic alkaline was used in ASP flooding.

Seawater was used in this study for aqueous solution preparation. Synthetic seawater was prepared using compositions shown in **Table 22**. Sodium chloride, calcium chloride, magnesium chloride, sodium sodium bicarbonate, and sodium sulfate were (ACS) reagent grade and obtained from Mallinckodt Baker, Inc. These salts and deionized water (resistivity = 18 MΩ.cm) were used to prepare seawater solution. Crude oil samples were used in this study. Crude oil samples were filtered using Berea sandstone and centrifuged before injected to the core sample.

Table 22—Seawater composition used in CT scan study.

Ions	Concentration, mg/L
Na^{+}	16,877
Ca^{2+}	664
Mg^{2+}	2,279
Ba^{2+}	0
Sr^{2+}	0
HCO_3^{-}	193
Cl^{-}	31,107
SO_4^{2-}	3,560
CO_3^{-}	0
TDS	54,680

Equipment

The experimental apparatus consist of core-flow set-up and HD 350 E X-Ray CT scanner. A simplified schematic diagram of the apparatus is shown in **Fig. 115**. The main components of the core flow set-up are core-holder, a pump, three liquid transfer accumulator, back pressure regulator and two absolute pressure transducers.

The core holder that is designed to accommodate core plug samples with diameter of 1" and length up to 12". The core holder is made of aluminum for scanning purpose because it has lower X-ray attenuation compared to commonly used metal materials. A rubber sleeve surrounds the core and is held by two end pieces at the end of the core holder. Confining pressure at the core is applied to injecting hydraulic oil to the cell using hand pump.

The injection system consist of positive displacement pump (ISCO 500 D syringe pump) equipped with a programMABle controller which can be set to deliver constant pressure or flow rate. The pump is connected to three accumulators to deliver brine, oil or chemical solutions. A set of valves were used to inject one of the above fluids to the core sample. Back pressure regulator was connected to the outlet and was used to control the flowing pressure inside the core sample.

The X-Ray CT scanner is a fourth generation Universal systems HD 350 E system with a resolution of 0.35x 0.35x 1 mm. This scanner is used to collect cross-sectional images along the core. Cross sectional scans of the core sample are made at regular intervals during the experiment. Each cross-sectional slice is 2 mm think and 6 or 18 mm apart. The data obtained from the CT scanner is transferred to a PC for image processing. The cross sectional images can then be used for porosity and saturation determination or reconstructed for flow visualization.

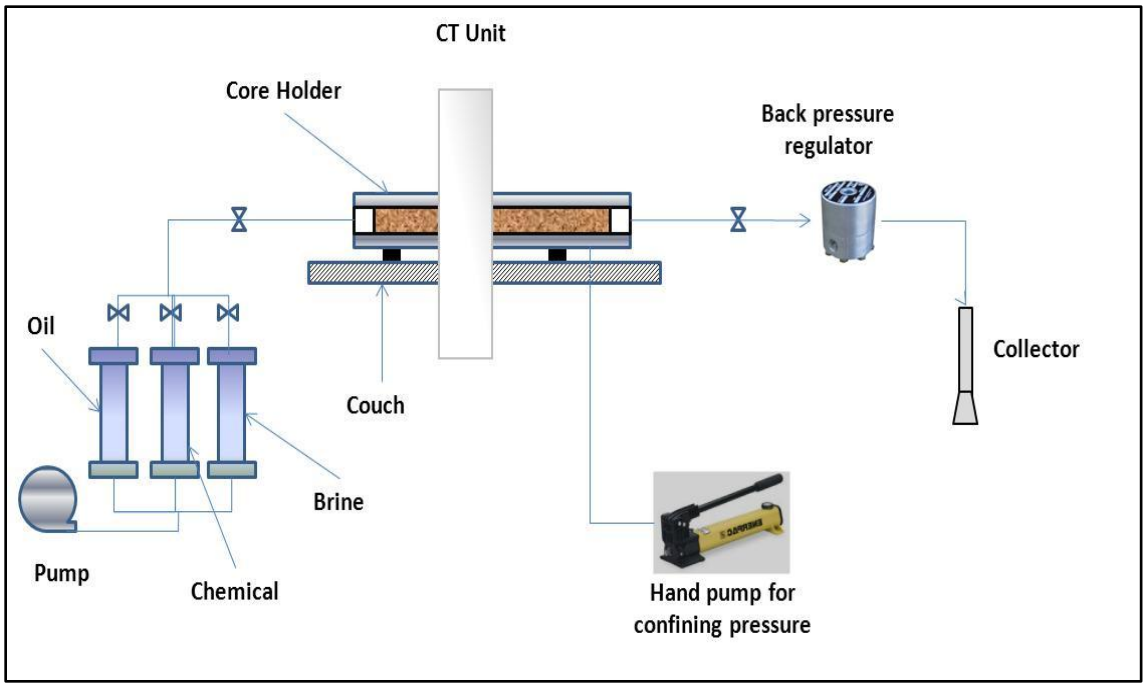

Fig. 115—Schematic for experimental set-up.

Procedure

Following are the steps for core preparation and core-flow experiments:

- Core samples were dried overnight in 95 ^{o}C oven.
- Core sample were load to the core-holder and confining pressure was applied followed by scan for dry core.
- Sample was vacuum saturated and 10 PV of brine was injected to the core to establish 100% water saturation.
- Base permeability to water was measured using different flow rates (1, 2, 4 and 8 cm^3/min) followed by scan (water saturated scan).
- Crude oil flood to displace movable water and establish irreducible water saturation (S_{wir}) followed by scan (scan at S_{wir}).

- Determine relative permeability to oil at S_{wir}, core sample was left in the core holder under confining and pore pressure for at least 8 hours before starting the next step.
- Water flooding started as a secondary recovery and 3 pore volumes were injected to establish residual oil saturation (S_{orw}) followed by scan (scan at S_{orw})
- Chemical flooding started as a tertiary recovery and one pore volume was injected. Several scans are taken in this stage to track the oil bank formation and displacement.

Result and discussion

Core flood studies

In this study four chemical flooding methods were conducted; alkaline-surfactant-polymer (ASP), surfactant-polymer (SP), polymer (P), and surfactant (S). All chemical flooding experiments were conducted in tertiary mode at residual oil saturation (S_{or}). Cores information used in this study are given in **Table 23**.

Table 23—Berea sandstone cores information used in CT scan studies.

Core number	CT-10	CT-11	CT-12	CT-15
Length (cm)	30.48	30.48	30.48	22.70
Diameter (cm)	2.51	2.51	2.46	2.48
Porosity (%)	19.7	18.9	18.9	19.2
Pemeability (md)	78	50	52	81
Temperature (^oC)	25	25	25	25
Chemical Process	SP	S	ASP	P
Chemical slug (PV)	1	1	1	1

Surfactant-polymer flood

Fig. 116 gives the porosity profile along the core used in this experiment with an average porosity of 19.7%. A uniform porosity distribution through the length of the core at vertical planes to the flow is shown in **Fig. 116**. The core flood experiment was conducted to study the flow behavior and oil bank formation during tertiary recovery stage using SP flooding. Formulations for all chemical slugs are given in **Table 24**. The saturation profile through the length of the core at the end of different flooding stages (at irreducible water saturation, water flooding, and SP flooding) is shown in **Fig. 117**. The figure shows the uniform increase in water saturation after water flooding the core with 3 PV to residual oil saturation (S_{orw}) from line 2 to line 3. At the end of the chemical injection, saturation was found to have maximum change in the core inlet and gradual reduction in water saturation change moving toward the core outlet. A sharp change in saturation is observed at the end of the core indicating a chemical front where a clear break in saturation continuity can be seen. This is an indication of good initial displacement, thus more injection is needed to assure complete displacement of any movable oil during the SP flood process.

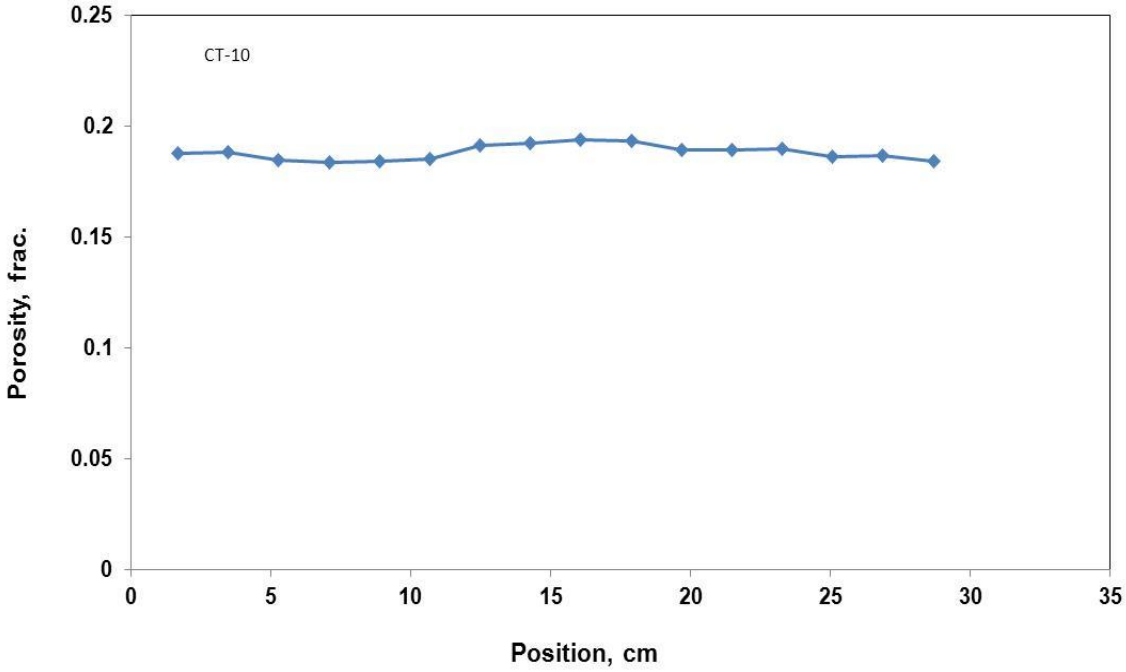

Fig. 116—Porosity distribution for core CT-10 used in SP flooding.

Table 24—Chemical formulation for chemical processes used in CT scan studies.

	Alkali	**Surfactant**	**Polymer**
Chemical flood	Organic Alkali, wt.%	Amphoteric, wt.%	AMPS, ppm
SP	NA	0.3	1,000
ASP	0.5	0.3	1,000
S	NA	0.3	NA
P	NA	NA	1,000

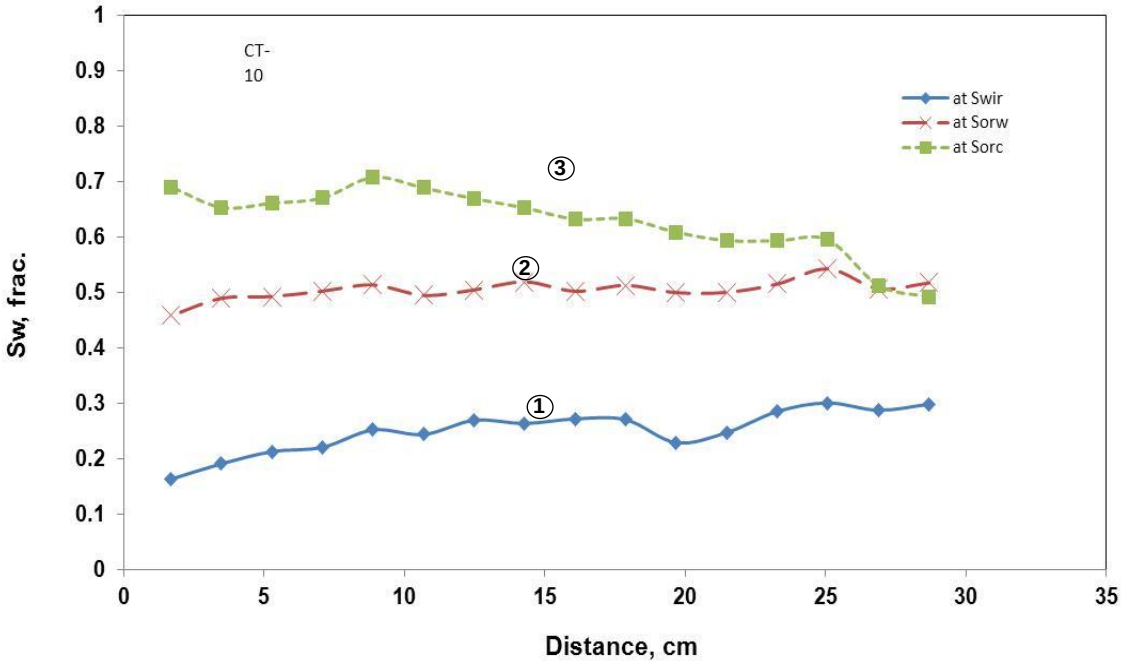

Fig. 117—Water saturation at different displacement stages (at irreducible water saturation, water flooding, and SP flooding) core CT-10.

Fig. 118 shows in-situ propagation and growth of the oil-bank during the chemical injection. Oil saturation was monitored in different positions of the core from inlet to outlet (5.28, 12.48, 17.88, 21.48. and 26.88 cm). Closer to the core inlet at 5.28 cm it can be seen the beginning of the formation of the oil bank followed with sharp reduction in the oil saturation as a sign of displacement by this SP flooding. The oil bank grows larger as traveling through the core and adding more oil to the bank.

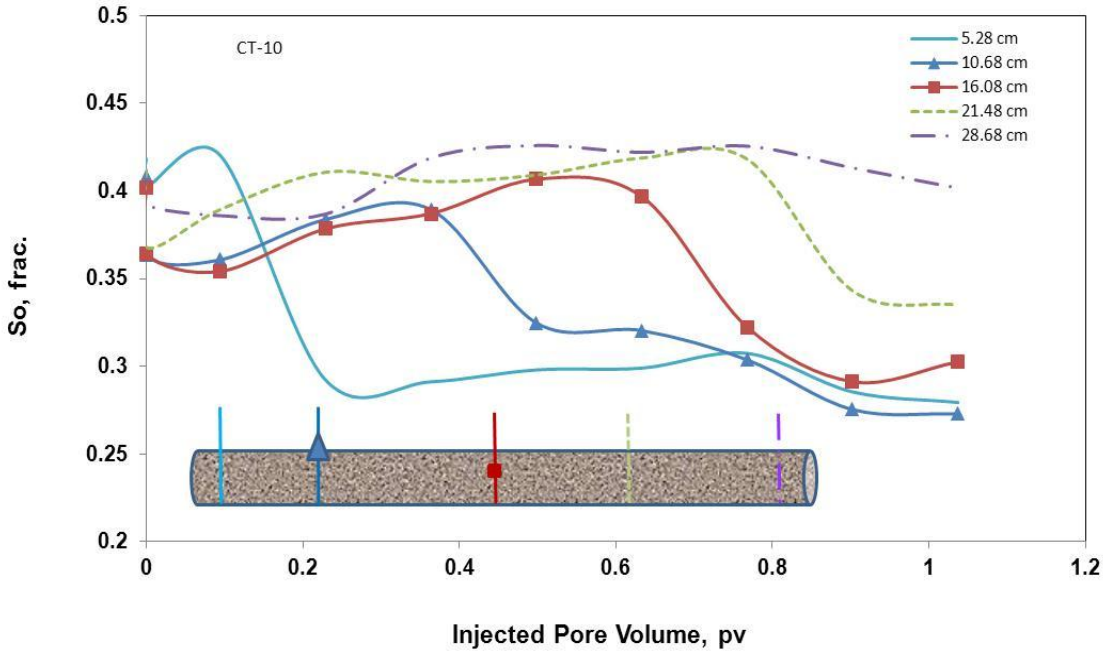

Fig. 118—Oil-bank propagation and growth dring SP injection (CT-10).

Fig. 119 shows the advance of the chemical front with injected volume at five time steps from 0 to 1.04 PV injected. Change in saturation profile is clear however it deviate from piston-like displacement. The chemical front has two regions; first region where gradual change in saturation was followed with a second region with sharper saturation change. Observation of the first region, shows that it starts at the highest water saturation for the core at that time step followed gradual reduction and end at a constant saturation around 0.67 (line 1). Second region shows a sharper change in saturation down to water saturation after water flooding was completed. It can also be noticed that the first region is growing as more chemical is injected however there is no change in region 2 which is closer to piston-like behavior. The development of two saturation regions can be explained by variation in the chemical flowing inside the core. Where part of the core is showing piston-like behavior and delay in flow or degradation of the chemical slug is happening in other part. The variation in the fluid flow inside the core is caused by high permeability streaks in the rock and variation in saturation can be seen clearly in (**Fig.**

120). In the **Fig. 120** the flow is dominated by one bedding and displacement in other layers are lagging. This behavior causes less efficiency in recovery when compared with a more uniform displacement (Piston-like).

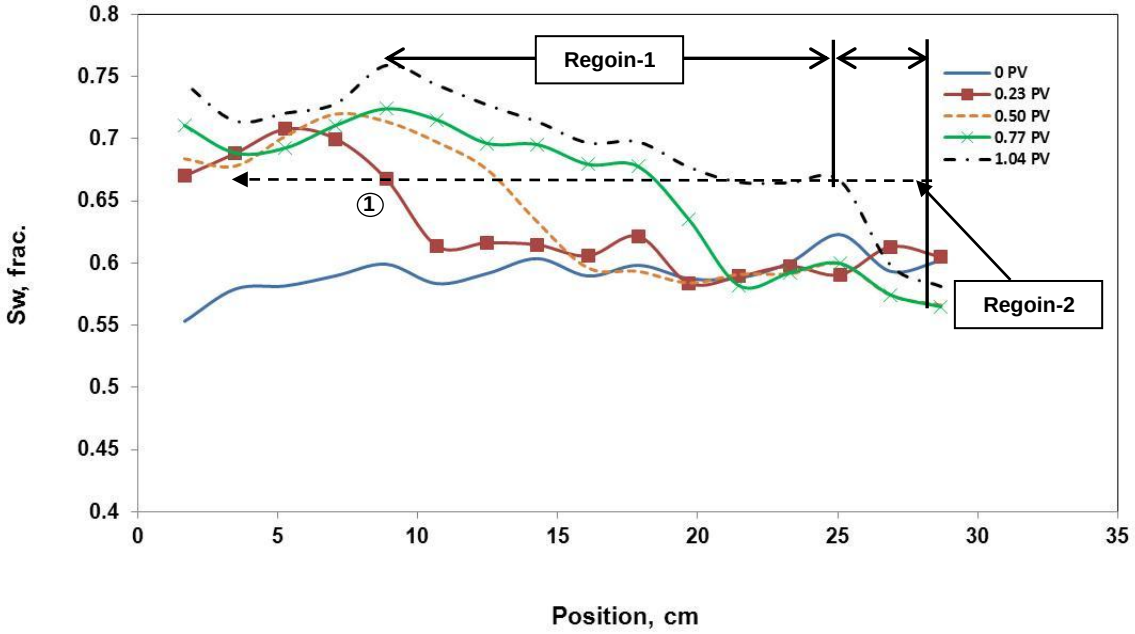

Fig. 119—Water saturation along the core at different injected pore volumes of SP flood (core CT-10).

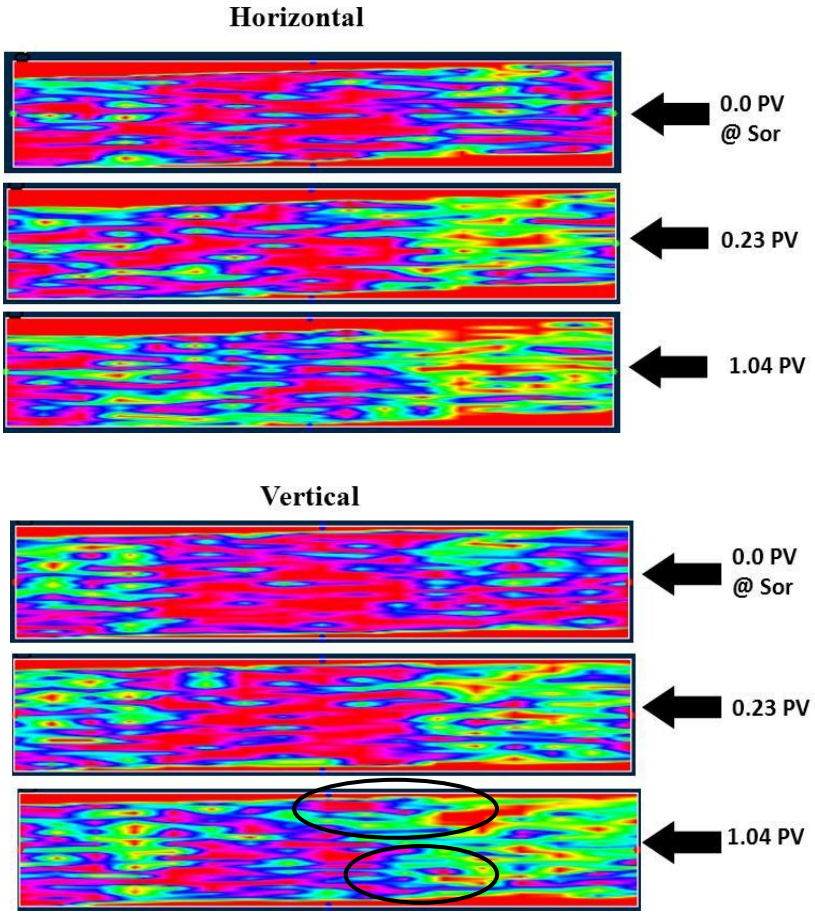

Fig. 120—Reconstructed axial image during SP flooding at different injected pore volumes into core CT-10, where dominant channel and smaller channels that caused to region of chemical front.

Alkali-surfactant-polymer flood

This experiment was conducted to study the effect of ASP flooding on the formation and propagation of the oil bank and chemical front. Alkaline is usually added to generate in-situ surfactant, minimize surfactant adsorption on the rock or alter the wettability to more water-wet. In this study the alkaline used was an organic alkali that has more tolerance to high hardness ions in the mixing and formation brines compared to conventional alkalis. **Fig. 121** shows the porosity profile along the core used in this experiment. The saturation profile for this core at three different stages, after oil, water,

and chemical flooding, is given in **Fig. 122**. As can be seen in **Fig. 122** there is recovery improvement after ASP injection similar to the SP flood. The water saturation shows a higher saturation value in the inlet with gradual decrease toward the outlet. However, a more complete displacement was achieved in this experiment compared with the SP were water front did not reach the end.

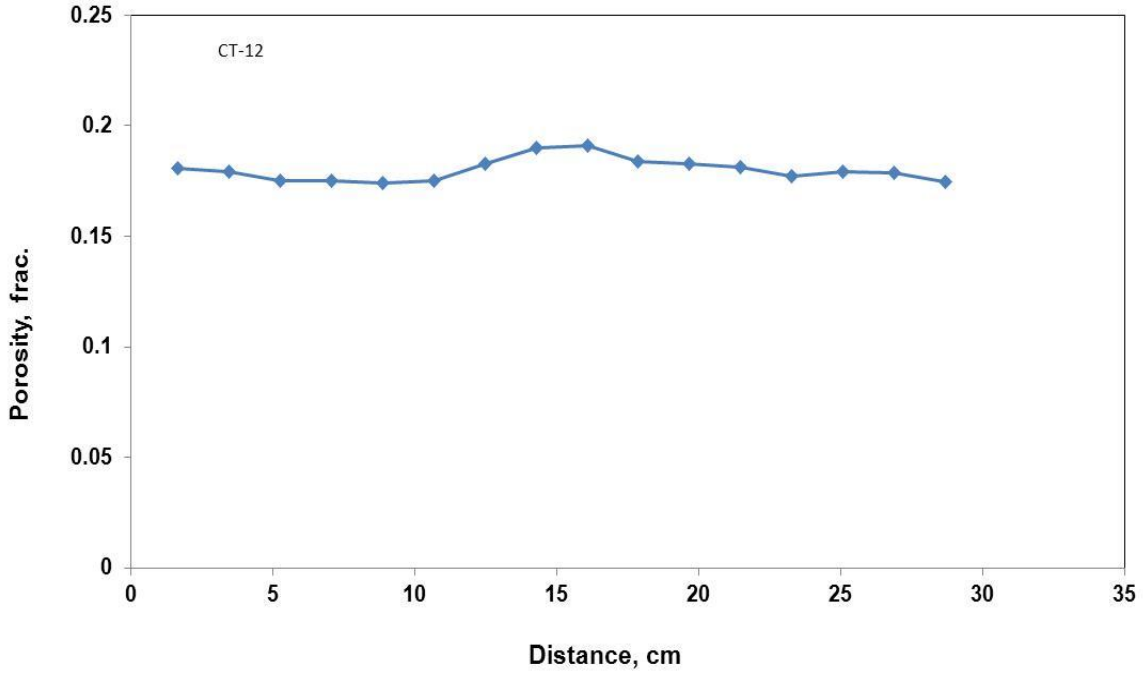

Fig. 121—Porosity distribution for core CT-12 used in ASP flooding.

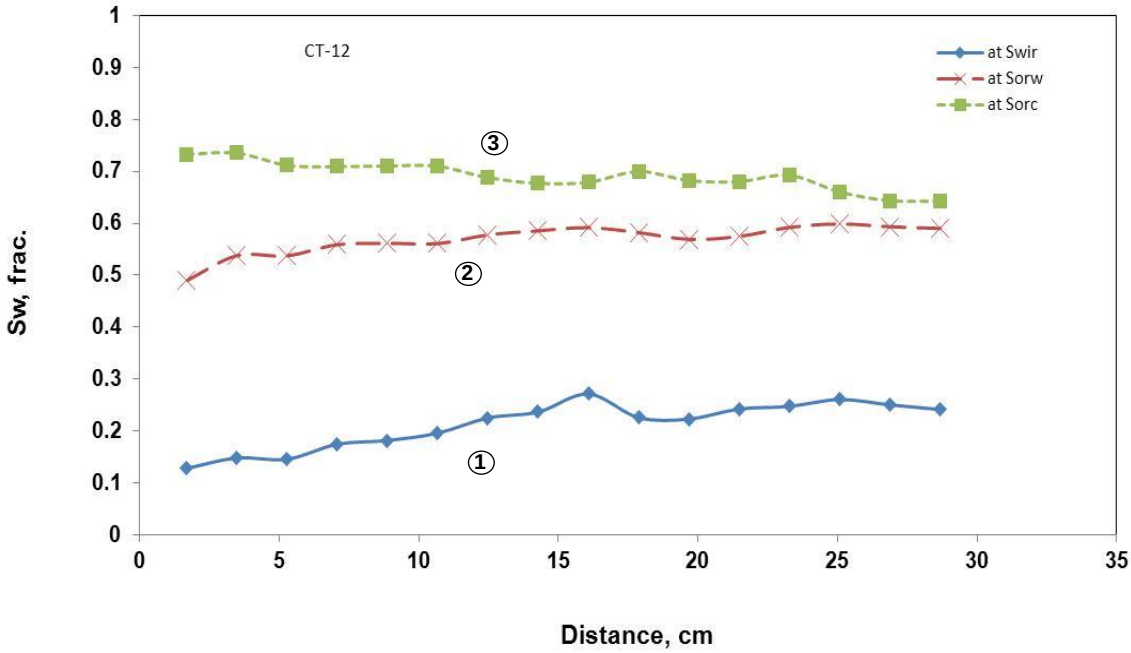

Fig. 122—Water saturation at different displacement stages (at irreducible water saturation, water flooding, and ASP flooding) core CT-12.

Fig. 123 shows the oil bank propagation in the core during the ASP injection. Saturation was monitored in five different locations along the core (5.28, 12.48, 17.88, 21.48, and 26.88 cm from inlet). Similar to the SP the oil bank start forming at 5.38 cm from the inlet and grows broader flowing through the core and recovering more oil.

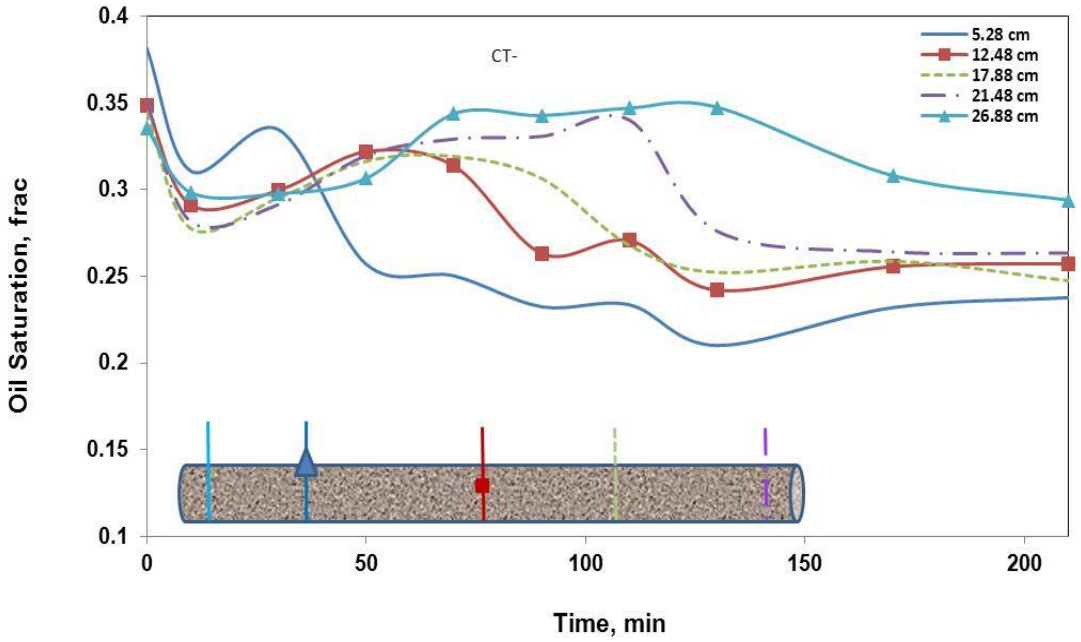

Fig. 123—Oil-bank propagation and growth dring ASP injection (CT-12).

Fig. 124 gives the advancement of the chemical front at five time steps (0, 70, 90, 130, and 170 min.). The chemical front starts with sharp saturation change in the initial stages of injection, however, the front start smoothening out and gradual saturation change was noticed in later times. As the front propagate in the core deviation from piston-like displacement increases. The deviation of the chemical displacement from sharp- piston-like front at the beginning of the core gradual saturation change shows the effect of the core length at the recovery studies using core flooding. If the core is not long enough the core will only see the piston-like behavior and will result in misleading higher recovery values.

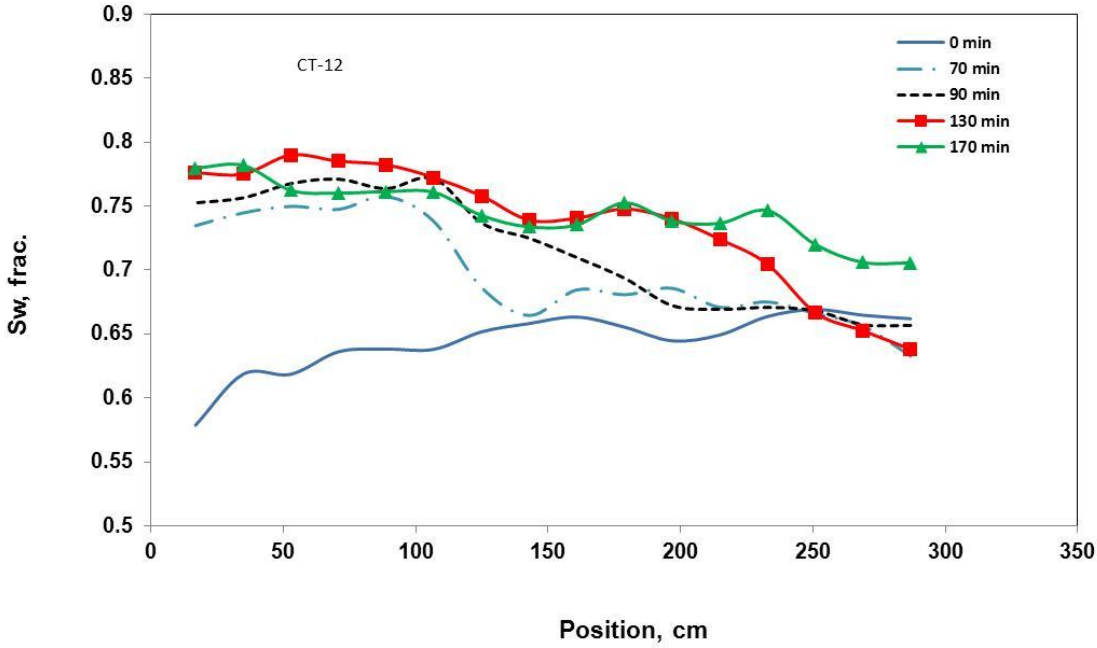

Fig. 124—Water saturation along the core at different injected pore volumes of ASP flood (core CT-12).

Fig. 125 presents flow channeling in this experiment (circled in the figure) no dominating channel was created during chemical flow inside the core. However, several channels were formed and chemical advancement was deviated from piston-like displacement. When compared to the first experiment where dominated channel was formed and moved ahead of other layers which give the piston like behavior in part of the advancing fronts.

SP and ASP processes give close recovery values of 31% and 29 %, respectively, of the residual oil after water flooding. These values were achieved following different displacement routs.

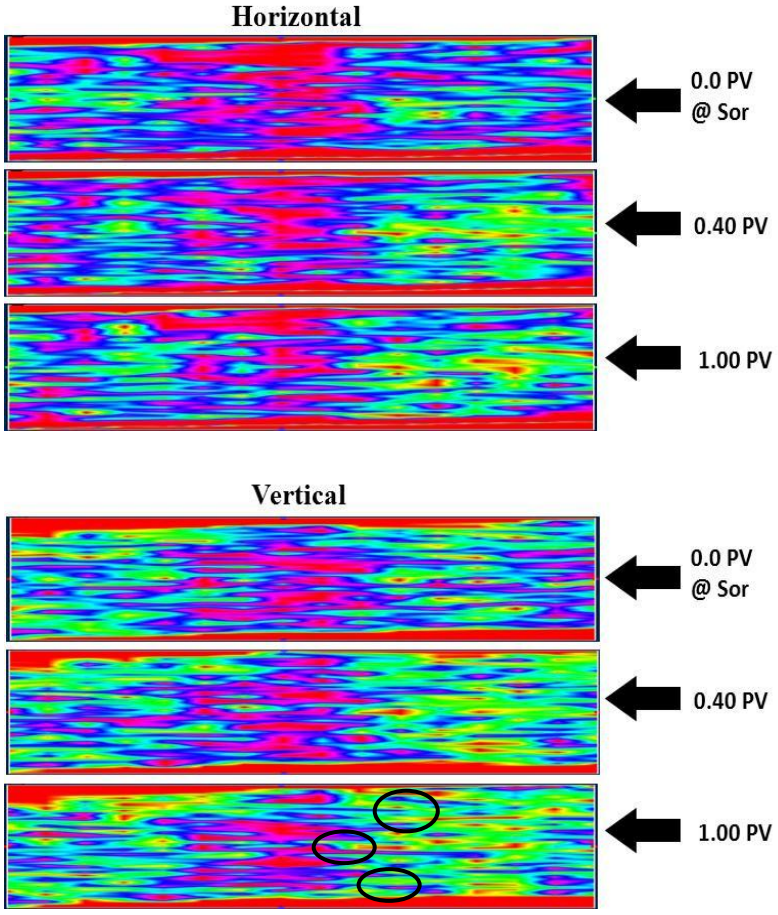

Fig. 125—Reconstructed axial image during ASP flooding at different injected pore volumes into core CT-12, where several channels were formed and caused deviation from piston-like displacement at chemical front.

Surfactant flood

In this experiment surfactant solution was injected to the core to evaluate recovery enhancement by this process. **Fig. 126** shows the porosity profile along the core used in this experiment with an average porosity of 18.9%. The saturation profile through the length of the core at different saturation stages (irreducible water saturation, water flooding, and chemical flooding) is shown in **Fig. 127**. An average of 4.4% increase in water saturation after injection surfactant to the core. However, no clear formation of an oil bank was observed. **Fig. 128** gives the saturation distribution inside the core. As

observed in the figure there is a spread of the injected chemical in the core with no clear advancing front and with small change in saturation not like the ASP and SP where front was observed and greater change in saturation that reflected in greater change in the color. After surfactant flooding was completed only traces of oil was recovered, less than 5% recovery.

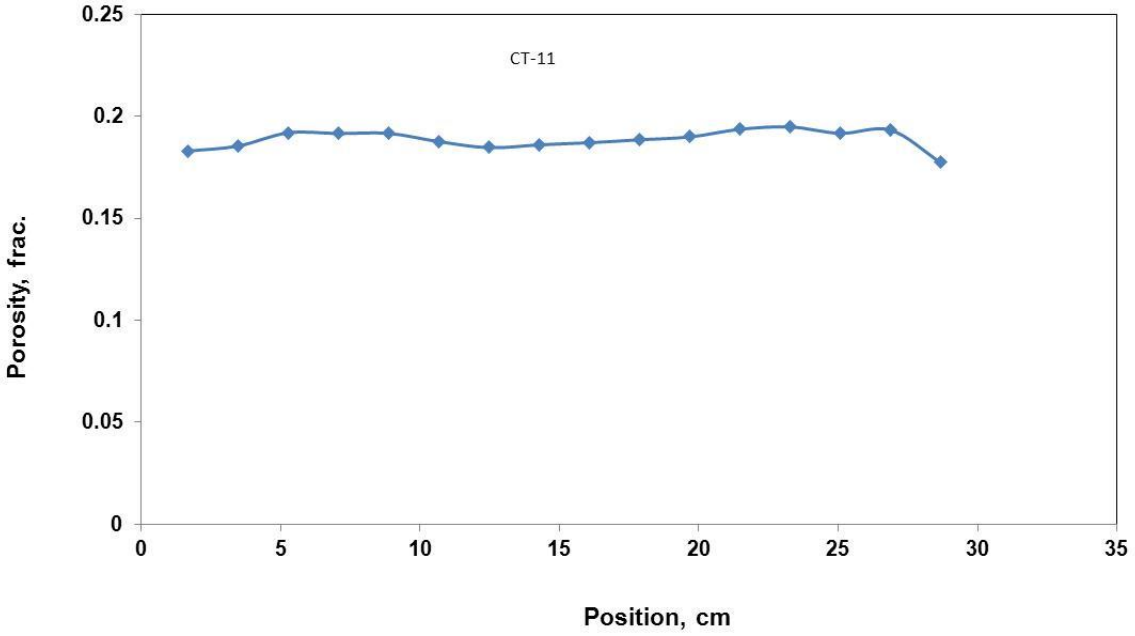

Fig. 126—Porosity distribution for core CT-11 used in S flooding.

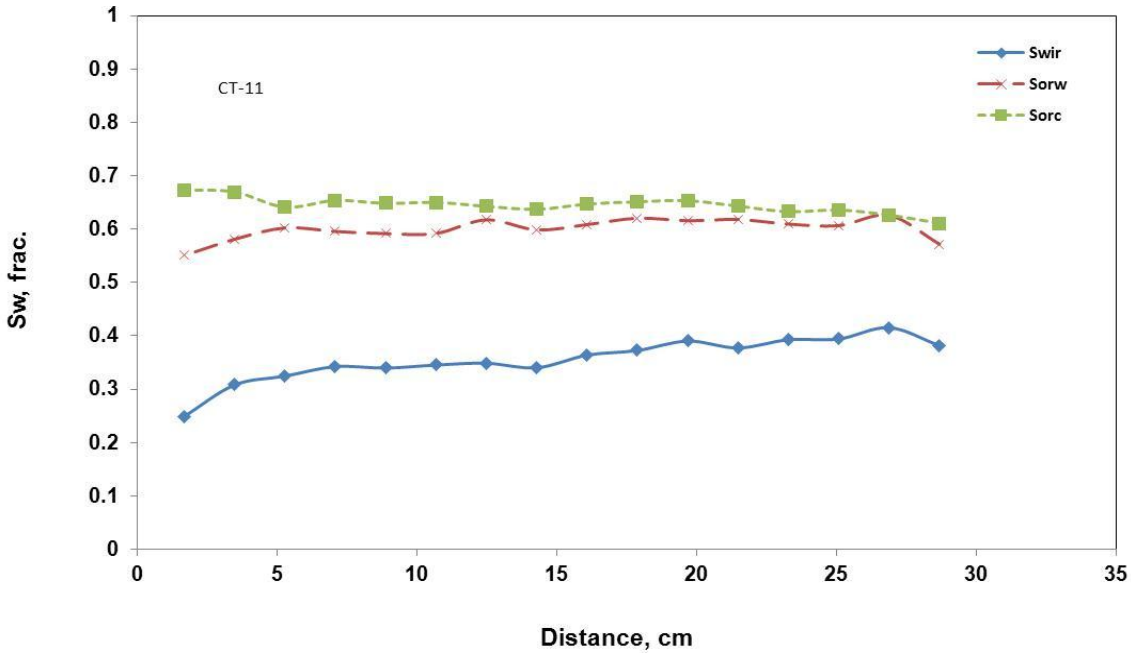

Fig. 127—Water saturation at different displacement stages (at irreducible water saturation, water flooding, and S flooding) core CT-11.

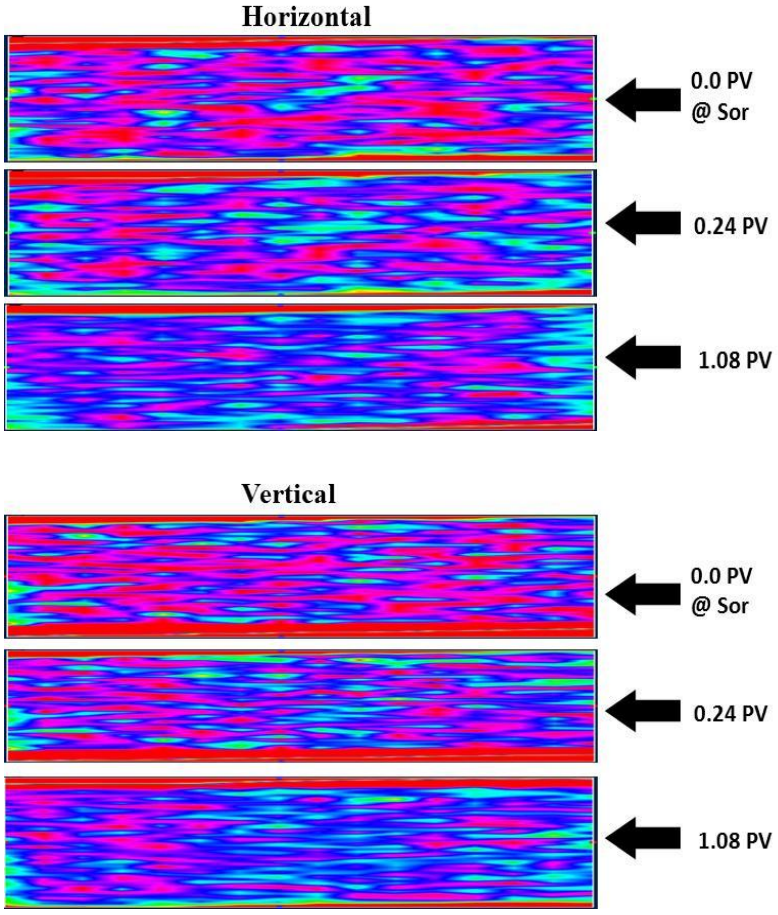

Fig. 128—Reconstructed axial image during ASP flooding at different injected pore volumes into core CT-11.

Polymer flood

In this experiment polymer flooding was evaluated by injecting one pore volume of the chemical and determines the recoverable oil. No surfactant was used so no reduction in IFT is expected. No clear chemical front advancement was observed in this experiment. **Fig. 129** shows the porosity profile at the core. **Fig. 130** gives the saturation profile at different injection stages and more oil recovered was gained compared to the water flooding stage. The recovery due to polymer flooding was around 18% of the oil in the core after water flooding. .

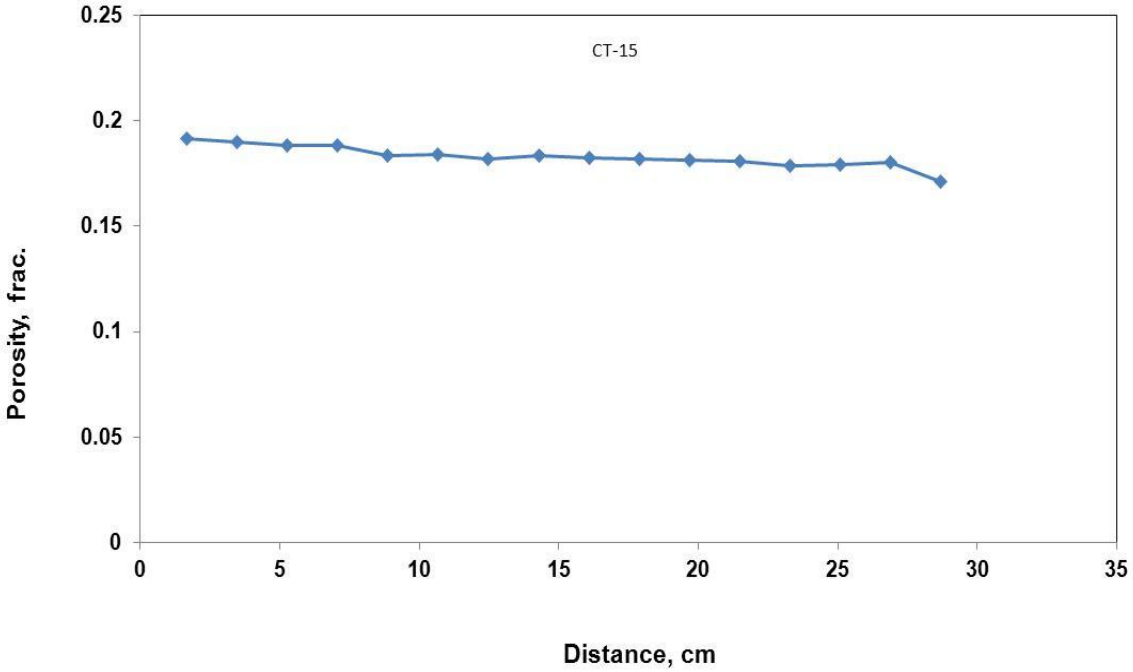

Fig. 129—Porosity distribution for core CT-15 used in P flooding.

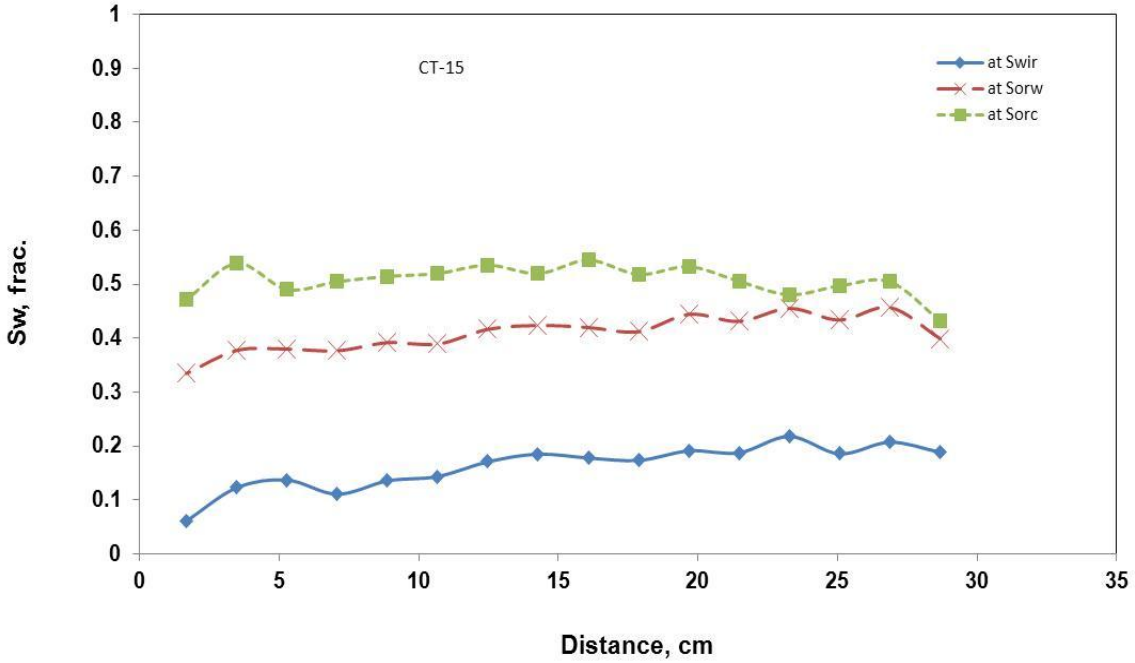

Fig. 130—Water saturation at different displacement stages (at irreducible water saturation, water flooding, and P flooding) core CT-15.

Conclusions

Based on the results obtained in this study the following conclusions can be drawn:

1. ASP and SP give the highest oil recovery compared to surfactant or polymer flooding.
2. Formation and propagation of the oil bank is a dynamic process and change in the oil saturation can be seen during different time steps of the chemical flooding.
3. CT scan can give an insight to the displacement of the front and help better understand different displacement mechanisms, in our case dominant channel verses multi-channels.
4. IFT is not enough to improve recovery, better mobility control is needed.
5. The pore structure plays an important role in having an effective chemical displacement.

CHAPTER IX
CONCLUSIONS AND RECOMMENDATIONS

The objective of this study was to evaluate ASP and SP flooding for an application in high salinity/high hardness reservoirs at high temperature using simple chemical formulation with low surfactant concentration using amphoteric surfactant. The evaluation included comparison with some anionic surfactants that are usually used in the industry for such application. In this study we tried to avoid the use of complicated chemical formulations including with main surfactant other chemical like cosurfactant, cosolvent, and salts in addition to polymer to recover residual oil. Traditionally the above formulation is used to generate microemulsion phase with help of proper salinity gradient through the reservoir. With this approach a tight control of reservoir and advancement of chemical slug need to followed. This may include reconditioning the reservoir by injecting a preflush ahead of the main slug to target the right salinity environment for micro-emulsion formation. To implement the salinity gradient brines with different qualities are needed which can add extra head and operational cost to the project in areas where there is scarcity of water supplies.

In Chapter II we studied precipitation and solubility of different alkaline spices used in the industry and two recently recommended novel alkalis sodium metaborate and organic alkali. The novel alkalis used in this study to overcome the need for water softening to prepare ASP solutions for chemical flooding operation. This will make using produced or seawater suitable for preparation media for the ASP solution. Second advantage of using these novel alkalis is reduction of possible plugging of the formation when chemical solution hit zone with high concentration of divalent cations are residence in the formation. This will also minimize the scale formation as what happen in some fields when they use ASP flooding. Organic alkali shows the best solubility in seawater and formation brine. Organic alkali shows no plugging when injected in cores flooded with seawater and minimum reduction in permeability when injected in cores with extremely high salinity brine with 230,000 ppm total dissolved solids (TDS).

In Chapter III Interfacial properties of the surfactant and alkali were studied. Several amphoteric surfactants were tested and screened using IFT studies. Several surfactant concentrations for each type were used during the screening process. SS-885 showed the lower IFT and was studied in details for different effects on the interfacial properties. Effect of salinity, mixing of brines, polymer type and concentration, alkali type and concentration

In Chapter IV rheological study of potential SP solutions were conducted. Amphoteric surfactant showed compatibility with polymer solution and can be used in chemical flooding. Effect of concentrations of two types of surfactants, anionic and amphotaric on chemical slug viscosity was studied. Amphotaric surfactant was found to have a preferable rheological attributes when compared to anionic surfactant. Amphoteric surfactant can maintain viscosity of chemical solution at high salinity and no reduction in viscosity was noticed when this type of surfactant was added to the solution. On the other hand, reduction in viscosity was measured when anionic surfactant was added to the solution.

In Chapter V several core flood experiments were performed using Berea sandstone cores. Different chemical flooding processes were evaluated using two amphoteric surfactants, two types polymer, and two types of alkalis were evaluated. Amphoteric surfactant showed association with two types of polymers, HPAM and AMPS, that caused reduction in surface activity until polymer-free aggregate concentration was reached. Increasing polymer concentration increases the surfactant concentration needed to reach to polymer-free aggregate concentration. When HPAM polymer used in preparing chemical slug, it shows higher injectivity decline compared to AMPS. Anionic surfactant showed less chemical retention due to the negative surface charge on Berea sandstone particles when this type of surfactant is used. No recovery was obtained during surfactant flooding, which prove that IFT reduction can’t improve recovery without the aid of mobility control by polymers.

In Chapter VI, ASP formulation prepared with anionic surfactant showed the best oil recovery compared to other chemical flooding processes. Although solutions

prepared with amphoteric surfactant shows the least IFT values they did not give the highest recovery. ASP solution prepared using organic alkali showed similar recovery when compared to high concentration surfactant formulation.

In Chapter VII core flood experiments using dolomite core was conducted. Chemical slug prepared with amphoteric surfactants showed higher recovery and lower chemical retention that is reflected in lower injection resistivity factor. High recovery values were gained when amphoteric surfactants were used with or without sodium carbonate addition. Adding sodium carbonate showed and improved recovery. ASP and SP solutions prepared using anionic surfactants shows lesser recovery and higher injection resistivity factors.

In Chapter VIII CT scan was used to visualize the chemical front progress, and formation and propagation of oil bank at different chemical flooding processes. Chemical was flowing in several channels during the chemical flooding process which limited the oil recovery to the invaded zone. The experimental results obtained from the core flooding experiment shows best recovery was during ASP and SP flooding with some residual reduction in permeability caused by using polymers. The lowest recovery was obtained during surfactant flooding, which prove that IFT reduction can't improve recovery without the aid of mobility control by polymers.

The following are recommendations from the study:

i. For effective use of amphoteric surfactant in sandstone rocks strategies to minimize adsorption should be used. In this study modified amphoteric surfactant to minimize adsorption showed better recovery in sandstone cores.
ii. Amphoteric surfactant is effective in lowering IFT with low concentrations and should be used in case of high divalent concentrations in preparation and formation brine.
iii. Develop concentration detection techniques for some challenging types of amphoteric surfactant. HPLC techniques using ELSD detector should be tested and evaluated.

iv. Improving core flooding setup attached to the CT scan facility to accommodate larger size core samples and minimize dead volumes for better saturation measurement. Include heating capability, better pressure detection arrangement and data acquisition system to expand the capability for more detailed recovery studies.

The following are the main recommendation for future studies:

i. Interaction between amphoteric surfactant with different types of polymers used in chemical flooding (partially hydrolyzed, AMPS and xanthan) should be examined to find which combination will give best flowing characteristics and least injectivity decline.

ii. Effect of pH on oil recovery and adsorption in sandstone and carbonate when using amphoteric surfactant to determine what will be best environment for using this type of surfactant for chemical flooding.

iii. Evaluate different strategies to minimize amphoteric surfactant in sandstone reservoirs.

iv. In-situ formation and propagation of oil bank during surfactant based chemical flooding processes should be examined deeply through simultaneously use of CT scan, core effluent and pressure profile (pressure tapes) in carbonate and sandstone reservoir and its effect on oil recovery.

REFERENCES

Abdullah, W., Buckley, J., Carnegie, A., John, Edwards, J., Fordham, E., Graue, A., Habashy, T., Hussain, H., Mentaron, B., and Ziauddin, M. 2007. Fundamentals of Wettability. *Oilfield Review*, **19** (2): 44-61.

Akin, S., and Kovscek, A.R. 2003. Computed tomography in Petroleum Engineering Research.*App.of X-ray CT in Geosci.* **215**:23-38.

Al-Hashim, H.S., Obiora, V., Al-Yousef, H.Y., Fernandez, F., and Noval, W. 1996. Alkaline Surfactant Polymer Formulation for Saudi Arabian Carbonate Reservoirs. Paper SPE/DOE 35353 presented at SPE/DOE Tenth Symposium on Improved Oil Recovery, Tulsa, Oklahoma, 21-24 April. doi: 10.2118/35353-MS.

Al-Muntasheri, G.A., Nasr-El-Din, H.A., and Zitha, P.L.J. 2008. Gelation Kinetics and Performance Evaluation of an Organically Crosslinked Gel at High Temperature and Pressure. *SPEJ*. **13** (3): 337-345. SPE 104071-PA. doi: 10.2118/104071-PA.

Al-Muntasheri, G.A., Zitha, P.L.J., and Nasr-El-Din, H.A. 2010. A New Organic Gel System for Water Control: A Computed Tomography Study. *SPEJ* **15** (1):197-207. SPE-129659. doi: 10.2118/129659-PA.

Alvestad, J., Gilje, E., Hove, A.O., Langeland, O., Maldal, T., and Schiling, B.E.R. 1992. Coreflood Experiments with Surfactant Systems for IOR: Computer Tomography Studies and Numerical Modeling. *J. Pet. Sci. & Eng*., **7:** 155-171.

Anderson, W.G. 1986. Wettability Literature Survey-Part 1: Rock/Oil/Brine Interactions and the Effects of Core Handling on Wettability. *JPT*, October: **38** (10): 1125-1144. SPE- 13932-PA. doi: 10.2118/13932-PA.

Anderson, W.G. 1987. Wettability Literature Survey-Part 5: The Effect of Wettability on Relative Permeability. *JPT*, November **39** (11): 1453-1468. SPE-16323-PA. doi: 10.2118/16323-PA.

Aoudia, M., Al-Harthi, Z., Al-Maamari, R.S., Lee, C., and Berger, P. 2010. Novel Alkyl Ether Sulfonates for High Salinity Reservoir: Effect of Concentration on Transient Ultralow Interfacial Tension at the Oil-Water Interface. *J. Surfact Deterg*. 13: 233-242.

Arihara, N., Yoneyama, T., Akita, Y, and Guo L.X. 1999. Oil Recovery Mechanisms of Alkali-Surfactant-Polymer Flooding. Paper SPE-54330 presented in the SPE Asia Pacific Oil and Gas Conference and Exhibition, Jakarta, Indonesia, 20-22 April. doi: 10.2118/54330-MS.

Austad, T., Fjelde, I., Veggeland, K., and Taugbol, K. 1994. Physicochemical Principles of Low Tension Polymer Flood. *Journal of Petroleum Science and Engineering*. **10** (3): 255-269. doi:10.1016/0920-4105(94)90085-X.

Austad, T. and Taugbal, K. 1995. Chemical Flooding of Oil Reservoirs 1.Low Tension Polymer Flood Using a Polymer Gradient in the Three-Phase Region. *Colloids and Surfaces A: Physicochemical and Engineering Aspects***. 101** (1): 87-97. doi:10.1016/0927-7757(95)03231-2.

Bataweel, M.A., and Nasr-El-Din, H.A. 2011a. Minimizing Scale Precipitation in Carbonate Cores Caused by Alkalis in ASP Flooding in High Salinity/High Temperature Applications. Paper SPE 141451 presented in the SPE International Symposium on Oilfield Chemistry, The Woodlands, Texas, 11-13 April. doi: 10.2118/141451-MS.

Bataweel, M.A., Nasr-El-Din, H.A., and Schechter, D.S. 2011b. Fluid Flow Characterization if Chemical EOR Flooding: A Computerized Tomography (CT) Scan Study. Paper SPE 149066-MS presented at SPE Saudi Arabia Section Technical Symposium and Exhibition, AlKhobar, 15-18 May. doi: 10.2118/149066-MS.

Berger, P.D. and Berger, C.H. 2009. Oil Recovery Method Employing Amphoteric Surfactants. US Patent No. 7,556,098.

Berger, P.D. and Lee, C.H. 2006. Improve ASP Process Using Organic Alkali. Paper SPE 99581 presented at the SPE/DOE Symposium on Improved Oil Recovery, Tulsa, Oklahoma, 22-26 April. doi: 10.2118/99581-MS.

Berger, P.D. and Lee, C.H. 2008. Composition and Process for Recovering Subterranean Oil Using Green Non-Toxic Biodegradable Strong Alkali Metal Salts of Polymerized Weak Acids. US. Patent No. 2008/0312108.

Bragg, J.R., Gale, W.W., McElhannon Jr., W.A., Davenport, O.W., Petrichuk, M.D., and Ashcraft, T.L. 1982. Loudon Surfactant Flood Pilot Test. Paper SPE 10862 presented at the SPE/DOE Third Joint Symposium on Enhanced Oil Recovery, Tulsa, OK, 4-7 April. doi: 10.2118/10862-MS.

Broze, G. 1999. *Handbook of Detergents: Properties.* New York: Marcel Dekker

Castor, T.P., and Somerton, W.H. 1977. Interfacial Instabilities in Porous Media. Paper SPE 6516-MS presented at the SPE California Regional Meeting, Bakersfield, California. 13-15 April. doi: 10.2118/6516-MS.

Cayias, J.L., Schechter, R.S., and Wade, W.H. 1975. The Measurement of Low Interfacial Tension via the Spinning Drop Technique. In ACS Symposium Ser. No. 8, Adsorption at Interfaces. American Chemical Society, Washington, DC, 234–247.

Chakravarthy, D., Muralidharan, V., Putra, E., Schechter, D.S. 2004. Application of X-ray CT for Investigation of CO2 and WAG Injection in Fractured Reserviors. Paper 2004-232 presented at the Petroleum Society's 5th Canadian International Petroleum Conference, Calgary, Alberta, Canada, 8-10 June.

Chen, H.L., Lucas, L.R., Nogaret L.A.D., Yang, H.D., and Kenyon, D.E. 2001. Laboratory Monitoring of Surfactant Imbibition with Computerized Tomography. *SPERE&E*, **4** (1): 16-25. SPE 69197. doi: 10.2118/69197-PA.

Cheng, K.H. 1986. Chemical Consumption During Alkaline Flooding: A Comparative Evaluation. Paper SPE 14944 presented at the SPE/DOE 5th Symposium on Enhanced Oil Recovery, Tulsa, Oklahoma, 20-23 April. doi: 10.2118/14944-MS.

deZabala, E.F., Vislocky, J.M., Rubin, E., and Radke, C.J. 1982. A Chemical Theory for Linear Alkaline Flooding. *SPEJ*, 245-258, Apr. 1982. doi: 10.2118/8997-PA.

Doe, P.H., Moradi-Araghi, A., Shaw, J.E., and Stahl, G.A. 1987. Development and Evaluation of EOR Polymers Suitable for Hostile Environments—Part 1: Copolymers of Vinylpyrrolidone and Acrylamide. *SPERE* **2**(4): 461-467. doi: 10.2118/14233-PA.

Doghaish, N.M. 2008. *Analysis of Enhanced Oil Recovery Processes—A Literature Review*. M.Eng., Dalhouse U. Canada.

Ferrel, H.H., Easterly, R.A., Murphy, T.B., and Kennedy, J.J.E. 1987. Evaluation of Micellar-Polymer Flood Projects in Highly Saline Environment in the El Dorado Field. Final report, DOE/BC/10830-6. (December).

Ferri, J. K., and Stebe, K. J. 2000. Which Surfactants Reduce Surface Tension Faster? A Scaling Argument for Diffusion-Controlled Adsorption. *Advances in Colloid and Interface Science.* **85** (1): 61-97.

Flaaten, A.K., Nguyen, Q.P., Pope, G.A., and Zhang, J. 2008. A Systematic Laboratory Approach to Low-Cost, High-Performance Chemical Flooding. Paper SPE 113469 presented at the SPE/DOE Improved Oil Recovery Symposium, Tulsa, Oklahoma, 19-23 April. doi: 10.2118/113469-MS.

Flaaten, A.K, Nguyen, Q.P, Zhang, J., Mohammadi, H., and Pope, G.A. 2010. Alkaline/Surfactant/Polymer Chemical Flooding Without the Need for Soft Water. *SPEJ*. **15** (1): 184-196. SPE- 116754-PA. doi: 10.2118/116754-PA.

Gardner, J.E., and Hayes, M.E. 1981. *University of Texas Spinning Drop Interfacial Tensiometer Model 500 Instruction Manual*. Department of Chemistry, University of Texas at Austin.

Goddard, E.D. and Ananthapadmanabhan, K.P. 1993. *Interactions of surfactants with polymers and proteins*. Boca Raton, Florida: CRC Press.

Gomaa, A.M., and Nasr-El-Din, H.A. 2010. Propagation of Regular HCl Acid in Carbonate Rocks: The Impact of an In-Situ Gelled Acid Stage. Paper SPE 130586 presented at the CPS/SPE International Oil & Gas Conference and Exhibition in China, Beijing, China, 8-10 June. doi: 10.2118/130586-MS.

Green, D.W. and Willhite, G.P. 1998. *Enhanced Oil Recovery*.Vol. 6, *SPE Textbook Series,* Richardson, Texas: SPE.

Guerra, E., Valero, E., Rodriguez, D., Castillo, M., Espinoza, J., and Garnja, G. 2007.Improved ASP Design Using Organic Compound-Surfactant-Polymer (OCSP) for La Salina Field, Maracaibo Lake. Paper SPE 107776 presented at the SPE Latin American and Caribbean Petroleum Engineering Conference, Buenos Aires, Argentina, 15-18, April. doi: 10.2118/107776-MS.

Hamaker, D.E., and Franzier, G.D. 1978. Nava Enhanced Recovery Pilot Design and Implementation. Paper SPE 7088 presented at the SPE Symposium on Improved Methods for Oil Recovery, Tulsa, Oklahoma, 16-19 April. doi: 10.2118/7088-MS.

Hirasaki, G.J. 2008.Recent Advances in Surfactant EOR. Paper SPE 115386 presented at the Annual Technical Conference and Exhibition, Denver, Colorado, 21-24 September. doi: 10.2118/115386-MS.

Hirasaki, G.J. 1991. Wettability: Fundamentals and Surface Forces. *SPEFE*, **6** (2): 217-226. doi: 10.2118/17367-PA.

Hirasaki, G. and Zhang, D.L. 2003. Surface Chemistry of Oil Recovery from Fractured, Oil-Wet, Carbonate Formation. Paper SPE 80988 presented at the International Symposium on Oilfield Chemistry, Houston, Texas, 5-8 February. doi: 10.2118/17367-PA.

Hou, J., Li, Zhenquan, Zhang, S., Cao, X., Du, Q., and Song, X. 2009. Computerized Tomography Study of the Microscopic Flow Mechanism of Polymer Flooding. *Transp. Porous Med*., **79** (3): 407-418.

Hove, A.O., Nilsen, V., and Leknes, J. 1990.Visualization of Xanthan Flood Behavior in Core Samples by Means of X-Ray Tomography. *SPERE*, **5** (4): 475-479. SPE 17342. doi: 10.2118/17342-PA.

Johnson Jr., C.E. 1976. Status of Caustic and Emulsion Methods. J*PT*, **20** (1): 85-92. SPE- 5561-PA. doi: 10.2118/5561-PA.

Kalpakci, B., Arf, T.G., Barker, J.W., Krupa, A.S., Morgan, J.C., Neira, R.D. 1990. The Low-Tension Polymer Flood Approach to Cost-Effective Chemical EOR. Paper SPE/DOE 20220 presented in SPE/DOE Seventh Symposium on Enhance Oil Recovery, Tulsa, Oklahoma, 22-25 April. doi: 10.2118/20220-MS.

Kalpakci, B., and Chan, K. S. 1985. Method of Enhanced Oil Recovery Employing Thickened Amphoteric Surfactant Solutions. US Patent No.4,554,974.

Khan, M.Y., Samanta, A., Ojha, K., and Mandal, A. 2009. Design of Alkaline/Surfactant/Polymer (ASP) Slug and Its Use in Enhanced Oil Recovery. *Petroleum Science and Technology*. **27** (17): 1926-1942. doi: 10.1080/ 10916460802662765.

Kim, D.H., Lee, S., Ahn, C.H., Huh, C., and Pope, G.A. 2010. Development of a Viscoelastic Property Database for EOR Polymers. Paper SPE 129971 presented at SPE Improved Oil Recovery Symposium, Tulsa, Oklahoma, 24-28 April. doi: 10.2118/129971-MS.

Krumrine, P.H., Mayer, E.H., and Brock, G.F. 1985. Scale formation During Alkaline Flooding. *JPT*, **37** (8): 1466 – 1474. SPE-12671-PA. doi: 10.2118/12671-PA.

Kurenkov, V.F., Hartan, H.G., and Lobanov, F. I. 2001. Alkaline Hydrolysis of Polyacrylamide. *Russian Journal of Applied Chemistry*, **74** (4): 543-554.

Lake, L. 1989. *Enhanced Oil Recovery*. Englewood Cliffs, New Jersey: Prentice Hall.

Lee, S., Kim, D.H., Huh, C., and Pope, G.A. 2009.Development of Comprehensive Rheological Property Database for EOR Polymers. Paper SPE 124798 presented at SPE Annual Technical Conference and Exhibition, New Orleans, Louisiana, 4-7 October. doi: 10.2118/124798-MS.

Levitt D.B., and Pope, G.A. 2008. Selection and Screening of Polymers for Enhanced-Oil Recovery. Paper SPE 113845-MS presented at the SPE/DOE Symposium on Improved Oil Recovery, Tulsa, Oklahoma, 20-23 April. doi: 10.2118/113845-MS.

Levitt, D.B., Jackson, A.C. Heinson, C. Britton, L.N., Malik, T., Dwarakanath, V., and Pope, G.A. 2009. Identification and Evaluation of High-Performance EOR Surfactants. *SPEREE*, **12** (2): 243-253. SPE 100089-PA. doi: 10.2118/100089-PA.

Li, J., Wang, W., and Gu., Y. 2003. Dynamic Interfacial Tension and Oil Shrinking Effect of Crude Oil in Alkaline Solutions. Paper 2003-139 presented at the Canadian International Petroleum Conference, Calgary, Alberta, 10 – 12 June.

Liu, S. 2007. *Alkaline Surfactant Polymer Enhanced Oil Recovery Process*. Ph.D. dissertation, Rice U., Houston, Texas.

Liu, S., Zhang, D.L, Yan, W., Puerto, M., Hirasaki, G.J, and Miller, C.A. 2008. Favorable Attributes of Alkaline-Surfactant-Polymer Flooding. *SPEJ* **13** (1): 5-16. doi: 10.2118/99744-PA.

Magbagbeola, O.A. 2008. *Quantification of the Viscoelastic Behavior of High Molecular Weight Polymers Used for Chemical Enhanced Oil Recovery*. M.S.E Thesis. University of Texas. Austin, Texas.

Mangalsingh, D., and Jagai, T. 1996. A Laboratory Investigation of the Carbon Dioxide Immiscible Process. Paper SPE 36134 presented at SPE Latin America/Caribbean Petroleum Engineering Conference, Port-of-Spain, Trinidad. 23-26 April. doi: 10.2118/36134-MS.

McAuliffe, C. 1973. Oil-in-Water Emulsions and Their Flow Properties in Porous Media. *JPT* **25** (6): 727-733. SPE-4369-PA. doi: 10.2118/4369-PA. doi: 10.2118/4369-PA.

Miller, C. A., and Neogi, P. 1985. I*nterfacial Phenomena, Surfactant Science Series, V. 17.* New York: Marcel Dekker, Inc.

Moradi-Araghi, A., Cleveland, D.H., Jones, W.W. and Westerman, I.J. 1987. Development and Evaluation of EOR Polymers Suitable for Hostile Environments: II: Copolymers of Acrylamide and Sodium AMPS. Paper SPE 16273 presented at the International Symposium on Oilfield Chemistry, San Antonio, Texas, 4–6 February. doi: 10.2118/16273-MS.

Muller, G. 1981. Thermal Stability of High-Molecular-Weight Polyacrylamide Aqueous solutions. *Polymer Bulletin* **5** (1): 31-37. doi: 10.1007/BF00255084.

Murtada, H., and Marx, C. 1982. Evaluation of the Low Tension Flood Process for High-Salinity Reservoir-Laboratory Investigation Under Reservoir Conditions. *SPEJ* **22** (6): 831-846. doi: 10.2118/8999-PA.

Nagarajan, R. 2001. Polymer-Surfactant Interactions. In "New Horizons: Detergents for the New Millennium Conference Invited Papers", published by American Oil Chemists Society and Consumer Specialty Products Association, Fort Myers, Florida.

Nasr-el-din, H.A., Green, K.A. and Schramm, L.L. 1994. The Alkaline/Surfactant//Polymer Process: Effects of Slug Size, Core Length and a Chase Polymer. *Rev. Inst. Franç. Du Pétrole*. **49** (4): 359-377.

Nasr-El-Din, H.A., Hawkins, B.F., and Green, K.A. 1991. Viscosity Behavior of Alkaline, Surfactant, Polyacrylamide Solutions Used for Enhanced Oil Recovery. Paper SPE 21028 presented at the SPE International Symposium on Oilfield Chemistry, Anaheim. California, 20-22 February. doi: 10.2118/21028-MS.

Nasr-El-Din, H.A., Hawkins, B.F., and Green, K.A.. 1992. Recovery of Residual Oil Using the Alkali-Surfactant-Polymer Process: Effect of Alkali Concentration. *J. Pet. Sci. & Eng*., **6** (4): 381-401.

Nasr-El-Din, H.A. and Taylor, K. 1993. Interfacial Tension of Crude Oil/Alkali Systems in the Presence of Partially Hydrolyzed Polyacrylamide. *Colloids and Surfaces*, **49**, 273-279.

Nasralla, R.A., Bataweel, M.A., and Nasr-El-Din, H.A. 2011.Investigation of Wettability Alteration by Low Salinity Water. Paper SPE 146322 presented at SPE Offshore Europe Oil and Gas Conference and Exhibition. Aberdeen, UK, 6-8 September.

Nelson, J.B., Lawson, D.R., Thigpen, D.R., and Stegemeier, G.L. 1984. Cosurfactant-Enhanced Alkaline Flooding. Paper SPE 12672 presented at the SPE/DOE 4th Symposium on Enhanced Oil Recovery, Tulsa, Oklahoma. 15-18 April. doi: 10.2118/12672-MS.

Peters, E.J., and Hardham, w.d. 1990. Visualization of Fluid Displacements in Porous Media Using Computed Tomography Imaging. *J Pet Sci and Eng.* **4** (2): 155-168.

Pye, D.J. 1964. Improved Secondary Recovery by Control of Water Mobility. *J. Pet. Technol*. **16** (8): 911-916. SPE 845-PA. doi: 10.2118/845-PA.

Rojas, M. R., Müller, A. J., A., and Sáez, E.: 2008. Shear Rheology and Porous Media Flow Of Wormlike Micelle Solutions Formed By Mixtures of Surfactants of Opposite Charge. *Journal of Colloid and Interface Science* **326** (1): 221–226.

Rosen, M.J. 2004. *Surfactants and Interfacial Phenomena*. Hoboken, New Jersey: John Wiley and Sons.

Salagera, J.L., Antóna, R.E., Sabatini, D.A., Harwell, J.H., Acostac, E.J., and Tolosa, L. I. 2005. Enhancing Solubilization in Microemulsions—State of the Art and Current Trends. *Journal of Surfactants and Detergents* **8** (1):3-21.

Schramm, L.L. 2000. *Surfactants: Fundamentals and Applications in the Petroleum Industry*. Cambridge, Massachusetts: Cambridge University Press.

Schramm, L.L., Mannhardt, K., and Novosad, J.J. 1991. Electrokinetic Properties of Reservoir Rock Particles. *Colloids and Surfaces*, **55**: 309-331.

Seright, R.S., Campbell, A.R., Mozley, P.S., and Han, P. 2010. Stability of Partially Hydrolyzed Polyacrylamides at Elevated Temperatures in the Absence of Divalent Cations. *SPEJ*, **15** (2): 341-348.

Shah, D.O., and Schechter, R.S. ed. 1977. *Improved Oil Recovery by Surfactant and Polymer Flooding*. New York: Academic Press.

Shen, P., Wang, J., Yuan, S., Zhong, T., and Jia, X. 2009. Study of Enhanced-Oil-Recovery Mechanism of Alkali/Surfactant/Polymer Flooding in Porous Media From Experiments. *SPEJ*, **14** (2): 237-244. SPE-126128-PA. doi: 10.2118/126128-PA.

Shupe, R.D. 1981. Chemical Stability of Polyacrylamide Polymers. *JPT,* **33** (8): 1513-1529. SPE-9299-PA. doi: 10.2118/9299-PA.

Siddiqui, S., and Khamees, A.A. 2004. Dual-Energy CT-Scanning Applications in Rock Characterization. Paper SPE 90520 presented at SPE Annual Technical Conference and Exhibition, Houston, Texas, 26-29 Sep. doi: 10.2118/90520-MS.

Sorbie, K.S. 1991. *Polymer-improved Oil Recovery*. Glasgow: Blackie and Son Ltd.

Standnes, D.C. 2001. Enhanced Oil Recovery From Oil-wet Carbonate Rock by Spontaneous Imbibition of Aqueous Surfactant Solutions. Ph.D. Thesis, Norwegian U. of Science and Technology/Stavanger U. College.

Stournas, S. 1984. A Novel Class of Surfactants with Extreme Brine Resistance and Its Potential Application in Enhanced Oil Recovery. Paper SPE 13029-MS presented at the SPE Annual Technical Conference and Exhibition, Houston, Texas, 16-19 September. doi: 10.2118/13029-MS.

Szabo, M.T. 1979. An Evaluation of Water-Soluble Polymers for Secondary Oil Recovery. Part II. *JPT*. **31** (5): 553-570. SPE-6601-PA. doi: 10.2118/6601-PA.

Taber, J.J., Martin, F.D. and Seright, R.S. 1997. EOR Screening Criteria Revisited - Part 1: Introduction to Screening Criteria and Enhanced Recovery Field Projects. SPERE 12 (3): 189-198. doi: 10.2118/35385-PA.

Taylor, K. and Nasr-El-Din H.A. 1996. Dynamic Interfacial Tension of Crude Oil/Alkali/Surfactant/Polymer Systems. in AOCS Monograph, "Dynamic Properties of Interfaces and Association Structures", D.O. Shah (Editor), Chapter 4, 80-125.

Thomas, S., and Farouq Ali, S.M. 2001.Micellar Flooding and ASP-Chemical Methods for Enhanced Oil Recovery. JCPT, **40** (2): 46-52.

Vinegar, H.J. 1986.X-Ray CT and NMR Imaging of Rocks. JPT, **38** (3): 257-.259. SPE 15277. doi: 10.2118/15277-PA.

Vinegar, H.J., and Wellington, S.L. 1987.Tomographic Imaging of Three-Phase Flow Experiments. *Rev. Sci. Instrum*. **58** (1): 96-107.

Wang, D., Jiecheng, C., Junzheng, W., Zhenyu, Y., and Yuming, Y. 1999. Summary of ASP Pilots in Daqing Oil Field. Paper SPE 57288-MS presented at the SPE Asia Pacific Improved Oil Recovery Conference, Kuala Lumpur, Malaysia, 25-26 October. doi: 10.2118/57288-MS.

Wang, D.M., Liu, C.D., Wu, W.X., and Wang, G. 2008. Development of an Ultra-Low Interfacial Tension Surfactant in a System with No-Alkali for Chemical Flooding. Paper SPE 109017-MS presented at the SPE/DOE Symposium on Improved Oil Recovery. Tulsa, Oklahoma, 20-23 April. doi: 10.2118/109017-MS.

Wang, D., Liu, C., Wu, W., and Wang, G. 2010. Noval Surfactants that Attain Ultra-Low Interfacial Tension Between Oil and High Salinity Formation Water Without Adding Alkali, Salts, Co-surfactants, Alcohol and Solvents. Paper SPE 127452 presented at the SPE EOR Conference at Oil & Gas WestAsia, Muscat, Oman, 11-13 April. doi: 10.2118/127452-MS.

Wang, Y., Liu, J., Liu, B., Liu, Y., Hongxing, W., and Chen, G., 2004. Why Does Scale Form in ASP Flood? How to Prevent from It?--A Case Study of the Technology and Application of Scaling Mechanism and Inhibition in ASP Flood Pilot Area of N-1DX Block in Daqing. Paper SPE 87469-MS presented at the SPE International Symposium on Oilfield Scale, Aberdeen, United Kingdom, 26-27, May. doi: 10.2118/87469-MS.

Wesson, L. L., and Harwell, J. H. 2000. Surfactant Adsorption in Porous Media. *Surfactants: Fundamentals and Applications in the Petroleum Industry*, Schramm, L. L., ed., Cambridge, Massachusetts: Cambridge University Press.

Winsor, P. 1954. *Solvent Properties of Amphiphilic Compounds*. London: Butterworth.

Withjack, E.M., Devier, C., and Michael, G. 2003. The Role of X-Ray Computed Tomography in Core Analysis. Paper SPE 83467 presented at SPE Western Regional/ AAPG Pacific Section Joint Meeting, Long Beach, California, 19-24 May. doi: 10.2118/83467-MS.

Young, T. 1805. An Essay on the Cohesion of Fluids, *Phil. Trans. R. Soc. Lond*. **95**:65-87, doi:10.1098/rstl.1805.0005

Zaitoun, A., and Potie, B. 1983. Limiting Conditions for the Use of Hydrolyzed Polyacrylamides in Brines Containing Divalent Ions. Paper SPE 11785-MS presented at the SPE Oilfield and Geothermal Chemistry Symposium, Denver, Colorado, 1-3 June. doi: 10.2118/11785-MS.

Zhang, D.L. 2005. *Surfactant-Enhanced Oil Recovery Process for a Fractured, Oil-wet Carbonate Reservoir*. Ph.D. dissertation, Rice U., Houston, Texas.

Zhang, J., Nguyen, Q.P., Flaaten, A.K., and Pope, G.A. 2008. Mechanisms of Enhanced Natural Imbibition with Novel Chemicals. Paper SPE 113453-MS presented at SPE/DOE Symposium on Improved Oil Recovery, Tulsa, Oklahoma, 20-23 April. doi: 10.2118/113453-MS.

Zhao, Z., Li, Z., Qiao, W., and Cheng, L. 2006. Dynamic Interfacial Tension Between Crude Oil and Octymethylnaphthalene Sulfonate Solution. *Energy Sources, Part A*, **28**: 1397-1403.

VITA

Name	Mohammed Abdullah Bataweel
Addres	P.O.Box 5645 Dhahran, 31311 Saudi Arabia
E-mail address	bataweel@yahoo.com
Education:	B.S., Mechanical Engineering, King Fahd University of Petroleum & Minerals (KFUPM), 1997. M.S., Petroleum Engineering, Herriot-Watt University, 2003. Ph.D., Petroleum Engineering, Texas A&M University, 2011.